ANTIBACTERIAL DRUG DISCOVERY: TARGETING RESISTANCE AND PERSISTENCE IN BACTERIA USING NOVEL SMALL MOLECULES

Ph.D THESIS

by

TIMSY BHANDO

DEPARTMENT OF BIOTECHNOLOGY
INDIAN INSTITUTE OF TECHNOLOGY ROORKEE
ROORKEE-247667(INDIA)
JULY, 2019

ANTIBACTERIAL DRUG DISCOVERY: TARGETING RESISTANCE AND PERSISTENCE IN BACTERIA USING NOVEL SMALL MOLECULES

A THESIS

Submitted in partial fulfilment of the requirements for the award of the degree

of

DOCTOR OF PHILOSOPHY

in

BIOTECHNOLOGY

by

TIMSY BHANDO

DEPARTMENT OF BIOTECHNOLOGY
INDIAN INSTITUTE OF TECHNOLOGY ROORKEE
ROORKEE-247667(INDIA)
JULY, 2019

INDIAN INSTITUTE OF TECHNOLOGY ROORKEE

STUDENT'S DECLARATION

I hereby certify that the work presented in the thesis entitled "**ANTIBACTERIAL DRUG DISCOVERY: TARGETING RESISTANCE AND PERSISTENCE IN BACTERIA USING NOVEL SMALL MOLECULES**" is my own work carried out during a period from July, 2013 to July, 2019 under the supervision of Dr. Ranjana Pathania, Associate Professor, Department of Biotechnology, Indian Institute of Technology Roorkee, Roorkee.

The matter presented in the thesis has not been submitted for the award of any other degree of this or any other institute.

Timsy

Dated : 18th September, 2019 **Timsy Bhando**

This is to certify that the above mentioned work is carried out under my supervision.

Dated : 18th September 2019 Ranjana Pathania

Ranjana Pathania
(Supervisor)

The Ph.D. Viva-Voce Examination of **Ms. Timsy Bhando**, Research Scholar, has been held on **18th September, 2019** at Department of Biotechnology, IIT Roorkee, Roorkee, INDIA.

18/9/19

Chairman, SRC

Rachna Chabe

Signature of External Examiner

This is to certify that the student has made all the corrections in the thesis.

Ranjana Pathania 18th Sep' 2019.

Signature of Supervisor

18.9.19

Head of Department

Dedicated to my parents

Abstract

Antibiotic resistance is one of the major global health concerns. Inappropriate and excessive use of antibiotics has led to the emergence of multi-drug resistant (MDR) bacterial strains, thus exacerbating the problem. Despite generous efforts, no new class of antibiotics have been approved against Gram-negative pathogens in over 50 years and antibiotic research is under a dry spell. The ESKAPE group of pathogens namely ***E****nterococcus faecium*, ***S****taphylococcus aureus*, ***K****lebsiella pneumoniae*, ***A****cinetobacter baumannii*, ***P****seudomonas aeruginosa* and ***E****nterobacter* species present a major threat worldwide due to their unequalled ability to escape the available antibiotic treatments. Only four new classes of antibiotics have been approved for clinical use in the last decade, all of which target Gram-positive pathogens and none of which exhibit a novel mechanism of action. Importantly, Gram-negative bacteria make up four of the six ESKAPE pathogens and present the most acute threat owing to their complex cell envelope structure that acts as a formidable barrier to the existing antibiotic arsenal. The increasing emergence of multidrug-resistant bacteria and the drying antibiotic pipeline calls for the development of new antibacterial agents and novel strategies that can help address the global threat of antibiotic resistance.

In an effort to explore new leads in the field of antimicrobial drug discovery against Gram negative bacteria, a whole-cell screening assay was performed on a collection of 10,956 small molecules against *Escherichia coli* ATCC 25922 and 30 hit compounds demonstrating remarkable antibacterial activity were identified. Herein, I describe the antibacterial spectrum, *in vitro* pharmacodynamics and mechanism of action (MOA) of one such lead series represented by IITR06144. IITR06144 exhibits an impressive broad spectrum activity against most MDR bacteria and a remarkable antibiofilm and anti-persister activity. It displays no associated toxicity, lack of resistance development and *in vivo* efficacy in a mice model of infection. With the aid of antisense RNA technology, fluorescence microscopy studies and use of *E. coli* gene mutants *etc.*, it was observed that IITR06144 inhibits the bacterial growth by causing DNA damage and consequently inhibiting the cell division machinery. IITR06144 is a promising antibacterial molecule displaying most features of a theoretically “ideal” antibiotic and extreme potential to overcome the problem of antibiotic resistance prevailing in the clinics.

The use of antibiotics in combination represents one of the most readily available strategies to combat infections caused by MDR pathogens. Synergistic antibiotic combinations are willingly accepted by clinicians as they aid the revival of old antibiotics and can overcome the problem of

toxicity associated with certain antibiotic classes. Hence, I further studied the ability of small molecule, IITR06144 to act in combination with clinically relevant antibiotics against a few representative ESKAPE pathogens. IITR06144 was observed to exhibit favourable synergistic interaction with vancomycin against Vancomycin Intermediate *Staphylococcus aureus* (VISA). The combination of IITR06144 and Vancomycin displayed excellent bactericidal activity, anti-biofilm activity and *in vivo* efficacy in *Caenorhabditis elegans* model of *S. aureus* infection.

Elucidating the mode of action for novel antibacterials identified in small molecule screens remains an arduous task that severely limits drug discovery efforts. In this respect, I exploited the previously established strategy of using chemical-chemical interactions to identify cellular targets of few aforementioned molecules from the phenotypic screen. Small molecules were combined with known antibacterials belonging to diverse chemical classes and mechanisms and screened for growth inhibition against *E. coli* MC1061, using a two-point dose matrix approach. This approach uncovered several synergistic combinations identifying a novel lead series antibacterial, IITR07865 which represents a new class of inhibitors targeting the bacterial cell wall synthesis.

Apart from drug resistance, the phenomenon of "drug tolerance" exhibited by a subpopulation of bacterial cells known as "persisters" ensues another major threat. Eradication of the persister populations in chronic ailments holds extreme importance for an improved long term recovery from recurring infections. In this part of the study, I first investigated the characteristics and mechanisms responsible for meropenem persistence in the ESKAPE pathogen, *A. baumannii*. Meropenem induced *A. baumannii* persisters were observed to exhibit enhanced efflux activity thus rendering them to be multi-drug tolerant. Further, I devised a mechanistic screen for novel anti-persister compounds leading to the identification of a GRAS (Generally Regarded As Safe) status small molecule with promising activity against bacterial persisters of *A. baumannii* and two other ESKAPE pathogens. This study has vital implications for the treatment of recalcitrant bacterial infections.

Overall, this work addresses the challenge of antibiotic resistance and endeavours to minimize or overcome the problem by the identification of new antibacterial agents, development of small molecule-combination regimens or targeting antibiotic tolerant organisms. Importantly, this study reports the identification of novel synthetic and natural scaffolds that demonstrate excellent potential and hold promise for use in clinics in the fight against antibiotic resistance.

Acknowledgement

Undertaking this PhD has been a truly life-changing experience for me and it wouldn't have been possible without the support and guidance that I received from numerous people. It is a pleasure to convey my gratitude to one and all who have contributed in one way or the other in this journey and in the compilation of this study.

Prime most I would thank the one above all, the omnipresent God, for answering my prayers and for giving me loads of strength to hurdle all the obstacles that came my way.

I would like to express my special thanks to my supervisor Dr. Ranjana Pathania for being a tremendous mentor to me. I lack in words to show my gratitude to her for providing me the perfect atmosphere and training to grow as a research scientist. I am also thankful to her for being an utmost source of inspiration and providing an excellent example as a successful woman microbiologist and professor. She has inspired me to become an independent researcher and helped me realize the power of critical reasoning and the importance of not having a minimalist approach in science. I can't thank her enough for all the freedom she gave me to wander intellectually. She has helped me not only in honing my research skills, but also helped me to develop into a stronger, confident and optimistic person. I am tremendously fortunate and could not have imagined having a better advisor and mentor for my PhD study.

I would like to extend my special thanks to Dr. Naveen K Navani for his constant support and encouragement. He always made himself available for the scientific discussions and insightful comments on my research work. His guidance helped me throughout and I have had the privilege of learning many things from him.

I express deep sense of gratitude and thankfulness to Prof. A. K. Sharma, Head, Department of Biotechnology for providing all the facilities within the department for carrying out unhindered research. A special note of thanks to my committee members Prof. Sanjoy Ghosh, Chairman SRC and Prof. R. Prasad, Chairman DRC; Prof. Partha Roy and Prof. P. Biswas for their help and constant encouragement. I sincerely thank Ministry of Human Resource and Development (MHRD) for providing financial assistance in the form of fellowship which buttressed me to perform my work comfortably.

I am also grateful to several mentors from my pre-IIT Roorkee days for their wisdom and encouragement. From the Institute of Microbial Technology, Chandigarh, I want to thank Dr. K.L. Dikshit under whose esteemed guidance I worked as a research intern after completing my masters. Dr. Dikshit's eternal enthusiasm and rigorous approach to science played an important role in nurturing my ardour for biology. I consider myself very lucky to have had the opportunity of working with such a great scientist during the initial years of my career. And from the Institute of Genomics and Integrative Biology, New Delhi where I underwent my masters dissertation; I want to thank my mentors Dr. Samantha Kohli and Dr. Rahul Jha who continue to inspire me till date. Also I would like to express my gratitude to Mr. Manish Tiwari, my Biology teacher at school for instilling my interest in the subject and who has been one of the most instrumental pillars in shaping my career goals.

I am indebted to my lab colleagues for providing a stimulating work environment. I am highly obliged to my seniors Rajnikant Sir, Tapas Sir, Parmesh Sir, Piyush Sir, Tamoghna Sir, Atin for their help that made me initiate my journey into research. I would like to express deep regards to Rajnikant Sir for his invaluable guidance, stimulating scientific suggestions and encouragement which helped me to tackle the 'tough times' in the initial period of my research. I would also like to thank my Juniors Amit, Vineet, Jawed, Mahak, Somok, Rajat, Shahnawaz, Anupama, Kuldip, Rinki and Abhiroop for their cheerful company and unconditional support throughout.

A special thank you goes out to Vineet, for being like a younger brother and the 'go to' person. I have some fond memories of the wonderful times and conversations we have shared, especially during our frequent lunches and dinners. I would specially like to thank Amit for the microscopy lessons. I am also grateful to Vivek Sir, Siva Sir, Rashmi Ma'am, Mangal Sir and Arun Sir for their help and guidance at all times. I would like to extend a heartfelt thanks to Rinki for her unselfish and unfailing support during the writing of this thesis. I fall short of words to express my gratitude towards her for providing me the much needed moral support.

I have also had the opportunity to mentor and work with several undergraduate and post graduate students during my PhD which has been a truly fulfilling experience. I would like to thank Ananth, Safuwan, Himanshu, Priyanka, Anand and Geetika for their support without which this work wouldn't have reached its destination.

Even more thanks goes to the good friends I made during my time at IIT Roorkee: Preeti Ma'am, Jyoti, Debpali, Pardeep, Benazir, Mukta, Anjali, Poonam and Sonam. They provided me with great friendship, great conversations, and constant encouragement. I would also like to thank Harshita, Shantanu, Tanusri, Urvashi, Divya, Reetika and Suruchi who have been incredible friends to me over the years. Their moral support has made all the difference. Also, I wish to specially thank my best friend Mangesh for his unconditional support and motivation throughout my PhD. I truly thank him for sticking by my side during my bad times, even when I was irritable and depressed.

Of course no acknowledgement would be complete without giving thanks to my family. I am very lucky to have been blessed with a loving and supportive family. I am indebted to my parents for beleieving in me, for their unconditional love and for all the sacrifices they have made for me. I am grateful to them for all that they have taught me about what it means to be a good person. I am extremely thankful to my mother for being a constant companion to me throughout the PhD process. I would like to thank my sisters and brothers in law for their emotional support and encouragement. Finally I would like to thank my little bundles of joy; my nieces Manya, Vanya, Rheeya and nephews Ansh and Tanishq for filling my life with so much laughter and playfulness. You guys are the sweetest people that surround me. Thank you so much!

Timsy

Contents

List of figures

List of tables

Abbreviations

ANOVA	One way analysis of variance
ATCC	American Type Culture Collection
ATP	Adenosine Triphosphate
CCCP	Cyanide 3-chlorophenylhydrazone
CDC	Centre for Disease Control and Prevention
cDNA	Complementary Dexyribose Nucleic Acid
CFU	Colony Forming Units
CLSI	Clinical and Laboratory Standards Institute
CRAB	Carbapenem Resistant *Acinetobacter baumannii*
CV	Crystal Violet
DAPI	4′, 6-Diamidino-2-phenylindole dihydrochloride
DEPC	Diethylpyrocarbonate
$DISC_3(5)$	3, 3'dipropylthiacarbocyanine
$DIBAC_4$	Bis-(1,3-Dibutylbarbituric Acid)Trimethine Oxonol
DMEM	Dulbecco's Modified Eagle's Medium
DMSO	Dimethyl suphoxide
DNA	Deoxyribonucleic acid
dsDNA	Double stranded DNA
EPIs	Efflux pump inhibitors
ESBL	Extended-Spectrum β-Lactamases
ESKAPE	*Enterococcus faecium, Staphylococcus aureus, Klebsiella pneumoniae, Acinetobacter baumannii, Pseudomonas aeruginosa,* and *Enterobacter* species
EtBr	Ethidium bromide
FDA	Food and Drug Administration

FIC	Fractional inhibitory concentration
FITC	Fluorescein isothiocyanate
FM 4-64	N-(3-Triethylammoniumpropyl)-4-(6-(4-(Diethylamino) Phenyl) Hexatrienyl) Pyridinium Dibromide
g	Grams
GFP	Green Fluorescent Protein
GRAS	Generally rRegarde As Safe
HIV/AIDS	Human Immunodeficiency Virus
HTS	High throughput screening
hVISA	Heterogenous Vancomycin intermediate *Staphylococcus aureus*
IAEC	Institute Animal Ethics Committee
ICU	Intensive Care Unit
IDSA	Infectious Diseases Society of America
IPTG	Isopropyl thio β, D-galactoside
Kan	Kanamycin
kDa	Kilodalton
L	Litre
LB	Luria Bertani
MATE	Multidrug and Toxic compound extrusion
MDR	Multiple drug resistance
MDR strain/bacteria	Multi Drug Resistant strain/bacteria
MFS	Major facilitator super family
mg	Milligram
MH	Mueller Hinton
MIC	Minimum Inhibitory Concentration
min	Minutes
ml	Milliliter

mM	Millimolar
MOA	Mechanism of Action/ Mode of Action
MRSA	Methicillin resistant *Staphylococcus aureus*
nm	Nanometer
OD	Optical Density
PAE	Post Antibiotics Effects
PAGE	Polyacrylamide Gel Electrophoresis
PBS	Phosphate Buffered Saline
PCR	Polymerase chain reaction
PDB	Protein Data Bank
PDR	Pan drug-resistance
pH	Power of hydrogen
RNA	Ribonucleic acid
RND	Resistance Nodulation Division
ROS	Reactive Oxygen Species
rpm	Rotation per minute
RT	Room Temperature
SDS	Sodium Dodecyl Sulphate
SEM	Scanning Electron Microscopy
SMR	Small multidrug resistance
sRNA	Small Ribonucleic Acid
TEM	Transmission Electron Microscopy
t-RNA	Transfer RNA
US/USA	United States of America
UTI	Urinary Tract Infections
UV	Ultraviolet

VISA	Vancomycin intermediate *Staphylococcus aureus*
VRE	Vancomycin-resistant enterococci
VRSA	Vancomycin resistant *Staphylococcus aureus*
WHO	World Health Organisation
WT	Wild type
XDR	Extremely-drug resistant
µg	Microgram
µl	Microliter
µM	Micromolar

1 Introduction

Bacterial infections have plagued humans throughout history. In the past 70 years, antibiotics have changed the world by saving and improving countless lives, establishing them as the cornerstones of all modern health systems. The success of modernized medicine, namely organ transplantation, cancer therapy, joint replacement, management of preterm babies, or even minor surgeries, might not have been possible without effective antibiotic treatment to keep bacterial infections in control [1]. However, excessive and injudicious antibiotic use has accelerated the emergence of multidrug resistant (MDR) bacteria causing significant morbidity and mortality across the globe [2]. The most dangerous and resistant bacteria have been clubbed under the acronym "ESKAPE" (***E****nterococcus faecium*, ***S****taphylococcus aureus*, ***K****lebsiella pneumoniae*, ***A****cinetobacter baumannii*, ***P****seudomonas aeruginosa*, and ***E****nterobacter* species) emphasizing their ability to evade killing by antibiotics [3],[4]. Of particular concern are the increase in cases of medical illness caused by the carbapenem resistant Enterobacteriaceae (CRE) and carbapenem resistant *Acinetobacter baumannii* (CRAB) [5].

The drug resistant superbugs survive the antibiotic onslaught by continually evolving to acquire sophisticated resistance mechanisms such as target site mutations, efflux pumps overexpression or acquisition of antibiotic modifying or degrading enzymes etc. [6]. Owing to the paucity of newer or better treatment options to combat the existing crisis of antibiotic resistance, we are slowly moving into the "post- antibiotic era", where even minor injuries would prove life threatening [7]. Given the proliferated emergence of resistance to existing antibiotics, there is an urgent need to discover novel chemical classes or modify the existing ones for improved efficacy [8],[9],[10],[11].

The use of combination therapy against serious bacterial infections is another viable approach that can be used to enhance the effectiveness and spectrum of known antibiotics [12]. Drugs in combination act on multiple targets and display the advantage of overcoming the emergence of resistance mutations [13]. The use of drugs, Augmentin (Amoxycillin-Clavulanic Acid) and Co-trimoxazole (Trimethoprim-sulfamethoxazole) in the clinics are few examples of the efficacy of combinations as antibacterial therapeutics [12], [151]. Combination therapy also showcases the power of improving the activity of antibacterial molecules which would have otherwise been discarded, due to toxicity [14].

Chemical genetics approach is one of the most widely used strategies for the discovery of novel antibacterial small molecules [15]. While forward chemical genetics involves the use of small molecules to assess their phenotypic effect on bacteria followed by target identification, reverse chemical genetics runs in the opposite direction [16]. The phenotype based whole-cell screening approach presents the advantage of overcoming the insurmountable outer membrane barrier in Gram negative pathogens besides also offering the possibility to identify growth inhibitory compounds that can act on novel single or multiple targets [17]. Hence, considering the advantages and efficacy of classical cell-based screens to identify potential antibacterials, recent years have witnessed resurgence in appreciating them, over target-based approaches [18].

Determining the MOA of novel leads identified in whole-cell phenotypic screens poses an appalling challenge and has been considered the rate determining step in any drug discovery program [15]. Although, no universal or systematic strategy for target identification exists, the classical biochemical approach employs the use of tagged/derivatised small molecules that act as a bait to its protein target [15]. Targets of β-lactam antibiotics, penicillin-binding proteins (PBP) were identified by affinity based pull down assays [19]. This approach has further undergone continued improvement enhancing the efficacy and sensitivity for target detection [20],[21]. Chemical genomic strategies have exploited the use of genome wide assemblage of overexpression or deletion clones that have been used to map antibiotic susceptibility phenotype to specific target genes [22],[23]. The successful discovery of a lipoprotein targeting inhibitor, MAC13243 by employing the *E. coli* ASKA library is one such example [9]. Moreover, antisense methodology to deplete bacterial strains from expressing essential proteins is another suitable approach that led to the discovery of platensimycin, a novel fatty acid biosynthesis inhibitor [24]. Identification and characterization of drug resistant clones is also a viable strategy that has proved useful to identify targets for the antibiotics rifampicin and novobiocin [25],[26]. Macromolecular synthesis (MMS) assays for target identification is also a preferred approach which involves the use of radioactively labeled precursors to identify inhibitors of DNA, RNA, protein, or cell wall biosynthesis [27]. This method can also aid the identification of molecules that target multiple pathways within the bacterial cell. Bacterial cytological profiling is a novel and powerful approach that has been recently developed to identify the cellular targets of unknown inhibitors using fluorescence microscopy techniques [28]. Promoter–reporter libraries also provide a signature phenotype in response to chemical stresses thus presenting an excellent tool for screening of novel antibacterial and MOA analysis [29]. Deep sequencing

technologies such as transcriptome profiling by RNA-Seq, transposon sequencing (Tn-Seq) and identification of suppressor mutants are newer and powerful approaches that have been used to study the MOA of novel antibacterials [30]. Further, chemical-chemical combination profiling also has demonstrated its potential in providing information about the target and MOA of novel antibacterial small molecules [31]. Recent reports on the identification of inhibitors of Dihydro Folate Reductase (DHFR) and Undecaprenyl Diphosphate Synthase by analysis of the synergistic and antagonistic interactions between known antibiotics and antibacterials with unknown MOA are an example [31],[32].

In the search for new antibacterial leads against the notorious Gram negative pathogens, our lab previously performed a whole-cell screening assay on a diverse collection of 10,956 small molecules for growth inhibition on the model organism, *E. coli* ATCC 25922. The screen identified 30 novel antibacterial leads belonging to diverse structural and chemical classes. The lead molecules demanded further characterisation on the basis of their antibacterial properties, pharmacodynamics, pharmacokinetics to be followed by evaluation of their toxicity and efficacy. It was also imperative to carry out mechanism of action studies for the novel leads by using a combination of the several approaches discussed above. All these studies were extremely crucial and would help in determining the therapeutic potential of the lead molecules discovered.

Further, the phenomenon of "Bacterial persistence" is of major clinical relevance, since it has been demonstrated to facilitate the emergence of antibiotic resistance [33]. The chronic and recalcitrant nature of infections caused by *Escherichia coli, Mycobacterium tuberculosis, Acinetobacter baumannii and S. aureus etc.* have been associated with their ability to exhibit drug tolerance in response to antibiotic stress or hostile environmental conditions [34]. Studying the underlying complex mechanisms of persistence hosted by the bacterial pathogens holds immense importance which would further facilitate the development of effective strategies to inhibit or eradicate them.

Thus, this thesis attempts to address the antibiotic apocalypse and endeavours to seek suitable solutions by employing diverse strategies such as (i) characterization of novel antibacterial agents, (ii) development of small molecule-combination regimens and (iii) characterization of the mechanisms of persistence and screening novel anti-persister molecules. The thesis has been divided into multiple chapters based on the above objectives. **Chapter 4** comprises the detailed characterization of a novel antibacterial small molecule belonging to the lead series IITR06144,

identified in a whole-cell screening assay on a collection of 10,956 small molecules against *Escherichia coli* ATCC 25922. The chapter is divided in two parts. The first section describes the antibacterial spectrum, *in vitro* pharmacodynamics and characteristics of IITR06144. The second part studies the mode of action of IITR06144 with the aid of chemical genetics, antisense RNA technology and fluorescence microscopy studies. **Chapter 5** evaluates the interaction of IITR06144 with clinically relevant antibiotics against a few representative Gram negative and Gram positive bacteria, with major focus on *Staphylococcus aureus*. **Chapter 6** exploits the strategy of utilising chemical-chemical interactions for the identification of cellular targets of uncharacterized antibacterials. This chapter studies the combination profiles of a few novel antibacterial molecules from the aforementioned phenotypic screen with a panel of fourteen known bioactives. This chapter discusses the chemical fingerprints and interaction profiles of several small molecules with special emphasis on IITR07865, which displayed a unique synergistic interaction with cell wall inhibiting and membrane targeting antibiotics. **Chapter 7** addresses the problem of antibiotic persistence prevailing in the clinics in reference to the dreadful nosocomial pathogen, *Acinetobacter baumannii* and the last resort antibiotics from the carbapenem class. It investigates and charactersises the mechanisms responsible for *A. baumannii* persistence in response to meropenem. It further describes the use of a systematic screening strategy for the identification of potent anti-persister compounds that target the bacterial membrane, induce oxidative stress mediated killing and inhibit antibiotic efflux. It reports the identification of GRAS (Generally Regarded As Safe) status molecules exhibiting promising activity against bacterial persisters of *A. baumannii* and two other ESKAPE pathogens. Finally, **Chapter 8** concludes the thesis and thoroughly discusses the implications of the current work. It summarizes the outcomes of the study and describes its significance and future prospects.

2 Review of literature

2.1 Antibiotic resistance – a serious global problem

Selman Waksman, a Ukrainian-American inventor and microbiologist coined the term antibiotics in 1939, where "anti" means against and "biotic" means "life" [35]. Hence, any substance that exhibits the ability to inhibit or kill bacteria could be outright called an "antibiotic". The history of antibiotic discovery dates back to the 1900s, when Paul Erlich, a German physician first reported the ability of some chemicals to target bacterial cells and discovered Salvarsan (arsphenamine), the first antimicrobial to be used for the treatment of syphilis [36]. This was a breakthrough discovery and Salvarsan became the first modern antibiotic. It was 30 years later, in 1939 when Sir Alexander Flemming stumbled upon the accidental discovery of a fungal mould that could inhibit the growth of *Staphylococcus aureus*, a deadly bacterium [37]. He later established the fungus, *Penicillium notatum* to produce the chemical Penicillin that was extremely safe and efficacious to be used against bacterial infections. Penicillin soon became the first successful "wonder drug" and saved the lives of numerous wounded soldiers during World War II [38]. Undoubtedly, the discovery of penicillin marked the beginning of the "modern era of antibiotics" and it was in 1945 that A. Flemming, along with Howard Florey, an australian pathologist and Ernest Chain, a German biochemist received the Nobel Prize in Medicine for its discovery and mass production [38]. A few years later in 1952, S. Waksman received the Nobel prize for his discovery of the first effective antibiotic against tuberculosis, streptomycin [39].

Antibiotic discovery swept a surge of unbridled optimism throughout the world, essentially transforming human health and revolutionizing the treatment of infectious diseases [40]. However, the increased use of penicillin both in the community and hospitals led to the emergence of bacterial strains that could resist its action. Penicillin resistance threatened the advances made in healthcare and propelled the discovery of newer beta-lactam antibiotics such as methicillin in 1959 [41]. Nonetheless by 1961, methicillin-resistant *Staphylococcus aureus* (MRSA) was identified, very much predicting the "antibiotic resistance" catastrophe that was to follow [41].

Unfortunately, resistance has eventually been reported to nearly all classes of antibiotics that were introduced thereafter (Fig. 2.1). It is estimated that antibiotic-resistant bacteria infect at least 2 million people per year in the U.S. itself causing approximately 23,000 deaths [2]. Antibiotic overuse, inappropriate prescribing, extensive use of antibiotics in livestock, poultry and agriculture accompanied by the availability of fewer new antibiotics are some of the major reasons that are held responsible for the mounting problem of antibiotic resistance [42]. Evidently, no new classes of antibiotics have been introduced since 1987 and this innovation gap is referred to as the "discovery void" (Fig. 2.1) [43].

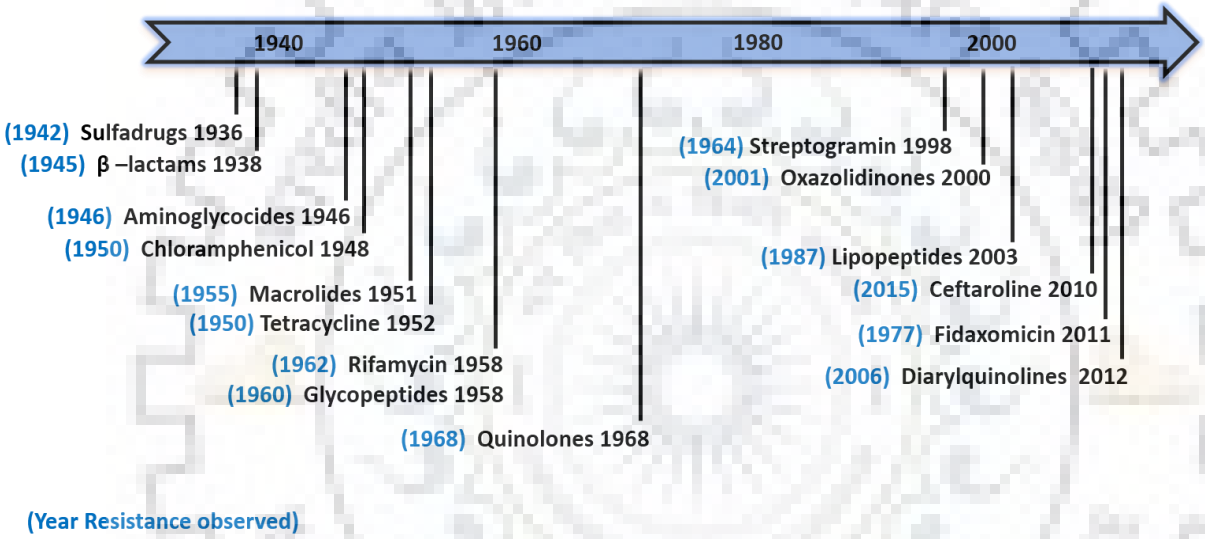

Figure 2.1: The antibiotic discovery and resistance timeline. The year in brackets indicate the year when resistance was reported against the respective antibiotic class in comparison to its year of introduction. Adapted from [44].

2.2 Ways to fight antibiotic resistance –the Global Action Plan (2014)

The burgeoning problem of antibiotic resistance if left unattended is expected to cast us back into the dark ages of medicine, where even minor injuries proved life threatening. Addressing the grim situation posed by the antibiotic resistant infections, the World Health Organization (WHO) in 2014 proposed the first Global Action Plan (GAP) on Antimicrobial Resistance (AMR) urging the member states to take concrete actions against the menace [45]. Antibiotic resistance has also been implicated to pose a huge economic burden, more so to the low income

countries [46]. Drug resistant infections, if left untreated by 2050, are estimated to cause 10 million deaths annually and cost around 100 trillion USD [46]. The Global Action Plan laid down five strategic objectives that are the key to tackle the global threat of AMR:

(i) To educate the global public and increase their awareness and understanding of the problem of AMR;

(ii) To optimise the unnecessary use of antimicrobial agents against humans and animals and to make efforts to improve the standard of diagnostic technologies available.

(iii) To encourage investment and research into the development of new antibiotics.

(iv) To limit the unscrupulous use of antimicrobials in the agricultural sector.

(v) Promote development of alternative strategies for both prevention and treatment of AMR such as the use of vaccines, phage therapy and probiotics.

2.3 The Global Priority list of antibiotic resistant pathogens

In the face of the ever increasing crisis of antibiotic resistance, coordinated efforts to revive and improve the successful drug discovery are essentially needed. In order to priortise research and development for the discovery of newer antibiotics in line with the Global action plan, WHO published its first priority list of antibiotic-resistant bacteria that cause significant mortality and morbidity and need immediate attention (Fig. 2.2) [47]. This list comprised of 12 groups of bacteria, categorized into three tiers namely, critical, high, and medium priority on the basis of the epidemiological data derived from the project DRIVE-AB Work Package 1B, "Setting, communicating and revising public health priorities" [3].

The four most important criteria that formed the grounds for categorization of the resistant pathogens were treatability, mortality, burden of health-care and the trend of resistance during the past 10 years. The critical priority category included the pathogens that are responsible for causing severe and often fatal bloodstream or urinary tract infections (UTI) in the clinics. These are the carbapenem-resistant *Acinetobacter baumannii*, *Pseudomonas aeruginosa*, and *Enterobacter* spp., apart from third-generation cephalosporin-resistant *Enterobacter* spp. Considering the fact that nine out of twelve antibiotic resistant pathogens in the global priority list were Gram-negative and no new antibiotics have been introduced against them in the past 20 years, the need for concerted efforts to foster research and development of newer antibiotics against them has been urged for.

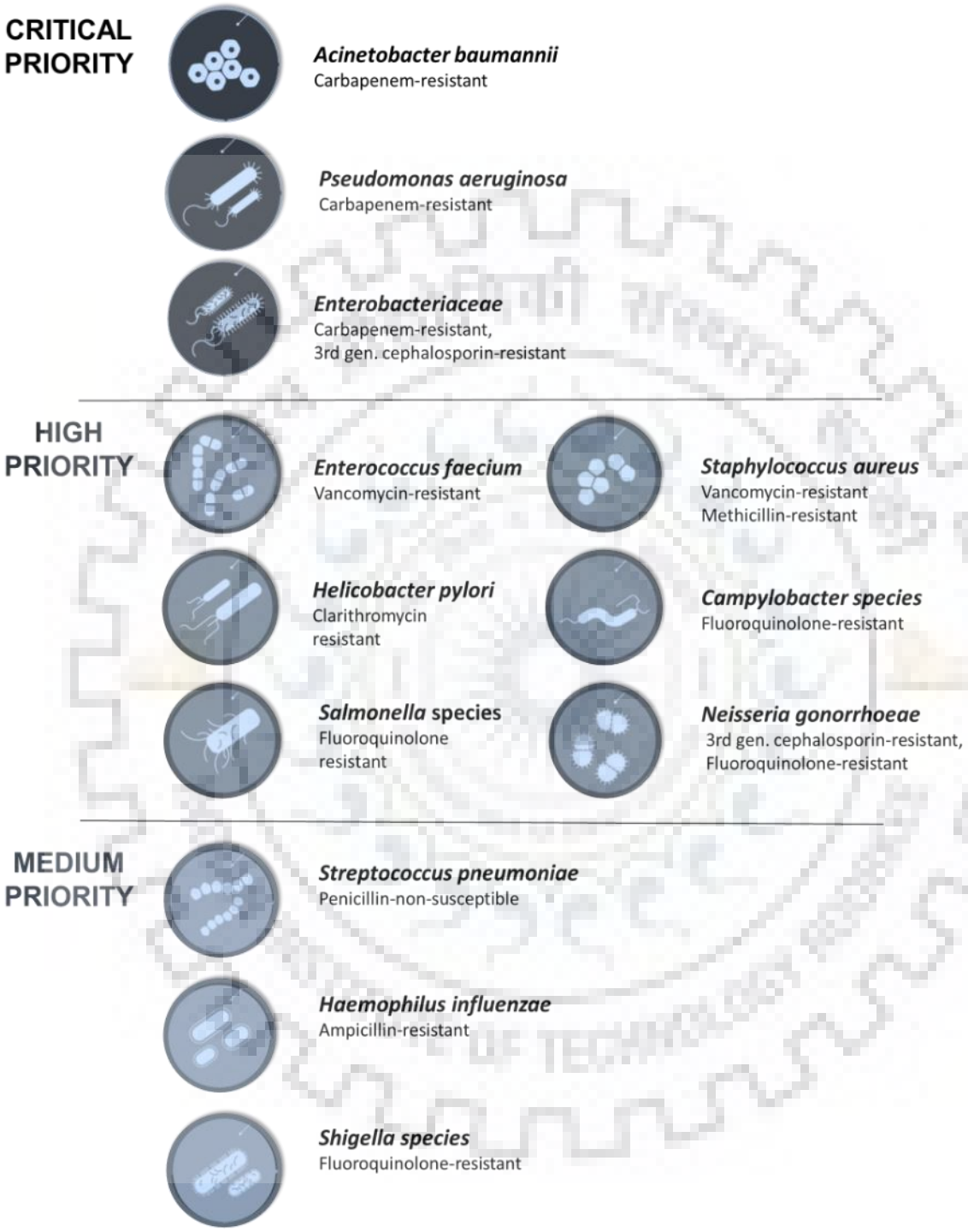

Figure 2.2: The Global priority list of antibiotic resistant pathogens as released by the World Health Organisation (WHO) in 2017. Adapted from [3].

2.4 What impedes the discovery of novel antibiotics?

Antibiotic discovery has slowed to a crawl and failed to keep up with the emergence of drug resistant pathogens. The three key barriers that contribute to the slow pace of novel antibiotic discovery have been discussed below [43],[48],[49]:

(i) **Regulatory barriers**: Although very few pharmaceutical companies are currently known to venture into novel antibiotic discovery, the regulatory barriers act as one of the major obstacles in the paths of very few who are willing. The difficulties in obtaining approval for new antibiotics, challenging design of clinical trials as approved by the Food and Drug Administration (FDA), the need for larger sample sizes and the high costs involved in carrying out clinical trials, make antibiotic discovery unattractive to the companies [48].

(ii) **Economic barriers**: Antibiotics are taken for a shorter duration of time in contrast to the drugs used to treat chronic infections such as diabetes, asthma and cholesterol. Also, the new antibiotics that are discovered are not immediately brought into the clinics and are in fact held by the doctors to be used as a last resort. Both these reasons are responsible for the extremely low returns on the investments made by the pharmaceutical companies, which refrains them from indulging into antibiotic discovery [48]. Antibiotic discovery and research both in academia and industry has suffered a setback due to the lack of funds to pursue the same.

(iii) **Scientific barriers:** It is the most significant and fundamental barrier which impedes antibiotic discovery. In depth knowledge of basic and fundamental science is needed to sustain the drug discovery efforts. Due to poor profit margins and low returns, the pharmaceutical companies have withdrawn themselves from research and development of newer antibacterial agents [48]. This has led to an increased burden on the shoulders of the academicians who alone aren't fully capable to overcome the discovery barriers. An interdisciplinary and concerted plan for novel antibiotic discovery needs to be taken in collaboration with industries [49]. Nonetheless, the task of finding the mechanism of action of novel antibacterials discovered in whole cell screening assays is especially daunting for the researchers since it requires both scientific expertise and economic support [50].

Considering the fact that Gram negative pathogens predominate the list of antibiotic resistant priority pathogens, as laid down by the WHO; it is imperative to discover novel antibacterials against them. However, this has been really challenging since the Gram negative bacteria harbour several intrinsic resistance mechanisms such as the presence of the lipopolysaccharide (LPS) containing outer membrane, which acts as a permeability barrier and is absent in the Gram positive pathogens (Fig. 2.3) [43]. The Gram negative outer membrane is an asymmetric lipid bilayer which slows down the passive diffusion of antibiotics across through it. Moreover, the LPS hosts a large number of porins which are responsible for active drug uptake and wide variety of efflux pumps that exclude antibiotics from reaching their cellular targets[51]. The Gram negative permeability barrier needs to be the focus of all the drug discovery screening programs and is one of the major reasons why target based approaches have failed to yield any novel antibacterial leads [49].

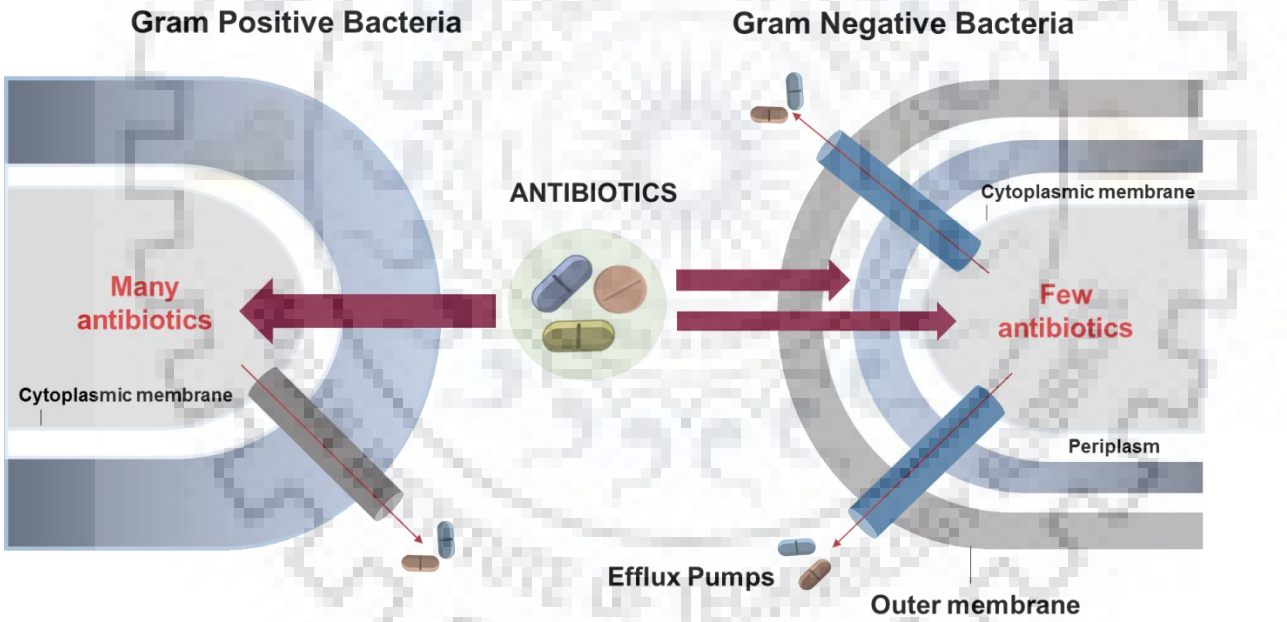

Figure 2.3: The Gram negative permeability barrier impedes antibiotic discovery. In contrast to the Gram positive bacteria, Gram negative bacteria consist of a complex outer membrane and several multidrug efflux pumps that restrict antibiotic entry and cause enhanced expulsion.

2.5 Mechanistic basis of antibiotic resistance

Bacterial cells evade killing by antibiotics by employing a repertoire of sophisticated mechanisms which they seem to have acquired over the span of millions of years (Fig. 2.4). The four major mechanisms of antibiotic resistance have been discussed below [52], [53]:

2.5.1 Antibiotic inactivation

Resistant bacteria express various enzymes that may inactivate the antibiotics even before it is able to bind to its target. These enzymes may work through the mechanism of hydrolysis, group transfer or redox mechanisms. Beta lactamases are the examples of hydrolytic amidases that cleave the b-lactam ring of the penicillin and cephalosporin antibiotics [54]–[57]. The enzymes known as esterases are responsible for macrolide antibiotic resistance while epoxidases lead to fosfomycin resistance [58]–[60]. The antibiotics aminoglycosides, chloramphenicol, macrolides and rifampicin undergo inactivation by group transfer enzymes that cause substitution with adenylyl, phosphoryl or acetyl groups etc [61]–[66].

2.5.2 Target modification or bypass

Target site modification is the second most favoured resistance mechanism after enzyme inactivation. The presence of mutations in the penicillin-binding proteins (PBPs), which are the essential proteins of cell wall synthesis, decreases their affinity to beta lactam antibiotics [67]–[69] Resistance to the macrolide and aminoglycoside class of antibiotics occurs through modifications in 23S rRNA and 16S rRNA respectively [70]–[74]. Fluoroquinolones resistance is known to occur through mutations in the binding sites of replication enzymes, DNA gyrase and topoisomerase IV [75], [76]. Bacteria might also develop an alternative pathway to overcome the need for a functional enzymes or it may overexpress their targets causing antibiotic sequesteration, for example in case of sulfonamide and vancomycin resistance respectively.

2.5.3 Activation of efflux pumps

Drug efflux is a major mechanism of resistance in both Gram-positive and Gram-negative bacteria. Resistant microbes maintain their normal physiology by effluxing out toxins, salts, heavy metal, antibiotics and biocides [77]. Efflux pump may be single component or multicomponent, latter being more prevalent in Gram negatives [78], [79]. The six major families of efflux pump comprises of the ATP-binding cassette (ABC) superfamily; the major

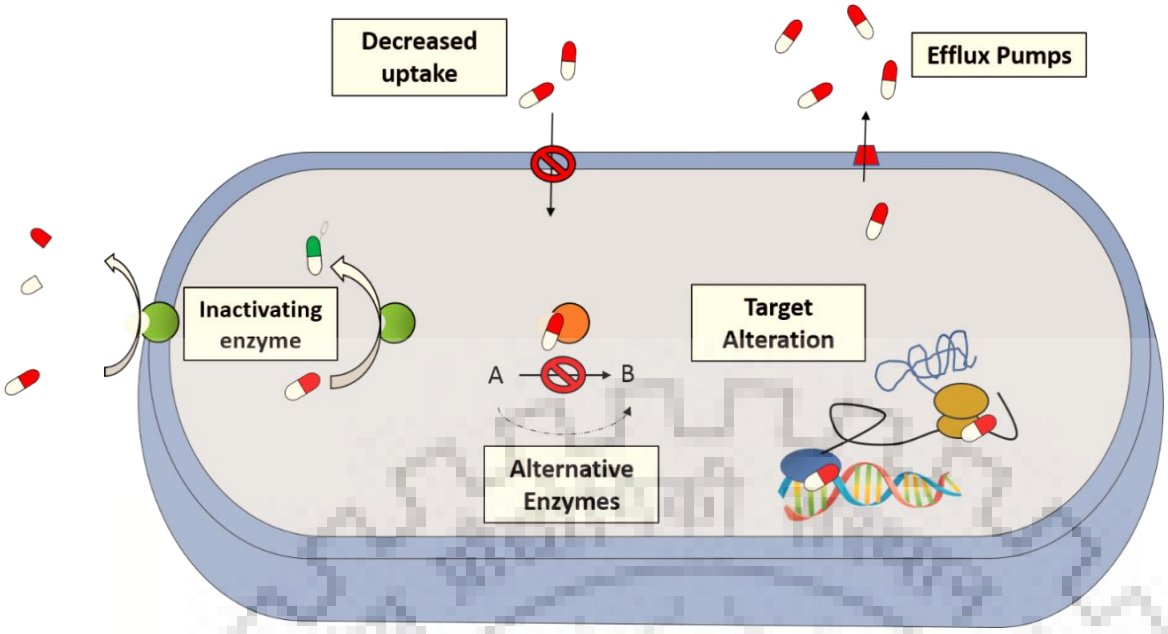

Figure 2.4: Molecular mechanisms responsible for antibiotic resistance in bacteria.

facilitator superfamily (MFS); the Multidrug and toxic compound extrusion (MATE); the small multidrug resistance (SMR) family; the resistance-nodulation-division (RND) superfamily; the drug metabolite transporter (DMT) superfamily [80]. Among the clinically important strains, RND pumps are most common in Gram negatives and are typically composed of a transmembrane protein, periplasmic protein and an outer membrane protein. The *E. coli* efflux pump, AcrAB-TolC system is the classical example of RND family efflux pump, which comprises of the inner membrane transporter (AcrB), periplasmic linker protein (AcrA), and outer membrane protein channel (TolC) [81]**.** RND pumps have broad substrate specificity and can transport antibiotics such as fluoroquinolones, chloramphenicol, β-lactams, tetracyclines and novobiocin [82]. In Gram positive bacteria, single component pumps of the MFS family are more common and cause efflux of tetracycline, fosfomycin etc. [82].

2.5.4 Decreased Outer membrane (OM) permeability

The outer membrane acts as a permeability barrier owing to its intricate and complex architecture which limits the passive diffusion of antibiotics. The downregulation of porin proteins and upregulation of efflux pumps present on the outer membrane further contribute in keeping the antibiotic concentration within the cells at a low level. Resistant bacteria display changes in the size, specificity, copy number of porins which ultimately affects the rate of antibiotic diffusion [83], [84]. Beta lactams, fluoroquinolones and chloramphenicol are examples of few antibiotics that use porins to gain entry into the Gram-negative outer membrane [85]. The porins OmpF, OmpC in *E.coli* and OprD in *P. aeruginosa* have been implicated to cause porin mediated antibiotic resistance [86], [87].

2.6 Biofilms as reservoirs of antibiotic resistance

Biofilms are communal structures of microorganisms concealed in an autogenic polymeric matrix made up of polysaccharides, proteins and extracellular DNA [88]. These surface attached microbial communities are responsible for more than 65% of human infections and have emerged as a major public health concern [89]. Owing to their high population densities and cellular proximity, biofilms act as a barrier to antibiotic diffusion and are notoriously difficult to eradicate [90]. Hence, high resistance of biofilm-associated infections to antibiotic therapy is one of the biggest clinical challenges. Biofilms also catalyse the exchange of genetic material among bacterial species serving as reservoirs of antibiotic resistance [91].

The biofilm communities are built in specific, defined steps that allow intense cellular interactions such as cell–cell communication and horizontal gene transfer [92]. The developmental stages of biofilm formation have been well scrutinized and concluded to consist of the following key stages (a) initial reversible attachment to a surface (b) irreversible attachment and micro-colony formation (c) formation of a three dimensional biofilm structure and (d) biofilm maturation followed by detachment and dispersal (Fig. 2.5) [93]. Biofilms are ubiquitous in nature comprising of either homogenous or heterogeneous bacterial populations in close proximity within the extracellular matrix. The Extracellular Polymeric Substances (EPS) matrix mainly comprises of exopolysaccharides that immobilize the biofilm cells, keeping them in long-term close proximity. Apart from EPS, the matrix is composed of carbohydrate-binding proteins followed by pili, flagella, adhesive fibers and extracellular DNA that provides a stabilizing platform for complex three dimensional biofilm architecture [94] [95]. In many Gram-negative bacteria, cyclic di-GMP (c-di-GMP) is a major intracellular signalling molecule involved in this process that promotes production of biofilm matrix and has been extensively implicated in the shift between sessility and motility in bacteria [95]. Cell to cell communication system known as quorum sensing (QS) also plays critical role in the maturation stage of biofilm formation. It regulates cell differentiation and development of biofilm structures. Cells in a biofilm produce and release QS signaling molecules that are used for intraspecies as well as interspecies communication. Several major types of QS systems such as N-acyl-homoserine lactone (AHL) systems and AI2/LuxS systems have been characterised in bacteria [96].

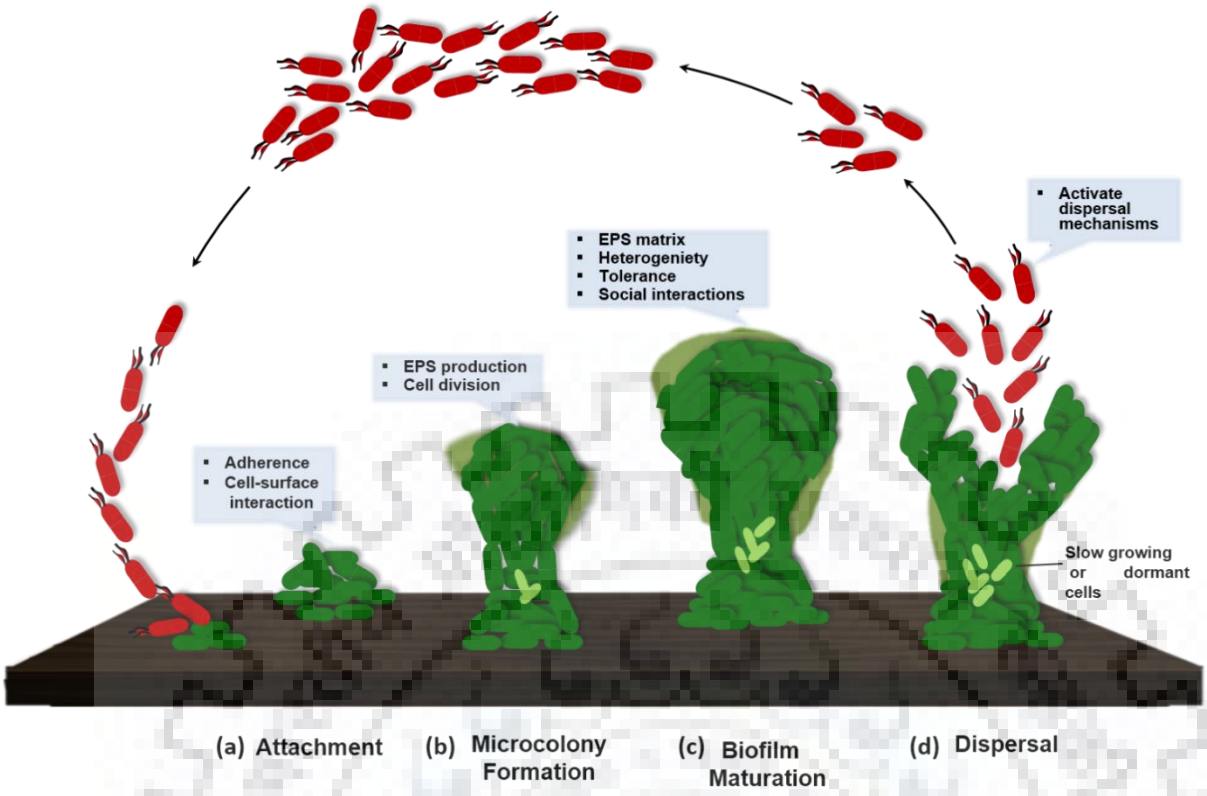

Figure 2.5: Stages of Biofilm formation: Biofilm formation is a complex multi-step process. The different stages of biofilm formation include (a) reversible attachment to the surface followed by (b) irreversible attachment (c) formation of microcolonies through extracellular matrix production and (d) formation of a mature three-dimensional biofilm architecture. Mature biofilms then disintegrate and distribute planktonic cells to new sites of infection in the human host.

2.6.1 Mechanism of resistance to antibiotics by biofilms

Pathogenic bacteria within the biofilm milieu employ both tolerance and resistance mechanisms to withstand antibiotic challenge. Resistance of bacterial biofilms to various classes of antibiotics and other antimicrobial agents is an acquired property of the bacterial cells in which the genetic makeup of cells changes either by mutations or integration of foreign DNA [90]. This bestows upon the cells, the ability to survive in the presence of high concentration of antibiotics (otherwise lethal for sensitive cells) even after the cells are dispersed from the EPS matrix. Tolerance, on the other hand, is the characteristic specific to biofilm, and is lost once the bacterial cells detach from EPS matrix. Based upon the evidence gained from the recent studies, the mechanisms by which biofilm associated bacteria survive in the presence of antibiotics and biocides are described as below (Fig. 2.6).

2.6.1.1 Extracellular polymeric substance (EPS) matrix as a diffusion barrier

The components of the extracellular polymeric substance (EPS) matrix act as plausible barrier for the penetration of antimicrobial agents and is known as the diffusion inhibition reaction in biofilms [97]. Glycocalyx, the extracellular polysaccharide containing structure is an integral part of biofilms and serves as one of the distinguishing features in antibiotic tolerance. It varies in thickness from 0.2-1μm and can accumulate antibiotic molecules up to 25% of its weight. The exoenzymes on the glycocalyx surface also inhibit diffusion and inhibition by antibiotics such as the presence of beta-lactamases on the *P. aeruginosa* glycocalyx [98]. Alginate, a major component of the mucoid biofilm produced by *Pseudomonas sp.,* is the primary antibiotic binding entity that limits the availability of aminoglycosides (tobramycin) to bacterial cells inside the biofilm [99].

2.6.1.2 Resistance gene dissemination by horizontal gene transfer

High cell density, increase in genetic competency, accumulation of eDNA and a physical environment favouring cell to cell contact enhances the uptake of antibiotics resistance genes between cells by horizontal gene transfer [100][101]. A common mechanism of horizontal gene transfer is via plasmid conjugation, for example, plasmids with antibacterial resistance genes readily transfer between the cells of *E. coli* and *Pseudomonas putida*. Conjugation has been shown to be 700-fold more favourable in biofilms as compared to free-living planktonic bacterial cells [102]. Type VI secretion system (T6SS) is also responsible for horizontal gene transfer in *Vibrio cholerae* biofilms. The T6SS machinery causes lysis of the neighbouring cells and uptake of DNA by natural competence [103].

2.6.1.3 Starvation and dormancy induced antibiotic tolerance in biofilms

Limitation of nutrient in the biofilm leads to slow growth rate, starvation of bacterial cells and metabolic dormancy that contributes to antimicrobial tolerance [104]. In biofilms, the number of bacterial cells in stationary phase significantly increases and so does their tolerance to antibiotics which rely majorly on metabolic activity of the cell for their action [105]. For instance, mature biofilms are less susceptible to antibiotic vancomycin [106]. Slow growth rate leads to one of the possible dormancy states of non-sporulating bacteria that is, viable-but-non-culturable state

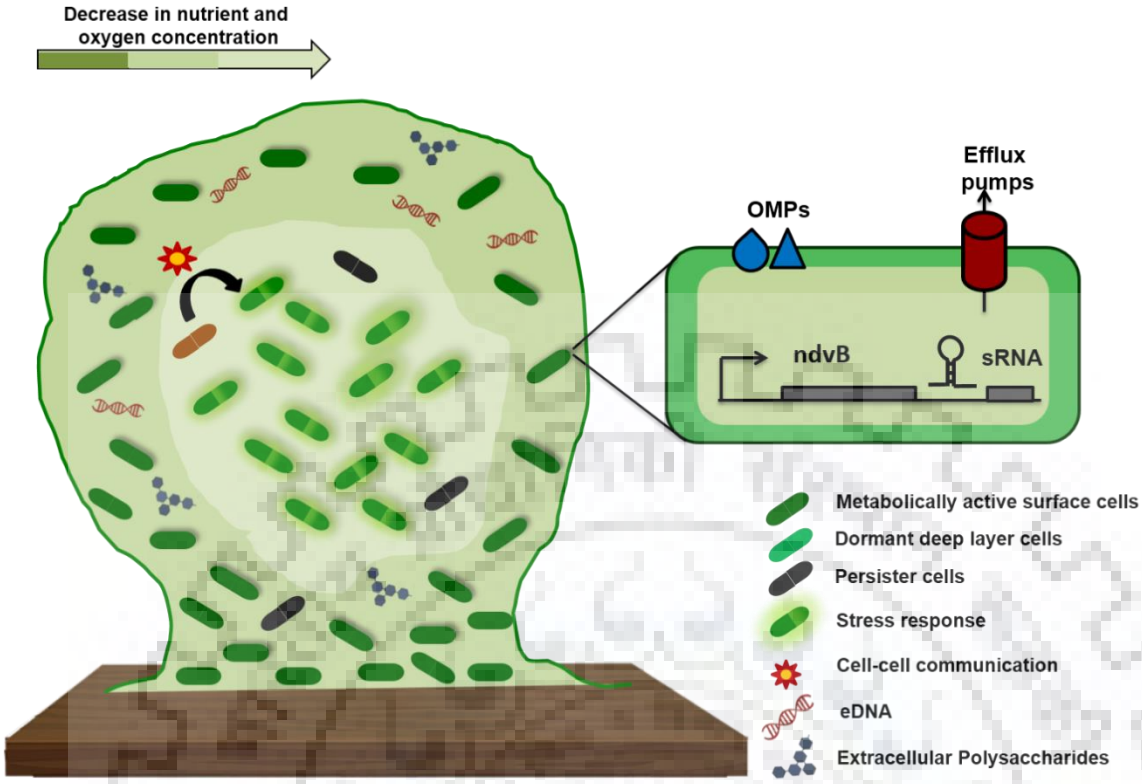

Figure 2.6: Major antibiotic resistance and tolerance mechanisms employed by bacterial biofilms. Biofilm cells (dark green) embed themselves in a mushroom-shaped matrix (shown in light green) and the biofilm attaches to a biotic or abiotic surface (brown rectangle). The various resistant mechanisms depicted in the figure are as follows : (1) nutrient gradient such that the biofilm core has less nutrient availability, (2) matrix exopolysaccharides, (3) extracellular DNA, (4) oxidative stress response and stringent response etc., (5) overexpression of multidrug efflux pumps and outer membrane proteins, (6) intercellular interactions (horizontal gene transfer, quorum sensing, multispecies communication etc.), (7) expression of biofilm specific genes and non-coding small RNAs and (8) presence of persister cells. Adapted and modified from [100].

(VBNC state). VBNC is a state of dormancy in which the organism fails to grow in rich media, while retaining viability parameters such as respiration, presence of rRNA and plasma membrane integrity [107]. The VBNC state of several pathogens such as *E. faecalis*, *S. epidermidis*, *Helicobacter pylori*, *Mycobacterium tuberculosis* and *H. influenza* has been found to be resistant to several antimicrobials [108].

2.6.1.4 Persister formation within biofilms

Biofilms contain a small fraction of bacterial population called "Persister cells" that survive antibiotic attack by shutting down their cellular targets [109]. Persister cells are a major culprit that account for the recalcitrance of biofilm associated infections *in vivo* and for their relapsing nature [110][111]. Persister cell formation has been linked to the actions of toxins, such as RelE and MazF, from toxin-antitoxin (TA) modules [112]. *E. coli* RelBE is one of the best studied TA module and cells expressing RelE from an inducible promoter display high tolerance to antibiotics - ofloxacin, cefotaxime and tobramycin [113]. Ectopic expression of other toxins such as MazF and HipA are also known to produce persistent cells in biofilms [114].

2.6.1.5 Quorum sensing

Quorum sensing (QS) is a cell-cell communication process that bacteria utilise to monitor changes in cell-population density and control group behaviours such as biofilm formation and virulence factor production. The QS system involves production, detection, and response to extracellular signalling molecules called autoinducers such as acyl homoserine lactone (AHL). Quorum sensing facilitates proper development of EPS matrix architecture and antibiotic resistance [115]. In *P. aeruginosa*, the expression of superoxide dismutase and catalase is regulated by quorum sensing AHL, which makes the cells resistant to oxidative stress in biofilms [115].

2.6.1.6 Efflux pumps

Multidrug resistance efflux pump are involved in resistance to metabolic active cells in biofilm [116]. Efflux pumps transport Homoserine lactone (HSL) across the cytoplasmic membrane. Studies in *P. aeruginosa* and *A. baumannii* involving the efflux pump mutant strains showed decrease in biofilm formation [117] [118]. In entero- and uropathogenic strains of *E. coli*, AcrAB-TolC is the most commonly found Multidrug Resistance (MDR) pump [119]. The protein TolC that act as outer membrane protein for AcrAB pump, aids in adherence of bacteria onto human epithelial cells (HEp-2) and in formation of biofilms [120]. AcrAB-TolC are also involved in bacterial colonization and persistence [77]. In *E. coli*, deletion of six genes coding for proton pumps, i.e. *emrD, emrE, emrK, acrD, acrE* and *mdtE* was shown to display decreased biofilm formation [121].

2.7 Persisters as evolutionary reservoirs of antibiotic resistance

Bacterial persisters were originally reported by Joseph Bigger in 1944 in a penicillin treated culture of *Staphylococcus aureus* [122]. Persister cells represent a phenotypically tolerant subpopulation of bacteria that survive exposure to lethal doses of antibiotics without undergoing any genetic changes. These specialised survivor cells are known to be the main culprits for the recalcitrant nature of chronic infections. *Mycobacterium tuberculosis*, *Salmonella typhimurium Burkholderia pseudomallei*, *Pseudomonas aeruginosa* and *Staphylococcus aureus* are examples of few pathogenic bacteria that have been associated with the occurrence of chronic recalcitrant infections [34].

As discussed previously, biofilms have a major role to play in chronic infections and this can be much attributed to their ability to harbour bacterial persister. However, persister populations are not only restricted to biofilm environment and might cause recalcitrant infections within the immunocompromised host such as those suffering from HIV infection or undergoing chemotherapy [123]. Not only this, persister cells can also persist within the immunocompetent host at sites where they could evade the immune system such as the central nervous system (eg. *Meningococcus* causing meningitis) and gastrointestinal tract (e.g. *Helicobacter pylori* causing gastroduodenal ulcers) [124].

Apart from being a threat to clinical therapy due to their antibiotic tolerance phenotype, persisters also have been implicated to accumulate genetic mutations thereby evolving to form resistant bacterial populations. Most studies describe persister cells to exhibit a state of dormancy and their ability to survive antibiotic exposure has been attributed to their 'target inactivation' phenotype [122], [125]. This severely limits the treatment options against them, since most of the discovered antibiotics act on active cellular targets such as DNA, RNA or protein synthesis *etc* [126]. However, the phenomenon of dormancy associated to persisters has been the subject of controversy and recent studies have shown persisters to harbour active mechanisms such as drug efflux [127].

The following passive and active mechanisms responsible for the occurrence and formation of persister cells within a population are as follows:

2.7.1 (p)ppGpp

Cells respond to stress by regulating the levels of an intracellular messenger (p)ppGpp which is an alarmone of the bacterial stringent stress response [128]. The levels of the regulatory nucleotide (p)ppGpp in the bacterial cells are controlled by the catalytic activity of enzymes RelA and/or SpoT in response to various environmental stresses such as nutrient limitation, heat shock, amino acid deprivation etc [129]. With respect to the persistence phenotype, cells expressing (p)ppGpp display low level of DNA replication, transcription as well as inhibit the cell division machinery [130]. Persistence to fluoroquinolones and beta lactams is known to occur by increased (p)ppGpp levels which inhibits DNA replication [131].

2.7.2 Toxin/Anti-toxin (TA) systems

Several (TA) systems are known to form the genetic basis of bacterial persistence. The TA system comprises of two genes encoded in an operon where the Anti-toxin (AT) molecule inhibits its complementary toxin (T) under normal growth conditions, but undergoes degradation under stressful environments. This leads to increased Toxin levels which ultimately inhibit important cellular processes such as replication or translation and arrests the growth of cells [132]. The toxins TisB and HokB induce persistence by forming pores thereby causing membrane depolarisation and a decreased proton motive force [133], [134]. The toxin TisB is upregulated as a result of DNA damage upon exposure to fluoroquinolone antibiotics [135]. The toxins YafQ and RelE bind to the 50S and 30S ribosomal units and act by inhibiting translation [136]–[139]. Toxins such as MazF and MqsR indirectly inhibit ribosome assembly by causing mRNA cleavage [140], [141]. The PasT toxin on the other hand, binds to the 50S subunit and directly inhibits 70S ribosome assembly [142]. A few toxin effectors such as HipA inhibit translation by targeting the tRNA. HipA phosphorylates the serine residue of tRNA synthetase and triggers (p)ppGpp formation which in turn induces persistence to β-lactam antibiotics [143], [144].

2.7.3 Indole: the signalling molecule

The signalling molecule indole has been shown to play an important role in bacterial persistence. Indole is formed within the bacterial cell by the enzyme tryptophanase which is

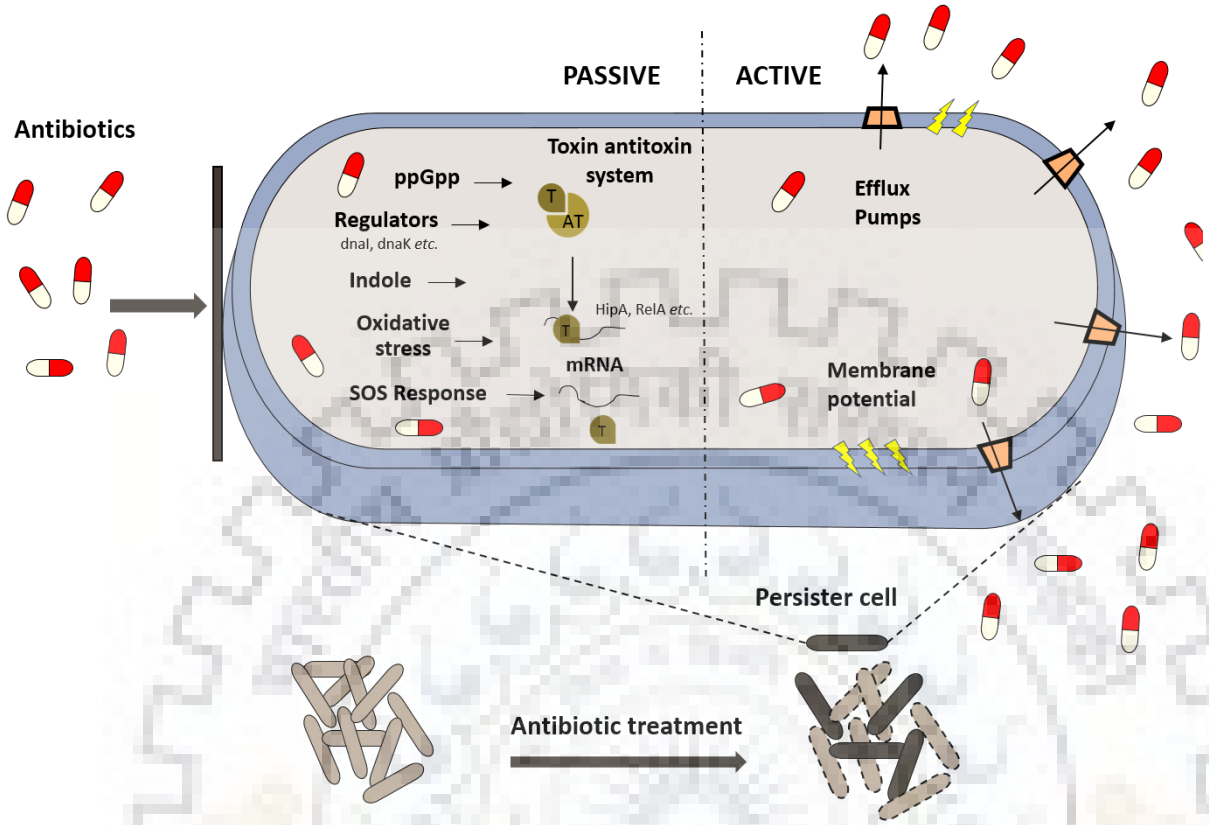

Figure 2.7: Molecular mechanisms facilitating antibiotic persistence in bacteria. Dormancy in persiters can be regulated by Toxin/Antitoxin modules released following signals from ppGpp and indole or in response to global regulators, oxidative stress, and the SOS response. Persister cells also harbor active efflux mechanisms and exhibit decrease in membrane potential.

encoded by the TnaA gene and acts upon the substrate tryptophan. The YafQ toxin of the YafQ/DinJ T/A system has been implicated to cleave the TnaA transcripts thereby reducing indole levels and inducing persistence.

2.7.4 Genes involved in cellular metabolism

Several genes that regulate the energy metabolism of bacteria have been reported to play an important role in regulating its persistence state. Some of these genes are (i) *phoU* gene of the phosphate uptake system *pstSCAB*, (ii) *ubiF* gene responsible for ubiquinone biosynthesis (iii) *sucB* gene of the tricarboxylic acid cycle pathway, (iv) *plsB* (*sn*-glycerol-3-phosphate acyltransferase) gene which regulates phospholipid metabolism and is required for persister

maintenance and (v) *glpD* (*sn*-glycerol-3-phosphate dehydrogenase) which encodes for the first step of the glycerol degradation pathway.

2.7.5 Global regulators/ other genes

Several heat shock proteins and genes involved in regulating the lipid metabolism also have been shown to regulate and maintain the persistence phenotype. For example, the heat shock protein DnaJ and lipid A biosynthetic protein PmrC from the Gram negative pathogen *S. enterica* serovar Typhimurium. The molecular chaperone DnaK in association with DnaJ and GrpE is also known to play an important role in persister maintenance by regulating the heat shock proteins and sigma factors σ^{32} and σ^{S} of the general stress response pathway.

2.7.6 Active Efflux mechanisms

Apart from exhibiting dormancy, persister cells are known to exhibit active mechanisms such as overexpression of the efflux machinery, that help them survive lethal antibiotic exposure. *E. coli* persisters were reported to upregulate their efflux mechanisms such as the AcrAB–TolC efflux pumps, leading to a reduced intracellular concentration of beta-lactam antibiotics [127].

2.7.7 The SOS response

The SOS response in bacteria is induced mainly in response to DNA damage and other stresses such as oxidative stress, antibiotic exposure or a due to a block in DNA replication [145]. The RecA protein is the major player that induces the SOS regulon which comprises of a battery of regulatory genes [145]. The TisB/TisR T/A module has been shown to undergo activation by the SOS response and lead to enhanced persistence against fluoroquinolone antibiotics [135]. The SOS-dependent DNA repair mechanisms have also been held responsible for resuscitation of *E. coli* persisters following exposure to fluoroquinolones. *E. coli* mutants deficient of the genes that form the SOS regulon have been observed to exhibit a low persister frequency. SOS-deficient mutants usually exhibit a considerable drop in the number of surviving persisters, particularly upon treatment with DNA-damaging agents [135], [146]–[149].

2.8 Novel antibiotic targets to overcome resistance: Thinking outside the box

The current pace of novel antibiotic discovery has inadvertently failed to equate the rate of emergence of resistance bacteria in the clinic, thus emphasizing the need for alternative strategies. Most antibiotics discovered so far act on single targets or enzymes and inhibit the three most essential pathways of the bacterial cell, i.e. the synthesis of DNA, RNA and proteins apart from the cell wall synthesis machinery. These single targeting antibacterials are prone to extreme selection pressures and readily undergo mutations to accumulate resistance. For example, as observed in the case of vancomycin and rifampicin antibiotics. Hence, it is imperative to look for alternate treatment strategies and more importantly discover novel cellular targets which are under the least predisposition of acquiring resistance.

One such promising strategy is to target the non-essential bacterial processes which are not crucial for its growth and survival but might become essential under stressful environments or at infection sites within the host (Fig. 2.8). These non-essential processes may be least subjected to resistance accumulation and thus would serve as ideal targets for antibiotic therapy. A few examples of these targets/processes would be the bacterial quorum sensing machinery, secretory systems, targets regulating persistence, toxin or virulence factor production, cell adhesion and genes encoding regulatory small RNAs or riboswitches. Some of these strategies have been discussed in the sections that follow.

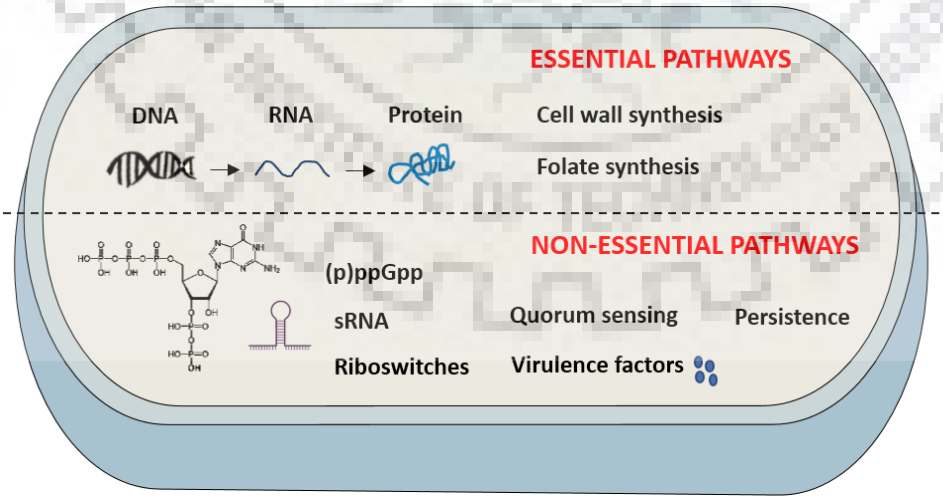

Figure 2.8: Novel targets for antibiotic discovery. Targeting the non-essential mechanisms of in bacteria such as quorum sensing, persister formation, virulence factor production, small RNA regulation etc. can be a viable approach to overcome drug resistance.

2.9 Mitigating antibiotic resistance by Combination therapy

An alternative approach to tackle the ever increasing problem of antibiotic resistance and the high rates of attrition in novel antibiotic discovery is the use of combination therapy for the treatment of bacterial infections [12]. Combination therapy is an attractive approach that has recently garnered a lot of attention worldwide since it displays the ability to revive the efficacy the old and existing antibiotics, which have been discarded due to the occurrence of resistance against them [13]. Since drugs in combination act on multiple cellular targets, combination therapy can help to overcome the rates of accumulation of resistance mutations [12]. Apart from broadening the antibacterial spectrum of a molecule, combination therapy also showcases the power of overcoming the toxicity related issues of some molecules, when administered as a monotherapy.

The antibiotic combination therapy is also commonly referred to as the antibiotic- adjuvant therapy where the adjuvant molecule could be an antibiotic or a nonantibiotic which improves the efficacy or overcomes the resistance mechanisms responsible for antibiotic failure [150]. The resistance mechanisms targeted by combinatorial therapy may include overexpression of multidrug efflux pumps, antibiotic inactivating enzymes or the formation of complex biofilms that extrude antibiotic diffusion across them (Fig. 2.9).

2.9.1 Antibiotic-antibiotic combinations

The most classical example of antibiotic combination therapy that has been used in clinics since 1968 is Trimethoprim-sulfamethoxazole combination which is extensively used for the treatment of urinary tract infections and gastrointestinal infections [151]. The mechanistic basis for administering two antibiotics in combination is that they may either (i) act on different targets of the same pathway or (ii) multiple targets of different pathways. The combination of Trimethoprim-sulfamethoxazole falls in the former category where both the molecules target the folic acid biosynthesis pathway but target different enzymes namely dihydropteroate synthase (target for sulfamethoxazole) and Dihydrofolate reductase (target for trimethoprim). A recent example of the inhibition of different targets within the same pathway is the combination of the natural product tunicamycin and β-lactam antibiotics such as oxacillin [152]. Tunicamycin was

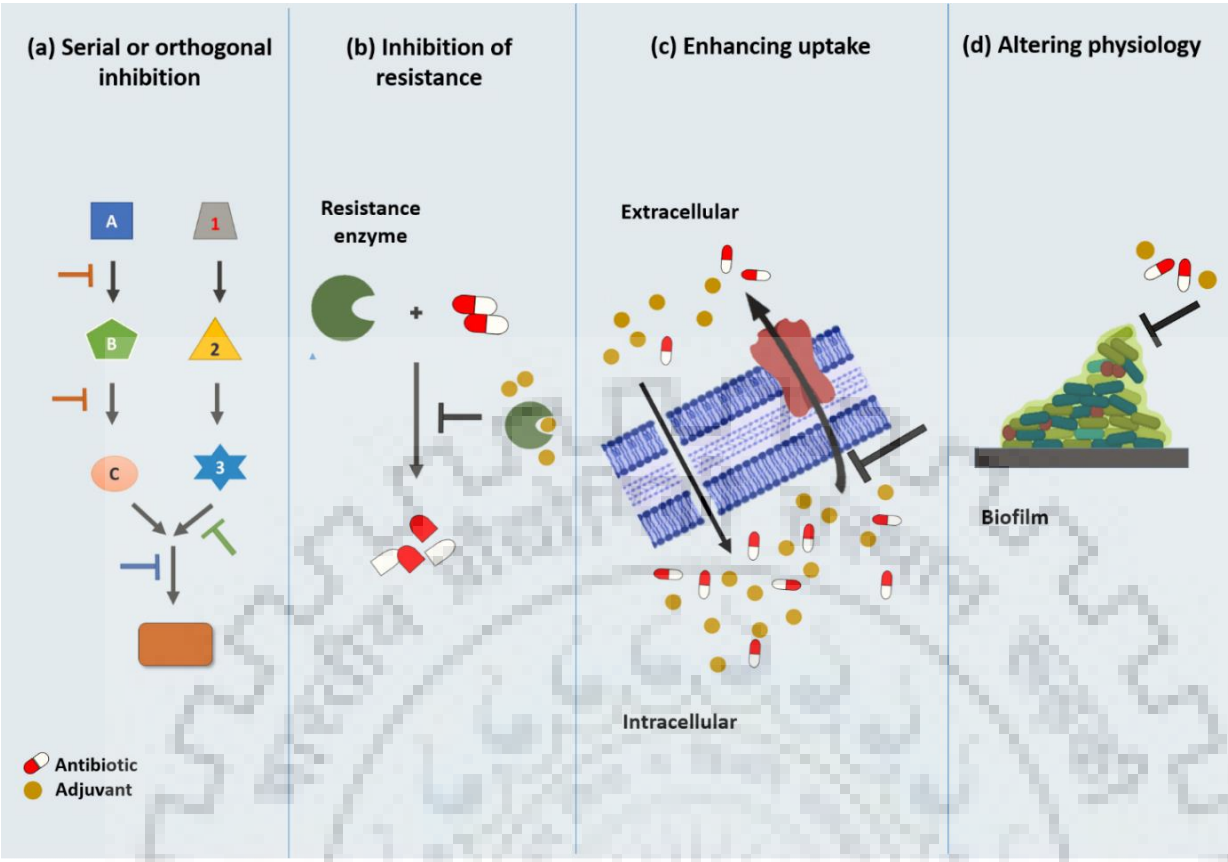

Figure 2.9: The antibiotic-adjuvant therapy can act through several mechanisms. (a) Synergistic activity between two compounds through serial or orthogonal inhibition of essential cellular pathways. (b) Inhibition of resistance enzymes that degrade or modify antibiotic to an inactive form. (c) Molecules that inhbit antibiotic efflux or cause enhanced antibiotic uptake (d) Compounds that can disperse or disrupt biofilms thereby increasing their susceptibility to antibiotics. Adapted from [153].

observed to be an inhibitor of cell wall teichoic acid in Gram positive bacteria and improved the efficacy of cell wall inhibiting antibiotic oxacillin in beta lactam resistant strains of *S. aureus* [152]. The combination of isoniazid, rifampicin, ethambutol and pyrazinamide which is widely used to treat *M. tuberculosis* infections is an example of antibiotic combination which acts on multiple pathways [154].

Antibiotic combinations might also act on orthogonal pathways such that in combination, one antibiotic potentiates the activity of the other [153]. The combination of the β-lactam antibiotic, penicillin and aminoglycoside class of antibiotics is one such example where the defective cell wall synthesis induced by penicillin has an orthogonal impact on the entry of aminoglycosides, thus potentiating its activity [155].

2.9.2 Antibiotic-adjuvant combinations

Adjuvant is an enzyme inhibitor or metal ion chelator: The clinically used combination of amoxicillin and clavulanic acid commonly known by the name augmentin is the most classic example of antibiotic-adjuvant combinations where clavulanic acid acts as an inhibitor of the enzyme, beta lactamases [156]. Other recently approved FDA drug combinations such as ceftazidime-avibactam and meropenem-vaborbactam against resistant Gram positive and Gram negative infections, also belong to the same category [157]. A natural product metallo-beta lactamase inhibitor, AspergillomarsamineA was recently discovered in a high throughput screen which inhibits NDM-1 producing *Klebsiella pneumoniae* strains by the mechanism of zinc chelation [158].

Adjuvant is an Efflux Pump Inhibitor (EPI): Efflux pump inhibitors can be used as adjunct molecules that can potentiate the activity of existing antibiotics by increasing the effective antibiotic concentration within the cell. Celecoxib, a nonsteroidal anti-inflammatory drug (NSAID) non antibiotic was recently reported to inhibit the MDR1 efflux pump of *S. aureus* making it sensitive to broad spectrum of antibiotics such as chloramphenicol, kanamycin, ciprofloxacin and ampicillin [159]. IITR08027, a recently discovered inhibitor of the AbeM efflux pmp of *A. baumannii* resensitises it to fluoroquinolone class of antibiotics [160].

Adjuvant is a membrane permeabiliser: Molecules that can permeabilise the Gram negative outer membrane can also be used as adjuvants in antibiotic therapy. SPR741, an antimicrobial peptide with poor antibacterial activity against Gram negative pathogens but permeabilises Enterobacteraceae and A. *baumannii* to rifampicin, fusidic acid clarithromycin [161]. SPR741 has successfully completed Phase I clinical trials recently [162].

Adjuvant is a Quorum Sensing Inhibitor (QSI) or disrupts preformed biofilms: The compound, meta-bromo-thiolactone (mBTL) inhibits two quorum sensing receptors in *P. aeruginosa*, LasR and RhlR thus inhibiting biofilm formation and virulence factor (pyocyanin) production [163]. Furthermore, preformed biofilms can be disrupted by the use of enzymes that degrade the quorum signaling molecule, AHL lactonase (AHLase). Recombinat lactonase from *Geobacillus kaustophilus* has been shown to disrupt preformed *A. baumannii* biofilms causing quorum quenching [164].

The most commonly used method to identify the type of interactions between two compounds in any drug combination screens is the checkerboard method [165],[166]. In this assay, both the drugs/compounds are individually diluted along the two axis of the plates such that each of the wells have a unique combination of concentration of the two agents. The effect of the two compounds in combination is compared to their individual effects in order to determine their efficacy. Fractional inhibitory concentration index (FICI) defined as the sum of the effective concentrations of the two compounds divided by the sum of the individual concentrations at their Mininum Inhibitory Concentration (MIC) when administered individually are calculated and represented in the form of an isobologram (Fig. 2.10) [166]. The FICI values are calculated by the formula:

$$FICI = FIC\text{-}A + FIC\text{-}B$$

where FIC, fractional inhibitory concentration; FIC-A, MIC of drug A in the presence of drug B divided by MIC of drug A alone; FIC-B, MIC of drug B in the presence of drug A divided by MIC of drug B alone. FICI value of <0.5indicate synegy, FICI > 0.5 indicates additive interaction or indifference and FICI > 4 denotes antagonistic interaction [166].

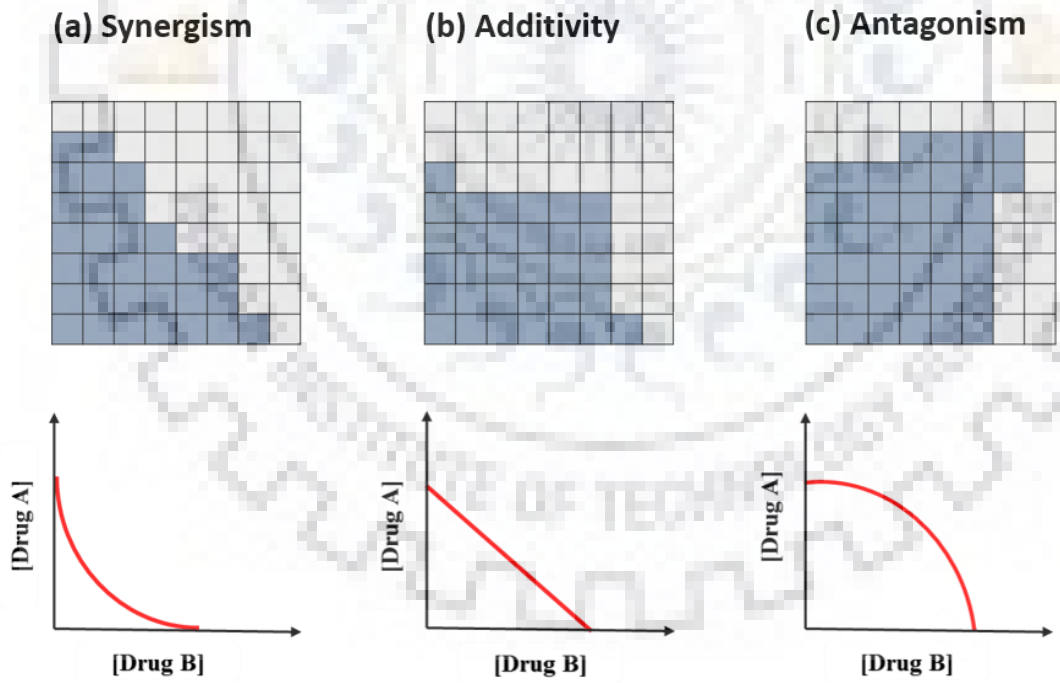

Figure 2.10: Representative isobolograms of the interaction between two compounds in a drug combination screen. The abscissa and ordinate represent the concentration of individual agents, and the the points plotted indicate the combination of concentrations of the two treatments required to reach a particular fixed effect e.g. growth inhibition. A concave curve indicates synergy, a convex curve denotes antagonism and a straight line represents an additive interaction or indifference.

2.10 Strategies for treatment of Biofilm associated infections

The physiological properties of biofilm confer the bacterial communities within them increased resistance to traditional antibiotic therapies. Hence, there is a dire need for the discovery of novel molecules or strategies that target both planktonic and biofilm associated cells (Fig. 2.11).

2.10.1 Aggressive antibiotic treatment regime

Biofilm infections are extremely difficult to handle in the clinical settings due to the restricted penetration of antibiotics through the matrix. Antibiotics like rifampicin, tetracycline, fusidic acid and those belonging to classes- quinolones, macrolides have higher penetration ability than β-lactams, aminoglycosides, glycoproteins and colistin. Combination of antibiotics rifampicin with fusidic acid and ciprofloxacin with vancomycin were reported to be bactericidal against Methicillin Resistant *S. aureus* (MRSA) biofilms [167]. Also, combination of azithromycin (AZM) and ciprofloxacin (CIP) has been reported to be synergistic against biofilm cells of *P. aeruginosa* [168]. Formation on indwelling medical devices such as central venous catheters (CVCs) can also be prevented by coating them with topical antibiotics. For instance, minoclycine/rifampin- coated CVCs are implanted in case of *S. aureus* catheter- related bloodstream infections [169].

2.10.2 Biofilm killing by essential oils/ Natural products

Essential oils are plant secondary metabolites with broad spectrum antibacterial activity [170]. Essential oils exert their antibacterial activity by multiple mechanisms such as inhibiting ATP synthesis and compromising membranes leading to leakage of metabolites and ions. They have also been reported to act as efflux pumps inhibitors and quenchers for quorum signaling molecules like AHLs [171]. Essential oils extracted from *Origanum vulgare*, carvacrol and thymol inhibit formation in *S. aureus* [172]. Combination between essential oils and conventional antibiotics is another strategy where essential oils are known to modify the uptake and tolerance of biofilm cells to antibiotics. Three essential oils cinnamon (*Cinnamomum zeylanicum*), tea tree oil (*Melaleuca alternifolia*), and palmarosa (*Cymbopogon martini*) have proved synergistic with the fluoroquinolone antibiotic, ciprofloxacin against established *P. aeruginosa* biofilms [173].

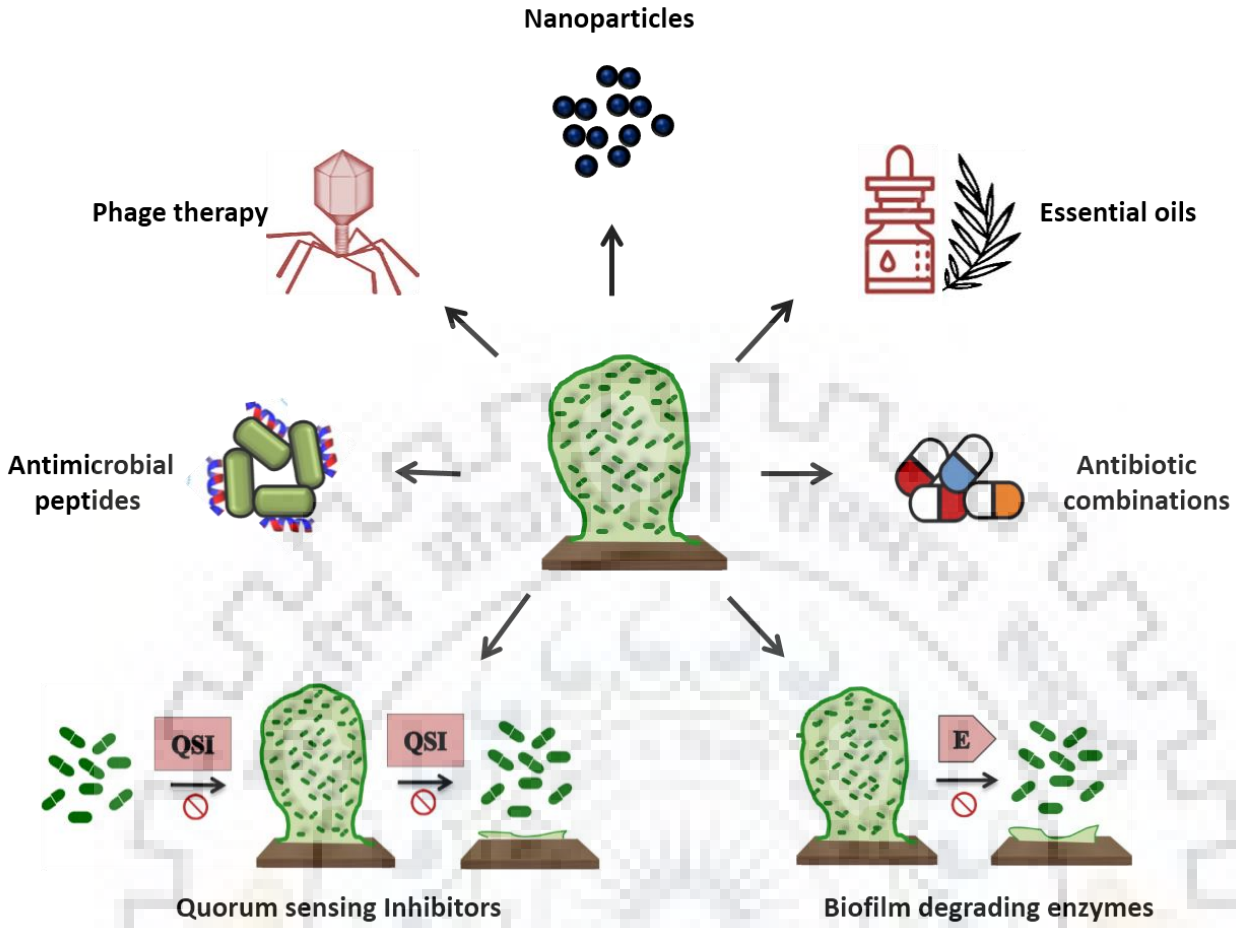

Figure 2.11: Strategies employed to tackle antibiotic resistance within biofilms

Carvacrol and thymol have also been identified to possess efflux pump inhibitory activity thus rendering the biofilm cells susceptible to otherwise ineffective antibiotics [174]. Since essential oils are multi-component in nature, they are believed to be more promising in preventing bacterial resistance.

2.10.3 Nanoparticles and their combination with antibiotics

Nanoparticles coupled with metals or natural product extracts have been shown to possess inhibitory activity against both planktonic and biofilm associated cells. NPs compromise the biofilm integrity by interacting with its polysaccharides, extracellular DNA, proteins, and lipids. Silver and Zinc oxide nanoparticles are reported to inhibit approximately 95% of *P. aeruginosa* biofilms [175],[176]. Biofunctionalized polymyxin B-capped silver nanoparticles (PBSNPs) were sythesised where PBSNPs displayed antibiofilm activity against multiple drug-resistant *Vibrio fluvialis* and *P. aeruginosa* [177].

2.10.4 Quorum sensing quenchers/Inhibitors

As discussed previously, the use of quorum sensing inhibitors or quencher molecules that weaken the biofilm architecture or its formation altogether is another promising approach (Uroz et al., 2009). Efforts to develop QS inhibitors have included screens of natural products, small molecule libraries, virtual screening, and used synthetic libraries derived from native AI structures [179]. The enzymes lactonase and paraoxonase are also known to degrade QS signals and display potential anti-biofilm strategy [180]. RNAIII-activating protein (RAP) and *arg* quorum sensing systems play important role for formation of *S. aureus* biofilms [181].

2.10.5 Antimicrobial peptides (AMP)

Antimicrobial peptides (AMPs) which are 15-30 amino acids long, positively charged peptides, produced by the innate immune represent another important approach to treat biofilms [95]. Peptides from the class cathelicidins such as BMAP-27, BMAP-28, SMAP-29 exhibit promising activity in eradication of preformed biofilms and killing of biofilm associated cells in MDR strain of *P. aeruginosa* [182]. Several *in vivo* studies have shown that combinations of nisin with daptomycin, indolicidin with teicoplanin and cecropin (1-7)-melittin-A (2-9) amide with ciprofloxacin potentiated the activity of antibiotics against biofilms [183]. However, AMPs have a few limitations such as their ability to bind to components of EPS matrix and other host molecules, which drastically reduces their effectiveness. Therefore, extensive preclinical efficacy studies are required before AMPs could be used for treatment.

2.10.6 Phage therapy

The use of bacteriophages is another strategy that is used to control and eradicate biofilms. Phage therapy takes advantage of the lytic cycle of virulent viruses that cause cell lysis, which confers them their antimicrobial activity. Staphylococcal phage K combined with another staphylococcal phage, DRA88 (MOI 10) could completely remove preformed biofilms of three *S. aureus* isolates after 48h of treatment. A filamentous phage overexpressing a repressor of the SOS DNA repair system in *E. coli* has been engineered to target metabolically inactive persister cells within biofilms [184]. Combinations of phages and antibiotics have also been tested against *S. aureus* and *K. pneumoniae* biofilms [185].

2.10.7 Matrix degrading enzymes

EPS matrix in biofilms facilitates the adhesion and protection of biofilm associated cells from antimicrobial activity of antibiotics. Therefore, use of enzymes that could inhibit and disrupt the EPS matrix formation and facilitates detachment is another approach. Various classes of enzymes, specifically proteases, deoxyribonucleases, and glycoside hydrolase have been exploited for the dispersal of medical biofilms. In *S. aureus*, ten secreted proteases have been identified till date, four of which namely SspA, SspB, ScpA, and aureolysin (Aur) have been shown to be involved in biofilm disruption [186]. Fungal strains of *Aspergillus clavatus* have also been isolated that produce enzymes- proteases, amylases and pectinases that can degrade *P. aeruginosa*, *B. subtilis* and *S. aureus* biofilms [187]. The EPS mass could also be reduced by DNase-1, dispersin B (DspB), α-amylase, while the cell number within biofilms could be controlled by the combination of enzymes with antibacterial agents [188],[189].

2.10.8 Anti-adhesion agents

A mannose analogue, mannoside M4284 has been reported to inhibit the adhesive function of type 1 pili and can be used to treat urinary tract infections (UTI) [190]. Mannosides can also be used in combination with trimethoprim- sulfamethoxazole (TMP-SMZ) against Uropthogenic *E. coli* (UPEC) isolates which were otherwise resistant to the two antibiotics [191]. Type-1 pili is an adhesive pili assembled by the chaperone/usher pathway (CUP) that plays a critical role in biofilm formation both on the host surface and for colonization of catheters and other surfaces in nosocomial settings. Pilicide compounds have been designed that bind to the chaperone and prevent pilus assembly in UPEC biofilm [95]. Curli are functional extracellular amyloid fibers produced by uropathogenic *E. coli* (UPEC) and other Enterobacteriaceae. Ring-fused 2-pyridone compounds such as FN075 and BibC6 are examples of curlicide compounds that inhibit curli biogenesis and polymerization in UPEC strains [192].

2.11 Strategies to inhibit bacterial persister cells

Bacterial persisters are seemingly dormant population of bacteria that evade the host immune response and are refractory to the action of antibiotics. Eradicating the persister populations pose a serious challenge and studies to understand the mechanisms underlying the persistence have recently been undertaken followed by the designing of appropriate strategies against them. Broadly, there are three main strategies that form the basis for most of the reported anti-persister therapies (Fig. 2.12).

2.11.1 Direct killing of persister cells

Bacterial persisters are known to exhibit a reduced metabolism and cellular dormancy such that the conventional antibiotics targeting the DNA, RNA, protein synthesis machinery fail to act. However, persisters require an intact cellular membrane to survive and therefore compounds inhibiting the bacterial membrane have been preferred candidates to be used for anti-persister therapies. SPI009 (1-((2, 4-dichlorophenethyl) amino)-3-phenoxypropan-2-ol) proved capable of directly killing non-multiplying cells of both Gram-negative and Gram-positive bacteria through extensive membrane damage [164], [165]. The essential oil carvacrol has been reported to exhibit excellent activity against both stationary phase cells and biofilms of *Borelia burgdorferi* by causing membrane disruption [195]. Art-175 is the first engineered phage endolysin to exhibit anti-persister activity against *A. baumannii* and *P. aeruginosa* [196], [197].

2.11.2 Sensitization and resuscitation of persister cells

Sensitisation of persister cells to inhibition by routine antibiotic therapy is another viable approach that has been shown to yield promising results.

2.11.2.1 Sensitisation by activation of antibiotic targets

Compounds that can activate the quasidormant state of bacterial persisters are attractive anti-persister molecules. The compound C10 and the fatty acid signaling molecule cis-2-decanoic acid have been shown to exhibit the ability to revert the persister phenotype in *E. coli* and *P. aeruginosa* cells thus rendering them sensitive to the action of antibiotics [198], [199].

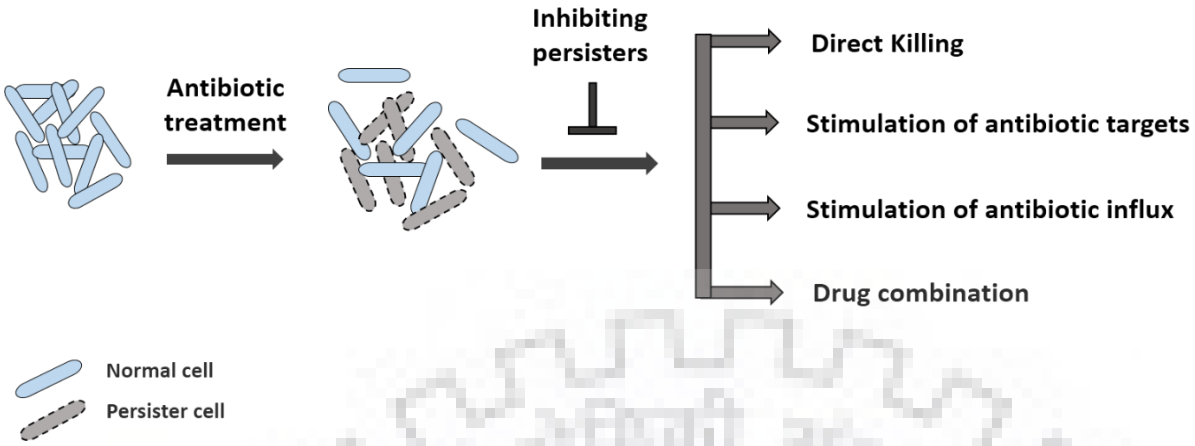

Figure 2.12: Strategies employed to tackle the problem of antibiotic persistence. While one of the strategies could be to inhibit or prevent persister cell formation, other strategies might target them by direct killing or inhibiting the determinants of persistence such as efflux pumps or by causing enhanced antibiotic uptake. Combinations of antibiotics can also prove effective against bacterial persisters.

2.11.2.2 Sensitisation by enhancing antibiotic influx

Bacterial persisters can be reverted to the antibiotic sensitive state by treating them with compounds that enhance antibiotic influx. These compounds could be metabolites, membrane permeabilisers or efflux pump inhibitors. The metabolites such as L-arginine, L-serine and mannitol have been reported to sensitise *S. aureus*, *P. aeruginosa* and *E. coli* persisters to aminoglycoside antibiotics [200]–[203]. While L-arginine acts by disrupting the membrane pH, L-Serine inhibits amino acid synthesis in persister cell. Treatment of persister cells with Silver ions is another viable strategy since they are known to cause membrane permeability and enhance antibiotic influx [204]. Since persisters exhibit active efflux mechanisms, the use of antibiotics in combination with efflux pump inhibitors such as PaβN and NMP have been shown to sensitise E. coli persisters to a broad panel of antibiotics [127]. The FDA approved calcium channel blocker, verapamil was recently reported to inhibit macrophage induced drug tolerance in Mycobacterium tuberculosis [205].

2.11.3 Combinations of conventional antibiotics to fight persistence

As discussed previously, combination antibiotic therapy is a promising approach to inhibit bacterial growth both in planktonic phase and in biofilms. Antibiotic combinations can also be exploited to target bacterial persisters. For example, the combination of daptomycin and cefoprazone was reported to inhibit both replicating and non-replicating cells of *Boreilia burgdorferi*, which is the causative agent for lyme disease [206]. Colistin in combination with gentamicin and ofloxacin inhibited persisters of Uropathogenic *E. coli* [207]. Recently, the combination of amikacin and colistin was shown to act on *A. baumannii* persisters by inhibiting its membrane potential [208].

2.11.4 Reducing persister formation

While anti-persister strategies that aim to eradicate the existing persister populations are promising, equally important are the approaches which can inhibit or reduce the formation of persisters. Inhibiting persister formation is a viable strategy to prevent the occurrence of chronic infections. Benzamide, benzimidazole compounds M64, M56, M59 and M34; identified as inhibitors of the quorum sensing regulon, MvfR demonstrated the ability to reduce *P. aeruginosa* persister formation and could be administered with the antibiotic ciprofloxacin [209], [210]. Mesalamine, an anti-inflamatory drug acts by decreasing polyphosphate levels in *E. coli* and *P. aeruginosa* persisters, thus making them prone to oxidative stress [211]. The alarmone (p)ppGpp is produced by the enzyme RelA and is known to regulates the stress reponse in bacterial persisters. Inhibitors of the enzyme RelA, for example Relacin which is a ppGpp analogue have been shown to decrease persister levels in Gram positive pathogens [128].

2.12 Chemical genetic approaches for novel drug discovery

Chemical genetics is defined as the study of biological systems using small molecules or chemicals [15]. It can be broadly divided into two categories (i) Forward Chemical Genetics and (ii) Reverse Chemical Genetics (Fig. 2.13).

As the name suggests, forward chemical genetics runs in the forward direction i.e from phenotype to protein. The forward chemical genetics approach requires the use of a small molecule library, a model organism against which the screening studies would be carried out and a phenotypic biological screening strategy [15]. Here, small molecules are screened against a biological system to study their ability to produce a desired phenotype for example, growth inhibition in case the screening was carried out to identify an antibacterial. Once a small molecule that produces the desired effect has been identified, detailed biological investigations need to be carried out to determine their cellular targets, which is a challenging task.

Reverse chemical genetics, on the other hand runs in the opposite direction and requires the identification of a target protein *a priori*, following which small molecules are screened for their ability to bind to the protein target and produce a phenotypic effect, for example inhibition of enzyme activity, in case the protein target was an enzyme [15]. Hence, reverse chemical genetics requires the pre-selection of a protein target, a small molecule library and a biochemical or biophysical assay appropriate for lead identification.

The target based approaches for drug discovery have witnessed numerous advances in technology paving the way for a modern drug discovery era, such as genetic manipulation of bacterial genomes, high throughput synthesis of chemical libraries, improved understanding of target protein structures which facilitates rational drug design, robotic handling systems for carrying out high-throughput biochemical assays and the availability of advanced computational tools to handle large amounts of data sets [212]. However, none of these advancements have been able to contribute to the discovery of promising new medicines, since the previous two decades. Several industrial failures have been reported in the target based screening approaches against Gram negative bacteria and much of these setbacks could be attributed to the presence of a formidable outer membrane barrier and efflux pumps [50], [213].

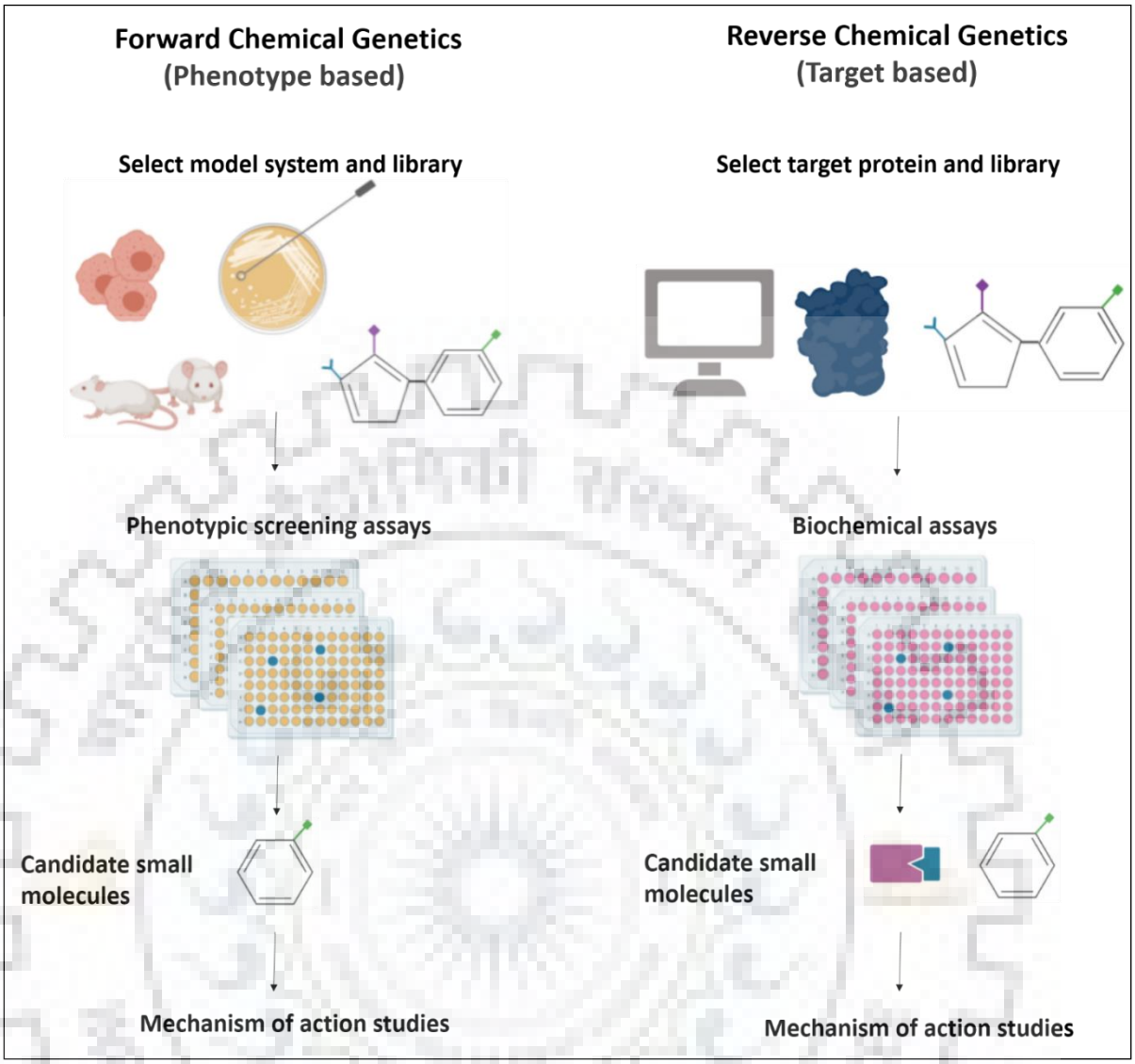

Figure 2.13: Forward and reverse chemical genetics approach for drug discovery. The forward chemical genetics approach requires the use of a small molecule library, a model system against which the screening studies would be carried out and a phenotypic biological screening assay such as growth inhibition. Upon identification of a lead compound, mechanism of action studies are carried out. Reverse chemical genetics or target based approach requires the pre-selection of a protein target, a small molecule library and a biochemical or biophysical assay appropriate for lead identification. Mechanism of action studies are further needed to validate the cellular activities.

2.13 Unconventional screening approaches for drug discovery

Considering the drawbacks of target based approaches and uncertainty of target identification in phenotypic strategies, recent years have witnessed the introduction of unconventional screening strategies which can overcome the limitations associated with the conventional strategies and hold great potential to yield favourable antibacterial leads [212], [214]. One of these approaches are the Target- based whole-cell screening strategies that can be used to identify small molecule inhibitors of certain cellular pathways [215]. This strategy demonstrates the potential to ease out the difficulties associated to target identification and can be used to find inhibitors of all genes provided whole cell screening assays could be designed to identify the same.

The identification of lamotrigine as an inhibitor of bacterial ribosome biogenesis is an example of the utility of phenotype based whole cell screening approach to identify compounds with novel mode of action [216]. Other unconventional screening strategies that are currently being exploited for novel drug discovery include screening in unconventional hosts and screening in nontraditional growth media [214].

2.13.1 Combinatorial drug discovery

The effectiveness of chemical combinations in the clinic has further opened up the avenue of using drug combinations as an alternative screening strategy to identify potential antibacterial molecules. The identification of four novel small molecule inhibitors which could augment the activity of novobiocin, a Gram positive specific antibiotic against Gram negative bacteria by causing membrane permeability is a successful example that followed this approach [217]. This approach can also aid the repurposing of already approved drugs as adjuvants to potentiate the action of antibiotics. For example, the antidiarrhoeal drug loperamide facilitated the uptake of the antibiotic minocycline in Gram-negative bacteria by disrupting their membrane potential [150]. Computational based screening of chemical combinations presents another useful strategy that can aid the rational design of favourable synergistic combinations by predicting their genetic interaction networks [218].

2.14 Strategies for target identification of novel antibacterials

Determining the mechanism of action (MOA) of novel leads identified in whole-cell phenotypic screens is a challenging task and has been considered the rate determining step in any drug discovery program [15]. The various strategies employed for the identification of the targets of novel antibacterials are discussed below:

1. Genetic strategy: Isolation and whole genome sequencing of drug resistant mutants may lead to the identification of cellular targets [19]. With the advent of next-generation sequencing technology, it has now become possible to parallelly sequence a large number of mutant strains, such as isogenic-sensitive or resistant mutants that can help to identify the drug targets in a rapid and inexpensive manner. For example: targets for the antibiotics novobiocin and rifampicin were identified by sequencing their resistant mutants [26],[25]. Cellular target for the antimycobacterial compound, pyridomycin was also identified by whole genome sequencing and subsequent genetic studies [219]. Although the strategy of sequencing mutants can lead to rapid target identification but it fails to yield results for compounds against which it is not possible to generate mutants. Also, sometimes this approach can lead to the identification of other pathways of resistance such as mutations in the regulatory regions of drug transporters and efflux pumps [19].

2. Biochemical strategy: Affinity based approaches coupled with high resolution mass spectrometry MS analysis methods can be used for the identification of protein targets [19]. Small molecule-affinity chromatography with stable isotope labelling of amino acids in cell culture (SILAC) can be used to assess the protein small molecule interactions on a proteome wide scale [21]. However, this approach comes with the challenge of immobilizing, modifying or labelling the small molecules which may hamper their cellular activity. Another approach that can be employed to assess the small molecule protein interaction without the need for modifying the small molecules is Drug Affinity Responsive target Stability (DARTS) [220]. Affinity based approaches suffer from the limitation of identifying only the high affinity interactions although several low affinity interactions would also be responsible for the biological activity of the small molecule [19].

3. Radioactivity based Macromolecular Synthesis (MMS) assay is another powerful approach that has been in use for the identification of the mechanism of action of unknown antibacterials

[19]. This assay can determine the effect of small molecules on the incorporation of radioactively labeled nucleotide and amino acids precursors of DNA, RNA and protein synthesis pathways [27]. It can also identify inhibitors of the cell wall synthesis and fatty acid synthesis pathways. Mechanism of action of the antimicrobial peptide daptomycin and repurposed antibacterial drug auranofin have been studied by this approach [221], [222] .

4. Bacteriological cytological profiling (BCP) is yet another fruitful strategy that has been exploited to identify the MOA of unknown compounds on the basis of the reference cytological profile of known antibiotics [28]. The MOA of novel compounds spirohexenolide A and NSC145612 against *E. coli* and *A. baumannii* have been identified using this method [28], [223].

5. Chemical genomic strategies such as the use of overexpression or deletion clones for target identification have been widely used [30], [224]. Compounds MAC 13243 and two other molecules targeting the periplasmic *chaperone* LolA and the enzyme DHFR of the folic acid synthesis pathway were identified by using the E. coli ASKA library of overexpressor clones [9], [22]. However the *E. coli* deletion library (KEIO collection) cannot be used in case if the small molecule targets en essential gene [225]. To overcome this limitation, the strategy of conditionally expressing complementary RNA transcripts via plasmids or CRISPR based constructs, come into rescue. The targets for the platensimycin (*fabF* gene), essential oils eugenol and carvacrol (*yidC* gene) and novel inhibitors of the cell wall synthesis pathway (*uppS* gene) were identified using this strategy [24], [32], [226]. Promoter–reporter libraries of GFP–promoter fusions can also be utilized to assess the transcriptional changes induced upon drug exposure [30]. These libraries can be beneficial in getting a mechanistic insight in case of unknown antibacterials. For example, stavudine (a nucleoside analog) was observe to induced transcription of LexA-repressed promoters (*lexA*, *recA*, and *sulA*) thus indicating the induction of SOS response [227]. Deep sequencing technologies such as transcriptome profiling by RNA-Seq, transposon sequencing (Tn-Seq) and identification of suppressor mutants are newer and powerful approaches that have been used to study the MOA of novel antibacterials [30]. Tn-Seq has been successfully employed to study the response of both Gram-negative and Gram-positive bacteria to tunicamycin (teichoic acid inhibitor) [228]. The strategy of sequencing suppressor mutants in a screen for inhibitors of bacterial ribosome biogenesis identified the anticonvulsant drug lamotrigine to target the translation initiation factor IF2, and inhibit ribosome biogenesis [216].

3 Objectives

Our lab has a long standing interest to tackle the problem of antibiotic resistance by employing various strategies such as:

(i) Screening of novel antibacterials from small molecule libraries by the aid of phenotype-based or target-based approaches followed by target identification [229].

(ii) Exploiting the use of combination therapy for the treatment of serious bacterial infections and improving antibiotic activity. These could include antibiotic-antibiotic or antibiotic-non antibiotic combinations.

(iii) Screening for novel inhibitors of determinants of antibiotic resistance such as Efflux Pump Inhibitors (EPI) [229],[160].

(iv) Screening for novel anti-persister compounds that can either directly kill persistent bacterial populations, re-sensitize them to the conventional antibiotic regime or interfere with the mechanisms of induction of persistence.

A small molecule library of 10,956 compounds was previously screened in the lab against the model organism, *E. coli* ATCC 25922 {Ph.D. Thesis: Dr. Tapas Bhattacharyya (2010-15)}. The screen led to the identification of 30 novel antibacterials which needed to be characterized on the basis of their antibacterial properties, mechanism of action, *in vitro* pharmacodynamics, *in vivo* toxicity and efficacy.

The specific aim of the research in this thesis was to overcome the existing crisis of antibiotic resistance and persistence. The four major objectives that were pursued to achieve this goal are as follows:

1. **Characterization of the antibacterial activity, *in vitro* pharmacodynamics and mechanism of action of small molecule IITR06144.**
2. **To study the combinations of IITR06144 with clinically important antibiotics.**
3. **Elucidating the mechanism of action of novel small molecules using chemical-chemical combinations.**
4. **Characterisation of the mechanisms of meropenem induced persistence in *A. baumannii* and identification of small molecule inhibitors thereof.**

4 Characterisation of the antibacterial activity, *in vitro* pharmacodynamics and mechanism of action of small molecule IITR06144

4.1 Introduction

Bacterial infections continue to pose a serious challenge to global public health. Inappropriate and excessive use of antibiotics has led to the emergence of multidrug resistant (MDR) and extensively drug resistant (XDR) bacterial strains that are impervious to most or all of the current antibiotics. Importantly, Gram negative bacteria make up four of the six "ESKAPE" pathogens and present the most acute threat owing to their complex envelope structure [4]. If the efficacy of the existing antibiotic arsenal continues to remain compromised, it is estimated to cause approximately 10 million deaths by 2050 annually and a cumulative loss of 100 trillion USD in the global Gross Domestic Product (GDP). Hence, the urgent and continuing need for the discovery of novel antibacterial agents against these notorious pathogens cannot be overemphasized.

In an effort to explore new antibacterial leads against Gram negative pathogens, a whole-cell screening assay was previously performed in our lab on a diverse collection of 10,956 small molecules for growth inhibition of the Gram negative model organism, *E. coli* ATCC 25922 [Unpublished work - PhD Thesis, Dr. Tapas Bhattacharyya]. The molecules were screened in 96-well microtiter plates at 50 µM concentration each. Primary screening led to the identification of 30 compounds with remarkable antibacterial activity, inhibiting >75% of *E. coli* growth and were therefore considered as potential antibacterial hits (Fig. 4.1). The primary screening data was observed to be reproducible, reliable and of high quality with Z' score of 0.81 [230].

The 30 antibacterial hits identified were further subjected to MIC determination as per CLSI guidelines, against *E. coli* ATCC 25922. Out of the 30 leads, the small molecule IITR06144 exhibited the most significant antibacterial activity inhibiting *E. coli* cells at the least MIC of 0.5 µg/mL. This study reports the antibacterial properties, pharmacodynamic parameters, *in vivo* efficacy and mechanism of action of the novel antibacterial small molecule IITR06144.

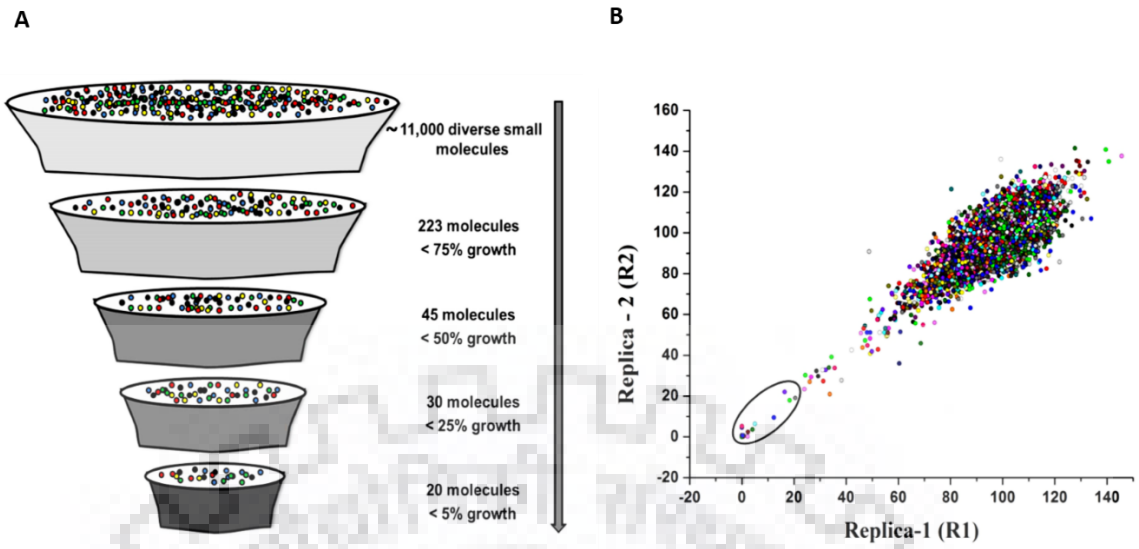

Figure 4.1: Screening of small molecule library for novel antibacterials. (A) Workflow for identification of antibacterial small molecules. A collection of 10,956 diverse synthetic small molecules was screened for growth inhibition against *Escherichia coli* ATCC 25922. Primary screening identified 223 compounds with potential antibacterial activity out of which 30 hit compounds displayed excellent activity inhibiting >75% of growth in comparison to the positive control. (B) Replicate plots for primary screen of growth inhibition. The screening was done in duplicates and the mean percentage growth of *E. coli* ATCC 25922 in the presence of 50 µM of each molecule was calculated by measuring optical density at 600 nm (OD600). The x and y axis values indicate the mean percent growth for each molecule in comparison to untreated control. The circle in the figure indicates the 30 molecules that inhibited >75% of growth and were identified as potential leads (Unpublished work – PhD Thesis of Dr. Tapas Bhattacharyya).

4.2 Results

4.2.1 Small molecule screening identified four antibacterials from the nitrofuran class

The 30 antibacterial hits were further subjected to MIC determination against a battery of Gram-negative bacteria including *A. baumannii* ATCC 17978, *Vibrio fluvialis* (L-15318), *E. coli* O157:H7 among others (Unpublished work – PhD Thesis of Dr. Tapas Bhattacharyya). IITR06144 exhibited the most significant antibacterial activity with the least MIC of 0.5 µg/mL against *E. coli* ATCC 25922. Three other compounds namely IITR06146, IITR07711, IITR01324 also showed remarkable activity (MIC range: 0.5-8 µg/mL) against *E. coli.*

Interestingly, all four of these compounds were observed to be structural analogues, belonging to the nitrofuran class (Fig. 4.2). Nitrofurantoin and furazolidone are two classical nitrofuran antibiotics administered for the treatment of uncomplicated urinary tract infections (UTIs) and enteritis respectively [231]–[233]. Since out of the four molecules, IITR06144 seemed to be most potent (MIC in the range 0.1-1 μg/mL) against all the pathogens tested, it was taken up for further investigations.

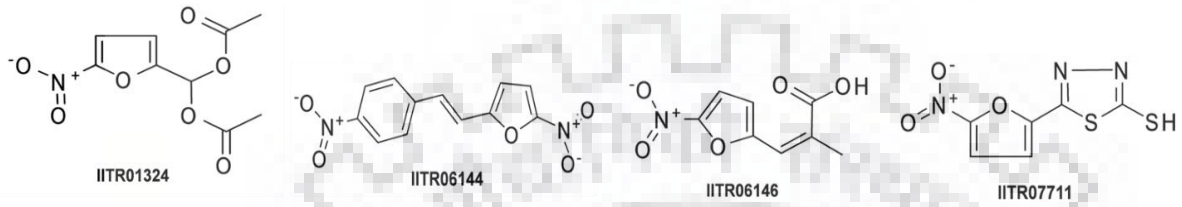

Figure 4.2: Chemical structures of the four nitrofuran compounds identified in the small molecule screen with potent antibacterial activity against *E. coli* ATCC 25922 namely IITR01324, IITR06144, IITR06146 and IITR07711.

The observation that IITR06144 [(E)-2-(4-nitrostyryl)-5-nitrofuran)] was the most potent molecule discovered in the screen, prompted us to investigate what imparted the compound its profound antibacterial activity. Structurally, IITR06144 comprised of a nitrobenzene and a nitrofuran moiety linked by carbon-carbon double bond formed by condensation of 5-nitro-2-furaldehyde and 4-nitrobenzaldehyde. Hence, I sought to identify its most active constituent by determining susceptibility of *E. coli* to both the molecules. The 5-nitro-2-furaldehyde component showed better activity (MIC: 1.5 μg/mL) than 4-nitrobenzaldehyde component (MIC: 25 μg/mL) when individually assayed. Clearly, the nitrofuran moiety in IITR06144 imparted a higher potency such that, in combination with nitrobenzaldehyde, its MIC decreased to 0.5 μg/mL.

4.2.2 IITR06144 is a broad spectrum antibacterial

The spectrum of activity of IITR06144 was further studied against common reference strains from the lab repository. The antibacterial spectrum of IITR06144 was compared to the two commonly used nitrofuran antibiotics, nitrofurantoin and furazolidone. IITR06144 displayed excellent activity against most Gram-negative bacteria, including the persistent and opportunistic pathogen *A. baumannii* (Table 4.1) [118].

Table 4.1: In vitro antibacterial activity of IITR06144 in comparison to structurally analogous antibiotics (minimum inhibitory concentration, MIC in µg/mL).

Bacteria	**MIC (µg/ml)**		
	IITR06144	**Nitrofurantoin**	**Furazolidone**
Gram- Negative:			
Escherichia coli ATCC 25922	0.5	10	1.2
Escherichia coli O157:H7	0.5	8	16
Acinetobacter baumannii ATCC 17978	0.5	>64	0.5
Acinetobacter baumannii AYE	0.5	32	>64
Shigella flexneri ATCC 9199	0.13	2	2
Burkholderia cepacia ATCC 25416	16	>64	32
Salmonella choleraesuis ATCC 10708	1	8	2
Salmonella enterica Serotype Typhimurium	0.25	8	1
Vibrio fluvialis (BD-146)	0.13	2	2
Vibrio fluvialis (L-15318)	0.13	2	16
Enterobacter sakazakii	0.5	8	2
Gram- Positive:			
Staphylococcus aureus ATCC 29213	0.5	16	2
Bacillus subtilis	2	16	2
Bacillus cereus ATCC 11778	0.5	16	4
Listeria monocytogenes	0.5	8	>32
Enterococcus faecium FH99	4	32	>32
***Mycobacterium* spp.**			
Mycobacterium smegmatis	0.25	8	1
Mycobacterium tuberculosis H37Ra	0.25	2	4
Mycobacterium bovis BCG	0.25	16	8

Table 4.2: Comparative *in vitro* activity of IITR06144, nitrofurantoin and furazolidone against clinical isolates.

Organism (no. of isolates)	MIC range (µg/ml)		
	IITR06144	**Nitrofurantoin**	**Furazolidone**
Gram- Negative:			
Escherichia coli **(8)**	0.1-1	6-12	0.2-1
Acinetobacter baumannii **(25)**	0.25 - 4	> 128	32 - ≥64
Klebsiella pneumoniae **(4)**	0.25 - 2	16 - >128	1-32
Shigella spp. **(6)**	0.5-1	16	8
Gram- Positive:			
Staphylococcus aureus **(6)**	0.5 - 1	6-48	1-16

It inhibited the growth of MDR *A. baumannii* strain AYE at 0.5 µg/mL, which is resistant to fluoroquinolones, aminoglycosides, rifampin, tetracycline and chloramphenicol [234]. IITR06144 was exceptionally active against *S. flexneri* (MIC: 0.13 µg/mL) which is a highly infectious pathogen and a leading cause of diarrhoeal deaths in the world (Table 4.1) [235]. IITR06144 also inhibited the Gram-positive bacterial pathogens *Staphylococcus aureus*, *Bacillus subtilis*, *Listeria monocytogens* and *Enterococcus faecium.* Importantly, IITR06144 showed impressive antibacterial activity against *Mycobacterium* spps.(MIC: 0.25 µg/mL). The activity of IITR06144 was further tested against a panel of clinical isolates and it was observed to display a broad spectrum inhibitory activity against both Gram negative and Gram positive bacteria with MICs in the range of 0.1-2 µg/mL. All the *A. baumannii* isolates tested showed resistance to nitrofurantoin and the last resort antibiotics, carbapenems but were extremely susceptible to the action of IITR06144 (Table 4.2).

Anaerobic bacteria are known to cause serious and life-threatening infections in immunocompromised patients. Difficult isolation, identification, and inadequate susceptibility testing are the major factors responsible for clinical failure of anaerobic therapy [236].

Furthermore, increasing resistance to the most commonly administered antibiotics metronidazole, piperacillin-tazobactam and meropenem has worsened the situation, thus emphasising the need for novel anti-anaerobic agent [236]. To this end, the antibacterial activity of IITR06144 against anaerobes was evaluated by the agar dilution method, as per CLSI guidelines [237]. IITR06144 displayed excellent bactericidal activity against all anaerobic strains tested (MICs in the range 0.060-0.25 µg/mL) namely *Bacteroides fragilis, Clostridium difficile, C. perfringes* including a metronidazole resistant isolate of *C. tetani* (Table 4.3). IITR06144 outcompeted metronidazole, nitrofurantoin and furazolidone against all anaerobic isolates studied. Since anaerobic infections are often polymicrobial in nature, empiric antibiotic therapy eliminates only the aerobic component of infection leading to adverse clinical outcomes. The remarkable antibacterial activity of IITR06144 implies that it holds great potential for the eradication of mixed aerobic and anaerobic bacterial infections.

Table 4.3: *In vitro* antibacterial activity of IITR06144 and comparative antibiotics against anaerobic bacteria.

Bacteria	MIC (ug/ml)			
	IITR06144	**Metronidazole**	**Nitrofurantoin**	**Furazolidone**
Clostridium difficile ATCC 9689	0.06	1	4	1
Clostridium perfringens ATCC 3629	0.25	2	16	2
*Clostridium tetani**	0.25	>32	16	4
*Bacteroides fragilis**	0.12	16	32	>32

*Clinical isolates. Source mentioned inAppendix 9.1

Oral consumption of antibiotics is known to alter the composition of gut microbiota significantly, disrupting the intestinal homeostasis thus causing a multitude of health problems. It is therefore imperative to analyse the potential of novel antibiotics on human microbiome during preliminary stages of any drug discovery program. Hence, I proceeded to assess the antibacterial activity of IITR06144 against a few laboratory strains of *Lactobacillus* in MRS medium by broth

Table 4.4: *In vitro* antibacterial activity of IITR06144 and comparative antibiotics against a few human commensal bacteria.

Bacteria	MIC (µg/ml)		
	IITR06144	**Nitrofurantoin**	**Furazolidone**
Lactobacillus fermentum	>64	16	32
Lactobacillus cassei	>64	64	64
Lactobacillus plantarum	>64	128	64
Lactobacillus brevis	>64	128	64
Lactobacillus gasseri	>64	128	64
Lactobacillus rhamnosus	>64	32	32
Streptococcus thermophilus	2	32	32
Leuconostoc mesenteroides	2	2	2

microdilution assay. It was particularly encouraging to observe that IITR06144 displayed no inhibitory effect on any of the *Lactobacillus* strains (up to 64 ug/mL) tested, while nitrofurantoin and furazolidone negatively influenced (MIC range: 16-128 µg/mL) their growth (Table 4.4). To rule out the speculation that MRS components or low pH of the MRS medium (pH 6.2 ± 0.2) would interfere with IITR06144 activity, *E. coli* O157:H7 was used as a control in the same assay. IITR06144 inhibited the growth of enterohaemorrhagic *E. coli* serotype O157:H7 in MRS broth but had no activity against the representative gut symbionts. However, IITR06144 inhibited *Streptococcus thermophilus* and *Leuconostoc mesenteroides* with MIC of 2 ug/mL (Table 4.4).

4.2.3 IITR06144 is bactericidal in action against *E. coli* ATCC 25922

Time kill kinetics assay was carried out to assess the killing potential of IITR06144 against *E. coli* ATCC 25922 in comparison to the nitrofuran antibiotics, nitrofurantoin and furazolidone. IITR06144 (at 1 ug/mL) was observed to be extremely bactericidal causing >3 $\log_{10}$ CFU/mL reduction in *E. coli* cells within 4 h of treatment, which was maintained up to 24 h (Fig. 4.3). In contrast, nitrofurantoin (at 12 μg/mL) and furazolidone (at 2 μg/mL) displayed delayed killing (after 8 h) followed by regrowth at 24 h time point. Thus, IITR06144 showed superior killing ability against *E. coli* in comparison to its analogous antibiotics.

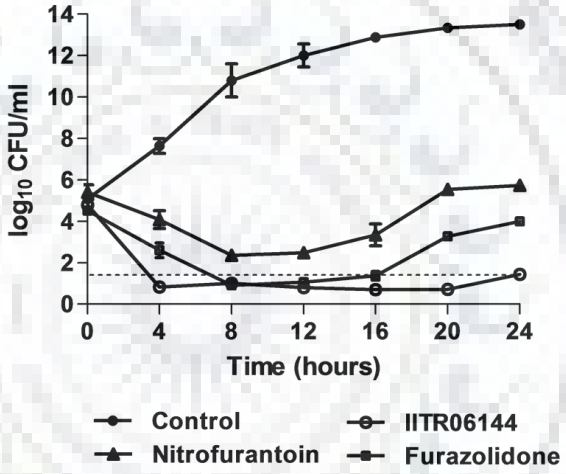

Figure 4.3: Time kill kinetics of IITR06144. Kinetics of bacterial killing by IITR06144 was studied in comparison to nitrofurantoin and furazolidone. *E. coli* ATCC 25922 (10^5 CFU/ml) was incubated with 2X MIC of IITR06144 and the number of viable cells were determined. The dashed line represents the limit of detection as 1.52 $\log_{10}$ CFU/mL. Each value represents the mean of three values and error bars denote the standard deviation.

4.2.4 IITR06144 exhibits an enhanced Post antibiotic effect (PAE)

Post antibiotic effect (PAE) is an important pharmacodynamic parameter which denotes the time for which bacterial growth remains suppressed following brief exposure to an antibiotic [238]. IITR06144 exhibited a longer PAE (2.2 h) and therefore enhanced persistence, than observed for nitrofurantoin (0.77 h) and furazolidone (1.03 h) (Fig. 4.4a). Considering the rapid

bactericidal nature of IITR06144, a 5 log bacterial killing was observed upon exposure and cells did not revive until 3 h after drug removal (Fig. 4.4b).

a

	Time required for unit $\log_{10}$ increase (h)	PAE (h)
Control	0.77	-
IITR06144	2.97	2.2
Nitrofurantoin	1.54	0.77
Furazolidone	1.80	1.03

b

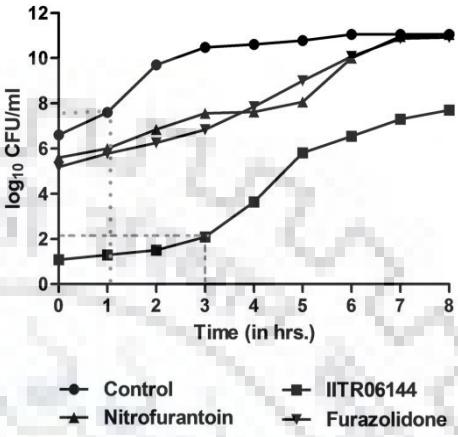

Figure 4.4: *In vitro* post-antibiotic effect (PAE) of IITR06144 against *E. coli* ATCC 25922. IITR06144 was added at a final concentration of 5X MIC and to bacterial cells in the logarithmic phase. Following exposure for an hour, culture was spun and washed twice with sterile buffer saline and the re-suspended cells were then incubated at 37 °C for a period of 8 h. (a) Calculated PAE for IITR06144, nitrofurantoin and furazolidone (b) Viable counts were determined before exposure and immediately after resuspension (0 h) followed by plating every 1 h. Each value represents the mean of three values and error bars denote the standard deviation.

4.2.5 IITR06144 exhibits least predisposition for resistance selection

The potential for emergence of resistance in *E. coli* cells against IITR06144 was also explored by the Spontaneous plating method. In comparison to nitrofurantoin, which selected mutants at a frequency of approximately 1×10^{-7} at 4X MIC, exposure to IITR06144 did not yield any resistant mutants. This observation suggested least predisposition for resistance selection in IITR06144 in comparison to nitrofurantoin.

4.2.6 IITR06144 is non-haemolytic to Red Blood Cells

To get a preliminary idea of toxicity of IITR06144, its ability to lyse human erythrocytes was evaluated . IITR06144 was observed to be non-haemolytic and hence non-toxic causing only 5.36±2.1% haemolysis (Fig. 4.5). In contrast, nitrofurantoin and furazolidone exhibited significant toxicity causing 43.8±3.3% (P value < 0.001) and 24.6±5.9% (P value < 0.01) haemolysis respectively, at 10 times their individual MICs (Fig. 4.5).

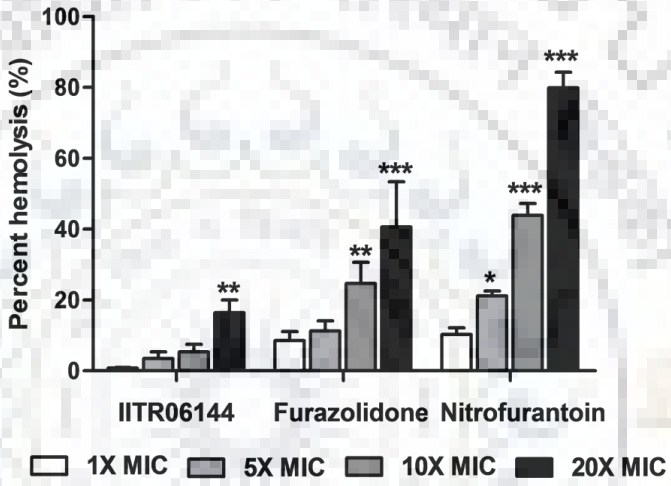

Figure 4.5: Haemolytic potential of IITR06144. Human erythrocytes were exposed to increasing concentrations of IITR06144, nitrofurantoin and furazolidone for 1 h. The absorbance was measured at 540 nm and percentage haemolysis relative to the positive control (0.1% Triton X-100) was determined. Statistical significance was evaluated by two-way ANOVA with Bonferroni's multiple-comparison test. *, P<0.05; **, P<0.01; ***, P<0.001.

4.2.7 IITR06144 is non-cytotoxic to human Peripheral Blood Mononuclear Cells

Further the effect of IITR06144 on the viability of human Peripheral Blood Mononuclear Cells (PBMCs) was assessed by MTT assay and therapeutic index (TI) was calculated. IITR06144 was found to possess no cytotoxicity with IC50 value of 32 μg/mL and a favourably large TI of 64, at par with nitrofurantoin and furazolidone (Table 4.5).

Table 4.5: *In vitro* cytotoxicity of IITR06144 in comparison to nitrofurantoin and furazolidone.

	MIC (µg/mL) in 10% FBS	Cytotoxicity (IC50)* (µg/mL)	Therapeutic Index (TI)
IITR06144	0.5	32	64
Nitrofurantoin	12	>128	>10.6
Furazolidone	2.4	>64	>26.6

*The concentration that showed less than 50% survival compared to untreated (solvent control), was taken to be the cytotoxic concentration. For nitrofurantoin and furazolidone, 128 µg/mL and 64 µg/mL were the highest concentrations tested in the experiment respectively and these did not show less than 50% survival.

4.2.8 IITR06144 can inhibit metabolically inactive bacterial cells in a stationary phase culture

As discussed previously, metabolically inactive persister cells are the major culprits responsible for recurrence and recalcitrance of chronic infections. Hence, the potency of IITR06144 against a stationary phase culture of *E. coli* ATCC 25922 was investigated, since it is known to possess persistent bacterial cells. Fig. 4.6 shows that IITR06144 efficiently inhibited the stationary phase persisters such that no viable cells were obtained upon treatment. In contrast, nitrofurantoin displayed decreased eradication even at 200 µg/mL, a concentration reached in the urinary bladder of patients with normal renal function.

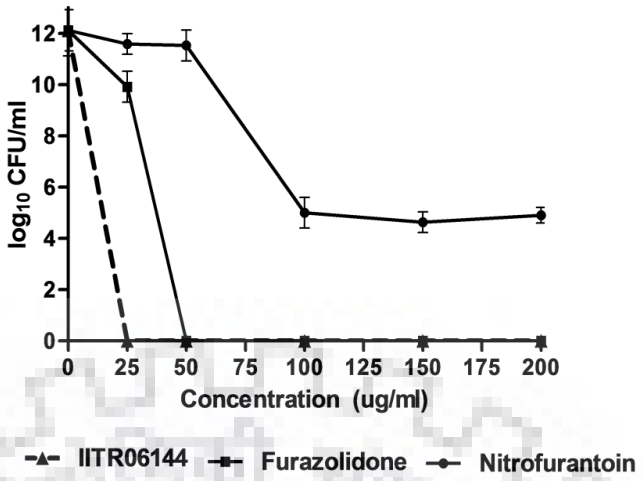

Figure 4.6: Killing of stationary phase bacterial cells by IITR01644. Stationary phase *E. coli* ATCC 25922 cells were treated with IITR06144, nitrofurantoin and furazolidone (at 0-200µg/ml) for 24 h and viable counts were determined. Each value represents the mean of three values and error bars denote the standard deviation.

Further, the membrane integrity of the IITR06144 treated population (treated with 25 µg/ml), which did not yield any culturable colonies on agar plates was assessed. This would help in determining the presence of any viable but non culturable bacterial cells. Therefore, a live-dead staining assay using the combination of two fluorescent dyes, FM 4-64 and Sytox green was performed. FM 4-64 is a lipophilic membrane staining dye while Sytox green is a nucleoid staining dye that can be used as an indicator dye for cells with compromised membranes. Sytox green is excluded from the membrane of viable cells and stains the dead cells green. Fluorescence microscopy of untreated *E. coli* cells and IITR06144 treated cells confirmed the presence of dead cells in the IITR06144 treated population (Fig. 4.7). Hence, IITR06144 was observed to inhibit all the cells in the stationary phase bacterial population.

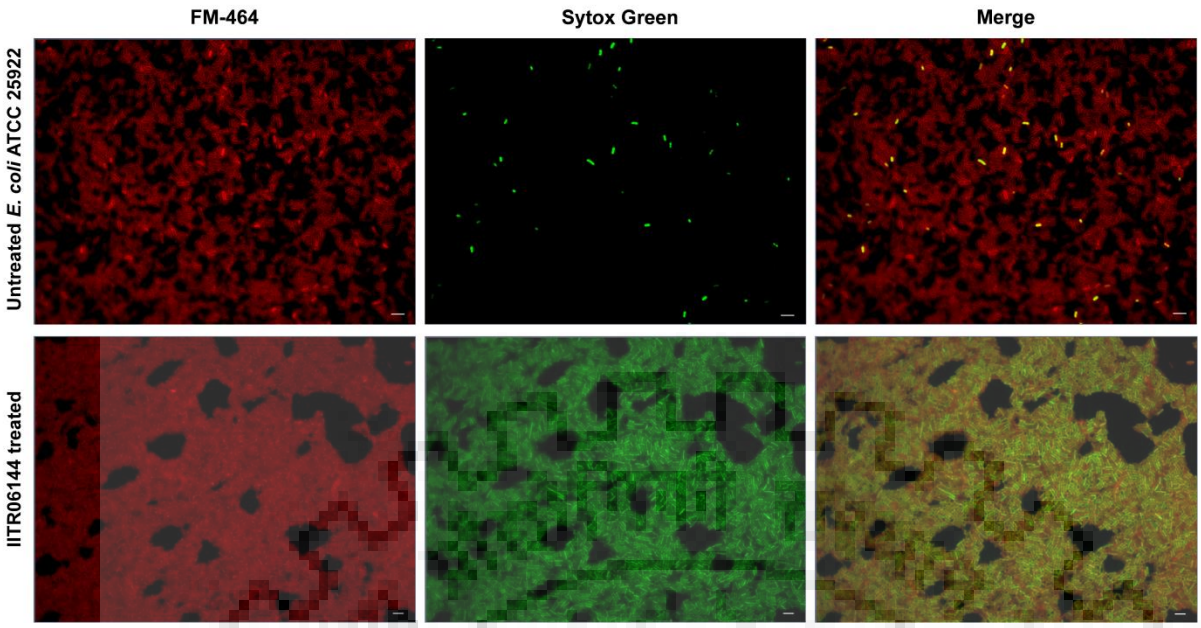

Figure 4.7: Fluorescence microscopic studies on stationary phase *E. coli* cells treated with 25 µg/mL of IITR06144 to assess their viability using combination of dyes FM 4-64 and Sytox green. Scale bar represents 5 µm.

4.2.9 IITR06144 can inhibit antibiotic induced persister cells

Further the efficacy of IITR06144 to inhibit antibiotic tolerant persisters was evaluated since these are responsible for the recalcitrance of chronic infections and also contribute substantially to the evolution of antibiotic resistance. A stationary phase culture of *E. coli* ATCC 25922 was exposed to extremely high concentration of ampicillin (300 µg/mL) for 14 hours in order to isolate ampicillin persisters. Isolation of ampicillin induced persisters was confirmed by determining the number of viable bacteria that survived ampicillin exposure by plating CFU at regular intervals upto 24 h. Ampicillin exposed culture exhibited the characteristic biphasic pattern of growth thus confirming the presence of true persister populations within them (Fig. 4.8).

Isolated persisters were further exposed to varying concentration of IITR06144, nitrofurantoin, furazolidone (at 4X and 8X MIC), ampicillin and kanamycin in order to compare their anti-persister activity. After 24 h of drug exposure, neither nitrofurantoin nor furazolidone displayed considerable killing ability against *E. coli* persisters. Treatment with 25X MIC of ampicillin (MIC: 4 µg/mL) and kanamycin (MIC: 2 µg/mL) also failed to inhibit the persister populations

(Fig. 4.9). On the contrary, IITR06144 caused a significant ~4 fold reduction in viable cell count at 4X MIC, while no colonies were detected at 8X MIC (Fig. 4.9).

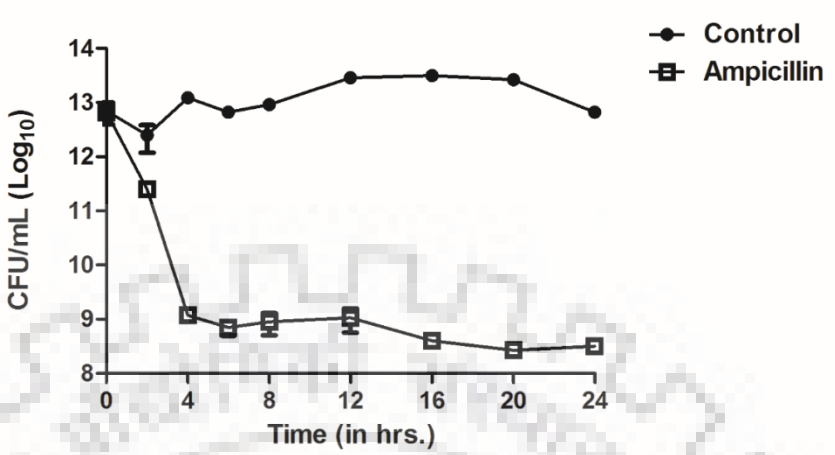

Figure 4.8: Kinetics of bacterial survival in *E. coli* ATCC 25922 upon treatment with 300 µg/mL of ampicillin in comparison to untreated control. Aliquots were extracted at regular intervals and the number of surviving bacteria were enummerated. Each value represents the mean of three values and error bars denote the standard deviation.

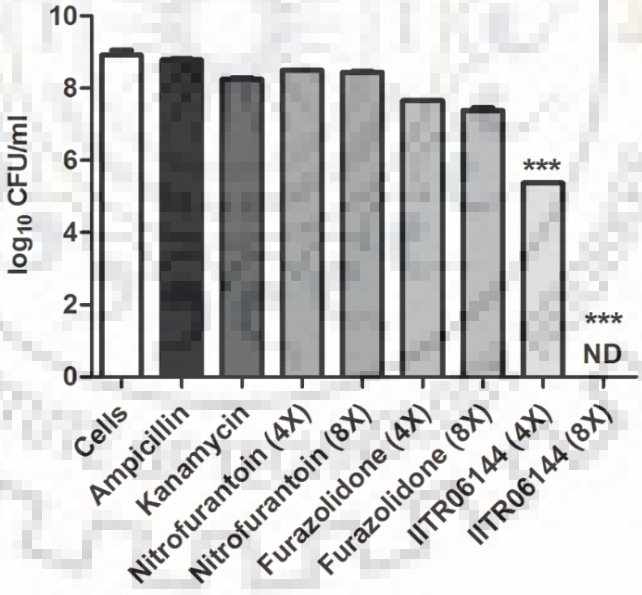

Figure 4.9: Killing of *E. coli* persister cells by IITR06144 and comparative antibiotics. Persister cells were isolated by treating stationary phase bacteria with 300 µg/ml ampicillin followed by exposure to IITR06144, nitrofurantoin and furazolidone (at 4X and 8X MIC), ampicillin (100µg/mL) and kanamycin (50µg/mL) for 24h and viable counts were determined. P values were determined by one-way ANOVA followed by Dunnett's multiple comparison test. ND: not detected. *, P<0.05; **, P<0.01; ***, P<0.001.

At 1/2X MIC, IITR06144 significantly inhibited *E. coli* biofilm formation by ~40±8% (P value < 0.001), which was comparable in activity to nitrofurantoin (~37±10%). However, furazolidone was observed to possess a poor antibiofilm activity, both at 1/4X MIC (P value ≥ 0.05) and 1/2X MIC (P value < 0.05) respectively (Fig. 4.11).

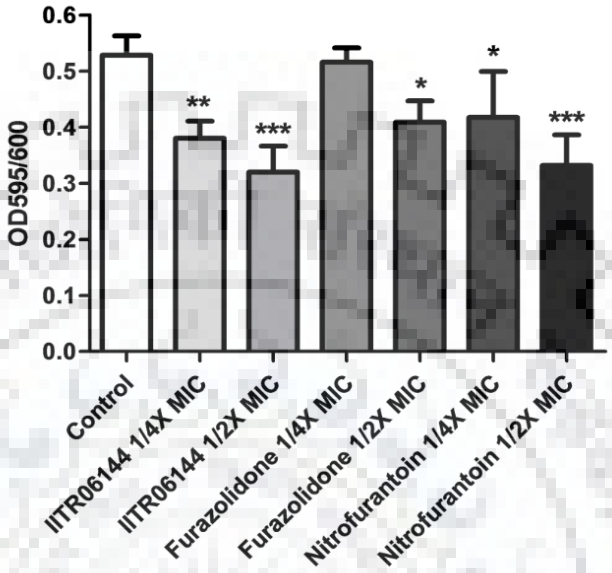

Figure 4.11: Inhibition of biofilm formation by IITR06144. The effect of IITR06144 and comparative antibiotics (at sub lethal concentrations) on *E. coli* MTCC 4296 biofilm formation was studied by crystal violet staining. Relative biofilm formation was determined as the ratio of the OD_{600} of the biomass (prior to staining) and OD595 of the stained biomass. Two-way ANOVA was performed, followed by Bonferroni's multiple-comparison test. *, P<0.05; **, P<0.01; ***, P<0.001.

4.2.11 IITR06144 can eradicate preformed UPEC biofilms

Drugs displaying bactericidal activity on slow replicating or non-replicating persisters are expected to effectively eradicate mature biofilms [240]. Therefore, we hypothesised that IITR06144 being a potent anti-persister compound could act on preformed biofilms as well. To this end, 2-day old biofilms of *E. coli* MTCC 4296 were treated with varying concentration of IITR06144 (1X-4X MIC) and the viable cell counts in comparison to untreated control were enumerated. IITR06144 at 2X MIC showed a significant reduction from 5.89±0.28 to 2.95±0.34 $\log_{10}$ CFU/mL (P value < 0.001) while nitrofurantoin (P value < 0.01) and furazolidone (P value < 0.05) displayed comparatively poor ability to eradicate established biofilms at similar concentrations (Fig. 4.12). IITR06144 could effectively reduce the biofilm

biomass in 48 h old biofilms formed by *E. coli* MTCC 4296 expressing green fluorescent protein at 4X MIC as visualised by fluorescence microscopy (Fig. 4.13).

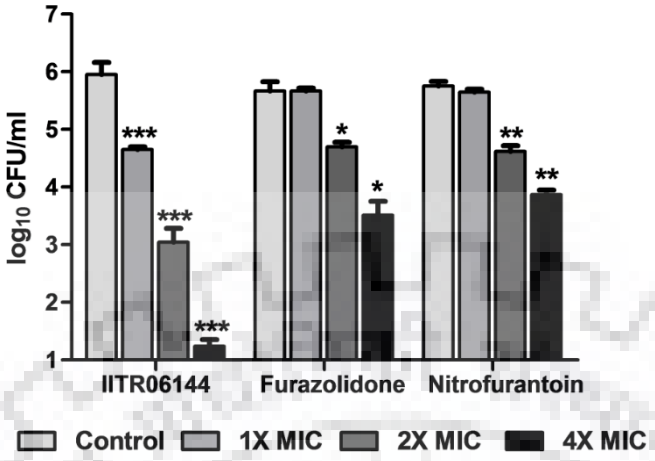

Figure 4.12: Disruption of preformed biofilms by IITR06144. 48 h old *E. coli* MTCC 4296 biofilms were treated with IITR06144 and comparative antibiotics for 12 h and number of biofilm associated cells that survived the treatment was determined. (Two-way ANOVA with Bonferroni's multiple-comparison test). Each value represents the mean of three values and error bars denote the standard deviation. P<0.05; **, P<0.01; ***, P<0.001.

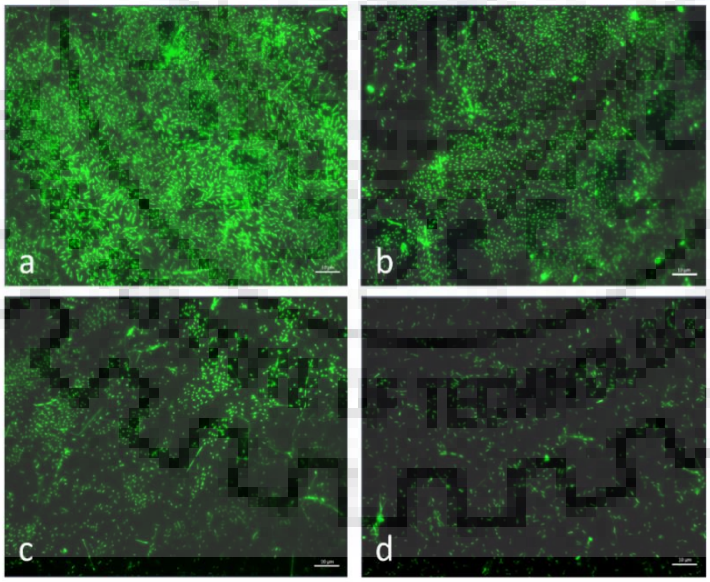

Figure 4.123: Ability of IITR06144 to disrupt preformed *E. coli* MTCC 4296 biofilms. 48 hour old biofilms formed by *E. coli* pNYL-GFP were treated with IITR06144 at 1X-4X MIC for 12 hours and visualised by fluorescence microscopy. (a) untreated biofilm (b) biofilms treated with 1X MIC (c) 2X MIC and (d) 4X MIC of IITR06144. Scale bar represents 10µm.

4.2.12 IITR06144 exhibits synergy with aminoglycosides and no negative interaction with other antibiotics

Combination therapy is frequently used in clinics to reduce the probability of emergence of drug resistance. Therefore, assessment of the compatibility of novel antibacterials with clinically relevant antibiotics holds immense importance. Hence, a checkerboard assay was undertaken against *E. coli* ATCC 25922, to determine the potential interactions between IITR06144 and representative antibiotics of different chemical classes. IITR06144 exhibited synergy with aminoglycosides such as kanamycin and amikacin [Fractional inhibitory concentration index (FICI): ≤0.5], while additive interaction was observed with other antibiotics (Table 4.6 and Table 4.7).

In *E. coli*, aminoglycosides are known to affect the membrane composition through incorporation of mistranslated membrane proteins, thereby causing increased cellular permeability and facilitating entry of other antibiotics. The basis of synergy between IITR06144 and aminoglycosides can be attributed to the alterations in membrane ultrastructure caused by aminoglycosides, ultimately leading to increased IITR06144 uptake [126]. Another probable reason for the synergistic interaction could be the occurrence of similar uptake transport mechanisms for aminoglycosides and nitrofuran antibiotics, although they may otherwise act on different cellular targets [241]. The antibiotic nitrofurantoin also has been previously shown to act in synergy with aminoglycosides thus corroborating that the synergistic interaction observed wasn't unique to IITR06144 and was class specific [242]. Encouragingly, also none of the antibiotic classes displayed any unfavourable or antagonistic interactions suggesting that IITR06144 may complement antibiotic therapy in the clinics.

Table 4.6: *In vitro* interaction of IITR06144 with representative antibiotics of different class as determined by the checkerboard assay.

Antibiotic	Class	FICI	Interaction
Penicillin	β-lactams	1	No interaction
Kanamycin	Aminoglycosides	0.375	Synergistic
Erythromycin	Macrolides	1.5	No interaction
Vancomycin	Vancomycin	0.625	No interaction
Rifampicin	Rifamycins	2	No interaction
Trimethoprim	Sulfonamides	0.625	No interaction
Fosfomycin	Fosfomycins	0.75	No interaction
Tetracycline	Tetracyclines	0.75	No interaction
Ciprofloxacin	Fluoroquinolones	1	No interaction
Polymyxin B	Polymyxins	1	No interaction

Table 4.7: *In vitro* interaction of IITR06144 with aminoglycoside antibiotics as determined by the checkerboard assay.

Antibiotic	MIC of Antibiotic (µg/ml)	MIC of IITR06144 (µg/ml)	MIC of antibiotic in presence of IITR06144 (µg/ml)	MIC of IITR06144 in presence of antibiotic (µg/ml)	FICI value	Type of interaction
Kanamycin	4	0.5	0.25	0.125	0.312	Synergistic
Tobramycin	2	0.5	0.0156	0.25	0.507	Synergistic
Gentamicin	0.5	0.5	0.125	0.125	0.5	Synergistic

4.2.13 IITR06144 treated cells exhibit an elongation phenotype

To gain insight into the mechanism of action of IITR06144, I first studied its effect on the morphology of bacterial cells. IITR06144 treated *E. coli* ATCC 25922 and *B. subtilis* cells exhibited strong filamentation in comparison to untreated control cells (Fig. 4.14A). Upon exposure to IITR06144, filamentous *E. coli* cells with cell size in the range 5-25 µm were observed, while untreated cells were only 1-2 µm long (Fig. 4.14). The *E. coli* morphology was also monitored by staining with membrane staining dye, FM 4-64FX and inhibition of septum formation in the elongated filaments was observed (Fig. 4.15).

(A)

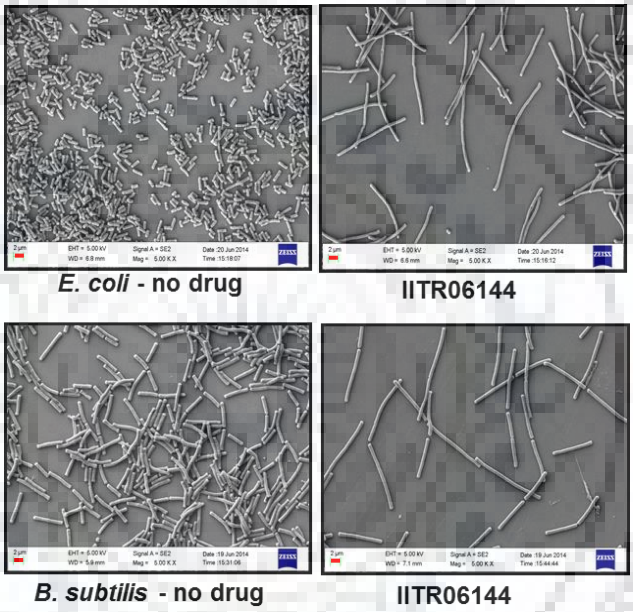

(B)

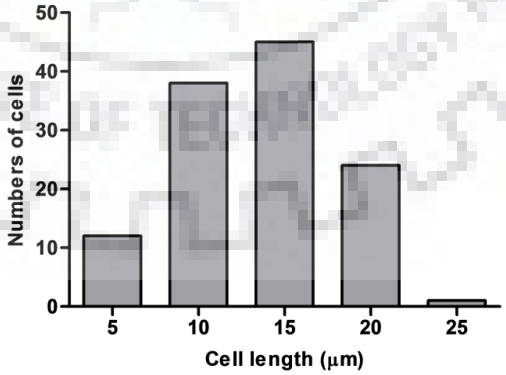

Figure 4.14 (A) Microscopy of *E. coli* ATCC 25922 and *B. cereus* cells with and without exposure to IITR06144 to study effect on cellular morphology. Scale bar is 2 µm (B) Frequency distribution of *E. coli* ATCC 25922 cell lengths after exposure to sub lethal concentration of IITR06144 for 2 h. Lengths of 120 cells from ten brightfield microscopic images were measured using ImageJ software.

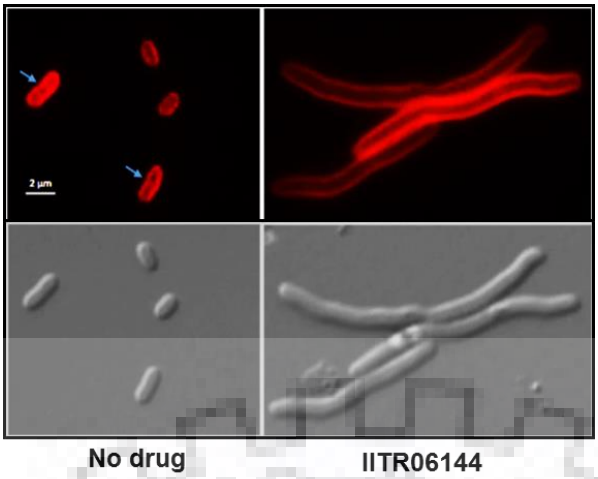

Figure 4.15: Effect of IITR06144 on septum formation. IITR06144 treated *E. coli* cells were stained with FM 4-64FX and visualised using fluorescent microscope. Respective brightfield image were also taken (bottom). Arrows indicate septa formation in untreated *E. coli* cells. Scale bar represents 2 µm.

Filamentation in bacteria is defined as the occurrence of anomalous growth when cells continue to elongate but cease to divide i.e. no septa formation occurs. The elongated cells are known to have multiple chromosomal copies since nucleoids continue to segregate and are regularly spaced along the filament. Filamentation may occur as a response to various stresses such as DNA damage eliciting the SOS response, partial inhibition of cell wall synthesis or inhibition of replication. An elongation phenotype in nitrofurantoin and furazolidone treated *E. coli* cells was also observed that has been previously attributed to the induction of SOS response upon treatment, thus leading to filamentation.

4.2.14 IITR06144 is a prodrug belonging to the nitrofuran class as revealed from whole genome sequencing of *in vitro* isolated *E. coli* mutant

The basic mode of action of nitrofuran antibacterials still remains largely unknown. Nitroaromatic compounds are considered as prodrugs since they are activated by the presence of intracellular reducing enzymes, which are specific to microorganisms. The reactive intermediates formed upon their reduction are further known to attack multiple targets within the bacterial cell such as ribosomal proteins, DNA, pyruvate metabolism, respiration machinery among other macromolecules. The biological activity and mechanism of these nitroaromatic compounds have been attributed to the redox potential of their 5-nitro groups. Nitrofurantoin and furazolidone display high redox potentials (−250 mV) whereas metronidazole

(nitroimidazole) exhibits low redox potential (−480 mV) and undergoes activation under anaerobic environment [243]. Considering the superior killing potential of IITR06144 over existing antibiotics in all the assays, it can be predicted to display a larger redox potential. Previous studies have demonstrated that the bacterial strains lacking the reducing enzymes display reduced susceptibility to nitrofurans, thus insinuating that enzymatic reduction is a prerequisite for their antibacterial activity [244].

Hence, the MIC of IITR06144 in *E. coli* Δ*nfsA*, which encodes for a major oxygen insensitive nitroreductase was evaluated. IITR06144 showed a 2-fold increase in MIC in *E. coli* Δ*nfsA* strain, thus validating its role as a prodrug antibacterial (Fig. 4.16). Similarly, nitrofurantoin and furazolidone also displayed 2 and 4 fold increase in MIC in *nfsA* mutant, in comparison to wild type respectively.

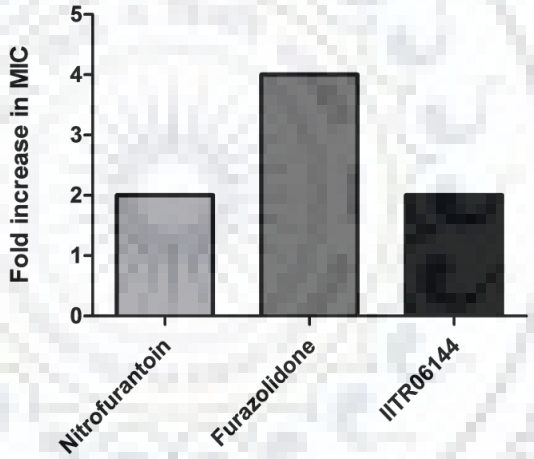

Figure 4.16: Relative MICs of IITR06144 and analogs in *E. coli* Δ*nfsA*. Fold change in MIC represents the average from three independent experiments.

Furthermore, in order to determine if IITR06144 may act through any specific target within the bacterial cells, an *E. coli* mutant displaying enhanced IITR06144 MIC (8 µg/mL) by the serial passaging method was isolated. The growth kinetics of the resistant mutant in comparison to wild type *E. coli* was further studied and the mutant was observed to display a growth defect (Fig. 4.17). The onset of growth in the resistant mutant exhibited a delay with a slower growth rate in comparison to the wild type strain, with an OD_{600} difference of 0.15 during the log phase at 37°C (Fig. 4.17).

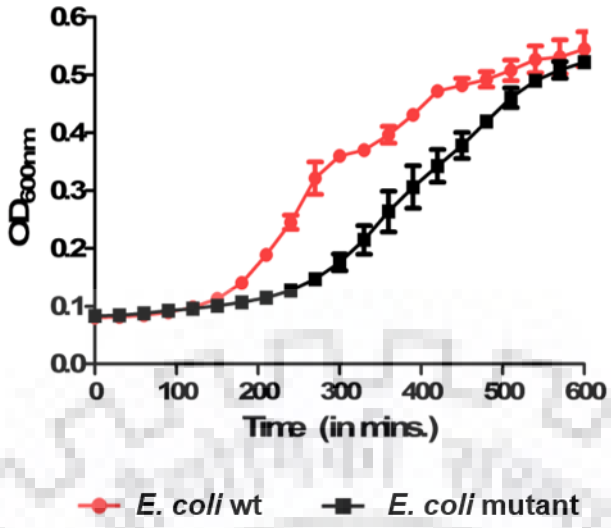

Figure 4.17: Growth curve of *E. coli* ATCC 25922 wild type in comparison to IITR06144 resistant mutant in the absence of IITR06144 at 37°C. Each value represents the mean of three values and error bars denote the standard deviation.

Further, the mutant was examined for the presence of cross-resistance to other antibiotics from related or different classes. Although the resistant mutant did not display cross-resistance to either nitrofurantoin or antibiotics from other classes, a modest 2 fold increase in MIC for furazolidone was observed (Table 4.8). Further, in order to assess the role of efflux pumps in acquisition of resistance to IITR06144, MIC of the mutant for IITR06144 was determined in presence of sub-inhibitory concentration of broad range efflux pump inhibitor, CCCP. Interestingly, CCCP (20µM) did not lead to reversal in IITR06144 MIC in the resistant mutant. This observation indicated that efflux pumps aren't involved in acquisition of IITR06144 resistance and that it is not a preferred substrate for efflux pumps.

Thereafter, whole genome sequencing of the mutant was performed to determine the presence of mutations in comparison to wild type strain. Although, the frequency of nitrofurantoin resistance in clinics is relatively low owing to its multi-targeting mode of action, resistance in *E. coli* has been primarily attributed to mutations in the genes *nfsA* and *nfsB*, that encode for oxygen-insensitive nitroreductases [245]. Interestingly, the isolated IITR06144 mutant did not show mutations in either of the two genes. However, an "in frame deletion" in the gene encoding for

Table 4.8: Cross resistance profile for IITR06144 resistant mutant for antibiotics representing varied chemical classes and mechanism of action.

	Cross resistance	Fold change
Nitrofurantoin	No	-
Furazolidone	Yes	2
Erythromycin	No	-
Fosfomycin	No	-
Ampicillin	No	-
Kanamycin	No	-
Tetracycline	No	-
Trimethoprim	No	-
Polymyxin B	No	-
Ciprofloxacin	No	-
Ampicillin	No	-
Rifampicin	No	-

Lumazine synthetase (*ribH*) at nucleotide positions 385-396, which has been recently implicated for *in vitro* nitrofurantoin resistance [341]. Lumazine synthase is an essential enzyme involved in flavin mononucleotide (FMN) biosynthesis, which acts as an important cofactor for bacterial reductases. Mutation observed in the *ribH* gene further confirmed the status of IITR06144 as a prodrug.

Several other missense and frameshift mutations were also observed that have been listed in Table 4.9 and Table 4.10. Considering the mutated genes to be putative direct targets, I also checked the susceptibility profile of few of these in *E. coli* knockout strains from the Keio collection. Surprisingly, most of these genes (such as *putC, cyoE, prpE, malJ, rpoS etc.*) displayed either no change or only a two-fold change in their susceptibility to IITR06144. This observation suggested that the mutated genes aren't the specific targets for IITR06144 but represent the off-target effects of IITR06144 i.e. mutations accumulated in the genome as a result of attack on multiple targets by the reactive reduced intermediates produced.

Table 4.9: Missense mutations observed in the IITR06144 resistant mutant upon whole genome sequencing.

	HGVS_ nomenclature	Amino acid Change	Reference	Altered	Gene Annotation/name
DR76_1272	c.1102G>A	p.Ala368Thr	C	T	degP_htrA_DO: peptidase Do family protein
DR76_1444	c.1168T>A	p.Trp390Arg	A	T	papC N-terminal domain protein
DR76_1452	c.706T>C	p.Trp236Arg	A	G	glutathionylspermidine synthase preATP-grasp family protein
DR76_1581	c.132C>G	p.Asp44Glu	C	G	conserved hypothetical protein
DR76_1801	c.277G>A	p.Ala93Thr	C	T	integrase core domain protein
DR76_2078	c.1197G>T	p.Leu399Phe	C	A	binding--dependent transport system inner membrane component family protein
DR76_2366	c.132G>C	p.Glu44Asp	C	G	conserved hypothetical protein
DR76_2585	c.383A>G	p.Glu128Gly	T	C	3-isopropylmalate dehydratase small subunit

DR76_2613	c.403T>A	p.Cys135Ser	T	A	integrase core domain protein
DR76_2648	c.795T>G	p.Ile265Met	T	G	T_den_put_tspse: conserved hypothetical family
DR76_2710	c.403A>T	p.Ser135Cys	T	A	integrase core domain protein
DR76_2710	c.199T>A	p.Tyr67Asn	A	T	integrase core domain protein
DR76_2763	c.130G>A	p.Gly44Arg	C	T	yjcZ-like family protein
DR76_2789	c.929C>T	p.Ser310Phe	G	A	glycosyl transferase 21 family protein
DR76_2922	c.908C>A	p.Ala303Asp	C	A	bacterial flagellin C-terminal helical region
DR76_3376	c.509T>C	p.Phe170Ser	T	C	inner membrane protein yddG
DR76_3395	c.830G>A	p.Arg277Gln	C	T	vgr_GE: Rhs element Vgr family protein
DR76_3395	c.791A>T	p.Tyr264Phe	T	A	vgr_GE: Rhs element Vgr family protein
DR76_3604	c.32T>C	p.Ile11Thr	T	C	periplasmic binding family protein
DR76_3825	c.136C>A	p.Arg46Ser	G	T	DNA polymerase III subunit delta
DR76_3826	c.591G>T	p.Met197Ile	C	A	dTMP kinase
DR76_3993	c.43G>A	p.Val15Ile	C	T	deoR C terminal sensor domain protein
DR76_4016	c.664A>C	p.Thr222Pro	A	C	bifunctional protein putA
DR76_4529	c.655A>G	p.Thr219Ala	A	G	cyoE_ctaB: protoheme IX farnesyltransferase
DR76_4542	c.392C>A	p.Thr131Asn	G	T	lumazine-synth: 6,7-dimethyl-8-ribityllumazine synthase

DR76_4605	c.764G>A	p.Gly255Asp	**C**	**T**	propionate--CoA ligase
DR76_4701	c.215T>G	p.Val72Gly	A	C	conserved hypothetical protein
DR76_4702	c.262A>G	p.Ile88Val	T	C	putative membrane protein
DR76_4703	c.7409T>C	p.Met2470Thr	A	G	adhes_NPXG: filamentous hemagglutinin family
DR76_4744	c.130A>G	p.Arg44Gly	A	G	yjcZ-like family protein
DR76_4952	c.704C>A	p.Ser235Tyr	C	A	

Table 4.10: Frameshift mutations observed in the IITR06144 resistant mutant upon whole genome sequencing.

	HGVS_ nomenclature	Amino acid Change	Reference	Altered	Gene Annotation/ name
DR76_208	c.309_313 delCGGTG	p.Gly 104fs	AGCACCG	AG	bacterial regulatory helix-turn-helix, lysR family protein
DR76_208	c.307_311 delATCGG	p.Ile 103fs	ACCGAT	A	bacterial regulatory helix-turn-helix, lysR family protein
DR76_524	c.15delA	p.Lys 5fs	GAAAAAAAA	GAAAAAAA	glpK Glycerol Kinase
DR76_1081	p.Phe518fs	c.1551 delT	CAAAA	CAAA	sigma-54 interaction domain protein
DR76_208	c.308_312 delTCGGT	p.Ile 103fs	CACCGA	C	bacterial regulatory helix-turn-helix, lysR family protein
DR76_1541	c.1440_1441 insTT	p.Asp 481fs	AT	ATTT	tetratricopeptide repeat family protein
DR76_1568	c.967delT	p.Phe 323fs	GAA	GA	inner membrane protein yeeR
DR76_1883	c.850dupG	p.Glu	CG	CGG	rpoS_proteo:

		284fs			RNA polymerase sigma factor RpoS
DR76_1965	c.414_415 insT	p.Lys 140fs	TAAA	TAAAA	conserved hypothetical protein
DR76_4015	c.1432delG	p.Ala 478fs	GC	G	sodium/proline symporter

4.2.15 IITR06144 causes bacterial DNA damage as observed by fluorescence microscopy, TUNNEL assay and use of *E. coli* mutants deficient in DNA repair

As discussed previously, reduction of nitrofuran prodrugs by bacterial flavoproteins (nitroreductase) is critical for their activation [244]. The highly activated species or intermediates thus produced hit multiple cellular targets leading to death. Bacterial DNA is a well-known target for these reduced intermediates speculated to undergo strand breakage [244]. As shown previously, IITR06144 treated *E. coli* cells exhibited an elongation phenotype which is indicative of the SOS response [246]. The SOS response involves a regulatory network of about 20 genes regulated by LexA and RecA that detect DNA damage leading to a halt in replication and division while repairing the DNA lesions [247]. Hence, induction of the SOS response in response to DNA damage causes cellular elongation phenotype in *E. coli* cells.

IITR06144, being a nitrofuran led to DNA fragmentation and occurrence of long and diffused nucleoids in drug treated *E. coli* cells as evident from DAPI staining in fluorescence microscopy (Fig. 4.18). TUNEL assay revealed that IITR06144 treatment led to DNA breaks and therefore enhanced incorporation of FITC-dUTPs in bacterial cells (Fig. 4.19).

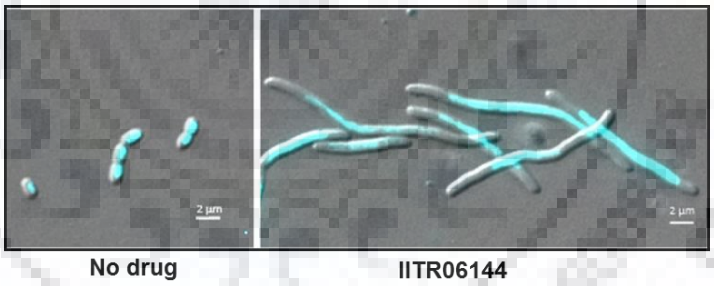

Figure 4.18: Fluorescence micrographs of *E.coli* ATCC 25922 cells treated with IITR06144 and stained with DAPI to study its effect on nucleoid. Image represents the overlay of individual brightfield and fluorescent images.

Furthermore, the susceptibility of *E. coli* mutants deficient in DNA repair mechanism to IITR06144 was determined. Consistent with previous reports, cells lacking *recA* and *uvrA* showed hypersensitivity to IITR06144 and also to its structurally related drugs, nitrofurantoin and furazolidone (Fig. 4.20) [248], [249]. This observation confirmed that IITR06144 exerts a lethal effect on bacterial DNA, which is repaired by the recombinational repair and excision repair mechanisms

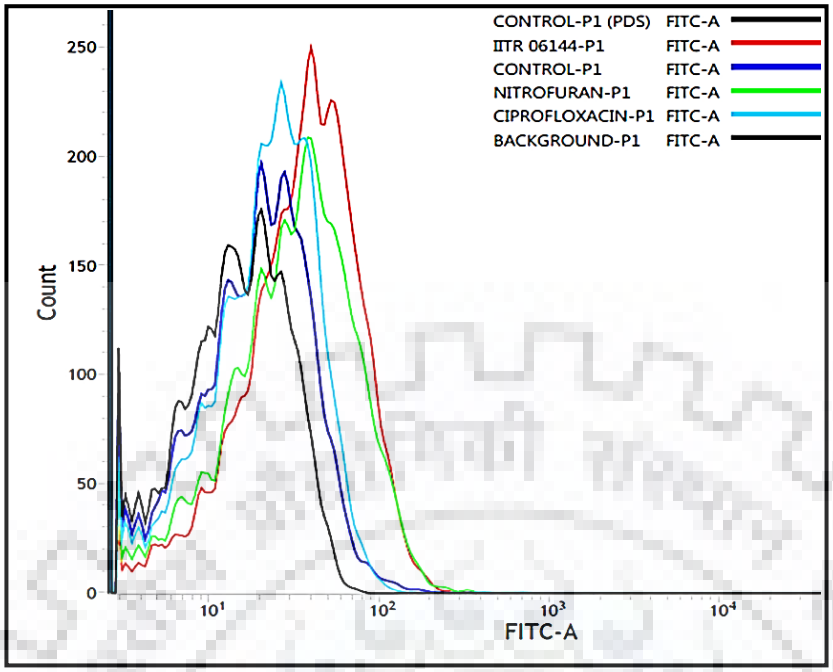

Figure 4.19: TUNEL assay coupled with flow cytometric analysis to quantify IITR06144 induced DNA damage in *E. coli* cells. *E. coli* cells were exposed to sub lethal concentration of IITR06144 for 2 hrs before TUNEL analysis. The x axis represents the relative FITC fluorescence, and the y axis (counts) is the number of cells. Nitrofurantoin and ciprofloxacin were taken as positive control antibiotics for the assay.

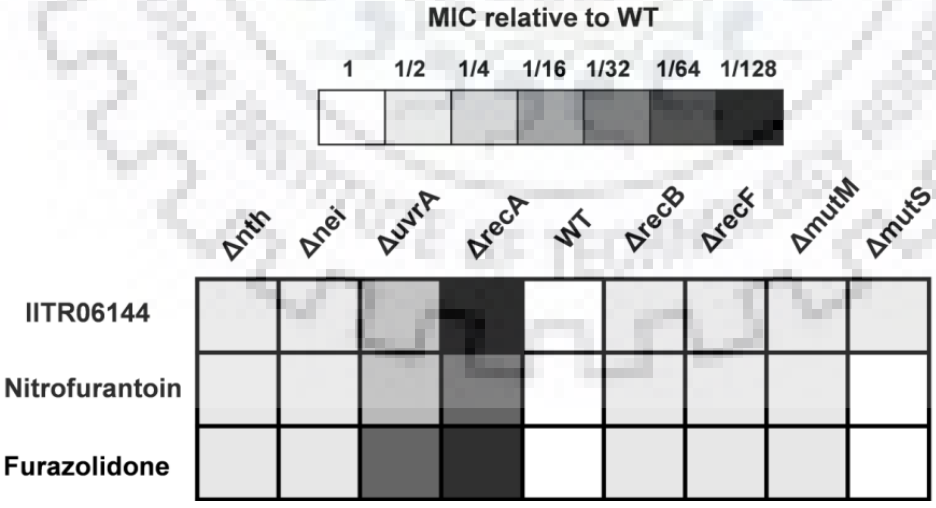

Figure 4.20: Heat map of relative MICs of IITR06144 in different *E. coli* mutants deficient in the DNA repair mechanism. Fold change in MIC represents the average from three independent experiments.

4.2.16 IITR06144 has no effect on the bacterial membrane potential

Membrane potential is an essential factor regulating the distribution of cell division proteins and their attachment to membrane [250]. Molecules that dissipate the transmembrane potential ($\Delta\Psi$) have been reported to perturb pathways modulating cell division and shape. Hence, it was further determined if the filamentous phenotype of IITR06144 treated cells was also a result of altered membrane potential apart from DNA damage. Drug treated cells were stained with the bis-oxonol dye $DiBAC_4$, which exhibits enhanced fluorescence upon membrane depolarisation. IITR06144 treated cells displayed fluorescence similar to control cells, in contrast to CCCP (10 µM), which is a known membrane potential inhibitor (Fig. 4.21). This observation suggested that IITR06144 did not exert its effect on *E. coli* morphology by dissipating the transmembrane potential.

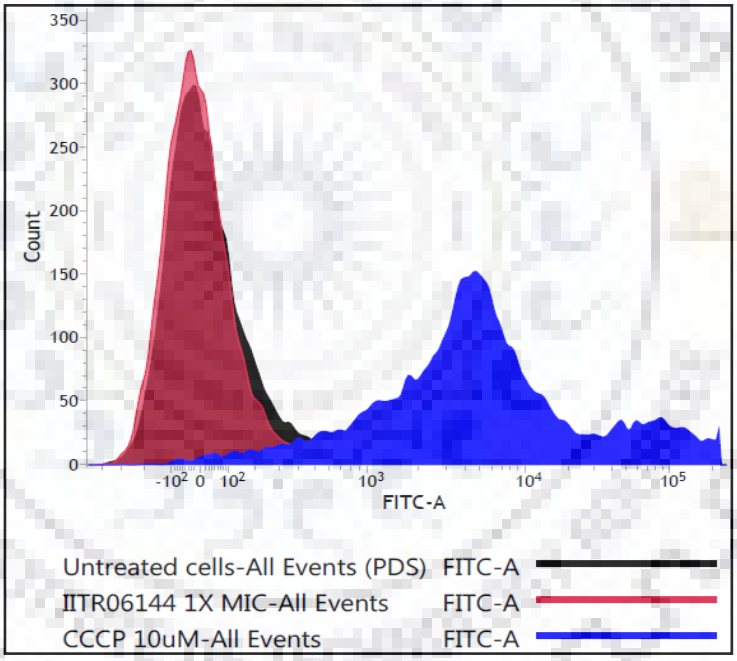

Figure 4.21: Effect of IITR06144 on bacterial membrane potential. *E. coli* ATCC 25922 cells were exposed to IITR06144 (1 µg/ml) and positive control, CCCP (10 µM) for 30 minutes. Upon further incubation with $DIBAC_4$ for 15 minutes, flow cytometry was used to determine fluorescence of IITR06144 treated cells with respect to untreated control.

4.2.17 IITR06144 causes a block in midcell Z-ring formation as evident from Immunofluorescence microscopy and Antisense studies.

The processes of DNA repair and cell division in *E. coli* are coordinated such that bacterial cells cease to divide until the damage has been repaired, as part of the SOS response [251]. Cell division in bacteria is executed by a macromolecular complex known as the divisome, where FtsZ protein plays a central role, localizing at the midcell forming Z rings and acting as a scaffold for assembly of cell division machinery[252]. The occurrence of replication inhibited or unsegregated nucleoids in *E. coli* cells is known to exhibit a block in cell division and inhibit midcell Z-ring formation [251]. Immunofluorescence microscopy using FITC-labelled Anti FtsZ antibody demonstrated extensive perturbation in the Z-ring morphology of IITR06144 treated cells, as a result of DNA damage (Fig. 4.22). Staining of IITR06144 treated cells with propidium iodide showed the presence of extensive DNA damage.

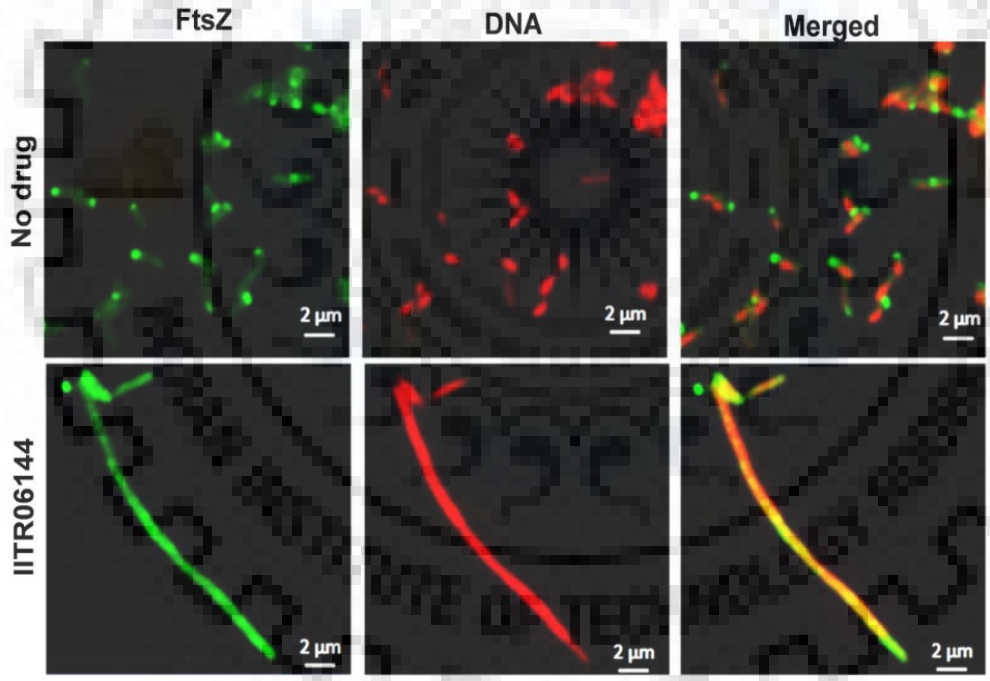

Figure 4.22: Subcellular localization of FtsZ in IITR06144 treated *E. coli* cells. The effect of IITR06144 on nucleoid segregation and Z-ring formation was studied by Immunofluorescence microscopy (IFM). Mid log *E. coli* ATCC 25922 were incubated with DMSO (vehicle) and 1.5ug/ml IITR06144 for 2 h. Cells were immunostained with polyclonal anti-FtsZ antibody followed by FITC-conjugated secondary antibody and nucleoids were visualized with Propidium iodide. IFM micrographs show localization of FtsZ (green) and nucleoids (red). This experiment was repeated thrice, and similar results were obtained.

In support of this observation, I further sought to find genetic evidence for effect of IITR06144 on the inhibition of Z-ring formation, by virtue of RNA silencing [253]. FtsZ antisense expressing construct, cloned in plasmid pHN678-FtsZ was transformed in *E. coli* BW25113 and antisense expression was induced by IPTG (70 µM). The susceptibility of the antisense expressing *E. coli* cells to FtsZ was determined by studying its growth profile in comparison to *E. coli* wild type strain carrying plasmid alone. The *E. coli* cells expressing ftsZ antisense were observed to display an increased sensitivity to low concentrations of IITR06144, thus corroborating that DNA repair and cell division are coordinated events (Fig. 4.23). *E. coli* cells expressing antisense of another essential gene, murA (plasmid pHN678-*murA*) served as a negative control for the experiment [254].

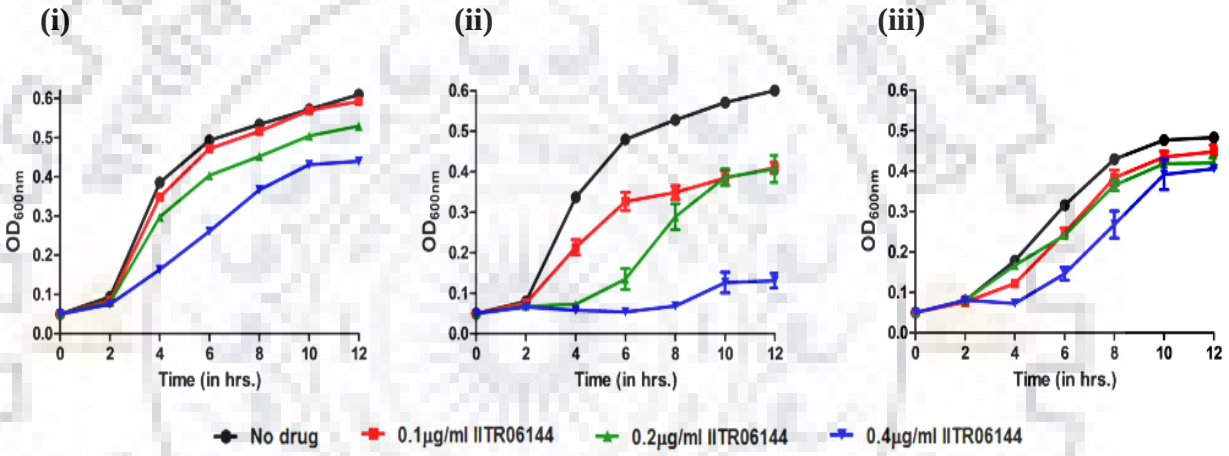

Figure 4.23: Effect of IITR06144 on growth of *E. coli* BW25113 expressing *ftsZ* antisense. *E. coli* cells expressing *ftsZ* Antisense (pHN678-*ftsZ*) was exposed to varying concentration of IITR06144 and growth was monitored spectrophotometrically at 600 nm. (i) Growth profile of control *E. coli* cells (*E. coli* BW25113-pHN678). (ii) FtsZ antisense expressing cells (*E. coli* BW25113-pHN678 *ftsZ*) (iii) murA antisense expressing cells (*E. coli* BW25113-pHN678 *murA*). Each value represents the mean of three values and error bars indicate standard deviation.

4.2.18 IITR06144 inhibits midcell Z-ring formation independent of SulA, MinC and SlmA

As discussed previously, cell division in bacteria is executed by the divisome complex, where FtsZ plays a central role, localizing at the division site and acting as a scaffold for assembly of cell division machinery [252]. SulA, accounts for most of the requirement for the SOS response, causing cell division to halt by sequestering FtsZ subunits, until genetic errors are corrected [252]. To investigate the possibility that IITR06144 may act indirectly through an

endogenous system of FtsZ assembly inhibition, such as the SOS-response activated SulA, the effect of IITR06144 treatment on the morphology of *E. coli* Δ*sulA* strain was examined. IITR06144 treatment resulted in cellular filamentation indistinguishable from that seen for the wild type bacteria, verifying that IITR06144 does not act through SulA for inhibiting cell division (Fig. 4.24). Two other proteins MinC and the nucleoid-occlusion factor, SlmA also act as endogenous inhibitors of cell division and regulate the positioning of Z-rings at midcell [252]. I further studied the effect of IITR06144 on the morphology of *E. coli* Δ*sulA*, Δ*minC* and Δ*slmA* cells. Microscopic studies revealed that these mutants exhibited inhibition of Z-ring assembly by IITR06144 which occurred independent of SulA, SlmA and MinC, as also reported previously for drugs mitomycin C and nalidixic acid [251] (Fig. 4.24).

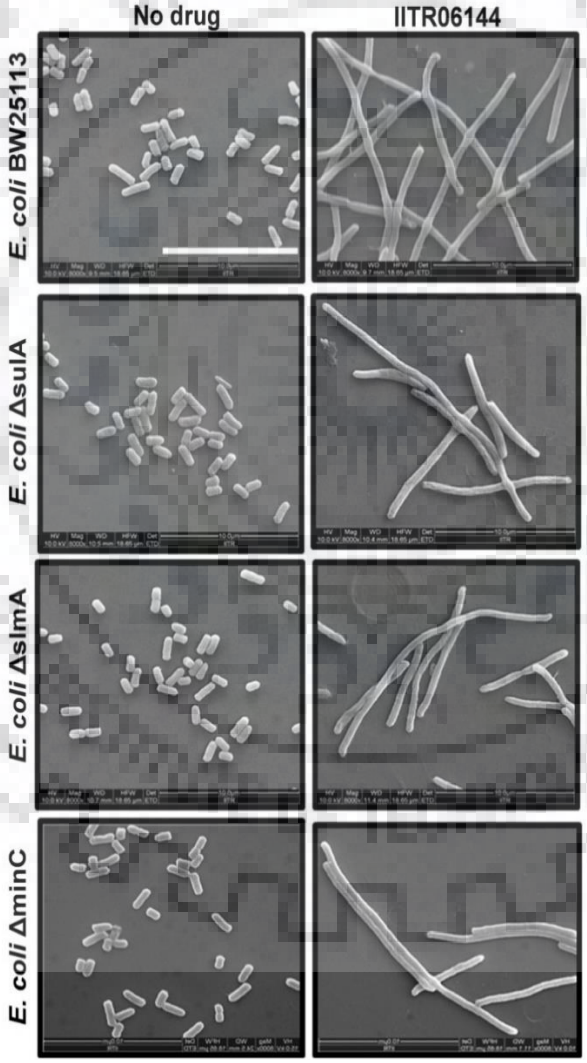

Figure 4.24: Effect of IITR06144 on cellular morphology of *E.coli* BW25113 wild type and *E. coli* Δ*sulA*, *E. coli* Δ*slmA*, *E. coli* Δ*minC* strains. Scale bar is 10μm. Shown are representative SEM micrographs of untreated and IITR06144 treated cells.

4.2.19 IITR06144 has no influence of FtsZ expression in treated *E. coli* cells

I came across a recent report on the antibacterial mechanism of natural product, resveratrol [273].The study reported resveratrol to exhibit a dual mode of action: it causes DNA fragmentation by induction of SOS response and also leads to cellular elongation, even in a SOS negative strain. Resveratrol was further established to suppress FtsZ expression (by immunoblotting) and hence Z-ring formation, regardless of induction of SOS response thus leading to cell death. Inspired by the study, I questioned if IITR06144 also might influence the expression of FtsZ in *E. coli* cells upon treatment. Hence, I performed Western blot using anti-FtsZ antibodies in *E. coli* cells upon treatment with IITR06144 (Fig. 4.25). As revealed by immunoblotting at increasing drug concentrations, IITR06144 seemed to have no effect on the expression of FtsZ in treated *E. coli* cells. Hence, I concluded that although IITR06144 induced DNA fragmentation independent of SOS, in a similar manner as of resveratrol but it did not induce cellular filamentation by decreasing FtsZ expression.

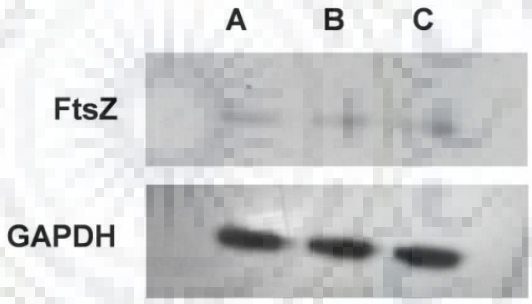

Figure 4.25: FtsZ expression levels measured by western-blot analysis. GAPDH was used an endogenous control for *E. coli* and FtsZ was detected using an anti-FtsZ antibody. Lane A) DMSO-treated cells were the negative control, no treatment. B) IITR06144 at 2.5X MIC C) IITR06144 at 4X MIC.

4.2.20 Reactive Oxygen Species (ROS) generation by IITR06144 is a consequence of damage to DNA and other macromolecules.

The effect of IITR06144 on ROS generation was evaluated using DCFDA as the oxidative probe [255]. As reported for bactericidal antibiotics, IITR06144 showed a dose dependent increase in fluorescence, suggesting that antibacterial killing by IITR06144 is followed by ROS generation. However, to ensure if ROS generation was actually a cause or consequence of cell

death, the growth pattern of *E. coli* cells supplemented with an antioxidant Vitamin C (5 mM) was analysed. Interestingly, pre-treatment of cells with Vitamin C did not preclude the inhibitory effect of IITR06144 (at 0.5 µg/mL) (Fig. 4.26). On the contrary, the antioxidant supplemented population showed a revival in growth when treated with methyl viologen (0.6 mM) (Inset: Fig. 4.26). This led us to conclude that ROS generation by IITR06144 was not the sole mechanism of bacterial death and was a consequence of the treatment.

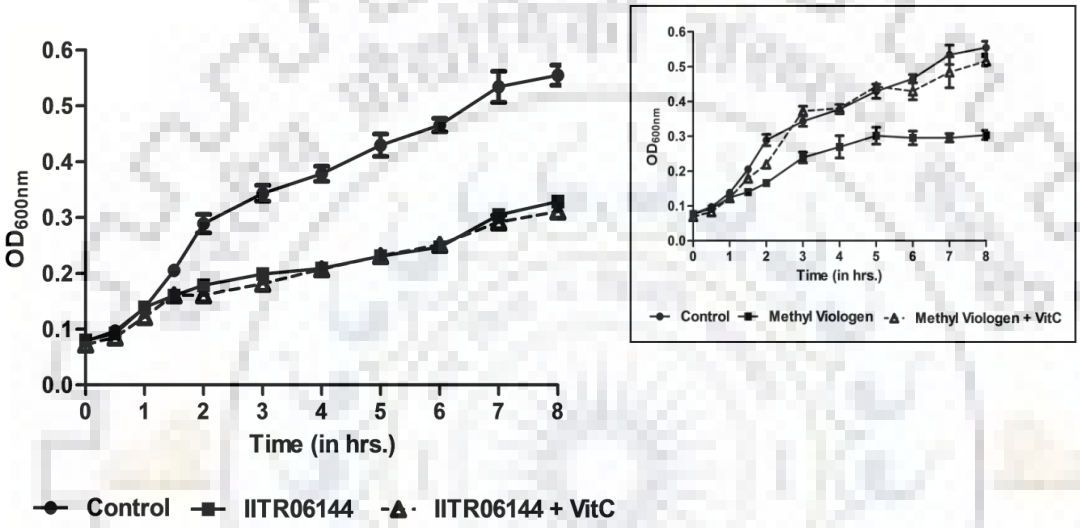

Figure 4.26: Growth profile of *E. coli* ATCC 25922 cells pretreated with Vitamin C (5 mM) in the presence of IITR06144. Box: Growth curve of Vitamin C pretreated *E. coli* cells in the presence of Methyl viologen (900 µM). Each value represents the mean of three values and error bars indicate standard deviation.

4.2.21 IITR06144 exhibits considerable efficacy and no *in vivo* toxicity in *A. baumannii* infection model

Encouraged by its potent *in vitro* antibacterial activity, I proceeded to evaluate the *in vivo* efficacy of IITR06144 in mice model of systemic infection. Initially, I assessed the toxicity of IITR06144 at an oral dose of 50 mg/kg body weight (mg/kg b.w.) in comparison to nitrofurantoin. All the drugs were administered to mice for 5 days and were regularly monitored for presence of adverse symptoms or mortality. The serum biochemical data did not show much difference between the IITR06144 and nitrofurantoin treatment groups, except for the increased levels of alkaline phosphatase (SGPT), and triglycerides in IITR06144 treated mice. In contrast, nitrofurantoin treatment showed increased cholesterol levels at similar dose (Table 4.11). Further, mice were challenged with MDR *A. baumannii AYE* and bacterial load in various organs upon IITR06144 treatment at varying doses was determined. IITR06144 (dose range: 50 to 6.25 mg/kg b.w.) showed a dose-dependent reduction in bacterial burden in the organs spleen, lung, kidney and liver (Fig. 4.27). At dosage, 25 mg/kg b.w., IITR06144 lowered the bacterial load in spleen ($p < 0.01$), in kidney ($p < 0.01$), liver ($p < 0.001$) and lung ($p < 0.001$) in comparison to the control group. In comparison, nitrofurantoin similarly reduced the bacterial infection but at a higher dose (i.e. 50 mg/kg b.w.).

Table 4.11: Biochemical parameters for assessment of *in vivo* toxicity of IITR06144 at oral dosage of 50 mg/kg b.w.

Serum components	Control	IITR06144	Nitrofurantoin
Bilirubin (mg/dl)	1.029±0.05	0.97±0.04	1.05±0.05
Creatinine (mg/dl)	0.538±0.15	0.384±0.16	0.42±0.1
Cholesterol (mg/dl)	30.85±2.1	24.87±5.4	35.24±2.3
Triglycerides (mg/dl)	20.34±0.05	31.54±0.15	20.34±0.17
ALP (IU/L)	3.32±1.2	4.52±0.85	6.1±1.34
AST or SGPT (IU/L)	6.48±0.05	9.63±1.5	5.89±1.9
ALT or SGOT(IU/L)	10.4±0.5	8.45±0.3	9.63±1.2

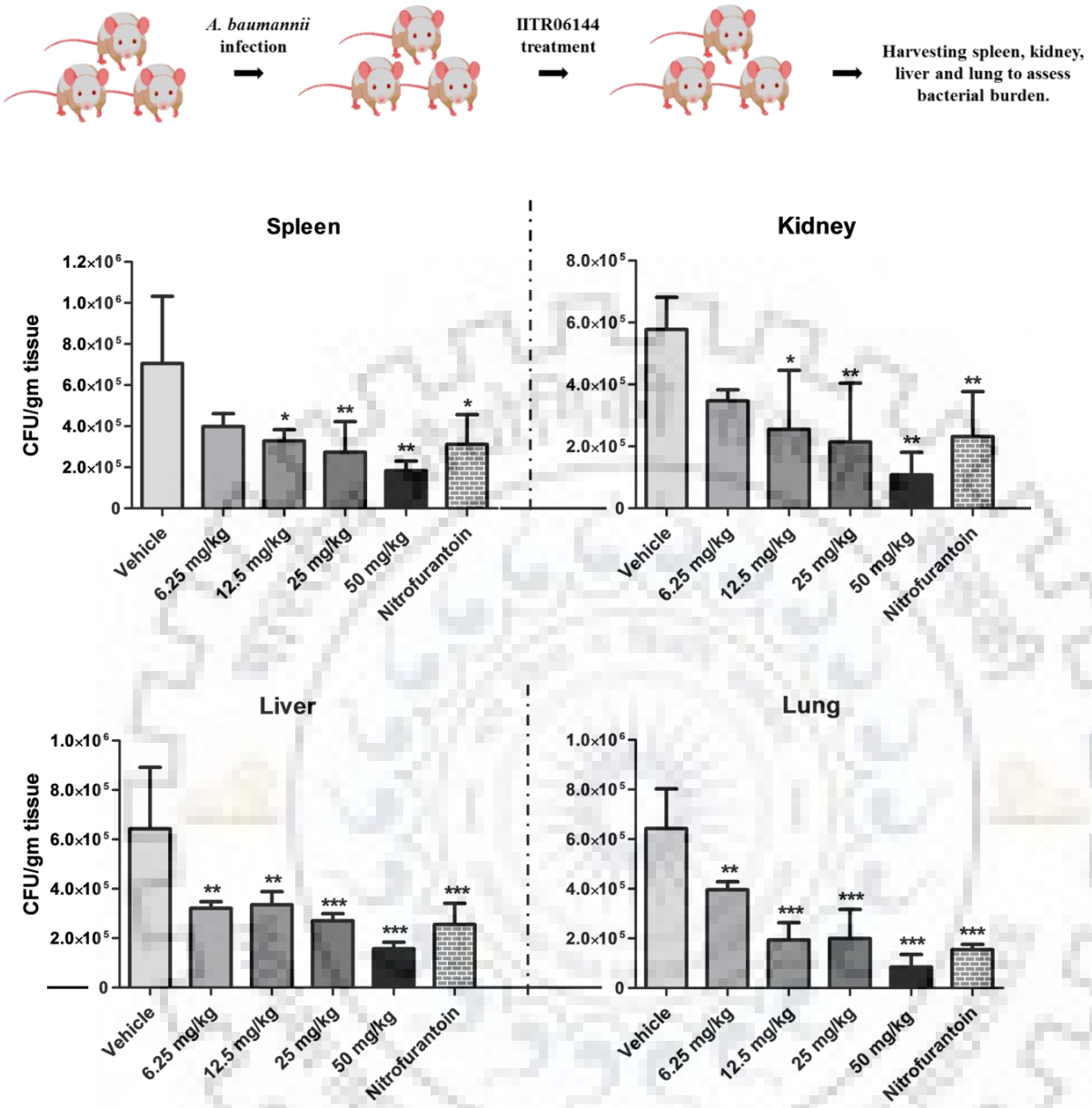

Figure 4.27: *In vivo* efficacy of IITR06144 in mice model of MDR *A. baumannii* systemic infection. IITR06144 at different doses was administered in *A. baumannii* AYE infected mice (n=5). After 4 days of drug dosing, mice were sacrificed and the bacterial burden in the organs (spleen, kidney, liver and lungs) was determined. The group of mice receiving vehicle only served as control. The y axis corresponds to the bacterial CFU obtained per gram of tissue. The *x* axis indicates the amounts of IITR06144 tested (mg/kg b.w.). Nitrofurantoin was administered at concentration 50 mg/kg b.w. P values were obtained using one-way ANOVA and Dunnett's multiple comparison test (*, P<0.05; **, P<0.01; ***, P<0.001). Error bars show standard deviation from five mice per treatment group.

4.3 Discussion

Antibiotic resistance is a global problem exemplified by the spread of resistance genes such as carbapenemases and emergence of clinical resistance to the "drug of last resort", colistin [49]. The pace of antibiotic discovery has inadvertently failed to keep up with the mounting crisis of antibiotic resistance and recalcitrant chronic infections. With the precipitous decline in drug development, attempts to either create or re-establish new antibiotic discovery platforms are continually being made [44]. Screening for novel prodrugs is one such attractive approach because of their selective toxicity towards microorganisms possessing specific activating enzymes. Prodrugs were originally discovered in the 1950s but were eventually discarded due to their lack of specificity and availability of newer or better antibiotics. Lack of novel scaffolds catering to the needs of drying antibiotic pipeline has led to a renewed interest into prodrug synthesis and discovery. Prodrugs are theoretically considered to be "ideal" antibiotics, owing to their broad spectrum activity, non-toxicity and ability to target both growing and dormant persister cells. 5-nitro antimicrobials such as those belonging to the nitrofuran, nitroimidazole and nitrothiazole classes are common examples of prodrug antibacterials [256]. Approximately 650 diverse 5-nitroimidazole compounds were recently reported with enhanced activity against a wide range of microbes, starting from the bacterial pathogen *Bacteroides fragilis* to the protozoan *Trichomonas vaginalis* [256]. Fleck et al performed a pilot screen for prodrug and identified three hits with excellent properties [257]. Moreover, nitroimidazoles and nitrofurans form much of the core of the anti-TB armamentarium targeting dormant TB bacilli [258],[259].

To address the lack of new antibacterials and need for compounds that can penetrate the complex envelope system of Gram negative bacteria, a small molecule screening of 11,000 compounds was performed against *E. coli.* The screen identified 30 antibacterial hits, out of which 4 molecules with significant antibacterial activity were observed to contain the nitrofuran nucleus. Thus, the screen worked in our favour and led to the serendipitous discovery of novel prodrugs from the nitrofuran class. The lead compound IITR06144 was studied extensively and found to exhibit excellent activity against all the Gram negative pathogens with MIC as low as 0.12 µg/mL, except for *P. aeruginosa* which are intrinsically resistant to nitrofurans. The antibacterial spectrum of IITR06144 was limited not only to the Gram negative pathogens but could also inhibit the Gram positive pathogens and mycobacterium spps studied. IITR06144 inhibited all the clinical isolates tested, inspite of their

resistance to nitrofurantoin, furazolidone, meropenem, ciprofloxacin, amikacin etc. with MICs in the range 0.12 - 2 µg/mL. Anaerobic bacteria are also known to cause life threatening infections and clinical resistance to commonly administered antibiotics metronidazole, piperacillin-tazobactam and meropenem have been reported. Interestingly, IITR06144 outcompeted metronidazole, nitrofurantoin and furazolidone against all the anaerobic isolates tested, with MICs in the range 0.06 – 0.25 µg/mL. Thus, IITR06144 holds great potential for the treatment of mixed aerobic and anaerobic infections, which routine empiric therapy fails to inhibit.

IITR06144 is structurally related to nitrofurantoin, an old antibiotic approved by FDA in 1953. Nitrofurantoin has undergone revival as a first line of treatment for uncomplicated UTIs, with increasing resistance to trimethoprim/sulfamethoxazole, fluoroquinolones concomitant with the rise in ESBL (Extended Spectrum Beta-lactamase) producing and carbapenem resistant bacteria [233]. The emergence of resistance to nitrofurantoin is relatively infrequent, owing to its multitargeting mode of action. However, with rampant empiric use and increase in over the counter sales, resistance as high as 34.3% have been reported in India[260]. Moreover, nitrofurantoin is ineffective against persistent uropathogenic *E. coli* infections and frequent cases of infection relapse have been reported [207].

In comparison to nitrofurantoin, IITR06144 showed a superior killing ability and rapid bactericidal nature against *E. coli* cells. IITR06144 displayed a longer PAE and a lack of cross resistance or antagonism to clinically relevant antibiotics. IITR06144 eradicated UPEC associated biofilms which are responsible for causing recurrent UTIs. IITR06144 also remarkably inhibited the dormant persister cells both in stationary phase and antibiotic induced environment, unlike nitrofurantoin and furazolidone. Moreover, in compliance with the multimodal mechanism of nitrofurans, it did not show any propensity towards the generation of single step resistant mutants. Hence, IITR06144 was observed to out-compete the existing nitrofuran antibiotics in most of the aspects studied.

Nitrofurans are known to act by inhibiting synthesis of DNA, RNA, glucose metabolising enzymes etc., out of which bacterial DNA has been considered as the major target[261]. *E. coli* nitroreductases reduce the nitroheterocyclic compounds into active metabolites that further cause DNA breakage [248]. The prodrug status of IITR06144 was confirmed by sequencing an isolated *E. coli* mutant with increased IITR06144 MIC which revealed mutation in lumazine

synthase (*ribH)* gene, which is responsible for cofactor synthesis required by reducing enzymes. Morphology studies further revealed a filamentous phenotype, which is a characteristic of SOS response and *E. coli* mutants of the DNA repair pathway showed hyper susceptibility. Hence, IITR06144 was observed to work through the canonical mode of action of nitrofurans. However, IITR06144 remarkably inhibited the nitrofurantoin resistant clinical isolates and no mutations were observed in the *nfsA* or *nfsB* genes of the *in vitro* mutant. Hence, IITR06144 could effectively overcome nitrofurantoin resistance and therefore can be postulated to (i) undergo activation by alternative pathways, which are not involved in nitrofurantoin resistance or to (ii) bypass general pathways involved in nitrodrug detoxification and (iii) overcome efflux mechanisms displayed by resistant isolates in the clinic [256].

IITR06144 caused elongation in an SOS negative strain and inhibited the Z-ring formation independent of SlmA and MinC proteins, as also shown for the drugs nalidixic acid, mitomycin c and hydroxyurea. Fluorescence microscopy and RNA silencing studies further revealed the disruption of coordination between DNA replication and cell division in *E. coli* cells treated with IITR06144. IITR06144 also proved efficacious in a murine model of septicemia against *A. baumannii* exhibiting reduction in bacterial burden in mice organs. The relatively modest *in vivo* efficacy of IITR06144 can be attributed to the lack of *in vivo* pharmacokinetic data that could have helped to decide dosing regime and route of administration. Studies to assess the *in vivo* pharmacokinetic parameters of IITR06144 will be undertaken in future followed by efficacy studies in mice models of urinary tract infection, wound infection and diarrhoea.

In summary, the results suggest that IITR06144 is a promising novel antibacterial molecule which is more potent than nitrofurantoin against aerobic and anaerobic Gram-negative and Gram-positive bacteria, including multidrug-resistant bacteria. No cross-resistance with antibiotics nitrofurantoin and furazolidone has been observed in the clinical strains. Further studies to determine the feasibility of IITR06144 as a therapeutic agent are warranted.

4.4 Experimental Procedures

4.4.1 Chemicals

The small molecule library was procured from Maybridge (Trevillett, UK). All antibiotics were purchased from Sigma-Aldrich (St Louis, MO, USA). Enzymes, dyes and molecular biology chemicals were purchased from Thermo Fisher Scientific (Waltham, MA, USA). Fluorescein (*FITC*) conjugated secondary antibody was purchased from Jackson ImmunoResearch Laboratories Inc. (PA, USA) and Dimethyl Sulfoxide (DMSO) was procured from Merck, Germany.

4.4.2 Bacterial strains and growth conditions

Strains of *Escherichia coli, Acinetobacter baumannii, Staphylococcus aureus, Salmonella enterica* subsp *enterica* Serovar Typhimurium, *Vibrio fluvialis* and others were grown in Mueller-Hinton broth (Merck, Germany). *Mycobacterium* strains were grown in Middlebrook 7H9 broth (HiMedia, India) supplemented with 10% OADC, 0.5% glycerol and 0.05% Tween-80 and Middlebrook 7H10 Agar (HiMedia, India) supplemented with 0.5% glycerol and 10% OADC as the solid medium. All strains were grown at 37°C with aeration at 180 rpm unless otherwise indicated. Strains of *Clostridium difficile, Bacteroides fragilis, Clostridium tetani and Clostridium perfringes* were maintained on Brain Heart Infusion (BHI) agar (HiMedia, India) containing 5% sheep blood under anaerobic conditions (80% nitrogen, 10% carbon dioxide and 10% hydrogen) at 37ºC in anaerobic workstation (Don Whitley scientific, UK). *Lactobacillus* strains were grown in MRS (deMan, Rogosa and Sharpe) broth (Difco, USA) at 37ºC under static conditions. *Streptococcus thermophilus* was grown in MRS medium at 42°C while *Leuconostoc mesenteroides* was grown at 30°C in M17 medium. Chloramphenicol antibiotic was used at 30 µg/mL for *E. coli* BW25113 in antisense studies. *E. coli* strains from the Keio collection were grown on LB (Luria-Bertani) medium agar plates containing 15 µg/mL kanamycin. All the strains, plasmids and primers used in the study are described in Appendix Table A1, A2 and A3.

4.4.3 Determination of Minimum Inhibitory Concentration (MIC)

MICs of small molecules and various antibiotics against *E. coli* ATCC 25922 were determined by the broth microdilution method in Mueller–Hinton medium, as per the CLSI guidelines. MICs of small molecules and various antibiotics against *E. coli* ATCC 25922 (10^5 CFU/mL)

was determined in 96-well plates and incubated at 37°C in static condition in a humidity controlled incubator (Kuhner LT-X). Growth was monitored after 12 h of incubation by reading absorbance at 600 nm. The lowest concentration of antibacterial which displayed no visible turbidity was considered its MIC. The MICs of IITR06144 and its comparative antibiotics against the anaerobic strains were determined by the agar dilution method, according to CLSI guidelines [262]. Briefly, serial 2-fold dilutions of the antibiotics were prepared and added to Brucella agar (HiMedia) supplemented with vitamin K1 (0.5 mg/L), haemin (5 mg/L) and 5% laked sheep blood. The bacterial inoculum was prepared equivalent to 0.5 Mc Farland and spotted (10 µl) onto the plates such that final inoculum is 10^5 CFU/spot. Plates were incubated at 37ºC in an anaerobic workstation and examined after 48 h. For MIC determination in *Mycobacterium* strains, cultures grown in Middlebrook 7H9 broth until OD_{600}~1 were 100 folds diluted in fresh medium and added to 96-well plates containing drugs. Plates were read at OD_{600} after 7 days of incubation at 37ºC in a humidity controlled incubator.

4.4.4 Time Kill Kinetics assay

To evaluate the bactericidal potential of IITR06144, the time-kill kinetics assay was performed as described earlier [10],[160]. *E. coli* ATCC 25922 cells (10^5 CFU/mL) were treated with IITR06144, nitrofurantoin and furazolidone at 2X MIC. 100ul aliquots were withdrawn at regular intervals and serial dilutions were plated onto MH agar plates. Plates were incubated at 37ºC under static condition and colony counts were determined after 24 h. Bacterial killing was assessed by plotting the mean viable counts (as $\log_{10}$ CFU/mL) versus time (in h).

4.4.5 *In vitro* Post-Antibiotic Effect (PAE)

Logarithmic phase *E. coli* ATCC 25922 cells (10^6 CFU/mL) were exposed to IITR06144 and comparative antibiotics at 5X MIC for 1 h in shaking condition at 37°C [160],[263]. Following the incubation of *E. coli* ATCC 25922 cells with IITR06144 and other antibiotics at 5X MIC, cells were centrifuged for 10 min at 4000 rpm at room temperature to remove the traces of drug. The cells were washed twice with 1X PBS and resuspended in fresh medium followed by further incubation at 37°C. At definite intervals after drug exposure (0, 1, 2, 3, 4, 5, 6, 7, 8 h), viable bacterial counts were determined by plating serial 10-fold dilutions on MH agar plates. The PAE was determined by the formula PAE = $T - C$ where, T is the time taken for unit $\log_{10}$ increase in inoculum (CFU/mL) versus the inoculum (CFU/mL) observed immediately after

antibiotic removal; and *C* is the time it takes to observe a $\log_{10}$ increase (CFU/mL) in an untreated control.

4.4.6 Determination of Frequency of Resistance (FOR)

The emergence of spontaneous resistance in *E. coli* ATCC 25922 against IITR06144 and nitrofurantoin was determined as described previously [160],[264]. 100 µL aliquot of (1×10^9 CFU/mL) *E. coli* cells were plated on MH agar plates containing drugs (at 4X MIC) in triplicates. The plates were incubated for 48 h at 37ºC in static conditions in a humidity controlled incubator. The colony count of the initial inoculum was verified by plating serial dilutions onto MH agar plates. The frequency of resistance was determined by dividing the average number of colonies obtained after 48 h on drug containing plates by the initial inoculum.

4.4.7 Haemolysis assay

Haemolytic activity of IITR06144 was assessed as described previously, with slight modifications [265]. Fresh human blood (10 mL) was extracted in a vaccutainer blood collection tube (Thomas Scientific) and centrifuged at 2500 rpm for 10 min. The supernatant was discarded, and the pellet was washed thrice with 1X PBS. The pellet was then diluted 1:5 (vol/vol) in 1X PBS and RBC suspensions (1 mL each) were incubated with varying concentration of IITR06144 and comparative antibiotics under at 37°C under static condition. The time of incubation was increased to 4 h instead of 35 minutes in the reference followed. The suspensions were then centrifuged at 2500 rpm for 10 min and the supernatant was carefully collected without disturbing the pellet. Haemolysis was monitored by measuring the absorbance of the released hemoglobin in the supernatant at 540 nm using a spectrophotometer. Triton-X 100 (0.1%) served as the positive control for the assay. Haemolysis levels were calculated by the formula: $100 \times (At - As)/Ac$ where Ac, As, and At are the absorbance of Triton-X 100, absorbance of solvent control and absorbance of the sample containing drug respectively. All experiments were performed in triplicates.

4.4.8 *In vitro* cytotoxicity

The cytotoxicity of IITR06144 on Peripheral Blood Mononuclear Cells (PBMCs) was determined by 3-(4,5-dimethylthiazol-2-yl)-2,5-diphenyl tetrazolium bromide (MTT) assay as described previously [266]. For cytotoxicity assay, Fresh PBMCs were isolated using HiSep™ LSM 1077 (Himedia) as per recommended protocol [267]. $2x10^6$ cells resuspended in Roswell

Park Memorial Institute medium (RPMI) with 10% fetal bovine serum (FBS) and L-glutamine were added to tissue culture treated 96-well plates (Nunc) for 24 h. Cells were then incubated in the presence of varying concentrations of IITR06144, nitrofurantoin and furazolidone at 37°C for 8 h in 5% CO2. Control cells were treated with similar percentage of dimethyl sulphoxide (DMSO) as in drug (vehicle control) The medium was then aspirated and 100 µl of 1X PBS containing 0.5 mg/mL MTT (Biobasic) dye was added to each well and incubated further for 4 h. Following incubation, MTT containing medium was removed and 100 µL of DMSO was added to dissolve the formazan crystals by gentle agitation. The OD was measured at 570 nm in a plate reader (Biotek). Absorbance values were expressed as percentage and inhibition with respect to solvent control was calculated.

4.4.9 Antibacterial activity against stationary phase cells and antibiotic exposed persister cells

Stationary phase bacterial culture and antibiotic exposed persisters were obtained by protocols described previously [257],[268]. *E.coli* ATCC 25922 cells grown to 0.5 OD_{600} in LB medium were diluted 100 times in fresh medium and grown for 16 h until they reach stationary phase. These were then divided into 1 mL aliquots in triplicates and subsequently treated with different concentrations of IITR06144, nitrofurantoin and furazolidone ranging from 25-200 µg/mL for 24 h in a shaker incubator. In case of control, the same volume of the solvent DMSO was added instead of the test antibiotic. The mean viable colonies were determined and represented as CFU/mL. In order to assess the membrane integrity of IITR06144 treated population which did not yield any culturable colonies on agar plates, fluorescence microscopy was carried out using the combination of two dyes. Treated *E. coli* cells were harvested and stained with membrane dye FM™ 4-64FX (1 µg/mL) and nucleoid stain Sytox green (1 µM) at room temperature for 15 minutes. A small volume (5µl) of cells was deposited on agarose pad and sealed with a clean coverslip. The cells were then observed under a Zeiss Axioscope A1 fluorescence microscope equipped with an AxioCam MRC digital camera using EC Plan-Neofluar 100X objective to assess viability.

Further, to determine the formation of antibiotic induced persister cells, stationary phase *E.coli* cells (from a 14 h old culture) were treated with 300 µg/mL ampicillin in LB medium for 24 h at 37 °C under shaking condition. Aliquots were withdrawn at regular intervals to determine the number of viable bacteria that survived ampicillin exposure. For the treatment of *E.coli*

persisters with IITR06144 and comparative antibiotics, ampicillin exposed cultures after 14 h of treatment were centrifuged and washed thrice with 1X PBS to remove any antibiotic traces. Isolated persisters were then resuspended in 1X PBS diluting upto four times the original volume. Ampicillin (100 μg/mL), Kanamycin (50 μg/mL), IITR06144, nitrofurantoin and furazolidone were added to each 1000 μL aliquot of persister cells at indicated concentrations followed by incubation at 37 °C for 24 h at 180 rpm. Control containing similar volume of solvent instead of compound or antibiotics was included. The viable colonies were determined after 24 h of incubation and represented as Log CFU/mL. Kill kinetics assay to study the rate of killing of persisters by IITR06144 (2X-8X MIC) was performed simultaneously by withdrawing aliquots at regular intervals to determine the viable cell count.

4.4.10 Biofilm inhibition and disruption assay

Biofilm formation by *E. coli* MTCC 4296 in the presence of IITR06144 and comparative antibiotics was assessed by crystal violet assay [118]. Disruption of preformed biofilms after 12h of IITR06144 treatment was studied, as described previously with slight modifications [257]. Log phase *E. coli* cells (OD_{600}~0.6) were 100 times diluted and added to 96-well microtiter plate containing test drugs at sub-inhibitory concentrations. Plates were kept under static condition in a humidity controlled incubator at 37°C for 48 h. Plates were then read at 600 nm and washed thrice with 1X PBS to remove the planktonic cells. Following fixation at 65ºC for 30 minutes (min), biomass was stained with 0.25% (w/v) crystal violet in methanol: 1X PBS (1:3) for 20 min. Following two brief washing steps, biofilms were quantified by addition of 33% acetic acid in methanol to dissolve the crystal violet adhered to biofilm forming biomass. Plates were read at 595 nm and relative absorbance ($OD_{595/600}$) was calculated. For studying the effect of IITR06144 on preformed biofilms, 48 h old *E. coli* MTCC 4296 biofilms made in 96-well plate as described above were treated with IITR06144 and comparative antibiotics at different concentrations (1X, 2X and 4X MIC). After 12 hrs of drug treatment, biofilms were washed twice and scraped using 0.5% triton-100 in 1X PBS. Viable count was determined in drug treated wells and compared to control wells exposed to similar volume of solvent (DMSO). For fluorescence microscopy studies on the effect of IITR06144 on preformed biofilms, *E. coli* MTCC 4296 was transformed with plasmid pNYL-GFP, a pZE21 derivative that constitutively expresses the green fluorescent protein. Biofilms made on coverslips for 48 hrs were treated with increasing concentrations of IITR06144 and visualised under Carl Zeiss fluorescence microscope.

4.4.11 *In vitro* interaction with antibiotics

In vitro interaction of IITR06144 with antibiotics was evaluated in *E. coli* ATCC 25922 by modified broth checkerboard assay as described previously [160],[166]. For determination of *in vitro* synergy, two fold serial dilutions of IITR06144 in combination with dilution of several antibiotics (one from each class) were prepared in a 96-well plate. Log phase bacteria at OD_{600} ~0.6 were 1000 times diluted and 100 µL of the inoculum was added to each well of the assay plate. Plates were then incubated for 16 h at 37ºC. Fractional inhibitory concentration index (FICI) was calculated using the formula [MIC of drug B in presence of drug A] / [MIC of drug B] + [MIC of drug A in the presence of drug B] / [MIC of drug A]. FICI scores were interpreted as follows: synergy (≤0.5), no interaction (0.5–4), or antagonism (4). For each drug combination, FICI ranges were reported from two biologically independent experiments.

4.4.12 Visualization of morphological changes in bacteria

Morphological changes in *E. coli* cells incubated with IITR06144 at sub-inhibitory concentration were observed under Scanning Electron Microscope (SEM) and fluorescence microscope [28]. Logarithmic phase *E. coli* cells (OD_{600} ~0.6) were diluted to OD_{600} ~0.1 and treated with sub-inhibitory concentration of the drug for 2 h. Treated samples were washed in 1X PBS and primarily fixed with 2.5% glutaraldehyde for 30 minutes at 4°C. Fixed cells were further dehydrated with an ethanol gradient (20%, 40%, 60%, 80%, 90% and 100%). The samples were then coated with a layer of gold and visualized under SEM.

For fluorescence microscopy, treated *E. coli* cells were harvested and fixed with 4% paraformaldehyde followed by staining with membrane dye FM™ 4-64FX (1 µg/mL) or nucleoid stain DAPI (0.3 µM) at room temperature for 15 minutes. A small volume (5µl) of cells was deposited on agarose pad and sealed with a clean coverslip. The cells were then observed under a Zeiss Axioscope A1 fluorescence microscope equipped with an AxioCam MRC digital camera using EC Plan-Neofluar 100X objective.

4.4.13 Isolation and whole genome sequencing of resistant mutant

E. coli mutant displaying increased MIC for IITR06144 was isolated by serial passaging method [269]. For the serial passaging studies, 1% inoculum of stationary phase culture of *E. coli* ATCC 25922 was added to tubes containing 3 mL fresh MH medium in the presence of 0.5 µg/mL (1X MIC) IITR06144 for 24 h at 37°C under shaking conditions at 180 rpm [269]. For

the second passage, the cells that survived the first exposure to IITR06144 were subsequently sub cultured (1% inoculum) into fresh medium containing 1 µg/mL IITR06144 (2X MIC) for 24 h at 37°C and 180 rpm. For the subsequent 3rd passage, 1% inoculum from the second exposure was added to tubes containing 2 µg/mL IITR06144 (i.e. 4X MIC) and incubated similarly as mentioned above. A 100 µL aliquot of cells that survived the third passage was then spread on drug containing plates (4X MIC IITR06144) and MIC of the colonies obtained was further determined by broth microdilution in order to confirm resistance generation. The genomic DNA of the resistant mutant was isolated, and sequencing was performed on Illumina HiSeq System at Aggrigenome Labs Pvt Ltd, Bangalore, India.

4.4.14 Assessment of DNA damage by IITR06144

DNA damage in bacterial cells was assessed using *in situ* Cell Death Detection Kit, Fluorescein (Roche, Germany) by Terminal deoxyribonucleotide Transferase (TdT)-mediated dUTP Nick End Labelling (TUNEL) assay [270]. Overnight culture of *E. coli* ATCC 25922 was 100 times diluted in LB broth and grown at 37 °C in shaking condition until log phase. The cells were diluted to OD_{600} ~0.1 and grown for 2 h at 37°C in the presence of IITR06144, ciprofloxacin and nitrofurantoin. At the end of incubation, cells were pelleted and fixed with 4% paraformaldehyde. TUNEL positive cells were quantitated by flow cytometry using BD FACSVerse™ (BD Biosciences, Franklin Lakes, NJ, USA) and the results were analysed using BD FACSuite™ software.

4.4.15 Membrane depolarization assay

E. coli cells grown to an OD_{600} ~0.5 were washed with PBS and further resuspended in PBS containing 5 mM glucose. Then, IITR06144 (at 1X MIC, 2X MIC) and carbonyl cyanide 3-chlorophenylhydrazone (CCCP) at 10 µM concentration were added to 1 ml aliquots of the cell suspension and incubated at 37 °C for 15 min. Fluorescent dye [$DiBAC_4$] (Sigma, USA) at concentration 1 µM was added to all the tubes and incubated for another 15 min at 37 °C. Fluorescence of the treated cells was analysed by flow cytometry using BD FACSVerseTM (BD Biosciences, Franklin Lakes, NJ) and compared to untreated control.

4.4.16 Immunofluorescence microscopy for visualisation of FtsZ

E. coli cells at OD_{600} ~0.1 were exposed to sub-inhibitory concentration of IITR06144 for 2h at 37°C with agitation. The cells were processed for immunofluorescence as described previously

[271]. Drug treated *E. coli* cells were harvested by centrifugation and washed twice in PBS. The cell pellet was then resuspended in 500 µl of PBS and 100 µl of fixative was added. Fixed bacterial cells were then added to poly-L lysine coated slides and let dry. The slides were washed with PBS and 10 µl of 2 mg/mL lysozyme was added followed by 20 min incubation. After a few washing steps, 2% BSA was added as a blocking agent. The slides were kept in a humid chamber for 30 min. Anti-FtsZ antibody (1:100 dilution in 2% BSA) was added to the slides after thorough washing and incubated overnight at 4ºC in the humid chamber. The next day the slides were washed 20 times with PBS and FITC labelled anti-rabbit antibody (1:500 dilution in 2% BSA) was added. After an incubation of 30 minutes, the slide was thoroughly washed with PBS and dried. Propidium iodide (0.1 mg/mL) was used to stain nucleoids and slides were visualized under Carl Zeiss fluorescence microscope. The images were processed using Zen software package.

4.4.17 Growth inhibition of antisense expressing *E. coli* strains

The effect of IITR06144 on growth of *E. coli* cells expressing antisense of *ftsZ* and *murA* genes was assessed by studying the bacterial growth at 600 nm [253],[272]. *E. coli* BW25113 cells carrying pHN678, pHN678 with an *ftsZ* antisense insert (pHN678- *ftsZ*) or pHN678 with a *murA* antisense insert (pHN678-*murA*) were grown for 10 h in LB broth supplemented with chloramphenicol (30 mg/L) at 37ºC in shaking condition. The cells were then diluted 100 folds in fresh LB-chloramphenicol medium and added to 96-well plates containing drugs at indicated concentration in the presence of optimised IPTG dose to induce the expression of *ftsZ* (50 µM) and *murA* (150 µM) antisense. Plates were read every hour using microplate reader (Biotek) to monitor the growth.

4.4.18 Quantification of FtsZ protein levels by western botting

Western blot analysis was performed to determine the FtsZ protein levels in IITR06144 treated *E. coli* ATCC 25922, as described previously [273]. *E. coli* cells at OD_{600} of 0.1 were treated with 2.5X MIC and 4X MIC of IITR06144 for 4 h. The cells were harvested and lysed using Bug Buster^{R} protein extraction reagent (Merck Millipore) for 35 minutes at room temperature with gentle shaking. Total protein in cell lysate was quantified by using BCA protein estimation kit (Thermo Scientific). 40 µg of total protein was resolved on 12% Glycine SDS-PAGE and the proteins were transferred to a nitrocellulose membrane. The membrane was incubated in 25 ml of blocking buffer {5% skimmed milk in PBS containing 0.05% Tween 20

(PBS-T)} for one hour at room temperature.The membrane was washed three times with PBS-T and then incubated with a 1:5,000 dilution of anti-FtsZ antibody (raised in rabbits at IVRI, Bareily) overnight at 4°C. GAPDH was used as an endogenous control for *E. coli* and was detected with anti-GAPDH antibody (Thermo Scientific) at a dilution of a 1:10,000 dilution. The membrane was then washed three times with PBS-T and incubated further with secondary antibody (horseradish peroxidase-conjugated goat anti-rabbit IgG antibody) at 1:10,000 dilution for 1 h at room temperature. Membrane was again washed three times with 25 ml of TBST buffer for 15 minutes each. The luminescent signal indicating the expression of FtsZ was detected using ECL substrate (Bio-Rad) for 1 minute at room temperature in the dark room. An autoradiography film (Kodak, USA) was exposed to the membrane and incubated for a span of 2 minutes in order to capture the signal. The film was developed, washed and scanned to obtain an image.

4.4.19 Effect of antioxidant pre-treatment on killing by IITR06144

The effect of pre-treatment with antioxidant Vitamin C (L-ascorbic acid) on IITR06144 killing was assayed in *E. coli* ATCC 25922 as described in Supplementary Methods [255]. Cells grown to OD_{600} of 0.6 in LB medium were 25 times diluted and divided into two equal parts such that one part was pre-treated with vitamin C (5 mM) while the remaining cells acted as control. Cells were kept for 20 min at 125 rpm at 37ºC after which they were transferred to 96-well plate containing different concentrations of IITR06144. Growth was monitored for up to 8 h at 37ºC under static condition using a plate reader. Methyl viologen (0.6 mM) served as a positive control for the assay.

4.4.20 *In vivo* efficacy studies in mice model of systemic infection

To assess *in vivo* efficacy, IITR06144 was administrated to female BALB/c mice (n=5) after 24h of *A. baumannii* AYE infection. Prior to infection, groups of 6-7 week old female BALB/c mice (n=5) were rendered neutropenic by intraperitoneal injection of cyclophosphamide consecutively for 2 days at 200 mg/kg body weight. Later, mice were intravenously infected with $1X10^7$ CFU of the *A. baumannii* AYE strain. IITR06144 (at 6.25, 12.5, 25, 50 mg/kg of body weight) or vehicle control (10% cremophore EL and 10% DMSO in PBS, pH 7.4) were orally administrated p.o. after 24 h of infection consecutively for 4 days. Animals were

euthanized on the 5th day of compound administration and Organs (spleen, kidney, liver and lung) were plated to assess the bacterial burden.

4.4.21 *In vivo* toxicity studies

Control group (n=5) was given vehicle (10% cremophore EL and 10% DMSO in 100 mM PBS, pH 7.4) while treatment group was orally administered with IITR06144 and Nitrofurantoin (at 50 mg/kg body weight) consecutively for 5 days at 24 h interval. Animals were monitored at regular time intervals for any unfavourable effects and on the 6th day, animals were kept without any dosing. Animals were later euthanized, blood was collected, and organ weights were assessed. Evaluation of biochemical parameters such as alanine aminotransferase (ALT), aspartate aminotransferase (AST), alkaline phosphatase (ALP), total bilirubin, creatinine, triglycerides and cholesterol was carried out as per the manufacturer's protocol (Erba, Mannheim, Germany).

4.4.22 Statistical analysis

All data were statistically analysed using GraphPad Prism 5 software (GraphPad Software). Results were expressed as mean of triplicate values, with error bars representing the standard deviations. Data was analysed using one-way ANOVA and two-way ANOVA followed by Dunnett's multiple comparison test or Bonferroni Post Hoc test and has been indicated in the figure legends. P value less than 0.05 ($P<0.05$) were considered to be statistically significant. None of the data points were excluded while performing statistical analysis. Lengths of *E. coli* cells upon treatment with IITR06144 were measured using ImageJ and frequency distribution of cell lengths was plotted on GraphPad Prism 5.

5 Studies on the combinations of IITR06144 with clinically important antibiotics against bacterial pathogens

5.1 Introduction

In the era of ever increasing antibiotic resistance, limited therapeutic options exist for treatment of infections caused by multidrug-resistant (MDR) pathogens. In order to keep up with the anticipated evolution of resistance, there is a dire need for novel antibacterial agents. However, novel antibiotic discovery is a challenging process and it is important to explore alternative treatment strategies in order to tackle bacterial infections. Combinatorial therapy is one such promising approach that aims to potentiate the activity of conventional antibiotics that seem ineffective when administered as a single agent [12] . The use of combination therapy is desirable since it not only limits the emergence of resistance but also broadens the antibacterial spectrum [13]. More importantly, it provides an added benefit of reduced toxicity thereby lowering the effective dose of each drug, in combination [14].

The potency of synergistic therapies to improve antibiotic efficacy and combat antibiotic resistance prompted me to develop a novel small molecule-antibiotic combination regime for treatment of bacterial infections. As discussed in chapter 4, a novel antibacterial small molecule, IITR06144 was discovered from a library of 11,000 small molecules against the Gram negative model organism, *E. coli* ATCC 25922. IITR06144 displayed excellent antibacterial activity against a broad range of bacterial isolates including multidrug-resistant Gram-positive, Gram-negative pathogens, *Mycobacterium* spps. and anaerobic bacteria.

This study was undertaken initially with the primary motive to evaluate the compatibility of IITR06144 with clinically relevant antibiotics belonging to different classes by studying their *in vitro* interaction using the standard checkerboard method against the Gram negative model organism, *E. coli* ATCC 25922 (Section 4.2.12). Encouraged by the *in vitro* interaction data against *E. coli* ATCC 25922, which showed IITR06144 to have no negative interactions with any of the antibiotic classes, I further sought to determine its combination profile in few other bacteria, belonging to the ESKAPE category such as *A. baumannii*, *K. pneumoniae* and *S. aureus*. The most promising small molecule-antibiotic combination was further evaluated for

its *in vitro* pharmacodynamic properties, activity against bacterial strains isolated from the clinic and *in vivo* efficacy in a nematode infection model.

5.2 Results

5.2.1 *In vitro* combinations of IITR06144 with antibiotics were screened by the checkerboard assay against *A. baumannii* AYE and *S. aureus* ATCC 29213

A. baumannii and *S. aureus* are two troublesome Gram negative and Gram positive ESKAPE pathogens respectively. *A. baumannii* AYE is a multidrug resistant strain which exhibits resistance to most β-lactams, aminoglycosides, fluoroquinolones, chloramphenicol, tetracycline, and rifampin [274]. *S. aureus* ATCC 29213 is a standard quality-control strain utilised in laboratory testing and displays a weak beta lactamase activity and oxacillin sensitivity [275]. Using the modified checkerboard method, the pairwise interaction of IITR06144 with several antibiotics belonging to different chemical classes was studied [166],[165]. The FICI values were calculated by the given formula:

$$FICI = FIC\text{-}A + FIC\text{-}B$$

(FIC, fractional inhibitory concentration; FIC-A, MIC of drug A in the presence of drug B divided by MIC of drug A alone; FIC-B, MIC of drug B in the presence of drug A divided by MIC of drug B alone). FICI value of <0.5 was considered to be synergistic, FICI > 0.5 meant additive interaction or indifference, FICI > 4 denotes antagonistic interaction.

Table 5.1 and 5.2 lists the MICs and FICIs displayed by IITR06144 in combination with several antibiotics against the reference strains *A. baumannii* AYE and *S. aureus* ATCC 29213 respectively. In both the strains, IITR06144 was observed to display a synergistic interaction (FICI<0.5) with kanamycin which belongs to the aminoglycoside class of antibiotics. The MDR strain, *A. baumannii* AYE also displayed favourable interaction with meropenem which is a last resort antibiotic of the carbapenem class. On the other hand, Vancomycin, which is considered as a 'gold standard' for the treatment of *S. aureus* infections showed a fourfold reduction in the MIC in combination with IITR06144 against *S. aureus* ATCC 29213.

Table 5.1: Fractional inhibitory concentration Index (FICI) of IITR06144 and various antibiotics against *A. baumannii* AYE as determined by the checkerboard method.

Antibiotic	MIC of Antibiotic	MIC of Antibiotic in combination	FIC of antibiotic	MIC of IITR06144 in combination	FIC of IITR06144	FICI*
Fosfomycin	64	64	1	0.5	1	2
Tetracycline	64	8	0.125	0.5	1	1.125
Kanamycin	512	128	0.25	0.125	0.25	**0.5**
Rifampicin	4	0.25	0.0625	0.25	0.5	0.5625
Meropenem	0.5	0.125	0.25	0.125	0.25	**0.5**
Trimethoprim	512	256	0.5	0.25	0.5	1
Norfloxacin	512	64	0.25	0.25	0.5	0.75

*Bold figures indicate synergistic interactions
FICI< 0.5 = synergy; FICI > 0.5 <2 = additive; FICI > 4 antagonistic; FICI: Fractional Inhibitory Concentration Index. MIC values are given in terms of µg/mL.

Table 5.2: Fractional inhibitory concentration Index (FICI) of IITR06144 and various antibiotics against *S. aureus* ATCC 29213 as determined by the checkerboard method.

Antibiotic	MIC of Antibiotic	MIC of Antibiotic in combination	FIC of antibiotic	MIC of IITR06144 in combination	FIC of IITR06144	FICI*
Vancomycin	0.5	0.125	0.25	0.125	0.25	**0.5**
Kanamycin	4	1	0.25	0.125	0.25	**0.5**
Rifampicin	0.004	0.004	1	0.25	0.5	1.5
Meropenem	4	1	0.25	0.125	0.25	**0.5**
Trimethoprim	8	4	0.5	0.125	0.25	0.75
Nalidixic Acid	32	8	0.25	0.5	1	1.25
Ampicillin	16	16	1	0.5	1	2

*Bold figures indicate synergistic interactions
FICI< 0.5 = synergy; FICI > 0.5 <2 = additive; FICI > 4 antagonistic; FICI: Fractional Inhibitory Concentration Index. MIC values are given in terms of µg/mL.

5.2.2 IITR06144 displayed synergy with aminoglycoside class of antibiotics in *A. baumannii* AYE, *S. aureus* ATCC 29213 and *K. pneumoniae* ATCC 700603.

Out of the various antibiotic-IITR06144 interactions studied, IITR06144 was observed to exhibit synergy with kanamycin against *A. baumannii* AYE and *S. aureus* ATCC 29213. This observation was further elaborated by studying its interaction with other antibiotics from the aminoglycoside class.

Similar to the previous observation where, IITR06144 interacted synergistically with aminoglycoside class of antibiotics against *E. coli* ATCC 25922 (Table 4.7); IITR06144 also exhibited a synergistic interaction (FICI <0.5) with amikacin, gentamicin *etc* in both *A. baumannii* AYE and *S. aureus* ATCC 29213, causing a four to eight fold reduction in the MIC of these aminoglycoside antibiotics (Table 5.3 and 5.4).

Table 5.3: Fractional inhibitory concentration Index (FICI) of IITR06144 and aminoglycoside antibiotics against *A. baumannii* AYE as determined by the checkerboard method.

Antibiotic	MIC of Antibiotic	MIC of Antibiotic in combination	FIC of antibiotic	MIC of IITR06144 in combination	FIC of IITR06144	FICI
Kanamycin	512	128	0.25	0.125	0.25	**0.5**
Gentamicin	512	128	0.25	0.125	0.25	**0.5**
Amikacin	4	0.5	0.125	0.125	0.25	**0.375**

*Bold figures indicate synergistic interactions
FICI< 0.5 = synergy; FICI > 0.5 <2 = additive; FICI > 4 antagonistic; FICI: Fractional Inhibitory Concentration Index. MIC values are given in terms of µg/mL.

The synergistic interaction between IIR06144 and aminoglycosides was also observed to occur in *Klebsiella pneumoniae* ATCC 700603, a Gram negative ESKAPE pathogen exhibiting ≥ 4 fold reduction in MICs of both IITR06144 and representative aminoglycosides when administered in combination (Table 5.5). Although, *K. pneumoniae* showed extremely high MIC for IITR06144 (64 µg/ml), its combination with aminoglycoside was observed to be synergistic causing a fourfold reduction in MIC (16 µg/ml). While the IITR06144-meropenem

combination in *A. baumannii* AYE showed FICI value of 0.5, in *K. pneumoniae* the combination was found to be additive in nature (FICI: 0.53).

Table 5.4: Fractional inhibitory concentration Index (FICI) of IITR06144 and various antibiotics against *S. aureus* ATCC 29213 as determined by the checkerboard method.

Antibiotic	MIC of Antibiotic	MIC of Antibiotic in combination	FIC of antibiotic	MIC of IITR06144 in combination	FIC of IITR06144	FICI
Kanamycin	4	1	0.25	0.125	0.25	**0.5**
Gentamicin	2	0.5	0.25	0.125	0.25	**0.5**
Amikacin	4	1	0.25	0.125	0.25	**0.5**
Streptomycin	8	2	0.25	0.125	0.25	**0.5**

*Bold figures indicate synergistic interactions
FICI< 0.5 = synergy; FICI > 0.5 <2 = additive; FICI > 4 antagonistic; FICI: Fractional Inhibitory Concentration Index. MIC values are given in terms of µg/mL.

Table 5.5: Fractional inhibitory concentration Index (FICI) of IITR06144 and various antibiotics against *K. pneumoniae* ATCC 700603 as determined by the checkerboard method.

Antibiotic	MIC of Antibiotic	MIC of Antibiotic in combination	FIC of antibiotic	MIC of IITR06144 in combination	FIC of IITR06144	FICI
Kanamycin	16	1	0.0625	16	0.25	**0.3125**
Amikacin	0.25	0.0156	0.0625	16	0.25	**0.3125**
Gentamicin	8	0.5	0.0625	16	0.25	**0.3125**
Meropenem	1	0.031	0.031	32	0.5	0.531

*Bold figures indicate synergistic interactions
FICI< 0.5 = synergy; FICI > 0.5 <2 = additive; FICI > 2 antagonistic; FICI: Fractional Inhibitory Concentration Index. MIC values are given in terms of µg/mL.

5.2.3 IITR06144 exhibited synergistic interaction with vancomycin against Methicillin sensitive *S. aureus* (MSSA) ATCC 29213.

Of all the studied pairwise interactions of IITR06144 with antibiotics against *S. aureus*, the most peculiar was found to be synergistic combination of IITR06144-vancomycin, since vancomycin antibiotic has been the mainstay for the treatment of infections caused by methicillin resistant *S. aureus* (Table 5.2) [276]. Since synergistic interaction of IITR06144-vancomycin exhibited in methicillin sensitive *S. aureus* ATCC 29213, I further sought to determine if this interaction also existed with methicillin resistant clinical strains of *S. aureus* by the checkerboard method.

5.2.4 IITR06144 exhibited synergistic interaction with vancomycin against MRSA clinical isolates that are vancomycin-susceptible *Staphylococcus aureus* (VSSA), heterogenous Vancomycin Intermediate *S. aureus* (hVISA) or Vancomycin Intermediate *S. aureus* (VISA).

The *in vitro* interaction of IITR06144 with vancomycin was further evaluated in clinical isolates of *S. aureus* procured from SGPGI Medical College, Lucknow, India and AIIMS, Bhopal, India. These strains were isolated from different sites in the human host such as sputum, blood, pus or were isolates of the urinary tract. As per previous studies done in the lab, all these strains displayed resistance to methicillin and oxacillin [229]. The susceptibility of the isolates to vancomycin was further determined by the broth microdilution assay as per the CLSI guidelines (Table 5.6) [275]. *S. aureus* clinical isolates that display vancomycin MICs of 2 μg/ml have been associated to therapeutic failure of vancomycin in clinics and known to exhibit the heterogenous vancomycin-intermediate *S. aureus* (hVISA) phenotype [276]. Hence, the clinical isolates that displayed MIC ≥2 μg/mL were further subjected to the Brain Heart Infusion (BHI) Agar screening assay to detect the presence of heterogenous Vancomycin Intermediate *S. aureus* (hVISA) or Vancomycin Intermediate *S. aureus* (VISA) strains (Fig. 5.1) [277].

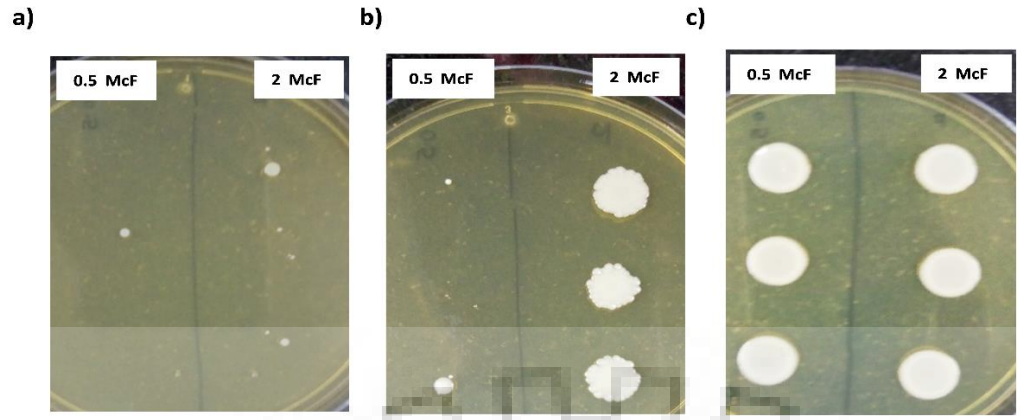

Figure 5.1: Brain Heart Infusion (BHI) Agar screening assay for detection of heterogenous Vancomycin Intermediate *S. aureus* (hVISA) or Vancomycin Intermediate *S. aureus* (VISA). BHI agar plates containing vancomycin (4 µg/ml) were spotted with 10 µl of 0.5 Mc Farland (McF) and 2 MC Farland (McF) *S. aureus* test isolates in triplicates. An isolate was considered to be hVISA when the 2 Mc Farland droplets had at least two colonies. Greater than 20 colonies were considered as Too Numerous to Count (TNTC) and the corresponding strain was considered to be VISA. (a) *S. aureus* ST1745 was observed to be hVISA while (b) *S. aureus* RPT U9 and (c) *S. aureus* RPT U13 were VISA isolates.

On the basis of the number of colonies obtained on BHI agar plates containing 4 µg/ml of vancomycin, strains were designated to be hVISA or VISA. The BHI Agar screening assay confirmed the isolate *S. aureus* ST1745 to exhibit heteroresistance to vancomycin while the isolates *S. aureus* RPT U9 and *S. aureus* RPT U13 were observed to be intermediately resistant to vancomycin (Fig 5.1). The remaining strains utilized in the study showed vancomycin sensitivity (MIC range: 0.5-1 µg/ml). Further combination studies were carried out to determine whether IITR06144 displayed the potential to act synergistically with vancomycin against vancomycin-susceptible *Staphylococcus aureus* (VSSA), heterogenous Vancomycin Intermediate *S. aureus* (hVISA) and Vancomycin Intermediate *S. aureus* (VISA). The results from the checkerboard assay revealed that 50% of the methicillin resistant isolates exhibited synergy with IITR06144 (Table 5.6). Interestingly, the three hVISA and VISA isolates also showed FIC values <0.5 thus indicating a synergistic interaction, such that the combinations showed ≥ fourfold reduction in vancomycin MIC, such that it could fall below the susceptibility breakpoint criteria, as laid down by the CLSI (Table 5.6).

5.2.5 Time kill studies confirmed the synergistic and bactericidal interactions between vancomycin and IITR06144 against Methicillin Resistant *S. aureus* (MRSA) and Vancomycin Susceptible *S. aureus* (VSSA) strain ST2071.

The synergistic interaction between IITR06144 and vancomycin observed by the checkerboard method was further validated using the time kill kinetics assay in Methicillin Resistant *S. aureus* (MRSA) ST2071 strain. *S. aureus* ST2071 is a sputum isolate exhibiting resistance to methicillin, oxacillin, ciprofloxacin, nalidixic acid, erythromycin and tetracycline [229]. The MIC of vancomycin and IITR06144 against ST 2017 was 1 µg/ml and 0.5 µg/ml respectively. Log phase cultures were exposed to IITR06144 and Vancomycin at concentrations 0.0625 µg/ml and 2 µg/ml respectively both alone and in combination for 24 hours and viable counts were determined at regular intervals. In a kill kinetics assay that employs two drugs in combination, synergy is defined as a ≥2-log10 decrease in CFU/ml in the combinations in comparison to its most active constituent, after 24 hour of treatment [166]. The combination of vancomycin and IITR06144 displayed excellent antibacterial activity and high rate of killing of *S. aureus* ST2071 exhibiting a ≥12-log10 decrease in comparison to the most potent agent individually i.e. vancomycin at 24 h (Fig. 5.2). This proved the combination of ITR06144-vancomycin to be bactericidal in nature and both the antibiotics acted in synergy to inhibit the Methicillin Resistant clinical isolate *S. aureus* ST2071.

Table 5.6: Fractional inhibitory concentration Index (FICI) of IITR06144 and vancomycin against clinical isolates of *S. aureus* as determined by the checkerboard method.

Strain no.	MIC of Vancomycin	MIC of Vancomycin in combination	FIC of antibiotic	MIC of IITR06144	MIC of IITR06144 in combination	FIC of IITR06144	FICI
MRSA ST2071	1	0.25	0.25	0.5	0.125	0.25	**0.5**
MRSA B10760	1	0.25	0.25	0.5	0.125	0.25	**0.5**
hVISA ST1745	2	0.125	0.0625	0.25	0.125	0.5	0.5625
MRSA ST3151	0.5	0.031	0.0625	1	0.5	0.5	0.5625
MRSA B10732	1	0.031	0.031	0.5	0.125	0.25	**0.281**
MRSA P4423	1	0.25	0.25	0.5	0.25	0.5	0.75
MRSA RPT U8	0.5	0.25	0.5	1	0.5	0.5	1
VISA RPT U9	2	0.5	0.25	0.5	0.125	0.25	**0.5**
MRSA RPT U10	1	0.015	0.015	0.25	0.125	0.5	0.515
VISA RPT U13	2	0.5	0.25	1	0.25	0.25	**0.5**

*Bold figures indicate synergistic interactions

FICI< 0.5 = synergy; FICI > 0.5 <2 = additive; FICI > 4 antagonistic; FICI: Fractional Inhibitory Concentration Index. MIC values are given in terms of µg/mL. Source of clinical isolates mentioned in Appendix 9.1.

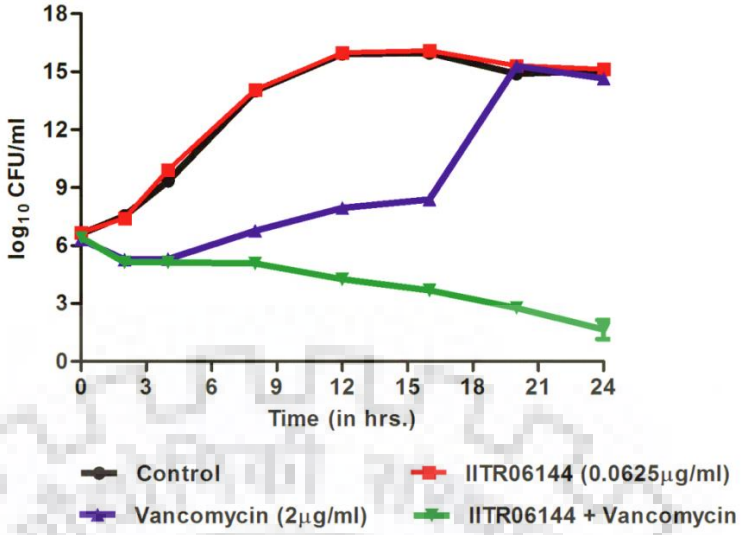

Figure 5.2: Kinetics of bacterial killing by combination of IITR06144 and Vancomycin in *S. aureus* ST2071 isolate. Cells were treated with IITR06144 alone (at 0.0625 µg/ml), Vancomycin alone (at 2 µg/ml) and a combination of IITR06144 and Vancomycin at similar concentrations. Aliquots were withdrawn at regular intervals and viable counts were determined up to 24 h of treatment.

5.2.6 Live dead staining confirmed the bactericidal interaction between vancomycin and IITR06144 against Vancomycin Susceptible *S. aureus* ST2071 (VSSA).

Fluorescence microscopy studies were further carried out to confirm the bactericidal activity of IITR06144-vancomycin combination against *S. aureus* ST 2071. Log phase cells of *S. aureus* ST 2071 were incubated with vancomycin, IITR06144 alone and in combination at concentration corresponding to 4X FIC of each antibiotic for 3 hours at 37º C and 180 rpm. The cells were subsequently washed with 1X PBS and analysed using LIVE/DEAD BacLight bacterial viability assay kit followed by fluorescence microscopy studies. The LIVE/DEAD kit uses a combination of two dyes, SYTO9 and PI where SYTO 9 stains all cells, both live and dead while Propidium Iodide (PI) is able to stain cells with compromised membranes, i.e. dead cells. LIVE/DEAD staining further validated the bactericidal potential of IITR06144 combination where untreated *S. aureus* cells displayed negligible PI signal indicating the presence of intact membrane. The combination of IITR06144 and vancomycin on the other hand displayed increased PI fluorescence in *S. aureus* cells suggesting that it causes cell death in contrast to individual drugs (Fig. 5.3).

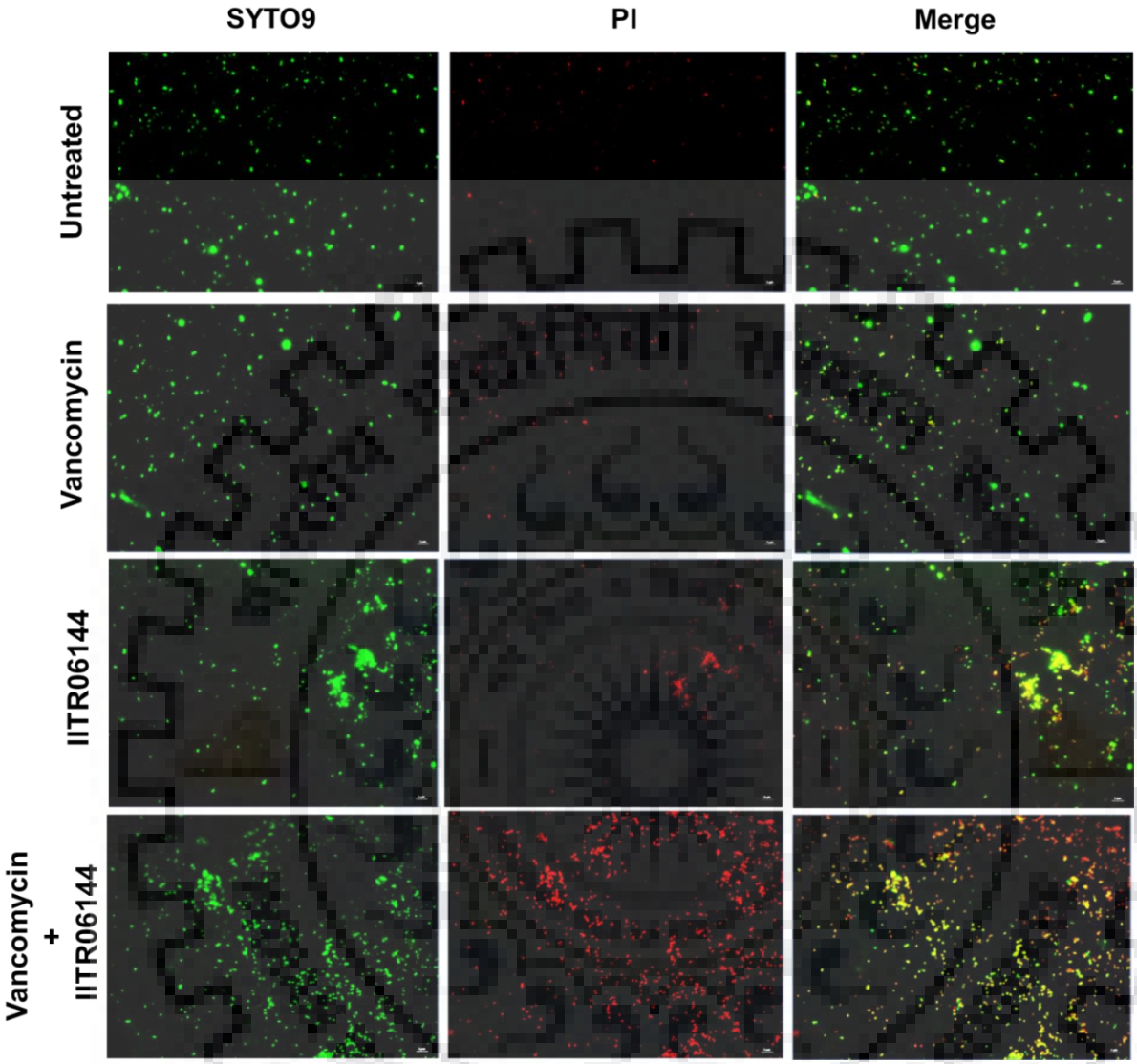

Figure 5.3: Fluorescence microscopy analysis for viability of *S. aureus* ST 2071 cells using LIVE/DEAD BacLight bacterial viability assay kit. Log phase cells of *S. aureus* ST 2071 were incubated with vancomycin, IITR06144 alone and in combination at 4X FIC for 3 hours. Following treatment cells were washed once with 1X PBS and stained with dyes SYTO9 and PI from the LIVE/DEAD BacLight bacterial viability assay kit. After 30 minutes of incubation, fluorescence microscopy studies were carried out to assess cell viability. Scale bar represents 1 µm.

5.2.7 IITR06144-vancomycin combination displayed an enhanced Post antibiotic effect.

The Post antibiotic effect **(**PAE) was studied in order to determine the duration for which the combination of vancomycin and IITR06144 remains effective against *S. aureus* cells after it has been removed from the medium, in comparison to drugs when administered alone. It was observed that *S. aureus* ST2071 cells when exposed to IITR06144 at concentration 0.125 μg/ml for 1 hour, prolong the PAE of vancomycin by approximately 30 minutes (Fig. 5.4). From the clinical viewpoint, the prolongation of PAE of vancomycin when combined with IITR06144 can turn out to be valuable for improving the treatment regimen and reducing the drug induced side effects [278],[263].

(A)

	PAE (in hour)
IITR06144	0.5
Vancomycin	1
Vancomycin + IITR06144	1.5

(B)

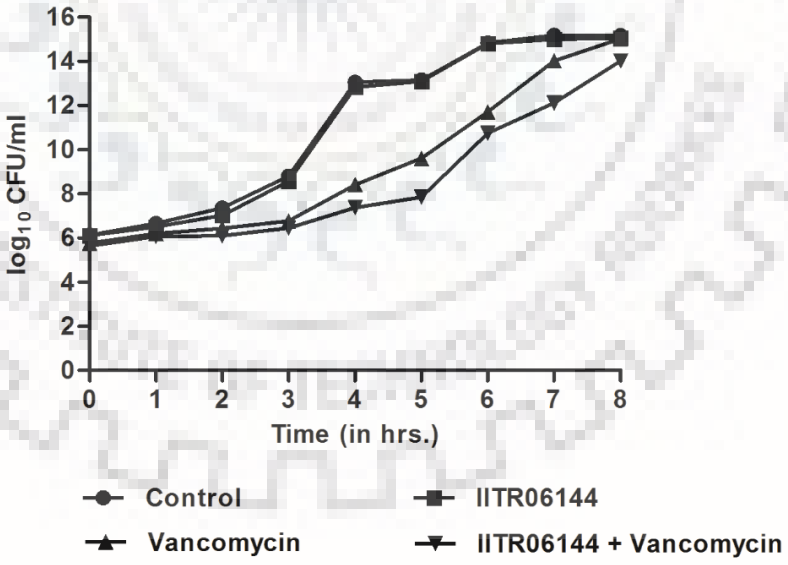

Figure 5.4: (A) Post Antibiotic effect of the combination of IITR06144 plus vancomycin in comparison with vancomycin alone treated cells of *S. aureus* strain ST 2071. (B) Viable counts were determined before exposure and immediately after resuspension (0 h) followed by plating every 1 hour. Each value represents the mean of three values and error bars denote the standard deviation.

5.2.8 IITR06144 displayed synergistic and bactericidal interactions with vancomycin against heterogenous Vancomycin Intermediate *S. aureus* ST1745 (hVISA).

Upon examination of the *in vitro* interaction between IITR06144 and vancomycin against the clinical isolates of *S. aureus*, it was observed that 50% strains showed FICI values ≤0.5 indicating synergy, a few strains displayed a borderline FICI (0.515-0.5625) which lied in the range of additive interactions. However, the chequerboard assay cannot be considered to be the only predictor of synergistic interactions and further assays need to be carried out to confirm the type of drug interactions. Evaluating the bactericidal effect of drugs in combination by performing the time kill kinetics assay is a viable and useful approach that has demonstrated the potential to identify synergistic combinations, including even the ones which did not display synergy in the chequerboard assay [279]–[282]. Hence, I further sought to evaluate the potential interaction between IITR06144 and vancomycin against the heterogenous Vancomycin Intermediate *S. aureus* ST1745 (hVISA) using the time kill kinetics assay. Vancomycin in combination with IITR06144 displayed excellent antibacterial activity exhibiting a ≥12-log10 decrease in CFU/mL in comparison to vancomycin alone, thus indicating synergy (Fig. 5.5). Thus IITR06144 was observed to act in synergy with vancomycin against hVISA isolate and this study revealed the importance of time kill assays over the chequerboard method.

5.2.9 IITR06144-vancomycin combination showed reduced frequency for resistance generation

The frequency of emergence of resistance against the IITR06144-vancomycin combination in *S. aureus* hVISA ST1745 was further evaluated by the large inoculum approach [264]. 10^9 CFU/mL of *S. aureus* cells were exposed to Vancomycin (at 2X MIC) alone and in combination with IITR06144 (at 0.5X MIC and 1X MIC) for 72 hours. The frequency of resistance (FOR) for the IITR06144-vancomycin combination was observed to be lower than that of vancomycin alone (Table 5.7).

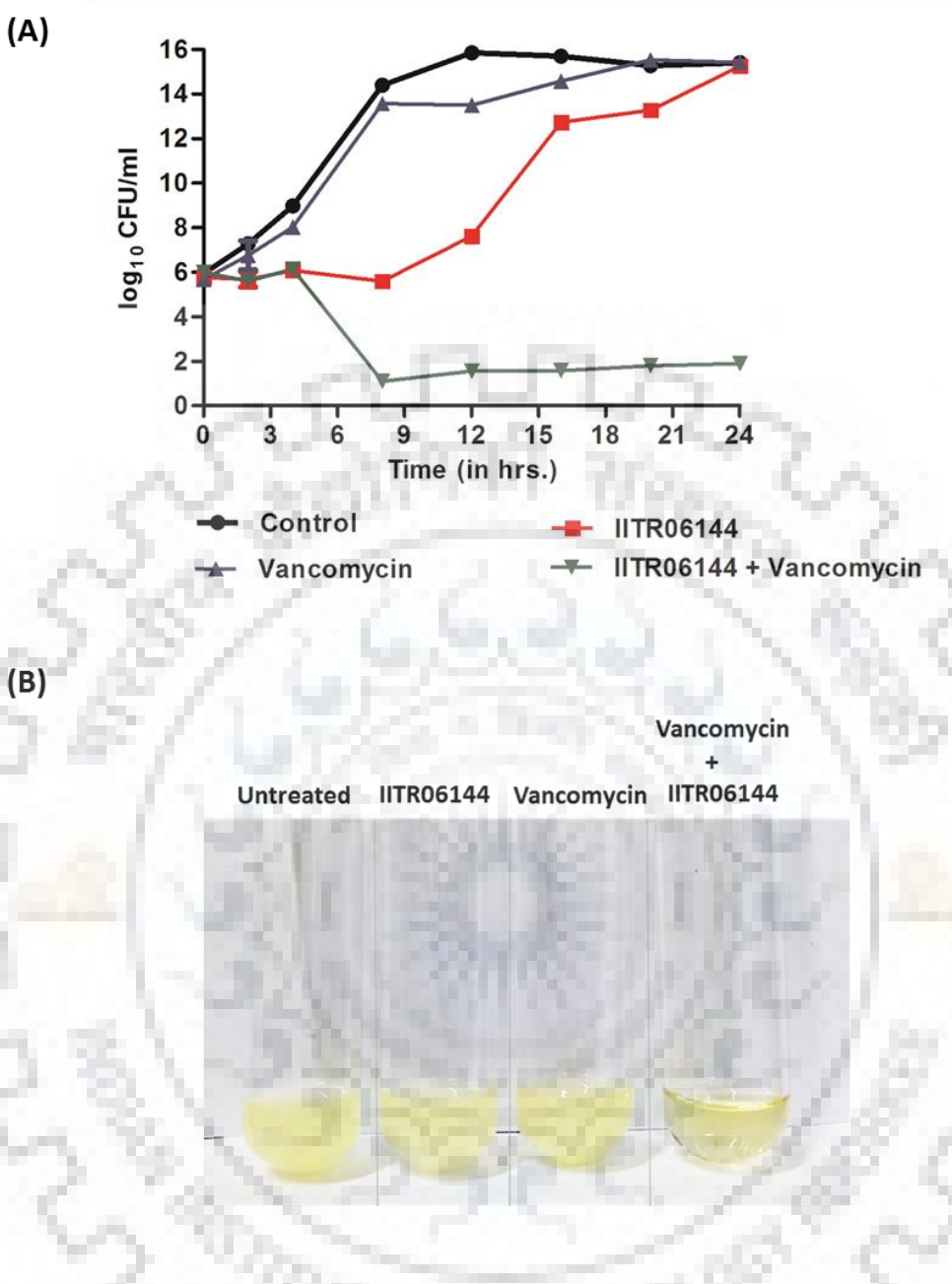

Figure 5.5: Kinetics of bacterial killing by combination of IITR06144 and Vancomycin in hVISA isolate *S. aureus* 1745. (A) Cells were treated with IITR06144 alone (0.5 µg/ml), Vancomycin alone (0.25 µg/ml) and with combination of IITR06144 and Vancomycin at similar concentrations. Aliquots were withdrawn at regular intervals and viable counts were determined up to 24 h of treatment. (B) Image of the culture tubes from the time kill kinetics assay after 24 hour of drug treatment. Corresponding CFU/ml was plated to determine the viable count.

Table 5.7: Frequency of resistance generation against hVISA *S. aureus* ST 1745 by IITR06144-vancomycin combination.

	Frequency of Resistance
Vancomycin (2X MIC)	$129 \pm 30 \times 10^{-7}$
Vancomycin (2X MIC) + IITR06144 (0.5X MIC)	$2 \pm 1 \times 10^{-9}$
Vancomycin (2X MIC) + IITR06144 (1X MIC)	$<10^{-9}$

5.2.10 IITR06144-vancomycin combination inhibited biofilm formation on abiotic surfaces.

Biofilms are highly organized communities of cells that possess unique characteristics in stark contrast to the characteristics of free-floating planktonic cells such that they are refractory to antibiotic treatment [115]. The ability of *S. aureus* to form recalcitrant biofilms on medical devices and hospital surfaces is a major concern in the hospital environments [283]. Hence, the ability of IITR06144 and vancomycin combination to inhibit *S. aureus* ST 2017 biofilm formation was further tested by the crystal violet biofilm staining assay in a 96-well microtiter plate. Biofilms were allowed to form for 48 hour in the presence of vancomycin (0.25 µg/ml) and IITR06144 (0.125 µg/ml) and percentage inhibition was calculated with respect to untreated control. Vancomycin and IITR06144 alone could inhibit biofilm formation by 35.9% and 34.3% respectively while in combination it could inhibit biofilm formation by 66% (Fig. 5.6). Hence, the combination of IITR06144 and vancomycin displayed great potential to inhibit the formation of *S.aureus* biofilm on abiotic surfaces.

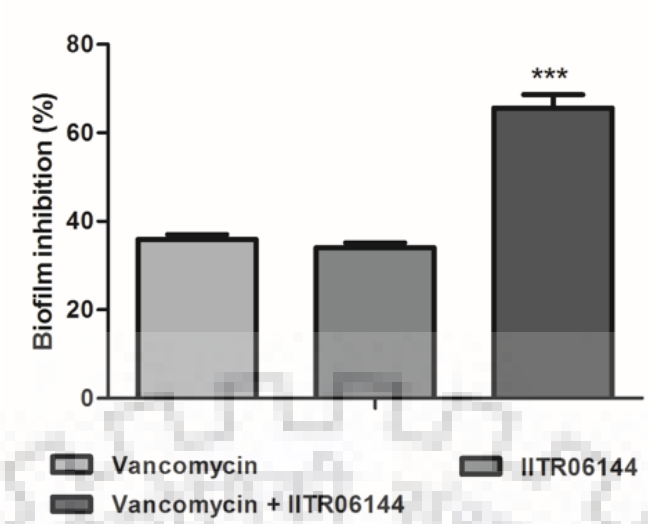

Figure 5.6: Percentage inhibition of *S. aureus* ST 2071 biofilm formation by the combination of IITR06144 and vancomycin using a 96-well crystal violet (CV) biofilm assay. Percentage biofilm inhibition was calculated by the formula = [(ODcontrol − ODtest) /OD control] × 100 where control OD is the absorbance of crystal violet in the absence of drug. Each value represents the mean of three values and error bars indicate standard deviation. P values were determined by one-way ANOVA and Dunnett's multiple comparison test (*, P<0.05; **, P<0.01; ***, P<0.001).

5.2.11 IITR06144-vancomycin combination exhibited haematocompatibility

The effect of IITR06144 and vancomycin alone and in combination on the haemolysis of isolated red blood cells was further studied, in order to get a preliminary idea of its toxicity (Fig. 5.7). All the concentrations tested displayed negligible haemolysis percentage, thus establishing the combination to be non-toxic.

5.2.12 IITR06144-vancomycin combination exhibited *in vivo* efficacy in *C. elegans* model of *S. aureus* infection.

To further evaluate the efficacy of the Vancomycin-IITR06144 combination *in vivo,* I employed the temperature-sensitive sterile mutant strain of *C. elegans* CF512 *fer-15*(*b26*)*II*:*fem-1*(*hc17*) *IV* [*fer-15*:*fem-1*] as the infection model. *C.elegans fer* mutant is sterile at room temperature and can lay eggs only at 15 °C [284]. Adult nematode were allowed to feed on *S. aureus* ST 2071 lawns spotted in the centre of NGM Agar plates for 48 hours [285].

Infected worms were then washed with M9 buffer and treated with vancomycin, IITR06144 alone and in combination for 24 hours at concentration corresponding to 1X FIC. The strategy has been outlined in Fig. 5.8. Worms were subsequently lysed and the number of viable bacteria were determined. The worms treated with IITR06144 combination displayed the presence of a significantly less bacterial burden in comparison to those treated with either of the drugs alone. Hence, the combination could effectively rescue the model nematodes from *S.aureus* infection (Fig. 5.9)

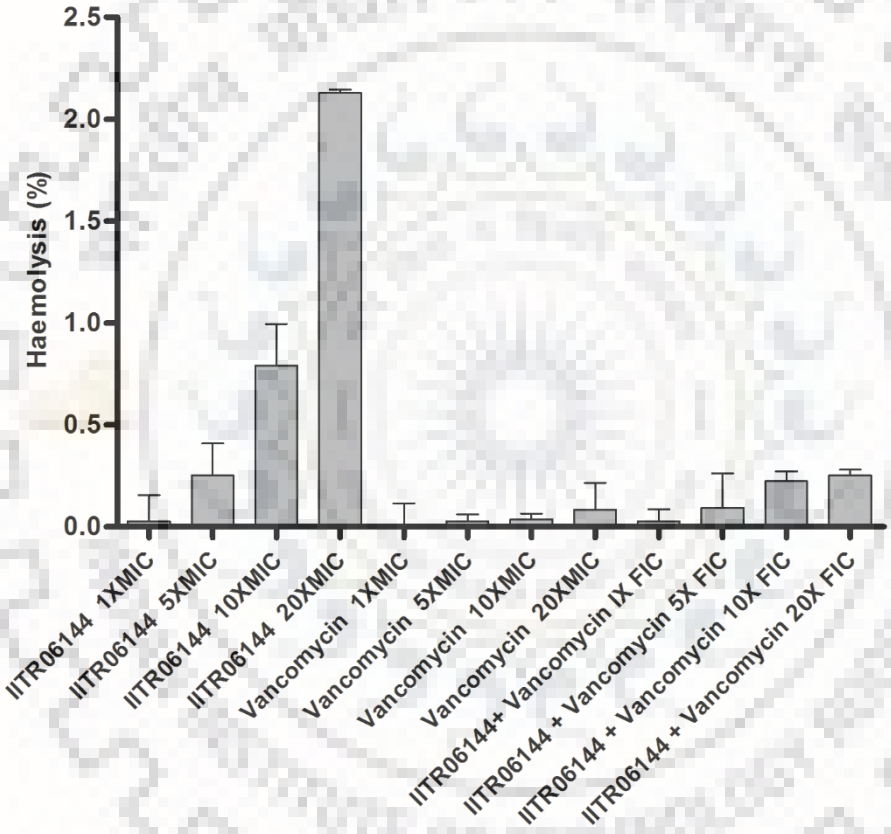

Figure 5.7: Percentage haemolysis by IITR06144 and Vancomycin alone at 1X, 5X, 10X, 20X of the MIC concentration and in combination (at concentrations 1X, 5X, 10X, 20X times the Fractional inhibitory concentration). Each value represents the mean of three values and error bars indicate standard deviation.

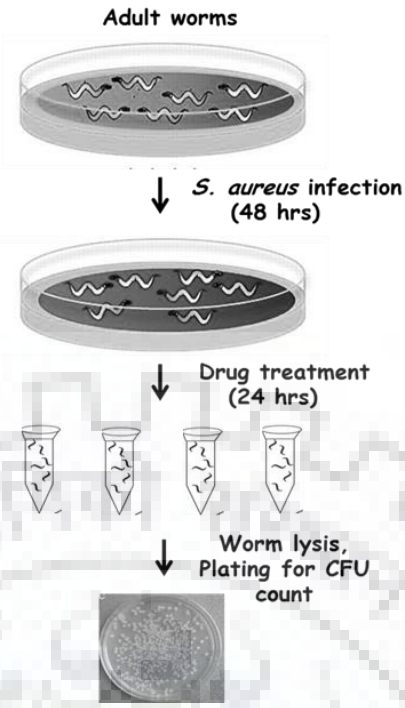

Figure 5.8: Schematic workflow for studying the *in vivo* efficacy of IITR06144-vancomycin combination in *C. elegans* infection model.

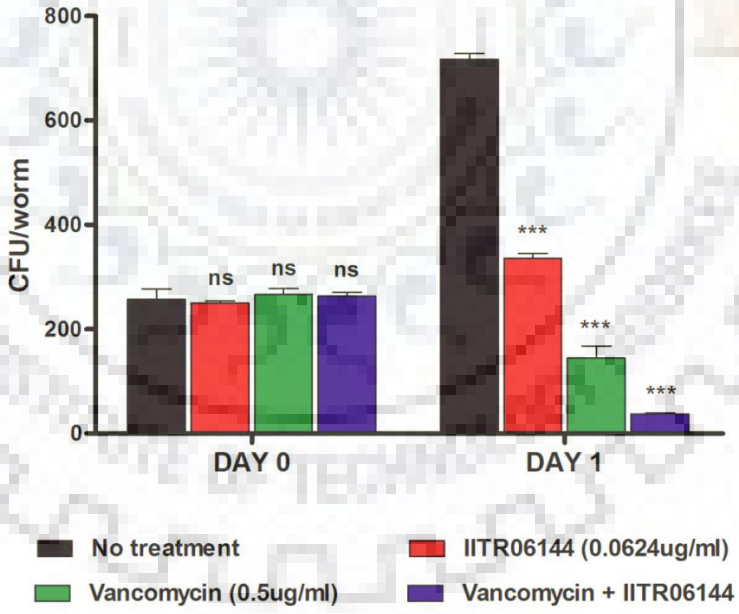

Figure 5.9: Effect of IITR06144-vancomycin on the number of live *S. aureus* cells within the worm gut. Adult worms were infected with *S. aureus* ST 2071 for 48 h and then transferred to M9 buffer supplemented with *E. coli* OP50, to which drug treatment alone or in combination were given. CFU were determined in the gut of 15 live worms removed from the plates before (0 day) and after 1 day of treatment. P values were determined by one-way ANOVA and Tukey's multiple comparison test (*, P<0.05; **, P<0.01; ***, P<0.001).

5.3 Discussion

Methicillin-resistant *Staphylococcus aureus* (MRSA) is one of the most dangerous gram positive pathogens that is known to cause human infections in community and hospital settings globally. Vancomycin is the most commonly used antibiotic against MRSA infections and has been considered to be the "gold standard" for treatment since decades. However, imprudent use of vancomycin has led to the emergence of clinical MRSA isolates with reduced susceptibility to the antibiotic [276]. Moreover, infections caused by heterogeneous vancomycin-intermediate *S. aureus* (hVISA) and vancomycin-intermediate *S. aureus* (VISA) infections are essentially life threatening. Limited treatment options for hVISA/VISA infections have further complicated the problem. Although, alternative antimicrobial agents, such as daptomycin, trimethoprim/sulfamethoxazole, linezolid, tigecycline and ceftaroline are a few viable options but they haven't been proved superior to vancomycin so far. Therefore, combination therapy may provide a potential treatment option for combating the grave situation caused by h-VISA/VISA. IITR06144 belongs to the nitrofuran class of antibiotics which are commonly prescribed for the treatment of uncomplicated Urinary tract infections. This is the first report which studies the combinatorial effect of a nitrofuran antibacterial with vancomycin against *Staphylococcus aureus*.

The objective of this study was to evaluate the synergy between IITR06144 and vancomycin against MRSA isolates that are vancomycin-susceptible *Staphylococcus aureus* (VSSA), hVISA, and VISA. IITR06144 belongs to the nitrofuran class of antibiotics which are commonly prescribed for the treatment of uncomplicated Urinary tract infections. Until now, there haven't been any reports assessing the combinatorial effect of this class of antibiotics with Vancomycin or other glycopeptides against *Staphylococcus aureus*. Time kill kinetics studies demonstrated their superiority over the classical chequerboard method to identify probable synergistic interactions and IITR06144 exhibited synergistic interaction with vancomycin in more than 50% of the isolates studied. IITR06144-vancomycin combination was observed to be bactericidal and demonstrated favourable *in vitro* pharmacodynamics properties such as enhanced Post antibiotic effect, anti-biofilm activity, haematocompatability and *in vivo* efficacy in a nematode model of *S. aureus* infection. Thus, the above described factors warrant the potential role of this combination in the treatment of *S. aureus* associated infections.

5.4 Experimental procedures

5.4.1 Bacterial strains and growth conditions

Acinetobacter baumannii AYE, *Escherichia coli* ATCC25922, *Staphylococcus aureus* ATCC 25913, *Klebsiella pneumoniae* ATCC 700603, and clinical strains of *S. aureus* were routinely grown at 37ºC with shaking at 180 RPM in Mueller Hilton Broth (HiMedia, India) and in Luria Bertani Broth (HiMedia, India). The clinical isolates used in the study were procured from SGPGI, Lucknow, India and AIIMS, Bhopal, India (Appendix Table 2).

5.4.2 Determination of Minimum Inhibitory Concentration (MIC)

MICs of IITR06144 and various antibiotics against *S. aureus* isolates were determined by the broth microdilution method in Mueller–Hinton medium, as per the CLSI guidelines. MICs were determined in 96-well plates and cells were incubated at 37°C in static condition in a humidity controlled incubator (Kuhner LT-X). Growth was monitored after 12 hour of incubation by reading absorbance at 600 nm. The lowest concentration of antibacterial which displayed no visible turbidity was considered its MIC.

5.4.3 Brain Heart Infusion Agar Screening Assay

BHI agar plates containing vancomycin (4 µg/ml) were spotted with 10 µl of 0.5 Mc Farland (McF) and 2 Mc Farland (McF) *S. aureus* test isolates in triplicates. An isolate was considered to be hVISA when the 2 Mc Farland droplets had at least two colonies. Greater than 20 colonies were considered as Too Numerous to Count (TNTC) and the corresponding strain was considered to be VISA.

5.4.4 Checkerboard assay to assess *in vitro* interactions

In vitro synergy of IITR06144 was evaluated in Gram negative and Gram positive isolates by modified broth checkerboard assay as described previously in section 4.4.11. In a 96-well plate, two fold serial dilutions of IITR06144 were prepared in combination with several antibiotics. Log phase bacteria at OD_{600} ~0.6 were 1000 times diluted and 100 µL of the inoculum was added to each well of the assay plate. Plates were then incubated for 16 h at 37ºC. Fractional inhibitory concentration index (FICI) was calculated using the formula [MIC drug B in presence of Drug A] / [MIC of drug B) + [MIC of drug A in the presence of drug B] / [MIC of drug A]. FICI scores were interpreted as follows: synergy (≤0.5), indifference (0.5–4), or

antagonism (>4). For each drug combination, FICI ranges were reported from two biologically independent experiments.

5.4.5 Time Kill Kinetics assay

To evaluate the bactericidal potential of IITR06144 alone and in combination with vancomycin, the time-kill kinetics assay was performed as described earlier (Section 4.4.4). *S. aureus* cells (10^5 CFU/mL) were treated with drugs alone or in combination and 100 µl aliquots were withdrawn at regular intervals and serial dilutions were plated onto MH agar plates. Plates were incubated at 37ºC and colony counts were determined after 12 h. Bacterial killing was assessed by plotting the mean viable counts (as $\log_{10}$ CFU/mL) versus time (in h).

5.4.6 *In vitro* Post-Antibiotic Effect (PAE)

Logarithmic phase *S. aureus* ST 2071 cells (10^6 CFU/mL) were exposed to IITR06144, vancomycin and combination for 1 h in shaking condition at 37°C [263]. Following the incubation with respective drugs, cells were centrifuged for 10 min at 4000 rpm at room temperature to remove its traces. The cells were washed twice with 1X PBS and resuspended in fresh medium followed by further incubation at 37°C. At definite intervals after drug exposure (0, 1, 2, 3, 4, 5, 6, 7, 8 hour), viable bacterial counts were determined by plating serial 10-fold dilutions on MH agar plates. The PAE was determined by the formula PAE = $T - C$ where, T is the time taken for unit $\log_{10}$ increase in inoculum (CFU/mL) versus the inoculum (CFU/mL) observed immediately after antibiotic removal; and C is the time it takes to observe a $\log_{10}$ increase (CFU/mL) in an untreated control.

5.4.7 Determination of Frequency of Resistance (FOR)

The emergence of spontaneous resistance in *S. aureus* ST 1745 against IITR06144, vancomycin and combination was determined as described previously. 10^9 CFU/mL of *S. aureus* cells were exposed to vancomycin (at 2X MIC) alone and in combination with IITR06144 (at 0.5X MIC and 1X MIC) for 72 hours. The plates were incubated for 48 h at 37ºC in static conditions in a humidity controlled incubator. The colony count of the initial inoculum was verified by plating serial dilutions onto MH agar plates. The frequency of resistance was determined by dividing the average number of colonies obtained after 48 h on drug containing plates by the initial inoculum.

5.4.8 Biofilm inhibition assay

Biofilm formation by *E. coli* MTCC 4296 in the presence of IITR06144 and comparative antibiotics was assessed by crystal violet assay [118]. Disruption of preformed biofilms after 12 h of IITR06144 treatment was studied, as described previously with slight modifications [257]. Log phase *E. coli* cells (OD_{600}~0.6) were 100 times diluted and added to 96-well microtiter plate containing test drugs at sub-inhibitory concentrations. Plates were kept under static condition in a humidity controlled incubator at 37°C for 48 h. Plates were then read at 600 nm and washed thrice with 1X PBS to remove the planktonic cells. Following fixation at 65ºC for 30 minutes (min), biomass was stained with 0.25% (w/v) crystal violet in methanol: 1X PBS (1:3) for 20 min. Following two brief washing steps, biofilms were quantified by addition of 33% acetic acid in methanol to dissolve the crystal violet adhered to biofilm forming biomass. Plates were read at 595 nm and relative absorbance ($OD_{595/600}$) was calculated.

5.4.9 Haemolysis assay

Haemolytic activity of IITR06144 was assessed as described previously, with slight modifications [265]. Fresh human blood (10 mL) was extracted in a vaccutainer blood collection tube (Thomas Scientific) and centrifuged at 2500 rpm for 10 min. The supernatant was discarded, and the pellet was washed thrice with 1X PBS. The pellet was then diluted 1:5 (vol/vol) in 1X PBS and RBC suspensions (1 mL each) were incubated with varying concentration of IITR06144 and comparative antibiotics under at 37°C under static condition. The time of incubation was increased to 4 h instead of 35 minutes in the reference followed. The suspensions were then centrifuged at 2500 rpm for 10 min and the supernatant was carefully collected without disturbing the pellet. Haemolysis was monitored by measuring the absorbance of the released hemoglobin in the supernatant at 540 nm using a spectrophotometer. Triton-X 100 (0.1%) served as the positive control for the assay. Haemolysis levels were calculated by the formula: $100 \times (At - As)/Ac$ where Ac, As, and At are the absorbance of Triton-X 100, absorbance of solvent control and absorbance of the sample containing drug respectively. All experiments were performed in triplicates.

5.4.10 *C. elegans* growth

C. elegans CF512 *fer-15*(*b26*)*II*:*fem-1*(*hc17*)*IV* [*fer-15*:*fem-1* worms] strain was used in this study which is a double mutant that does not make a germ line at 25°C [284]. These worms were routinely maintained on nematode growth medium (NGM) agar plates seeded with *E. coli*

OP50 at permissive temperatures (15°C or 20°C) for propagation using standard procedures [286]. For the assays, they were used at restrictive temperature (25°C) in order to induce sterility.

5.4.11 *In vivo* efficacy studies in *C. elegans* model of infection

C. elegans were used to test the efficacy of IITR06144-vancomycin combination in an *in vivo* model of *S. aureus* infection [285]. Adult worms infected with *S. aureus* ST 2071 for 48 hours were washed with M9 buffer containing 1 mM sodium azide (inhibits expulsion of bacteria from the worm intestine) to remove external bacteria. Worms were added to microcentrifuge tube containing M9 buffer supplemented with cholesterol (10ug/ml) and *E. coli* OP50 and then treated with vancomycin, IITR06144 alone and in combination at concentration corresponding to 1X FIC. The numbers of live *S. aureus* bacteria in the worm intestine were determined before and after 24 h of treatment. For this, 15 worms were vortexed at maximum speed for one minute in M9 buffer containing 400 mg of 1.0-mm silicon carbide particles, which can disrupt the worms but does not affect bacterial survival. The resulting suspension was plated and the bacterial CFU per worm calculated using the formula: (average colony number × dilution factor × volume of worm lysate)/(volume of lysate plated × number of worms) [287].

6 Elucidating the mechanism of action of novel small molecules using chemical-chemical combinations

6.1 Introduction

Undoubtedly, antibiotic resistance has emerged as one of the major global health concerns that has jeopardized the advancement in modern medicine. The unscrupulous use of antibiotics in hospitals, poultry and agriculture industry has led to the uncontrolled proliferation of resistant bacterial strains such as vancomycin-resistant *Enterococcus faecium*, and carbapenem resistant *Acinetobacter baumannii*, taking a toll on thousands of lives worldwide [3].

Needless to say, the best remedial strategy to tackle antibiotic resistance is the continued discovery and development of novel antibiotics. The use of phenotypic cell based assays or target based approach are the two most common strategies employed in antibacterial screening platforms [17]. Considering the shortcomings of target based methods for drug discovery, whole cell phenotypic screening is mostly favored and has witnessed resurgence in recent years [17], [18]. However, target identification of small molecule antibacterials identified in a phenotypic screen poses a tedious and formidable challenge to the researchers [16].

Several strategies such as the use of chemical genetics, biochemical approaches, stress responsive whole-cell biosensors, bacterial cytological profiling (BCP) etc. have been utilised to elucidate the mechanism of action (MOA) of novel small molecules [9],[21],[29],[28]. Chemical-chemical profiling is a novel and unique approach that has been exploited to link compound interactions with their mode of action [31]. Both synergistic as well as antagonistic chemical interactions have proved invaluable in studying the interactions of biological pathways and deciphering MOA of novel growth-inhibitory small molecules [31],[32].

In this study, the strategy of chemical-chemical interaction profiling for 12 novel antibacterials screened out of a small molecule library, with a panel of 14 known bioactives against *Escherichia coli* MC1061 was followed [31]. The combination profiles unfolded numerous intriguing synergistic, additive or antagonistic interactions. One of the small molecules, IITR07865 was taken up for further studies since it was observed to display unique synergistic interactions with antibiotics targeting the bacterial cell wall and cell membrane. The MOA of

IITR07865 was studied by the use of fluorescence microscopy, protein based biochemical assays and spectrofluorometric assays. The antibacterial spectrum, killing kinetics, *in vitro* toxicity and anti-persister activity of IITR07865 was also determined. The chemical-chemical interactions profile also identified a few other molecules that exhibited synergistic or additive interactions with multiple bioactives. Considering the possibility of these molecules to be membrane active, membrane potential and permeability assays were performed to get an insight into their mechanism of action.

6.2 Results

6.2.1 Small molecules exhibit lower Minimum Inhibitory Concentration (MIC) against the hyperpermeable mutant, *E. coli* MC1061 in comparison to wild type *E. coli* ATCC 25922.

A library of ~11,000 small molecules was screened against *E. coli* ATCC 25922 and 30 molecules with antibacterial properties were discovered (Fig. 4.1). From the 30 novel antibacterial leads, 12 small molecules were selected on the basis of their structural diversity and availability. These 12 compounds were screened against *E. coli* MC1061, which is an outer membrane hyperpermeable mutant and exhibits hypersensitivity to antibiotics [31]. These molecules were subjected to combination profiling with 14 known antibacterial agents representing diverse mechanisms and chemical classes. For example, the various antibiotics used were ampicillin, kanamycin, chloramphenicol, tetracycline, fosfomycin, polymyxin B, erythromycin, cefotaxime, norfloxacin, vancomycin, rifampicin, sulfamethoxazole, and trimethoprim. Triclosan, which is a widely used biocide was also included in the screen [289]. These antibiotics or bioactives target the bacterial cell membrane, cell wall synthesis, DNA synthesis, protein synthesis, fatty acid synthesis and folic acid synthesis pathways. The strategy followed for the study has been outlined in Fig. 6.1.

MICs of each of the small molecule and bioactive were determined against *E. coli* MC1061 in 96-well plates as per the CLSI guidelines [275]. Table 6.1 and Table 6.2 show the MIC of small molecules and 14 bioactives against the strain, *E. coli* MC1061. As expected, the small molecules could inhibit *E. coli* MC1061 at lower concentration in comparison to wild type *E. coli* ATCC 25922 (Table 6.1).

6.2.2 Combination Screening was based on a two point dose matrix approach

Instead of using the conventional checkerboard for screening the interactions, a previously established two point dose matrix approach was followed [31]. In this method, molecules were screened on the basis of their ability to inhibit growth at 0.125X (1/8X) and 0.25X (1/4X) of their MIC, in combination with bioactives in contrast to when given alone. This approach makes the screening process less tedious, reliable and also saves on the amount of small molecules required. Average absorbance data obtained from two independent combination screens at 0.125X and 0.25X MIC was calculated.

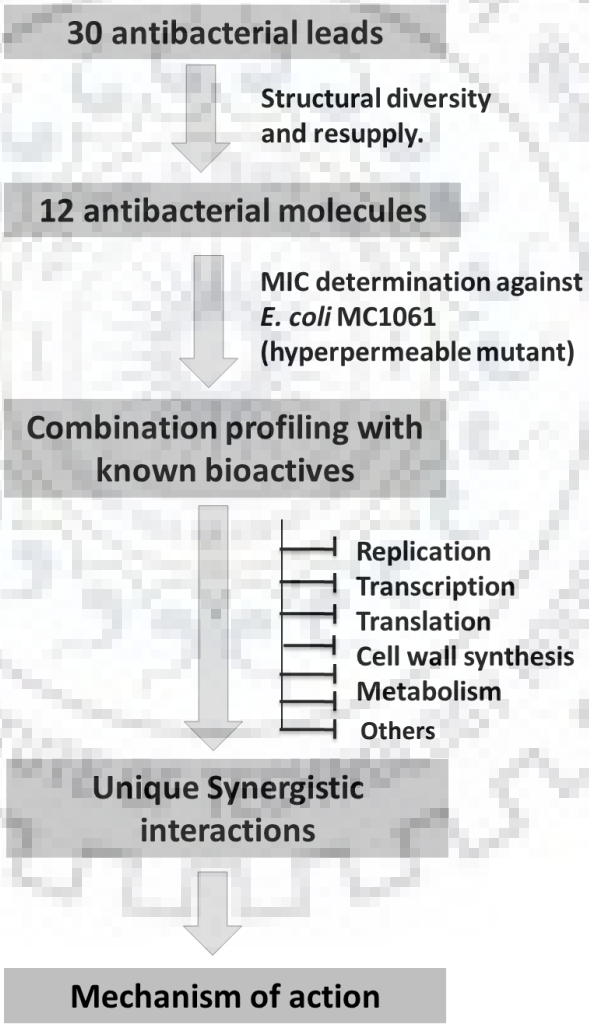

Figure 6.1: Workflow followed to study the interaction profiles of novel antibacterial small molecules derived from small molecule screening with known antibiotics/bioactives.

Table 6.1: Minimum Inhibitory Concentration (MIC) of 12 antibacterial small molecules against *E. coli* ATCC 25922 and *E. coli* MC1061.

S No.	Small molecules	MIC (µg/ml) in *E. coli* ATCC 25922	MIC (µg/ml) in *E. coli* MC1061
1.	IITR00205	16	16
2.	IITR06033	64	0.25
3.	IITR07480	16	64
4.	IITR07806	32	4
5.	IITR07865	32	8
6.	IITR08276	8	8
7.	IITR08540	64	4
8.	IITR07347	16	16
9.	IITR01324	4	1
10.	IITR07952	32	16
11.	IITR08524	16	2
12.	IITR08345	16	16

6.2.3 Combination ratios for the small molecule-bioactive screen were calculated

Further the "combination ratio" was computed, which is defined as the ratio of the percent growth of cells exposed to the small molecule-bioactive combinations divided by the percent growth in the presence of only the bioactives [31]. Two compounds were considered to be synergistic when they displayed combination ratio of 0.25 or lower which correspond to >75% growth inhibition, in combination [290]. The combination ratios (CR) were calculated by using the following formula:

$$\textbf{Combination ratio (CR)} = \frac{\dfrac{\text{O.D of combination}}{\text{O.D of positive control}}}{\dfrac{\text{O.D of bioactives}}{\text{O.D of positive control}}}$$

Table 6.2: Minimum Inhibitory Concentration (MIC) of known bioactives against *E. coli* MC 1061.

Bioactives	MIC (µg/ml)	Biological Target
Ampicillin	8	Cell wall biosynthesis
Chloramphenicol	0.25	50S ribosome
Erythromycin	1	50S ribosome
Fosfomycin	4	Cell wall biosynthesis
Tetracycline	0.25	30S ribosome
Triclosan	0.0625	Fatty acid biosynthesis/multiple targets
Vancomycin	256	Cell wall biosynthesis
Kanamycin	2	30S ribosome
Polymyxin B	0.007	Lipopolysaccharide/membrane
Cefotaxime	0.031	Cell wall biosynthesis
Norfloxacin	0.007	DNA gyrase
Rifampicin	2	RNA polymerase
Sulfamethoxazole	128	Folic acid biosynthesis
Trimethoprim	0.25	Folic acid biosynthesis

Further, the average combination ratios obtained from the screening were plotted individually for each bioactive, both at 1/4X and 1/8X MIC (Fig. 6.2A and 6.2B). From the scatter plots, it was observed that synergistic interactions in all the combinations screened were observed only at 1/4X MIC (and not at 1/8X MIC).

The combination ratios of all the small molecule-bioactive combinations were further compiled and represented in the form of heat map to facilitate the analysis of the type of interaction (Fig 6.3). Synergistic interactions were represented in red colour while black colour represented the pairs exhibiting antagonistic interactions.

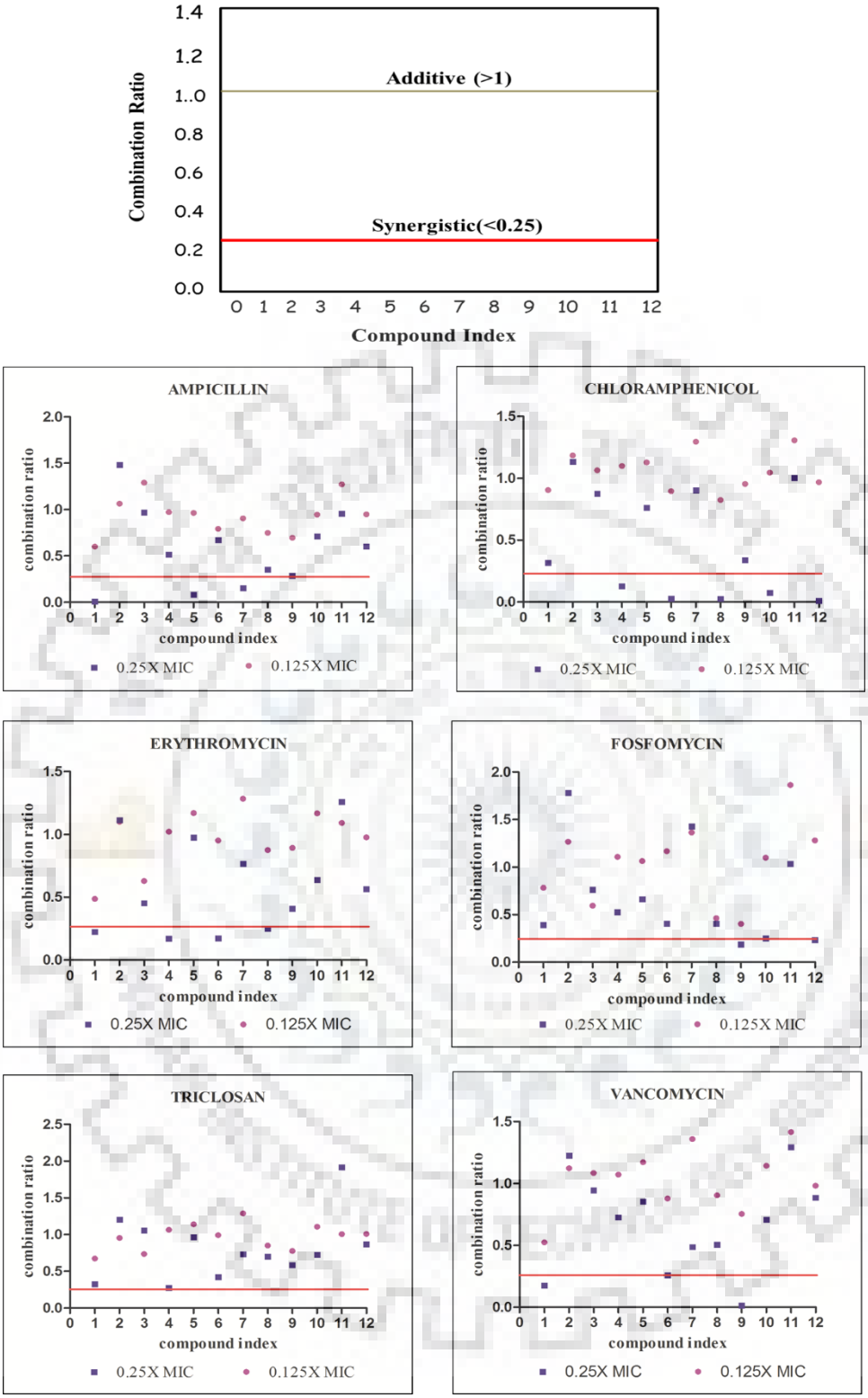

Figure 6.2A: Combination ratio profiles of 12 small molecules with six known bioactives (Ampicillin, Chloramphenicol, Erythromycin, Fofomycin, Triclosan and Vancomycin) at 0.25X and 0.125X MIC. The average combination ratios of two replicates have been plotted. Red line indicates combination ratio of ≤0.25 which exhibits >75% growth inhibition and was considered to be synergistic. Compounds found below this line were judged as hits.

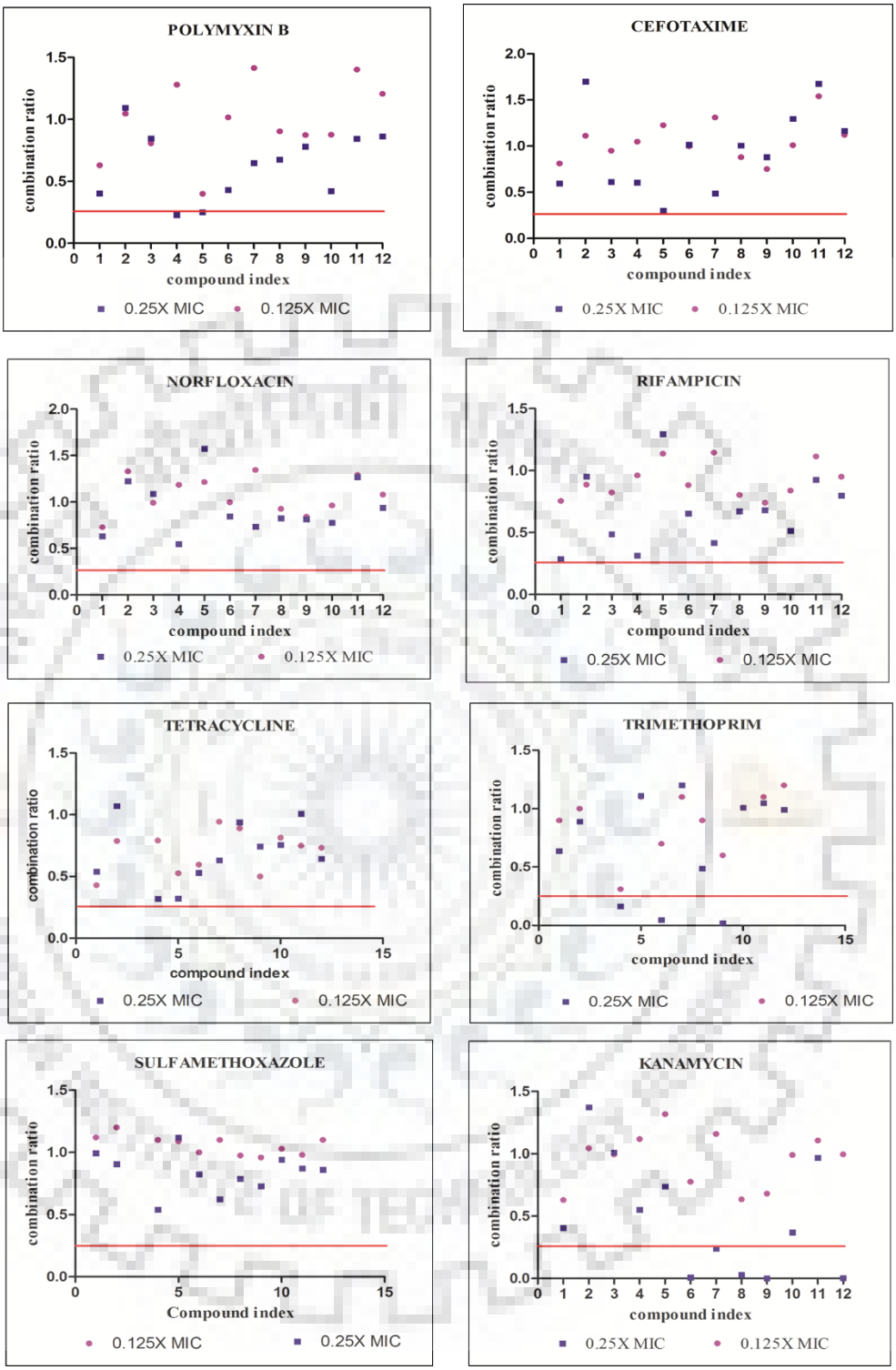

Figure 6.2B: Combination ratio profiles of 12 small molecules with other bioactives (Polymyxin B, Cefotaxime, Norfloxacin, Rifampicin, Tetracycline, Trimethoprim, Sulfamethoxazole and Kanamycin) at 0.25X and 0.125X MIC. The average combination ratios of two replicates have been plotted. Red line indicates combination ratio of ≤0.25 which exhibits >75% growth inhibition and was considered to be synergistic. Compounds found below this line were judged as hits.

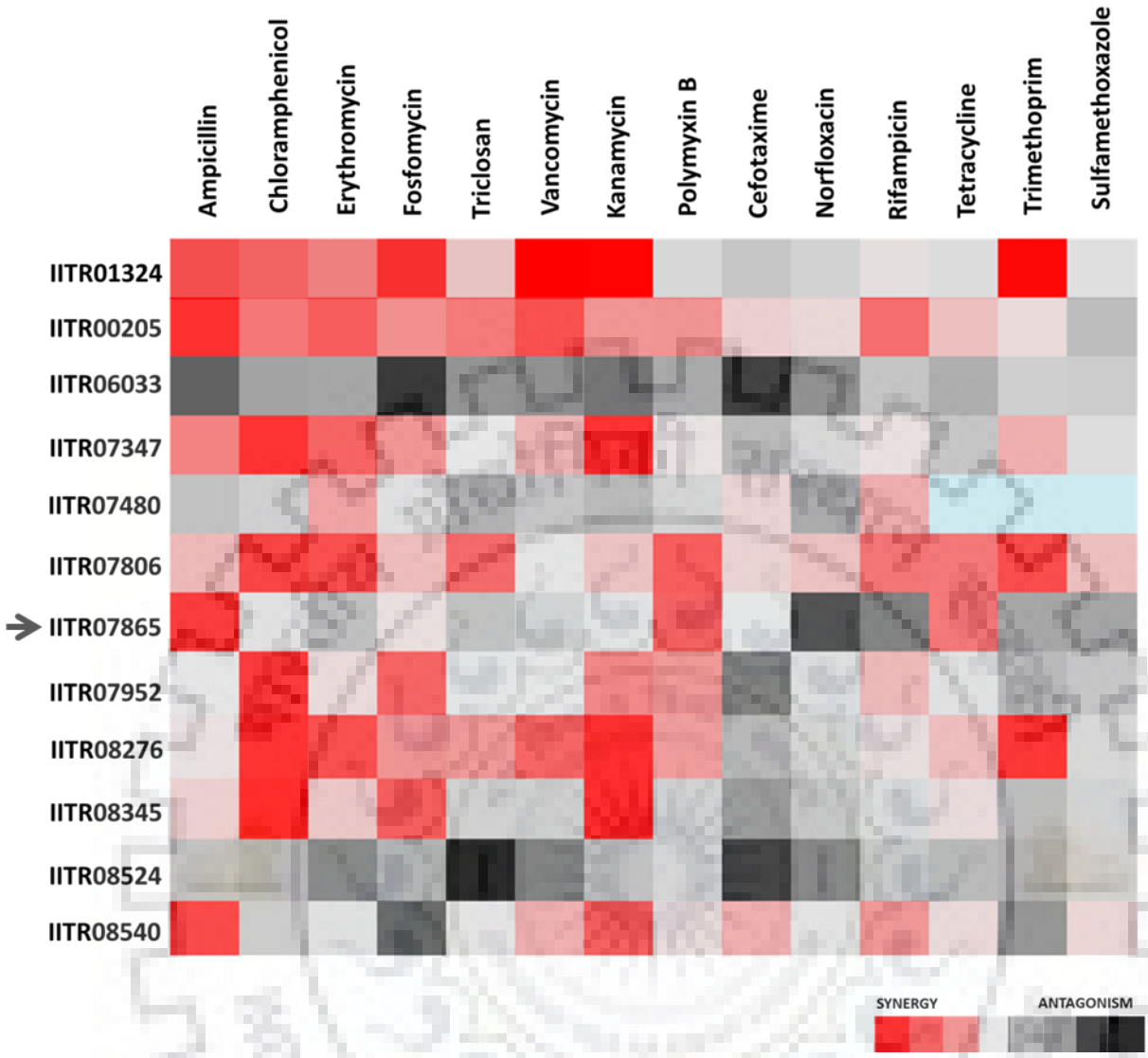

Figure 6.3: Chemical-chemical interaction profiles of 12 antibacterial small molecules and known bioactives at 1/4X MIC. Highly synergistic interactions are represented in red. Arrow indicates the combination profile of IITR07865. (Blue: data not determined)

6.2.4 Chemical-chemical interaction profile was analysed for the type of interaction

The small molecule-bioactive interaction profile was further analysed and revealed the occurrence of several synergistic, additive or antagonistic interactions. Most of the drug pairs showed additive interaction which indicates indifference upon combining two molecules. From the heat map it was evident that the antibiotics (or bioactives), kanamycin and chloramphenicol exhibited the most no. of favourable interactions (n=4) with the small molecules. The small molecule IITR07806 showed the most number of interactions followed by IITR08276. As

reported in literature, the combination profile screen also demonstrates the ability to cluster molecules on the basis of their interaction profile [31]. Interestingly, the molecules IITR07347, IITR08276 and IITR08345 exhibited a somewhat similar chemical fingerprint (Fig. 6.4). On close analysis, it was observed that the fingerprint of IITR07347 and IITR08276 closely matched each other while in case of IITR08345, it was found similar for half of the bioactives. Upon structural analysis of these molecules, it was interesting to note that all the three molecules belonged to the same chemical class, comprising of 5-Nitro-2-Thienyl moiety. This observation reaffirmed the importance of combination screens of clustering similar molecules. Three molecules namely IITR01324, IITR07806 and IITR08276 were observed to exhibit synergy with the antibiotic trimethoprim. IITR07865 exhibited favourable interaction with ampicillin and polymyxin B. IITR08540, on the other hand displayed synergy with the antibiotics ampicillin and kanamycin.

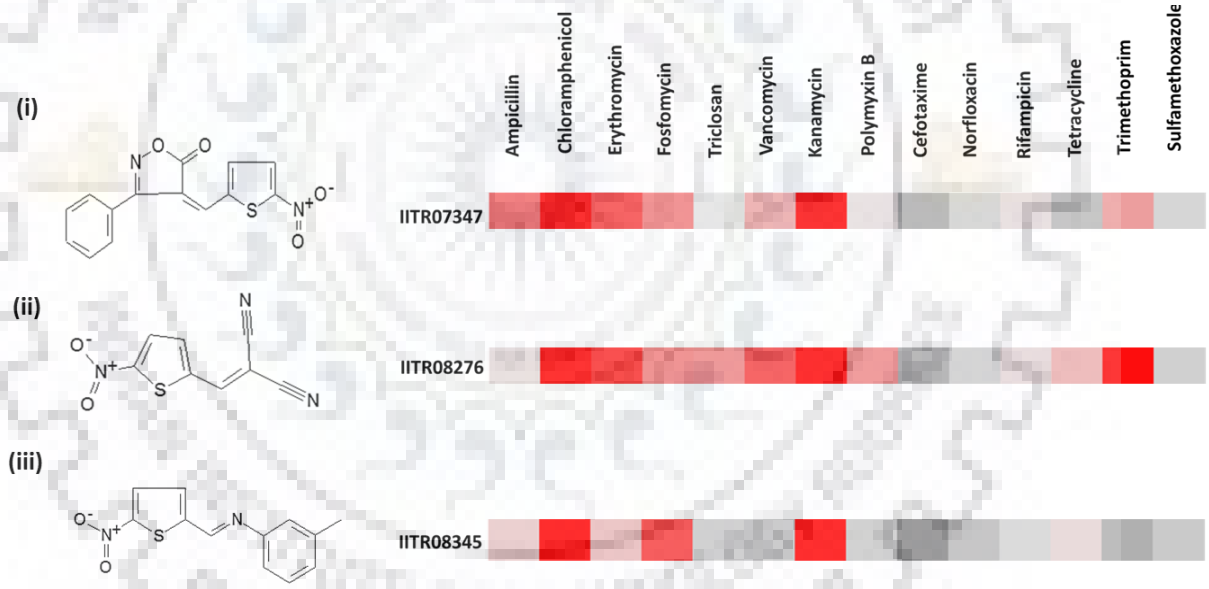

Figure 6.4: Structures and interaction profiles of the small molecules IITR07347, IITR08276 and IITR08345 that displayed similar chemical fingerprint.

6.2.5 IITR07865 displayed synergy with antibiotics targeting the bacterial cell wall and cell membrane

IITR07865 was observed to exhibit a combination ratio of 0.08 with Ampicillin (highly synergistic) and 0.25 with Polymyxin B. Further, I evaluated the combination ratio of IITR07865 with five other antibiotics which are known to inhibit bacterial cell wall synthesis namely, meropenem, oxacillin, cefepime, penicillin G and aztreonam, Interestingly, IITR07865 showed excellent synergy with all five cell wall targeting antibiotics, with low combination ratio of Meropenem (0.04), Penicillin G (0.05), Oxacillin (0.08), Cefepime (0.16), Aztreonam (0.5) as shown in Table 6.3. Thus, the small molecule IITR07865 was observed to interact distinctly and favourably with inhibitors of cell wall synthesis. Following the previously established concept of Loewe additivity which states that, two compounds form a synergistically interacting pair if they have a similar mode of action or similar target within the bacterial cell [291]. Hence, I assumed IITR07865 to target the bacterial cell wall synthesis machinery. IITR07865 also displayed synergy with polymyxin B and could be assumed to target the cell membrane as well [292]. However, both these speculations needed further experimentation for validation.

Table 6.3: Combination ratio profiles of IITR07865 with cell wall targeting antibiotics at 1/4X MIC.

Antibiotic	Combination Ratio
Ampicillin	0.08
Cefotaxime	0.5
Penicillin G	0.05
Oxacillin	0.08
Cefepime	0.16
Meropenem	0.04
Aztreonam	0.5

6.2.6 IITR07865 treated *E. coli* cells displayed a rounded morphology

Analysing the morphology of bacterial cells upon treatment with novel antibacterial agents can also facilitate the identification of their mechanism of action [293]. Hence, I exposed *E. coli* Δ*tolC* cells with sub inhibitory concentrations of IITR07865 and performed fluorescence microscopic studies to study its effect on their morphology. *E. coli* Δ*tolC* is the mutant strain which is deficient of a major bacterial efflux pump, TolC [294] (MIC of IITR07865 in *E. coli* Δ*tolC* = 8 µg/ml). Fluorescence microscopy using the combination of membrane staining dye FM 4-64FX and DNA staining dye, DAPI revealed the occurrence of rounded phenotype in IITR07865 treated *E. coli* cells (Fig. 6.5). This observation was further validated by performing Scanning Electron Microscopy (SEM) studies and formation of rounded or ovoid cells upon IITR07865 treatment was observed (Fig. 6.6).

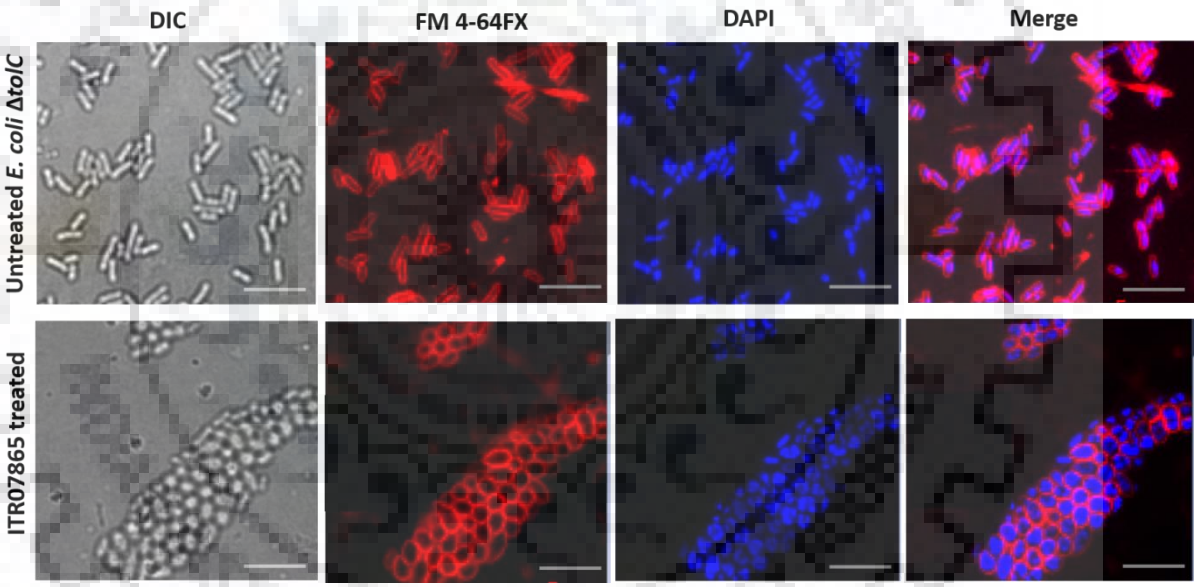

Figure 6.5: Fluorescence microscopy images of untreated and IITR07865 treated *E. coli* Δ*tolC*. Cells were stained with FM 4-64FX (1µg/ml) and DAPI (0.2µM). Scale bar represents 5 µm.

The rounded bodies obtained upon IITR07865 treatment are known as spheroplasts and represent bacterial cells that lack intact cell wall [293]. Peptidoglycan synthesis inhibitors such as fosfomycin, vancomycin and the beta-lactam antibiotics have been implicated in spheroplast formation in Gram negative bacteria [295]. Exposure to other antibiotics that inhibit protein synthesis (e.g. chloramphenicol) or folic acid synthesis inhibitors (e.g. trimethoprim and sulfamethoxazole) may also induce spheroplast formation in bacterial cells [293].

However, it is worth noticing that not all beta-lactam antibiotics lead to spheroplast formation. Aztreonam is a monocyclic beta lactam that causes the formation of elongated rod like *E. coli* cells upon treatment [296]. The difference in the beta-lactam induced morphological changes can be attributed to the affinity of different antibiotics to various Penicillin Binding Proteins (PBPs), which are a group of enzymes that play an essential role in cell wall biosynthesis [297]. Aztreonam demonstrates high affinity for PBP-3 leading to formation of filaments. On the other hand, meropenem has high affinity for PBP2 and PBP4 and leads to the formation of spherical or ovoid cells by inhibiting these targets [298]. Fluorescence microscopy studies on *E. coli* ATCC 25922 demonstrated ovoid, filamentous and spherical morphologies in cells treated with meropenem, aztreonam and IITR07865 respectively (Fig. 6.7). Thus the morphology of IITR07865 treated *E. coli* cells was observed to more closely resemble meropenem treatment, thus indicating IITR07865 to inhibit cell wall synthesis by acting on common cellular targets.

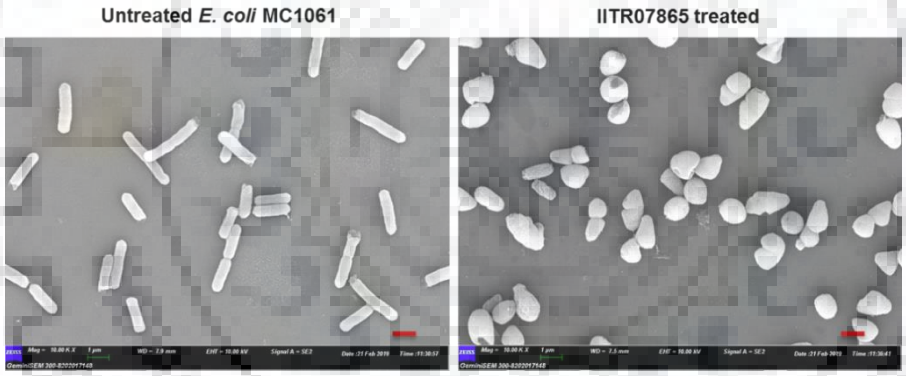

Figure 6.6: Scanning electron microscopy (SEM) micrographs of *E. coli* MC1061 cells treated with sub-inhibitory concentration of IITR07865. Images were taken at magnification 10000X and scale bar represents 1 µm.

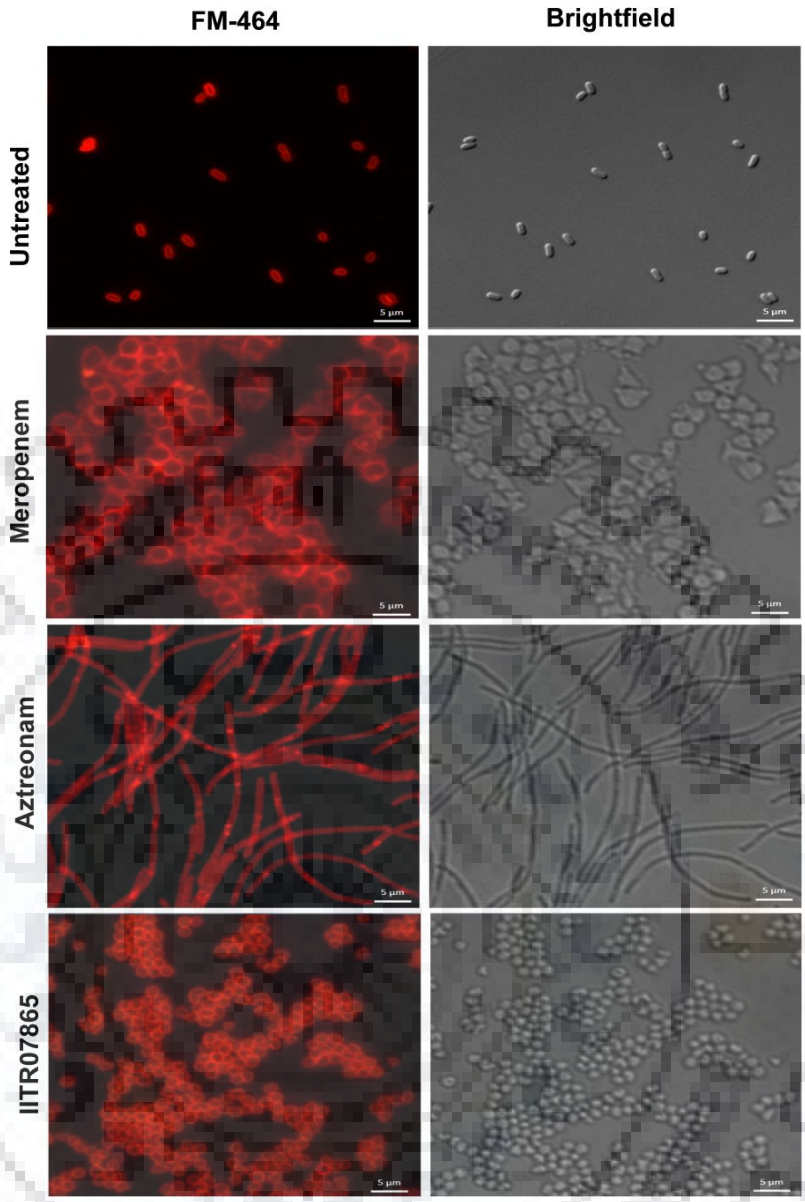

Figure 6.7: Fluorescence microscopy studies to assess morphological changes in *E. coli* cells upon IITR07865 exposure in comparison to other cell wall targeting antibiotics. *E. coli* ATCC 25922 were treated with antibiotics meropenem, aztreonam and IITR07865 and stained with FM 4-64FX (1 µg/ml). Scale bar represents 5 µm.

6.2.7 IITR07865 inhibited cell wall synthesis by acting on PBP 2 and PBP 4

The chemical-chemical interaction profile and morphological studies so far indicated IITR07865 to have mechanism of action similar to that of cell wall synthesis inhibitor, meropenem. Hence, in order to confirm our speculation, I performed a PBP binding and competition assay with IITR07865, as per the previously published protocol [299]. This

protocol requires the use of isolated bacterial membrane fractions, which contain PBPs and the fluorescent derivative of penicillin, Bocillin FL as a reporter. A PBP targeting antibacterial may compete for similar binding sites as of Bocillin FL thus causing decreased fluorescence signal, in comparison to no drug treated membrane fractions. Isolated membrane fractions were preincubated with IITR07865 and subsequently incubated with Bocillin FL [300]. Samples were run on SDS Page following which gels were scanned to analyse fluorescence. Meropenem was used as a positive control for the assay. As discussed previously, meropenem is known to possess highest affinity for PBP2 and PBP4 followed by PBP6, PBP3, PBP1b and PBP1a [298]. Upon visualising the gel on a fluorescence scanner, the intensity of two bands at positions corresponding to PBP2 (MW-70.8 KDa) and PBP4 (MW 51.8 KDa) were found to decrease in the presence of IITR07865 and meropenem (Fig. 6.8).

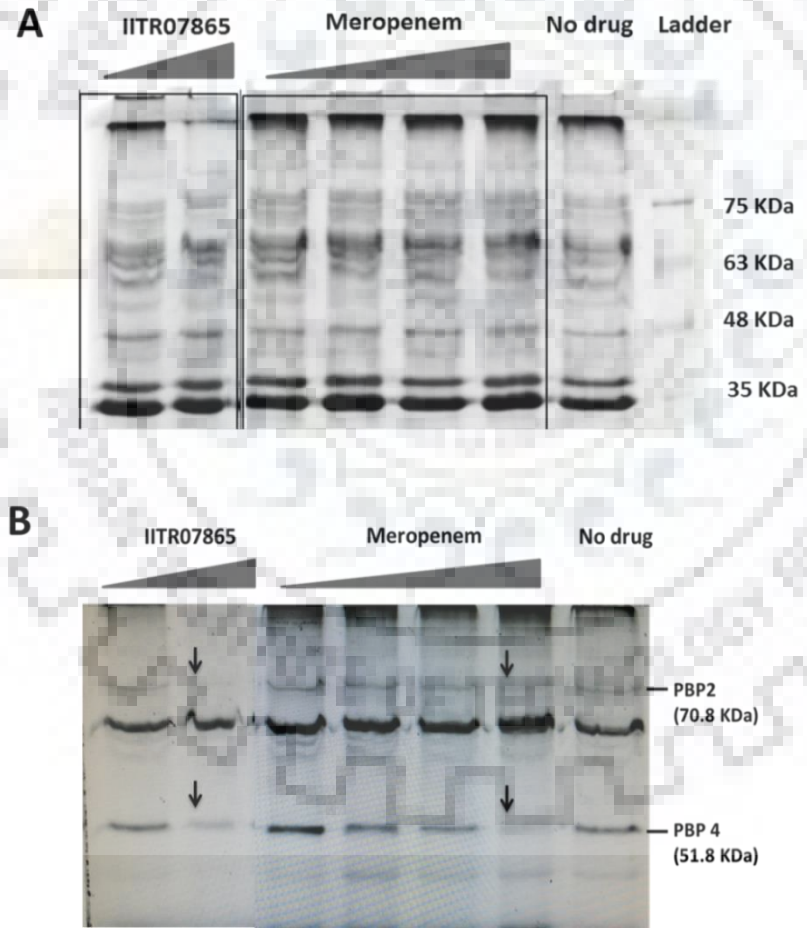

Figure 6.8: Bocillin FL based PBP binding assay for target identification of IITR07865. (A) SDS PAGE gel after staining with Coomassie brilliant blue. (B) SDS PAGE gel scanned with Typhoon FLA 9500 instrument using a 488-nm excitation wavelength (IITR07865 at concentration of 8 µg/ml and meropenem at 0.032, 0.064, 0.128, 0.256 µg/ml).

6.2.8 IITR07865 exhibited a broad spectrum antibacterial activity and is bactericidal in nature

Further, I sought to analyse the antibacterial spectrum of IITR07865 against a panel of Gram negative and Gram positive strains from the lab repository (Table 6.4). IITR07865 was observed to inhibit wild type *E.coli* ATCC 25922 and Enterohemorrhagic *E.coli* O15:H7 (EHEC) at 32 µg/ml. However, it was observed to have low inhibitory potential against the two Gram negative ESKAPE pathogens, *A. baumannii* and *P. aeruginosa* both exhibiting MIC of 128 µg/ml. *Salmonella enterica* Serotype Typhimurium was observed to exhibit greater susceptibility to IITR07865 (MIC of 8 µg/ml). The activity of IITR07865 was further studied against a few clinical isolates of *E. coli* and one each of *A. baumannii* and *K. pneumonia*e. The *E. coli* strains

Table 6.4: *In vitro* antibacterial activity of IITR07865 in several bacteria.

	IITR07865 MIC (µg/ml)
Gram Negative :	
E. coli ATCC 25922	32
E. coli O157:H7	32
Acinetobacter baumannii AYE	128
Shigella flexneri ATCC 9199	64
Pseudomonas aeruginosa MTCC 2453	128
Salmonella choleraesuis ATCC 10708	128
Salmonella enterica Serotype Typhimurium	4
Gram Positive :	
Staphylococcus aureus ATCC 29213	64
Bacillus cereus ATCC 11778	128
Enterococcus faecium FH99	64
***Mycobacterium* spp.**	
Mycobacterium smegmatis	64

studied were isolates causing Urinary Tract Infection (UTI) and exhibited multidrug resistance. IITR07865 demonstrated a fairly good activity against them with MIC in the range 8-64 µg/ml. Clinical isolates of *A. baumannii* and *K. pneumoniae* showed MIC of 128 µg/ml and 64 µg/ml respectively.

Table 6.5: *In vitro* antibacterial activity of IITR07865 against clinical isolates of Gram negative pathogens. Numbers in brackets indicate the no. of isolates tested.

Bacteria	IITR07865 MIC (µg/ml)
E. coli (10)	8-64
A. baumannii (1)	128
Klebsiella pneumonia KPC2 (1)	64

6.2.9 The combination of IITR07865 and meropenem is synergistic and bactericidal

Further, time-kill kinetic study for IITR07865 was performed against *E. coli* ATCC 25922 to identify whether it is bacteriostatic or bactericidal in nature. *E. coli* cells were exposed to varying concentration of IITR07865 and the number of viable bacteria at regular intervals was determined. Since, IITR07865 caused a >3 log reduction of the bacterial inoculum in comparison to untreated control, it was observed to possess a bactericidal activity (Fig. 6.9).

Since, IITR07865 exhibited synergistic interaction with cell wall targeting antibiotics with combination ratio <0.25, I further analysed its interaction with meropenem by means of time kill kinetics assay. Small molecules that show greater than 2 $\log_{10}$ killing in comparison to the most effective agent in the small molecule-antibiotic pair are considered to exhibit synergy. Hence, IITR07865 showed a synergistic and bactericidal killing activity against *E. coli* ATCC 25922 such that no viable bacteria were obtained after 12 h of treatment up to 24 h (Fig. 6.10)

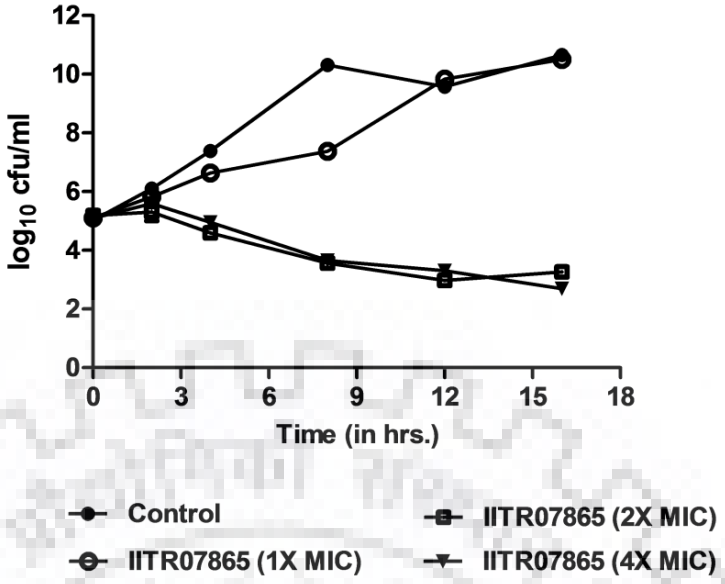

Figure 6.9: Time kill kinetics of IITR07865 against *E. coli* ATCC 25922. *E. coli* (10^5 CFU/ml) cells were incubated with 1X, 2X and 4X MIC of IITR07865 and the number of viable cells were determined. Each value represents the mean of three values and error bars indicate standard deviation.

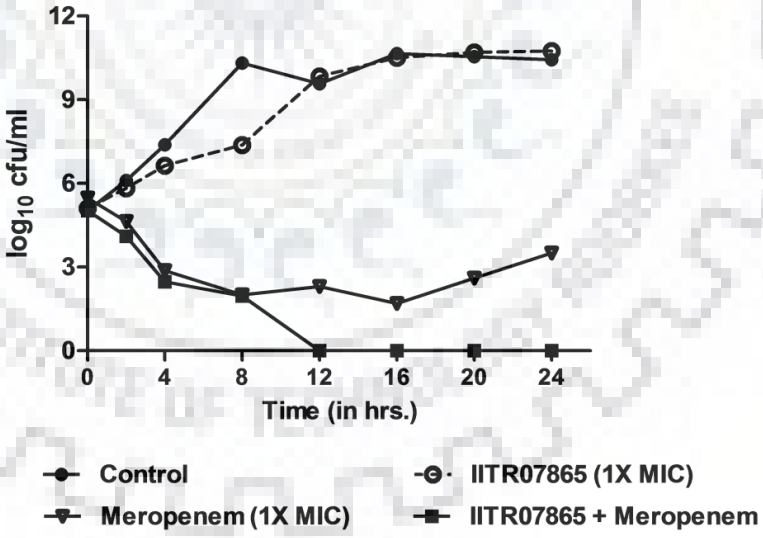

Figure 6.10: Time kill kinetics of IITR07865 in combination with meropenem against *E. coli* ATCC 25922. *E. coli* (10^5 CFU/ml) cells were incubated with 1X MIC each of IITR07865 and meropenem and the number of viable cells were determined. Each value represents the mean of three values and error bars indicate standard deviation.

6.2.10 IITR07865 is non-haemolytic to Red Blood Cells

To get a preliminary idea of toxicity of IITR07865, I evaluated its ability to lyse human erythrocytes at 4X and 8X MIC observed against *E. coli* MC1061. IITR07865 was observed to be non-haemolytic and hence non-toxic causing only 0.49±0.1% haemolysis at 8X MIC (Table 6.6).

Table 6.6: Haemolytic potential of IITR07865.

	Haemolysis (%) w.r.t to Triton-X 100 (100%)
IITR07865 (at 4X MIC)	0.26 ± 0.02
IITR07865 (at 8X MIC)	0.49 ± 0.1

6.2.11 IITR08276, IITR07347 and IITR01324 cause membrane depolarization

As discussed previously, the chemical combination screen identified a few other small molecules that displayed favorable interactions with several bioactives. For example, the compounds IITR07806 and IITR08276 displayed synergy with antibiotics chloramphenicol, erythromycin, kanamycin and trimethoprim. Such compounds could be considered to display promiscuous synergistic interactions, as per previous reports [31]. In an effort to understand the mode of action of such molecules, I investigated the possibility of these molecules to act on membrane either by affecting its membrane potential or permeability. This was assessed with the aid of membrane potential sensitive fluorescent probe, 3, 3'dipropylthiacarbocyanine {$DiSC_3(5)$} and membrane permeability indicator dye, Sytox Orange.

The transport of electrons through the electron transport chain (ETC) is responsible for the generation of a Proton Motive Force (PMF) across the bacterial membrane, which is necessary for ATP synthesis [301]. Bacterial PMF comprises of two components, $\Delta\Psi$ and ΔpH which represent the electric potential and proton gradient across the membrane respectively [14]. The cationic dye $DiSC_3(5)$ displays the potential to identify dissipaters of both the $\Delta\Psi$ and ΔpH component of PMF. Compounds that cause enhanced $DiSC_3(5)$ fluorescence are considered to be potential dissipaters of $\Delta\Psi$, while the ones that cause decrease in fluorescence, act by affecting the ΔpH component of PMF [14]. Verapamil, a known inhibitor of bacterial membrane potential was used as positive control for the assay [302].

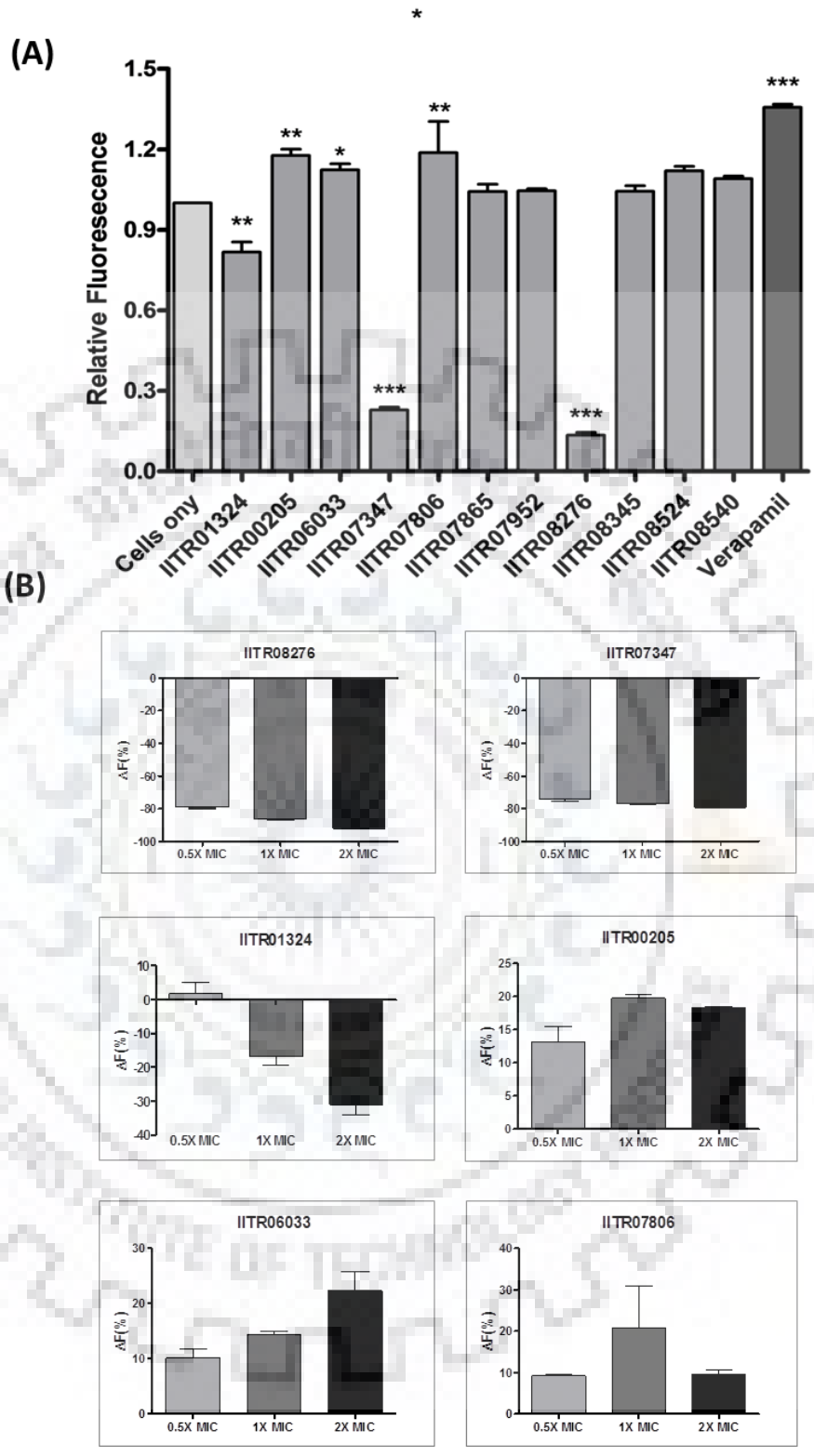

Figure 6.3: Membrane potential assay for small molecules from the chemical combination screen. ***E. coli*** **cells were incubated with $DiSC_3$ (0.5 µM) and exposed to small molecules (at 1X MIC). Fluorescence was measured at the excitation-emission wavelengths of 620-680 nm. P values were determined by one-way ANOVA followed by Dunnett's multiple comparison test (*, P<0.05; **, P<0.01; ***, P<0.001).**

IITR07347 and IITR08276 showed a significant decrease in $DiSC_3(5)$ fluorescence ($P<0.001$), thus indicating them to be potential disruptors of the ΔpH component of PMF (Fig. 6.11A). This observation established the reason for the promiscuous synergies displayed by IITR08276 and IITR07347 with several bioactives. IITR01324 was also observed to affect the membrane potential and showed decrease in $DiSC_3(5)$ fluorescence ($P<0.01$). The assay revealed the compounds IITR00205, IITR06033 and IITR07806 to exhibit an increase in fluorescence, thus indicating them to be potential dissipators of the bacterial membrane potential ($P<0.01$). Dose response curves for these compounds were plotted to assess their concentration dependent effect on the $DiSC_3(5)$ fluorescence at 0.5X - 2X MIC. IITR01324, IITR08276 and IITR07347 displayed a concentration dependent decrease in fluorescence (Fig. 6.11B). Similarly, dose response curves for IITR00205 and IITR06033 showed increase in fluorescence as the concentration of drug was increased (Fig. 6.11B). However, IITR07806 failed to show a concentration dependent effect. This observation was found to be surprising considering the fact that out of the 14 small molecules studied, IITR07806 showed favourable interaction with maximum number of bioactives. This would indicate though that the membrane depolarization effect displayed by IITR07806 was only a consequence of cell death and does not indicate its mechanism of action. However, this speculation would need further validation.

6.2.12 IITR00205, IITR06033 and IITR07865 cause increased membrane permeability

The membrane permeability assay using the fluorescent dye, sytox green revealed the compounds IITR06033 and IITR07865 to show a significant increase in fluorescence ($P<0.001$) thus indicating the occurrence of compromised membranes. It was interesting to note that in the combination screen, IITR07865 was observed to act in synergy with Polymyxin B which is also a membrane targeting antibiotic. This assay further established the small molecule IITR07865 to have a dual targeting mechanism of action; it acted on bacterial cells by inhibiting the cell wall synthesis machinery and increasing membrane permeability. Small molecule IITR00205 showed a slight increase (approximately 1.2 fold) in fluorescence (Fig. 6.12A). Dose response curves for each of the three compounds were further plotted and they revealed a concentration dependent effect thus validating the mechanism of action of the three compounds (Fig. 6.12B).

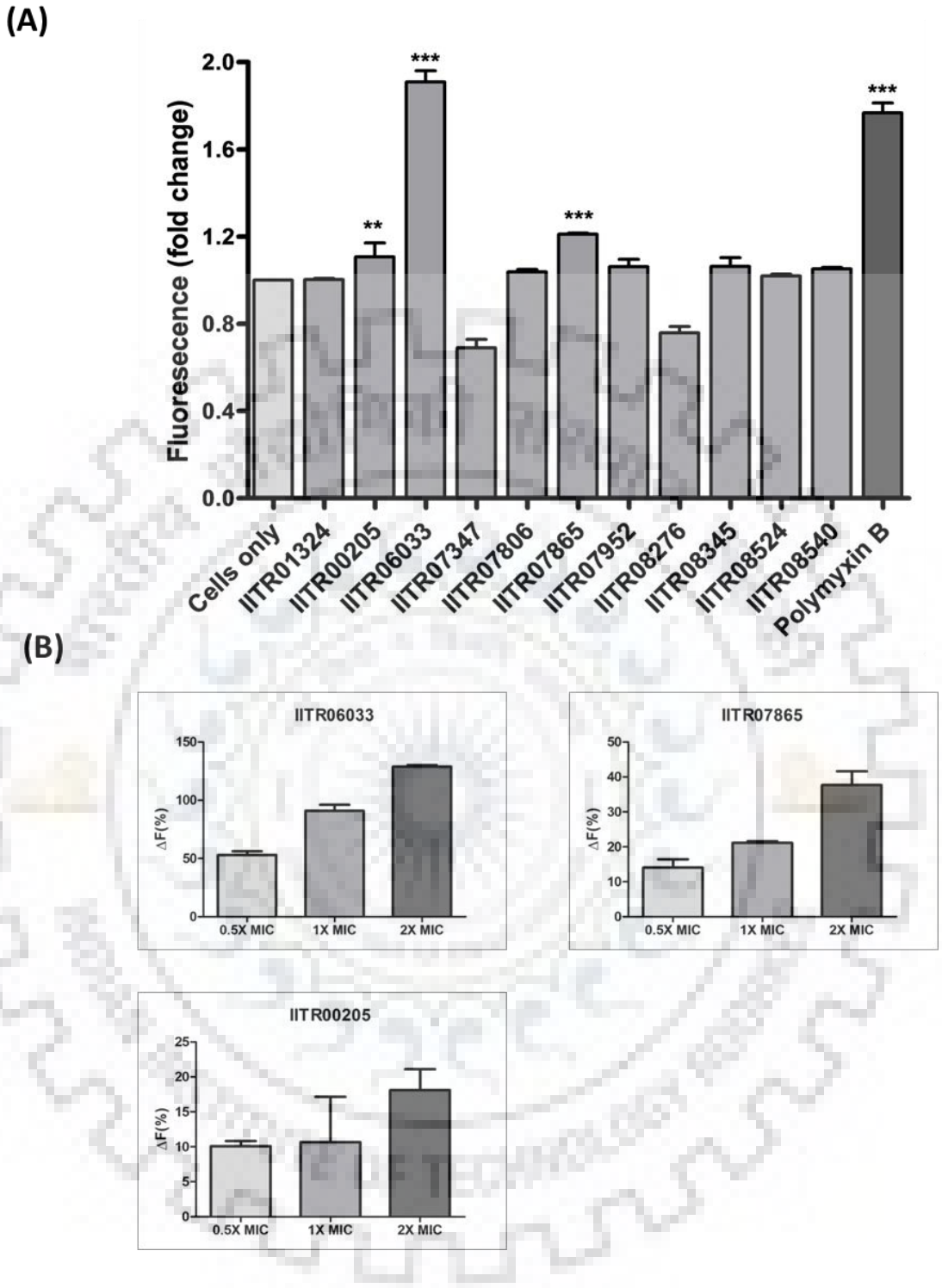

Figure 6.12: Membrane permeability assay for small molecules from the chemical combination screen. *E. coli* cells were incubated with Sytox Orange (1 µM) and exposed to small molecules (at 1X MIC). Fluorescence was measured at the excitation-emission wavelengths of 547-570 nm after 30 minutes of incubation. P values were determined by one-way ANOVA followed by Tukey's multiple comparison test (*, P<0.05; **, P<0.01; ***, P<0.001).

6.2.13 *In vitro* cytotoxicity of the small molecules was evaluated

At the early stages of lead identification, an initial assessment of the toxicity of a drug candidate can be obtained on the basis of its therapeutic index. The therapeutic index (TI) is calculated by dividing the IC50 values obtained from *in vitro* cytotoxicity studies by the Minimum Inhibitory Concentration values. A drug is considered to have a good safety profile if its Therapeutic Index is ≥10 [303]. Hence, I performed *in vitro* cytotoxicity studies on isolated human PBMCs of each of these small molecules at 10X MIC to get a preliminary idea about their toxicity. Assessment of *in vitro* toxicity was extremely important since some of the small molecules were observed to target membrane, thus insinuating them to possess toxicity against eukaryotic cells. The MTT assay for *in vitro* cytotoxicity revealed the compounds IITR01324 and IITR08345 to be extremely safe at 10X MIC causing no or negligible cell death. On the contrary, IITR07952, IITR00205, IITR07347, IITR08540 and IITR06033 were observed to be significantly toxic ($P<0.001$) causing approximately 60-75 % cell death (Fig. 6.13). The compounds IITR07865, IITR07806, IITR08276 cause approximately 25-35 % cell death at 10X MIC. The toxicity of these compounds could be reduced and overcome by using them in combination with the antibacterial agents that exhibited favorable interactions with them [13].

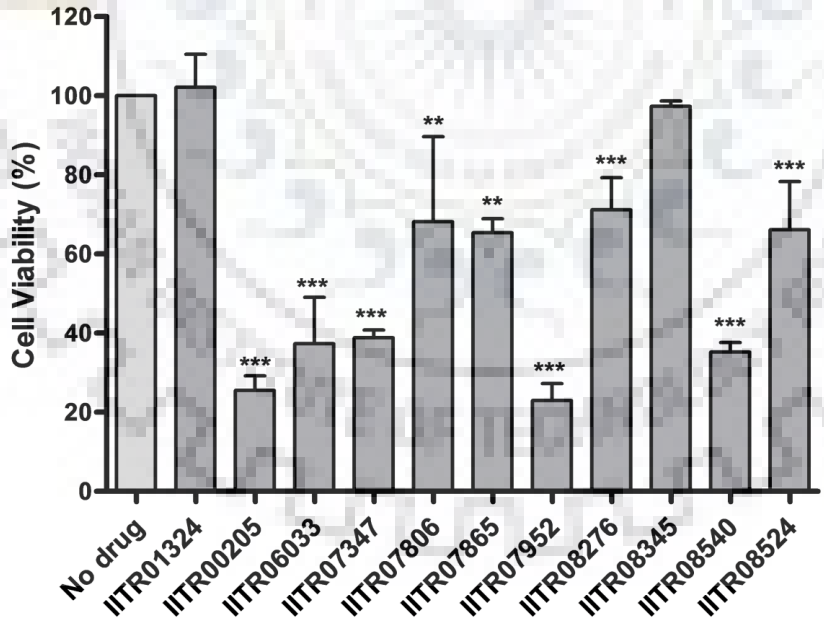

Figure 6.13: Cytotoxic effects of small molecules from the combination screen against human Peripheral Blood Mononuclear Cells (PBMCs). MTT assay was used to assess the toxic effect of small molecules at 10X MIC. Percent viability was calculated with respect to no drug (solvent only) control. P values were determined by one-way ANOVA followed by Dunnett's multiple comparison test (*, P<0.05; **, P<0.01; ***, P<0.001).

6.2.14 IITR07865 exhibited excellent anti-persister activity against ampicillin induced persisters of *E. coli* ATCC 25922

On the basis of the observation that IITR07865 acted on dual targets within the bacterial cell i.e. the cell wall and cell membrane. I was encouraged to see if it would also possess antibacterial activity against persisters since membrane active agents are considered to be potent anti-persister compounds [304]. Persister cells of *E. coli* ATCC 25922 were isolated by treating stationary phase bacteria with 300 µg/ml ampicillin (for 14 h). These were then exposed to 2X and 4X MIC of IITR07865 and viable counts were determined at regular intervals up to 24 h. Interestingly, IITR07865 at 2X MIC exhibited a bactericidal activity against ampicillin induced persisters causing a >3 log reduction in the viable cell count. Moreover, at 4X MIC IITR07865 exhibited a superior rate of killing such that all persisters were eradicated within 24 hours of treatment (Fig. 6.15).

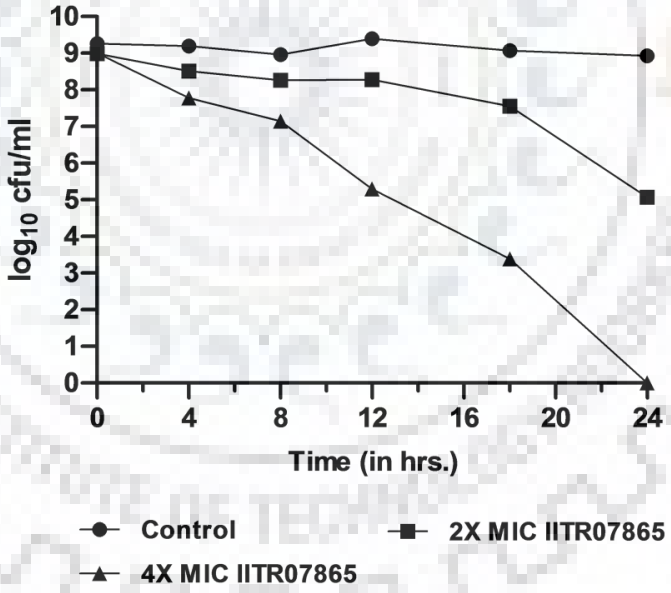

Figure 6.14: Kinetics of persister killing by IITR07865 in *E. coli* ATCC 25922. Ampicillin induced persisters were isolated and exposed to 2X and 4X of IITR07865. Aliquots were withdrawn at regular intervals and the number of surviving bacteria were enumerated. Each value represents the mean of three values and error bars indicate standard deviation.

6.3 Discussion

Elucidating the mode of action (MOA) for novel antibacterials identified in small molecule phenotypic screens remains a daunting task that limits drug discovery efforts. Previous studies have established that the MOA of unknown antibacterials can be determined by studying their combinations with compounds of known biological activity [31]. The combination study of small molecules with known bioactives gives an idea about their interaction and aids the identification of their targets [242] . As per the concept of Loewe additivity, two compounds are known to form a synergistically interacting pair if they have a similar modes of action or share similar targets within the bacterial cell [305].

My combination screen revealed the occurrence of several synergistic (CR <0.25), additive (CR >0.25), or antagonistic interactions (CR >1). The small molecules IITR07806 and IITR08276 displayed a large number of favourable interactions indicating their promiscuous nature, which was later confirmed by membrane potential and permeability assays. The combination profile screen also clustered the molecules IITR07347, IITR08276 and IITR08345; all belonging to the same chemical class, on the basis of their interaction profiles. The small molecule IITR07865 interacted synergistically with ampicillin, meropenem, aztreonam etc. (cell wall synthesis inhibitors) and Polymyxin B (cell membrane inhibitor). Since bacterial cell wall synthesis and cell membrane are attractive targets for antibacterial drug discovery and IITR07865 was observed to act through both, it was taken up for detailed analysis.

IITR07865 treated cells displayed a rounded/ovoid rounded phenotype, similar to the phenotype shown by cell wall targeting antibiotic, Meropenem. Formation of rounded bodies or spheroplasts by Meropenem has been attributed to its affinity for the cell wall synthesis protein, PBP2/PBP4. PBP binding and competition assay showed IITR07865 and meropenem to have similar targets though the affinity in each case might differ, considering the extremely low MIC of meropenem (0.12 µg/ml) against *E. coli* in comparison to IITR07865. IITR07865 displayed a bactericidal activity and interacted synergistically with meropenem in time-kill kinetic assay. It was also observed to exhibit an excellent anti-persister activity against *E. coli* cells. IITR07865 increased bacterial membrane permeability but had no effect on the membrane potential. Upon analysis of the structure of IITR07865 closely, it was observed to possess a biguanide moiety which is also present in the commonly used biocide, chlorhexidine (Fig. 6.15)

[289]. Infact, IITR07865 represented exactly half of the structure of chlorhexidine except for the presence of an extra

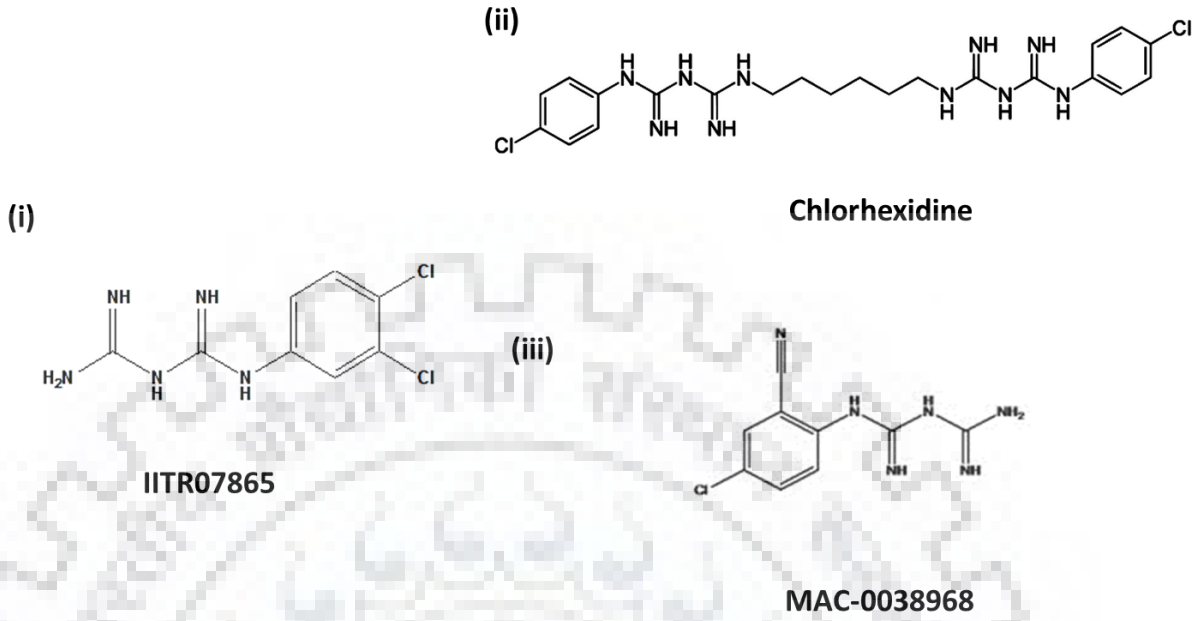

Figure 6.15: Chemical structures of (i) IITR07865, (ii) Chlorhexidine and (iii) MAC-0038968. IITR07865 closely resembles Chlorhexidine and MAC-0038968 although they act on different targets within the bacterial cell.

chlorine atom. It was interesting to observe that chlorhexidine, although a known membrane targeting compound did not cause the occurrence of rounded/ovoid structures (microscopy for chlorhexidine treated *E. coli* cells was performed, data not shown). Moreover, IITR07865 also closely resembled a previously reported inhibitor of the enzyme Dihydro Folate Reductase (DHFR) of the folic acid synthesis pathway, MAC-0038968 [31]. This molecule was discovered in a chemical combination screen and displayed unique synergistic interaction with sulfamethoxazole. IITR07865, on the other hand displayed additivity/indifference with sulfamethoxazole.

IITR07865 was observed to be non-hemolytic and relatively safe exhibiting only 25-35 % toxicity to eukaryotic cells at 10X MIC. The safety index of IITR07865 could be possibly reduced or overcome by using it in combination with synergistically interacting antibacterial agents. Despite the dual targeting potential of IITR07865, it displayed high antibacterial activity against most Gram negative and Gram positive bacteria with MIC in the range of 32-128 µg/ml. Structure Activity Relationship (SAR) studies need to be carried out in future to

improve the antibacterial potential of IITR07865 without compromising its safety profile. This study also discovered a few other molecules that act on the bacterial cells by causing increased membrane permeability and membrane depolarization. Small molecules which dissipated the bacterial membrane potential could be also evaluated for their efflux inhibitory activity. However, further studies need to be carried out to ascertain whether these observations are a result of off-target membrane activity or represent the true targets for these compounds.

6.4 Experimental procedures

6.4.1 Bacterial strains, antibiotics and other reagents

The strains used for the study were *E. coli* MC1061, *E. coli* Δ*tolc* and *E. coli* ATCC 25922. A panel of Gram negative and Gram positive reference strains and clinical isolates from the lab repository were also used. The growth and culture conditions have been described in the experimental procedures section of chapter 4. 12 small molecules from the in house collection of 11,000 small molecule library were used, which were procured from Maybridge and were dissolved in DMSO at a concentration of 50 mM. Antibiotics used in this study were procured from Sigma-Aldrich Corporation and were dissolved in the conditions as recommended.

6.4.2 Determination of minimum inhibitory concentrations

The minimum inhibitory concentrations (MIC) of small molecules and known antibiotics were determined to characterize their growth inhibition by the 96-well microbroth dilution method, as per the CLSI guidelines. Detailed protocol has been described in the experimental procedures section of chapter 4.

6.4.3 Small molecule-bioactive Combination profiling

Based on the minimum inhibitory concentrations (MIC), I calculated the 1/4 th and 1/8 th MIC values of both known antibiotics and small molecule. Experiments were done in duplicates by the two point dose matrix approach. *E. coli* MC1061 was grown overnight in 3 ml of MHB media. The cells were then diluted 1:100 in fresh media and allowed to grow until the OD_{600} reached 0.4-0.5. The cells were then diluted 1:1000. These were tested in 96- well micro well plates (according to two point dose matrix method) with a total volume of 200 µl and incubated at 37°C with 80% humidity for 16 hours before determining optical density at 600 nm.

6.4.4 Morphological studies using fluorescence microscopy

E. coli Δ*tolc* cells were grown overnight in 3 ml of MHB media. They were then diluted 1:100 in fresh media and allowed to grow until the OD_{600} reached 0.4-0.5. Cells were diluted to 0.1 OD and treated with sub inhibitory concentration of IITR07865 (2X MIC) and incubated for 2 h at 37°C. Agarose pads were made using 1 % agarose. FM 4-64(N-(3-Triethylammoniumpropyl)-4-(6-(4-(Diethylamino) Phenyl) Hexatrienyl) Pyridinium Dibromide) a membrane staining dye and 0.2 µM of DAPI (4′,6-diamidino-2-phenylindole) a blue fluorescent stain, which binds AT regions of dsDNA were added to cells treated with IITR07865 and incubated for 15 minutes at room temperature in dark. A 10µL aliquot of cells was added to agar pad and covered it with a cover slip followed by observing the cells under Zeiss Axioscope A1 fluorescence microscope.

6.4.5 Scanning Electron Microscope (SEM) sample preparation

Logarithmic phase of *E. coli* MC1061 cells (OD_{600} ~0.6) were diluted to OD_{600} ~0.1 and treated with sub-inhibitory concentration of the drug for 2 h. Treated samples were resuspended in 1X PBS and primarily fixed with 2.5% glutaraldehyde for 30 minutes at 4^{o}C. Fixed cells were further dehydrated with an ethanol gradient (20%, 40%, 60%, 80%, 90%, and 100%). The samples were then coated with a layer of gold and visualized under SEM. Detailed protocol has been mentioned in the experimental procedures section of chapter 4.

6.4.6 PBP binding and competition assays

Bacterial membranes for the PBP binding and competition assay were isolated and prepared according to previously published protocols [299],[300]. *E. coli* ATCC 25922 was grown overnight in 3 ml of LB media. The cells were then diluted 1:100 in fresh media and allowed to grow in 200 ml LB until they reached stationary phase. The bacterial cell pellets were collected and suspended in a 20 mM potassium phosphate -140 mM NaCl (KPN) buffer (pH 7.5). The cells were then lysed using a cell disruptor (Constant system Ltd) at a pressure of 25 psi, and cell debris was removed by centrifugation at $12{,}000 \times \boldsymbol{g}$ for 30 min. The supernatant was centrifuged at $150{,}000 \times \boldsymbol{g}$ for 40 min at 4°C for isolation of membranes. The protein concentration in the membrane preparations was estimated by BCA assay using bovine serum albumin as a standard. For the PBP competition assay, membrane preparations (40 µg each) were incubated with IITR07865 (8 µg/ml) and Meropenem (0.12, 0.24 µg/ml) at increasing concentration and were incubated for 20 minutes at 30^{o}C. Later, Bocillin dye (30 µM) was added to it and further incubated for 20 minutes at 30^{o}C. At the end of the incubation, 4X loading dye was added (up to 1X concentration) and samples were kept at 100^{o}C in a dry bath

for 3 minutes. Membrane proteins from the competition assay mixtures were then separated by electrophoresis using an SDS-polyacrylamide gel (12%) system. For PBP visualization, gels were scanned by the Typhoon FLA 9500 instrument using a 488-nm excitation wavelength (emission, 520 to 530 nm) corresponding to the peak absorption of Bocillin. The same gel was also stained with coomassie brilliant blue stain to confirm equal loading of membrane protein in all lanes.

6.4.7 Time Kill kinetics assays

E. coli ATCC 25922 cells were grown overnight in 3 ml of MHB media. Time dependent killing of IITR07865 and combination with meropenem was studied by diluting cells freshly at 0.4 OD at 600nm, 1000 times into different sterile culture tubes containing MHB media and different concentrations of the drugs individually or in combination. Samples were treated at 37ºC and shaking at 180 rpm. Aliquots were withdrawn at regular intervals, serially diluted in 1X PBS, and plated on MH agar plates to determine the viable bacterial counts up to 24 h of treatment. Detailed protocol has been mentioned in the experimental procedures section of chapter 4.

6.4.8 Membrane potential assay

The transmembrane potential was determined with the fluorescent probe, 3'-dipropylthiacarbocyanine {$DiSC_3(5)$}. *E. coli* MC1061 cells were grown overnight in 3 ml of MHB media. Cells were then diluted 1:100 in fresh media and allowed to grow until the OD_{600} reached 0.4-0.5. Bacterial cells were then washed twice with 1X PBS buffer and then resuspended in 1X PBS to an optical density at 600 nm of 0.3. $DiSC_3(5)$ was added at a final concentration of 0.5 µM, and the cells were incubated, with constant stirring to let the dye stabilize. Compounds were then added at sub inhibitory concentrations to the $DiSC_3(5)$ pre-incubated cells and fluorescence was measured after 30 min of incubation at excitation and emission wavelengths of 620 and 680 nm respectively using a plate reader (SpectraMax M2e).

6.4.9 Membrane permeability assay

The membrane permeability assay was determined with the fluorescent dye Sytox Orange. *E. coli* MC1061 was grown overnight in 3 ml of MHB media. The cells were then diluted 1:100 in fresh media and allowed to grow until the OD_{600} reached 0.4-0.5. *E. coli* MC1061 cells were then washed twice with 1X PBS buffer and then resuspended to an optical density at 600 nm of 0.3. Following the addition of Sytox orange at a final concentration of 1 µM, the cells were incubated with constant stirring in order to let the dye stabilize. Compounds were then added at

sub inhibitory concentrations to the dye pre-incubated cells and fluorescence was measured at excitation and emission wavelengths of 547 and 570 nm respectively using a plate reader (SpectraMax M2e).

6.4.10 Haemolysis assay

Haemolytic activity of IITR07865 at 4X and 8X MIC was assessed as described previously in the experimental procedures section of chapter 4. Haemolysis was monitored by measuring the absorbance of the released hemoglobin in the supernatant at 540 nm using a spectrophotometer.

6.4.11 *In vitro* cytotoxicity studies

The cytotoxicity of small molecules on Peripheral Blood Mononuclear Cells (PBMCs) was determined by 3-(4,5-dimethylthiazol-2-yl)-2,5-diphenyl tetrazolium bromide (MTT) assay. Fresh PBMCs were isolated using HiSep^{TM} LSM 1077 (Himedia) and $2x10^6$ cells were resuspended in Roswell Park Memorial Institute medium (RPMI) and incubated in the presence of 10X MIC of small molecules at 37°C for 8 h in 5% CO_2. Control cells were treated with similar percentage of dimethyl sulphoxide (DMSO) as in drug (vehicle control) The medium was then aspirated and 100 µl of 1X PBS containing 0.5 mg/mL MTT (Biobasic) dye was added to each well and incubated further for 4 h. Following incubation, MTT containing medium was removed and 100 µL of DMSO was added to dissolve the formazan crystals by gentle agitation. The OD was measured at 570 nm in a plate reader (Biotek). Absorbance values were expressed as percentage and inhibition with respect to solvent control was calculated.

6.4.12 Persister killing assay

Stationary phase *E.coli* cells (from a 14 h old culture) were treated with 300 µg/mL ampicillin in LB medium for 24 h at 37°C under shaking condition for 14 h. Persisters were isolated by washing thrice with 1X PBS to remove any antibiotic traces and subsequently diluted upto four times the original volume in 1X PBS. IITR07865 (at 2X and 4X MIC) were added to each 1000 µL aliquot of persister cells followed by incubation at 37°C for 24 h at 180 rpm. Control containing similar volume of solvent was included. The rate of killing of persisters was determined by withdrawing aliquots at regular intervals to determine the viable cell count by plating.

7 Characterisation of the mechanisms of meropenem induced persistence in *A. baumannii* and identification of small molecule inhibitors thereof.

7.1 Introduction

The discovery of antibacterial drugs in the 1940s represents one of the most important developments in the history of modern medicine. However, imprudent and indiscriminate use of these "magic bullets" worldwide has eroded their efficacy and led to a global crisis. The emergence of multidrug resistant (MDR) and extensively drug resistant (XDR) bacterial strains has further exacerbated the problem causing more than 23,000 deaths per year in the United States [2]. With the ever increasing rise in "global resistome" and significant decline in novel antibiotic discovery, there is an urgent need for alternative strategies to tackle the current predicament.

Acinetobacter baumannii is one of the most troublesome Gram-negative ESKAPE pathogens, responsible for causing a wide range of hospital acquired infections, including urinary tract infections, secondary meningitis, wound infections and ventilator-associated pneumonia [306]. The Infectious Disease Society of America (IDSA) has declared *A. baumannii* as one of the 'red alert' pathogens, thus highlighting the threat it poses to the healthcare systems [4]. In addition to the organism's high levels of intrinsic resistance, *A. baumannii* exhibits extreme genetic flexibility and remarkable ability to acquire resistance determinants in response to selective environmental pressure [234]. The uncanny ability of this bacterium to resist desiccation, survive harsh environmental conditions, including hospital settings and form biofilms, both on medical devices and biological surfaces qualifies it to be a dreadful nosocomial pathogen [306]. Alternatively, *A. baumannii* is also known to enter a physiological state where it becomes refractory or tolerant to the action of antibiotics [307],[308]. This phenomenon referred to as 'persistence" is the major cause for relapsing infections in clinical settings [125]. Eradication of the persister populations in chronic ailments holds extreme importance for an improved long term recovery. Meropenem, tigecycline, rifampicin and polymyxin B are commonly administered against *A. baumannii* infections in hospital settings, although increasing incidence of both resistant and persistant isolates have limited their efficacy against recurrent and chronic infections [309]. Therefore, screening for novel agents

that can inhibit the antibiotic tolerant bacterial cells presents an unusual challenge and can provide a successful alternative in the fight against chronic infections. Since most of the clinically important antibiotics act on DNA, RNA or protein targets that exhibit quiescence during "persistent" infections; membrane-active agents have emerged as an important new means of eradicating recalcitrant dormant bacteria [310],[311]. Furthermore, recent studies have reported the crucial role of reactive oxygen species (ROS) and active efflux mechanisms for drug tolerance in persistent populations [312],[127].

In this study, I examined the ability of *A. baumannii* to produce antibiotic tolerant persisters to four clinically relevant antibiotics from different classes, both in planktonic phase as well as biofilms. Since carbapenem class of antibiotics *are* the last resort drugs against *A. baumannii* infections, the antibiotic meropenem remained the main focus for the study. In addition, I investigated the characteristics and mechanisms of meropenem tolerance in *A. baumannii*. Furthermore, I screened a library of small molecules encompassing the GRAS (Generally Regarded As Safe) status against *A. baumannii* for potential "anti-persister" compounds based on their ability to target the bacterial membrane, cause increased ROS production and inhibit multidrug efflux pumps. The screen identified thymol to possess excellent inhibitory activity against *A. baumannii* persisters.

To our knowledge, this is the first study that utilizes a mechanism based screen to identify novel anti-persister compounds against *A. baumannii*. I also present evidence that meropenem tolerant *A. baumannii* persisters exhibit enhanced efflux activity. Importantly, this study for the first time reports the discovery of GRAS status natural compounds demonstrating excellent inhibitory activity against *A. baumannii* persisters. These findings can have vital implications for the improved treatment of recalcitrant *A. baumannii* infections in the clinics.

7.2 Results

7.2.1 Meropenem, Tigecycline, Rifampicin and Polymyxin B induced persister formation in *A. baumannii.*

The occurrence of persistence in *A. baumannii* AYE in response to four clinically relevant antibiotics meropenem, tigecycline, rifampicin and polymyxin B was assessed. *A. baumannii*

AYE is susceptible to all the four antibiotics with MICs as follows: Meropenem (0.5 µg/ml), Tigecycline (0.25 µg/ml), Rifampicin (8 µg/ml) and Polymyxin B (0.5 µg/ml). A stationary phase culture (12 h old) of *A. baumannii* AYE culture was exposed to high concentrations of Meropenem (100X MIC), Tigecycline (100X MIC), Rifampicin (50X MIC) and Polymyxin B (40X MIC) for 12 h under shaking conditions and the number of bacteria that survived the treatment was determined. *A. baumannii* AYE was observed to form persisters against all the four antibiotics exhibiting maximum persistence frequency (0.59%) for meropenem (Fig. 7.1). The antibiotics rifampicin, tigecycline and polymyxin B also displayed high persistence frequency such as 0.4144%, 0.4188% and 0.43% respectively. The Minimum Inhibitory Concentration (MIC) of the isolated persisters against respective antibiotics was further determined by the microbroth dilution method and they did not exhibit resistance. The isolated persisters were subsequently regrown into LB medium and passaged up to three generations followed by determination of MIC and persistence frequency after each passage. The persister fractions did not show any change in their susceptibility to any of the antibiotics, in comparison to the parent culture and exhibited similar persister frequencies. This observation suggested that during the period of antibiotic exposure, none of the resistance mechanisms were acquired and hence confirmed the isolation of true persister fractions.

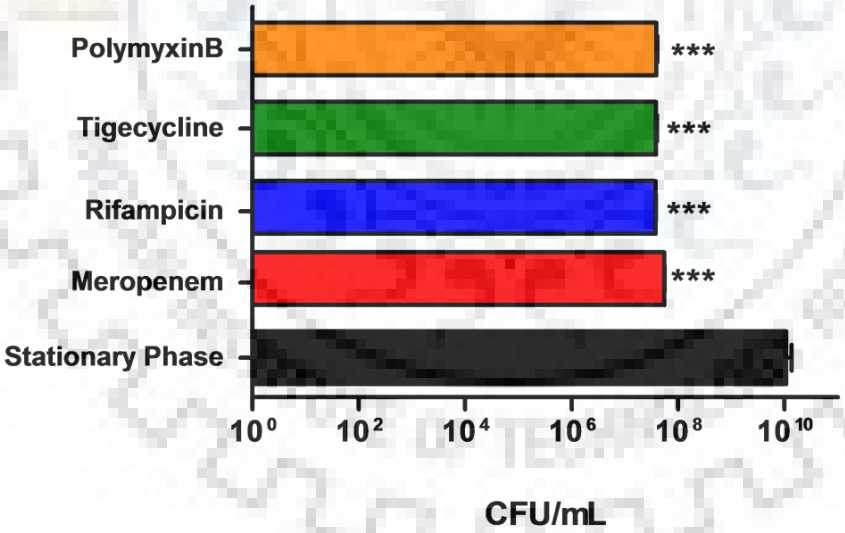

Figure 7.1: Persister fractions obtained in *A. baumannii* AYE upon exposure to Meropenem, Tigecycline, Rifampicin and Polymyxin B. Stationary phase planktonic cells were treated with high concentrations of Meropenem (100X MIC), Tigecycline (100X MIC), Rifampicin (50X MIC) and Polymyxin B (40X MIC) for 12 h under shaking conditions at 37°C. The dilutions were made and spotted onto a LB plate using the drop plate method to enumerate the colony forming units in the sample. P values were determined by one-way ANOVA followed by Tukey's multiple comparison test (*, P<0.05; **, P<0.01; ***, P<0.0001). Each value represents the mean of three values and error bars indicate standard error.

7.2.2 Meropenem induced *A. baumannii* persister revealed a typical biphasic killing pattern

Persisters represent a subpopulation of bacteria that exhibit dormancy and tolerance to bactericidal antibiotics [125]. This dormant state is characterised by a typical biphasic killing pattern in the presence of antibiotics [313]. These display an initial drastic killing of bulk of the bacterial population followed by the occurrence of a plateau phase where only the surviving persister fractions sustain. The biphasic pattern killing pattern has been observed to be both time and concentration dependent [308]. However, in case of *A. baumannii*, increasing the meropenem concentration has been shown to have no effect on persister eradication thus complicating its treatment efficacy. When stationary phase cells of *A. baumannii* AYE were exposed to meropenem at 100X MIC, a rapid decrease in viable bacterial count (up to 3.5 log) was observed until 8 h, followed by relatively constant CFU count after 24 h of treatment (Fig. 7.2). This biphasic killing pattern confirmed the presence of meropenem tolerant *A. baumannii* persisters. The MIC of the isolated persister cells against meropenem was further determined and no change in meropenem susceptibility was observed. The persisters were further re-inoculated into fresh LB medium and subsequently exposed to 100X MIC of meropenem. The cultures grown from persister cells also displayed the biphasic killing pattern and led to the formation of a similar fraction of persisters after drug exposure, thus confirming the non-heritability of persistence.

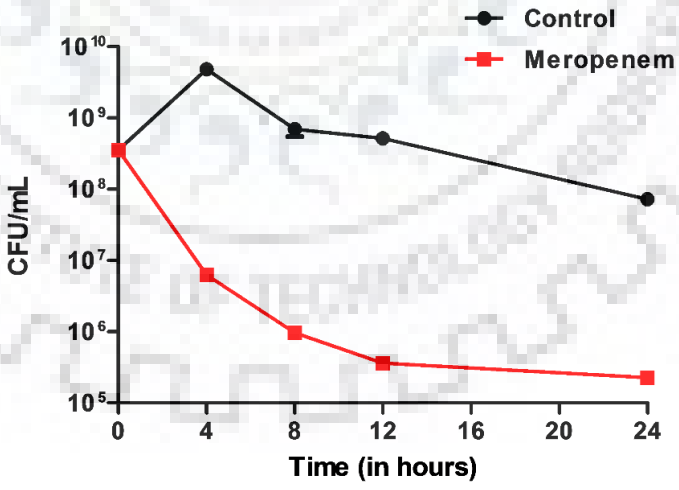

Figure 7.2: Kinetics of survival of *Acinetobacter baumannii* AYE upon treatment with 100X MIC of meropenem. 12 h old stationary phase culture of *A. baumannii* AYE were treated 100X MIC of meropenem and aliquots extracted after 4, 8 and 12 and 24 h. The number of surviving bacteria were enummerated at indicated intervals. Each value represents the mean of three values and error bars indicate standard error.

7.2.3 Meropenem induced *A. baumannii* persister formation under biofilm conditions

As discussed previously, *A. baumannii* exhibits a remarkable ability to adhere and form biofilms on both biotic and abiotic surfaces such as epithelial cells, site of wound infections, hospital surfaces and medical devices. Biofilm communities are known to contain persister subpopulations which are responsible for their recalcitrant and relapsing nature. Hence, I assessed the levels of persister fractions in *A. baumannii* AYE biofilms. 48 h biofilms grown in 96-well microtitre plate under static conditions were exposed to meropenem at 100X MIC. Persister levels were detected after 12 h of antibiotic exposure and the numbers of surviving fractions were enumerated. *A. baumannii* AYE formed biofilms on polystyrene surfaces by attaching 8.15±0.13 log cfu/ml. A significant fraction of biofilm associated cells i.e. 5.06±0.02 log cfu/ml were observed to survive exposure to bactericidal concentration of meropenem (Fig. 7.3). The level of persister formation in *A. baumannii* AYE biofilms was calculated to be 0.08±0.02%.

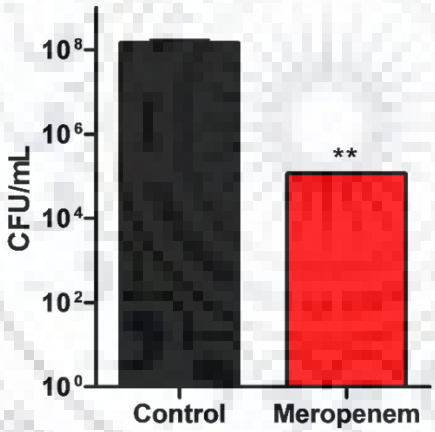

Figure 7.3: Persister levels in *A. baumannii* AYE biofilms exposed to meropenem at 100X MIC. 48 h old biofilms were treated with meropenem for 12 h and the number of surviving persisters were enumerated and plotted. P values were determined by unpaired t-test (two-tailed) (*, P<0.05; **, P<0.01; ***, P<0.0001). Each value represents the mean of three values and error bars indicate standard error.

7.2.4 Meropenem induced *A. baumannii* persisters exhibit multidrug tolerance

Persisters are considered to be dormant bacterial cells that exhibit inactive targets and thus may impart tolerance to a wide variety of antibiotics. I further investigated the tolerance of meropenem induced persisters towards three antibiotics namely rifampicin, tigecycline and

polymyxin B; which act on different cellular targets. Cross-tolerance to rifampicin (50X MIC), tigecycline (50X MIC) and polymyxin B (40X MIC) was measured by exposing a fraction of meropenem induced persisters with them for 12 h. The fraction of meropenem induced persisters that survived exposure to rifampicin, tigecycline and polymyxin B was compared to the surviving fraction of stationary phase cells [314]. It was observed that a significant fraction of meropenem persisters survived exposure to the antibiotics tigecycline and rifampicin (Fig. 7.4). Hence, cells isolated by meropenem treatment exhibited a high degree of tolerance to tigecycline and rifampicin. This could be attributed to the presence of overlapping mechanisms of persistence between meropenem induced persisters and persisters of tigecycline and rifampicin. On the contrary, meropenem induced persisters did not survive polymyxin B treatment and extremely low fractions of surviving bacteria were obtained. This indicated that the mechanisms responsible for persistence to meropenem and polymyxin were exclusive to each other and cannot occur simultaneously [315].

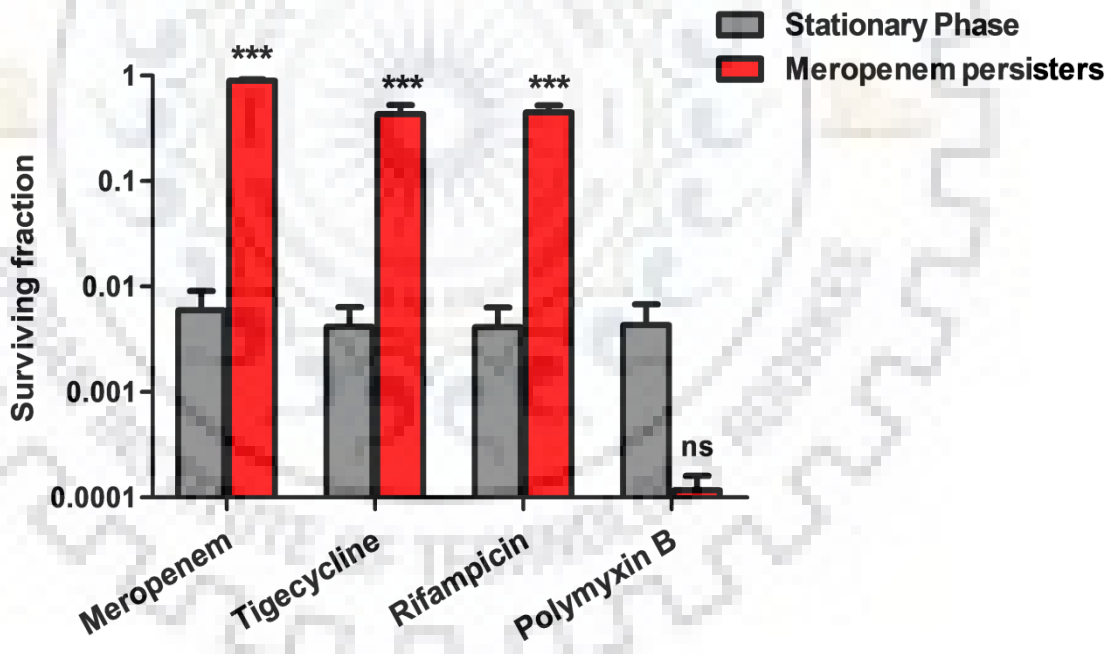

Figure 7.4: Meropenem induced *A. baumannii* persisters are multidrug tolerant. Fraction of surviving *A. baumannii* cells were determined after 12 h treatment of (i) a stationary phase culture and (ii) isolated meropenem persisters with meropenem (100X MIC), rifampicin (50X MIC), Tigecycline (50X MIC) and Polymyxin B (40X MIC). Statistical significance was calculated using two-way ANOVA followed by Bonferroni post hoc test test (*, P<0.05; **, P<0.01; ***, P<0.0001). Each value represents the mean of three values and error bars indicate standard deviation.

7.2.5 Meropenem induced *A. baumannii* persisters exhibit filamentous phenotype

I further studied the morphology of meropenem induced *A. baumannii* persisters by staining them with lipophilic membrane staining fluorescent dye, FM 4-64FX. While stationary phase *A. baumannii* cells exhibited the typical cocci shape with lengths of 1-2 µm, few cells in the meropenem persister fractions displayed elongation phenotype with cell size in the range 3-6µm (Fig. 7.5). This observation was specially intriguing since treatment of *A. baumannii* with sub inhibitory concentrations of meropenem, imipenem and other carbapenems have been reported to form larger and rounded spheroplasts [316],[317]. Several factors such as nutritional status of the bacterial cells, osmotic stress or desiccation stress are known to affect the morphology of *A. baumannii* cells [318]. A recent study reported the presence of elongated rod-like cells in stationary phase cultures of colistin-heteroresistant strains of *A. baumannii* [318]. The mechanism for the elongation phenotype observed in a fraction of meropenem isolated persisters is currently unknown, and would need further investigation.

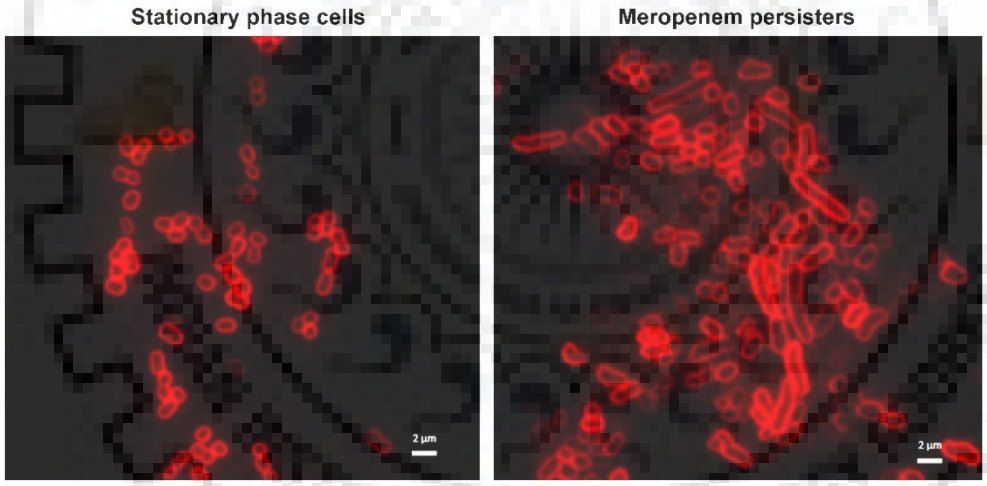

Figure 7.5: Effect of meropenem exposure (at 100X MIC) on the morphology of *A. baumannii* cells. Cells were stained with FM 4-64FX and visualised using fluorescent microscope. Scale bar represents 2 µm.

7.2.6 Meropenem induced *A. baumannii* persisters exhibit active antibiotic efflux

Recent studies have reported the crucial contribution of active efflux mechanisms towards bacterial persistence in *E. coli* and *Mycobacterium* species [205],[127]. Fluorescence based single cell microscopic studies revealed lesser accumulation of antibiotics within the persister cells thus indicating increased efflux or poor membrane permeability. The role of active efflux mechanisms in persistence was further confirmed by transcriptomic analysis of antibiotic induced persister fractions followed by the use of knockout strains of a set of efflux genes [127]. Considering the hypothesis that *A. baumannii* cells exhibit meropenem persistence by upregulating its efflux machinery, fluorescence microscopy studies on isolated meropenem persisters were performed. The accumulation of the beta lactam antibiotic BOCILLIN^{TM} FL Penicillin (BOCILLIN) was studied in the persister populations in comparison to stationary phase *A. baumannii* AYE cells. BOCILLIN is a fluorescent derivative of penicillin which has been recently employed to assay the the activity of efflux pumps by measuring its accumulation [127]

Interestingly, the accumulated antibiotic concentration of BOCILLIN in meropenem persisters was observed to be lower in comparison to stationary phase cells thus indicating that meropenem persisters enhance the expression of efflux pump genes in order to survive exposure to otherwise lethal doses of meropenem (Fig. 7.6).

7.2.7 Meropenem induced *A. baumannii* persisters exhibit membrane depolarization

Membrane potential refers to the presence of an electrochemical gradient across the inner membrane of bacterial cells leading to the generation of a proton motive force (PMF) which aids proton transfer across membrane thereby producing ATP [301]. Bacterial membrane potential and intracellular ATP levels are known to influence the phenomenon of persistence such that decreased PMF leads to a characteristic low metabolic activity in dormant persister cells. Several Toxin-Antitoxin (TA) systems have been implicated to affect the bacterial membrane potential leading to persistence [131]. To investigate if meropenem induced persisters in *A. baumannii* AYE exhibited any alteration in their membrane potential in comparison to stationary phase cells, I used the fluorescent Anionic lipophilic dye, $DiBAC_4(3)$, that enters depolarized cells causing an enhanced fluorescence intensity [319]. Since membrane potential of bacterial cells is also known to be influenced by its growth phases, the fluorescence intensity of exponential phase cells to the stationary phase cells and meropenem persisters in the $DiBAC_4(3)$ assay was further compared [320]. It was interesting to observe that meropenem induced persisters of *A. baumanii* AYE exhibited a significant increase in $DiBAC_4(3)$ fluorescence ($p< 0.0001$), thus indicating membrane depolarization and a decreased PMF, which is the characteristic of persistence in *E. coli* cells (Fig. 7.7).

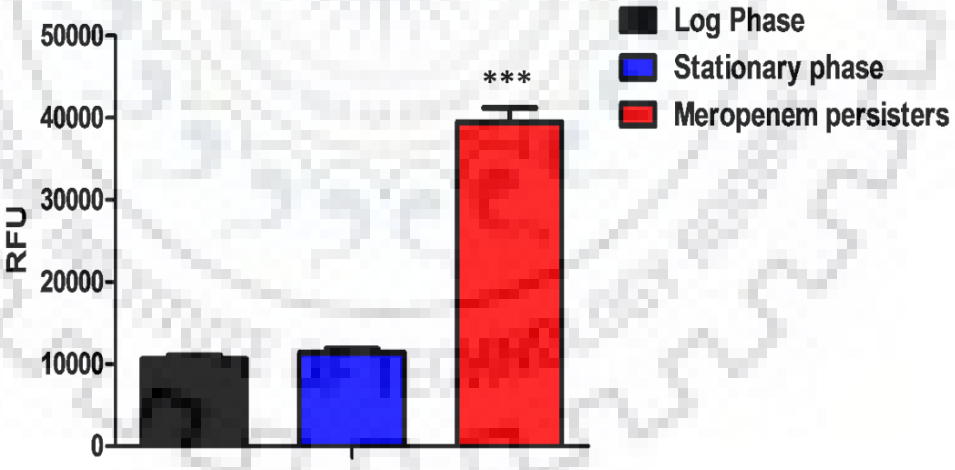

Figure 7.7: $DiBAC_4(3)$ based assay to assess the membrane potential of meropenem induced *A. baumanii* AYE persisters in comparison to exponential phase and stationary phase cells. Isolated persisters were incubated with 10 µM $DiBAC_4(3)$ for 30 minutes at 37°C and washed twice with 1X PBS. Fluorescence was recorded in a spectrophotometer at excitation-emission of 490/516 nm and Relative fluorescence unit (RFU calculated by dividing fluorescence with absorbance at 600 nm). P values were determined by one-way ANOVA followed by Tukey's multiple comparison test (*, P<0.05; **, P<0.01; ***, P<0.0001).

7.2.8 Meropenem treated cultures of *A. baumannii* indicate the presence of Viable But Non Culturable (VBNCs) bacteria: evidence from metabolic activity assay.

As discussed previously, bacterial persisters represent a subpopulation that exhibits a state of dormancy characterized by low metabolic activity [321]. Hence, I sought to evaluate the respiratory activity of meropenem induced *A. baumannii* persisters by the {2,3-bis[2-methyloxy-4-nitro-5-sulfophenyl]-2H-tetrazolium-5-car-boxanilide (XTT) assay. Metabolic activity of stationary phase culture (12 h old) of *A. baumannii* AYE were compared with meropenem induced persister cells and exponential phase culture. The XTT assay is based on the reduction of the tetrazolium dye, XTT into a water soluble formazan product, which correlates to respiratory activity and the levels of NADH within the bacterial cell [322]. The number of CFU in the three cultures of *A. baumannii* AYE i.e the log phase, stationary phase and meropenem exposed populations were normalized prior to setting up the experiment (Fig 7.8). The assay revealed the meropenem induced *A. baumannii* persisters to exhibit a significantly high respiratory activity in comparison to stationary phase and exponential phase cells (Fig. 7.9). This observation indicated the presence of Viable But Non culturable (VBNC) populations apart from persisters in the meropenem treated *A. baumannii* cultures, which obscured our measurement of persister metabolism.

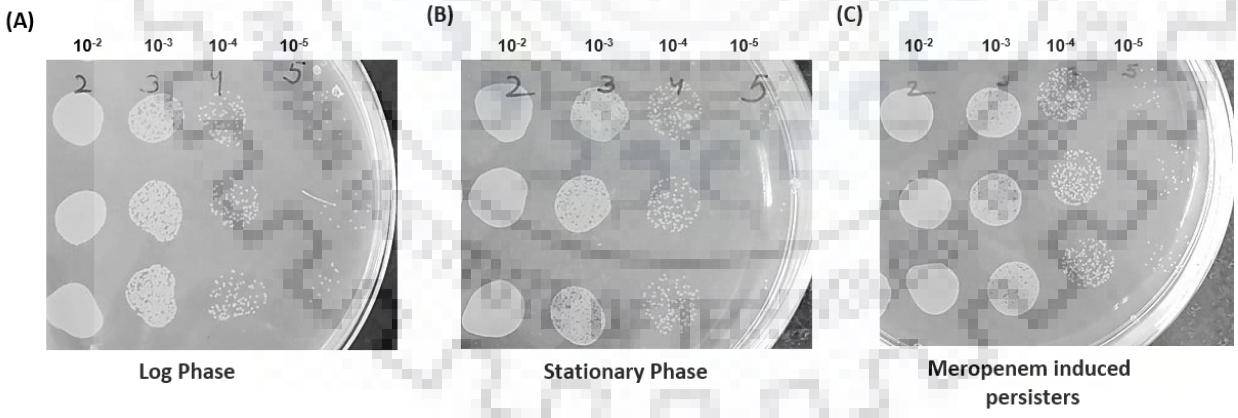

Figure 7.8: Normalisation of the Colony Forming units (CFU) of *A. baumannii* AYE cells grown upto (A) Log/exponential phase (B) Stationary phase (upto 12 hours) and (C) meropenem induced persisters isolated by treating 12 hour old culture of *A. baumannii* AYE with meropenem (at 100X MIC) for 12 hours. The CFU of each of these were normalized in 1X PBS and serial dilutuions were spotted (20 µl each) onto LB agar plates such that countable number of colonies were obtained in the 10^{-5} dilution of each condition.

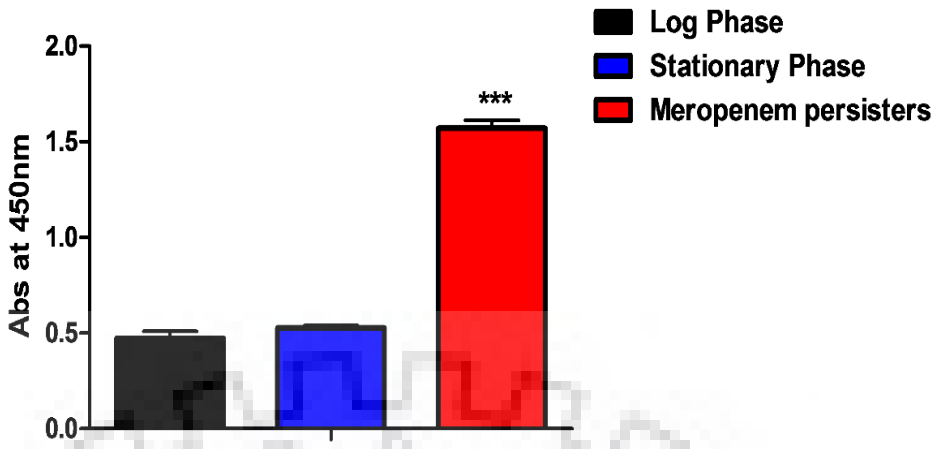

Figure 7.9: Assay for the determination of metabolic activity of meropenem induced *A. baumannii* AYE persisters in comparison to stationary phase and exponential phase cells. XTT (0.5 mg/ml) used in combination with menadione (50 µM) was added to isolated persisters in 1X PBS and incubated for 2 h. Absorbance was read at 450 nm to assess the reduction of XTT. P values were determined by one-way ANOVA followed by Tukey's multiple comparison test (*, P<0.05; **, P<0.01; ***, P<0.0001).

7.2.9 Mechanism based screening identifies potential anti-persister compounds against *A. baumannii*

In order to tackle the problem of antibiotic persistence prevailing in clinics, discovery of novel compounds that can inhibit bacterial persisters is much needed. Hence, I devised a mechanism based screen for the screening and discovery of potent anti-persister compound against meropenem induced persisters of *A. baumannii*. An in house collection of GRAS status small molecules was screened for their ability to target three major mechanisms of bacterial persistence i.e. membrane barrier, efflux pumps and oxidative stress. The Minimum Inhibitory Concentrations (MIC) of the small molecules against *A. baumannii* AYE were initially determined using broth microdilution method as per the CLSI guidelines (Table 7.1). The structures of the GRAS compounds used in the study have been given in Figure 7.10, except for clove oil and origanum oil which are mixtures of essential oils.

The compounds carvacrol, thymol, cinnamaldehyde, clove oil and eugenol were observed to have good antibacterial activity against *A. baumannii* AYE with MICs in the range 125-500 µg/mL. Other compounds such as linalool and origanum oil inhibited *A. baumannii* at a higher MIC of 1 mg/ml. Compounds that showed MIC values >1mg/mL were excluded from further screening assays.

Table 7.1: Antibacterial activity of GRAS status small molecules against *A. baumannii* AYE in terms of their Minimum Inhibitory Concentration (MIC).

Compounds	Minimum Inhibitory Concentration
Carvacrol	125µg/ml
Cinnamaldehyde	250µg/ml
Clove Oil	500µg/ml
Eugenol	500µg/ml
Thymol	250µg/ml
Origanum oil	1mg/ml
Linalool	1mg/ml
Curcumin	>8mg/ml
Berberine	>8mg/ml
Chlorogenic Acid	>8mg/ml
Piperine	>8mg/ml

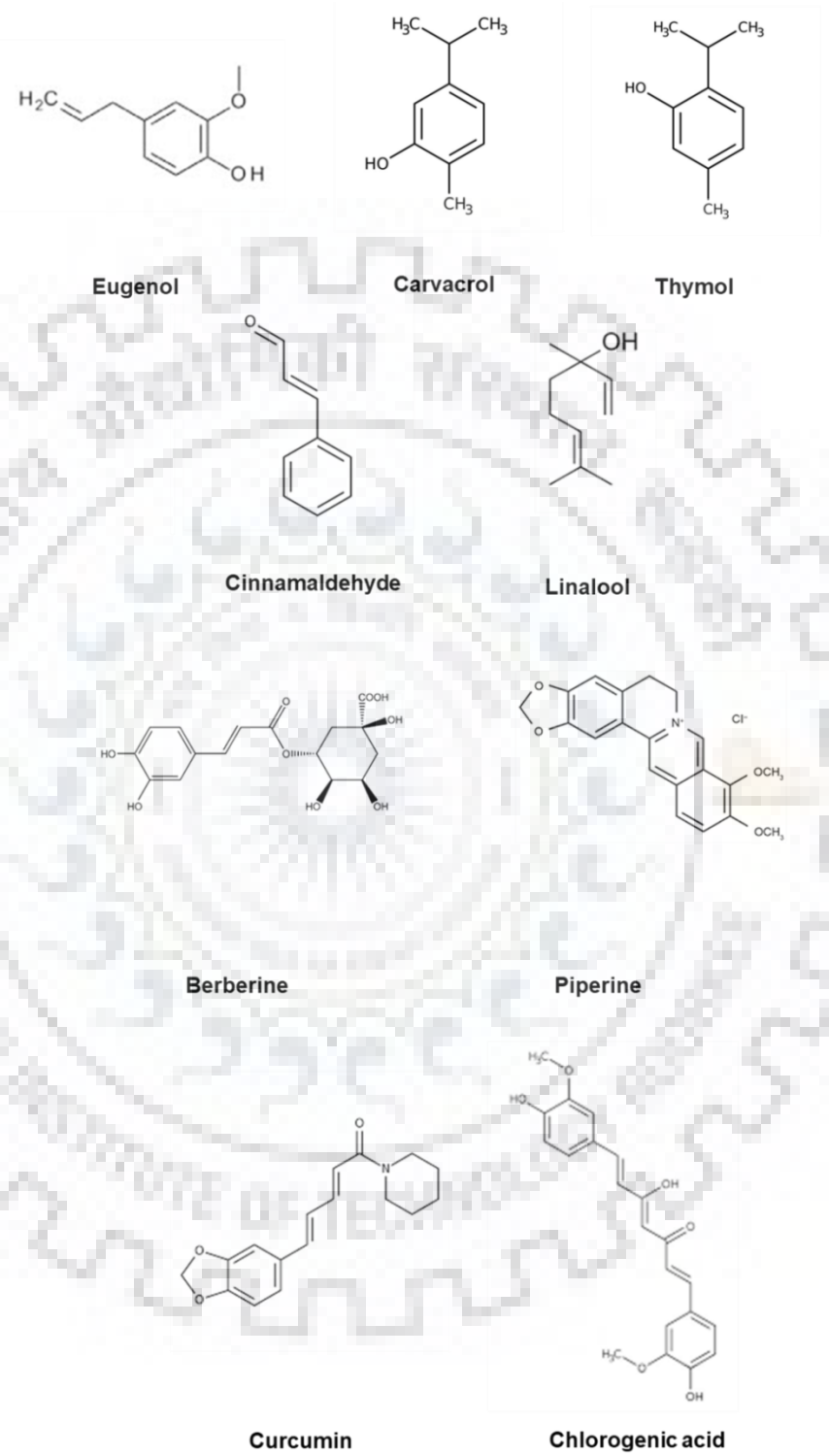

Figure 7.10: Structures of GRAS status compounds used in the study to determine their inhibitory activity against *A. baumannii* AYE.

7.2.10 Thymol, carvacrol and linalool cause outer membrane permeability in *A. baumannii*

The most common strategy to directly kill persister cells is through extensive damage of the bacterial membrane. Hence, I examined the potential of the GRAS compounds to cause membrane permeability in *A. baumannii* cells by the aid of fluorescence based assays. Fluorescent dye N-phenyl-1-napthylamine (NPN) was used to evaluate the outer membrane damaging potential of the small molecules. N-phenyl-1-napthylamine (NPN) is known to bind to the outer leaflet of the cell membrane, where it exhibits fluorescence in the hydrophobic environment. Exponential phase cells of *A. baumannii* AYE (OD_{600} = 0.6) were washed and resuspended in 5mM HEPES to an OD_{600} of 0.3. Cells were further incubated with sub inhibitory concentrations of small molecules for 30 minutes followed by the addition of NPN (10 µM). Fluorescence was immediately measured at an excitation and emission of 350 and 420 nm respectively using a plate reader. The outer membrane permeability assay revealed the compounds thymol, carvacrol and linalool to exhibit maximum potential to permeabilise the *A. baumannii* outer membrane (Fig. 7.11).

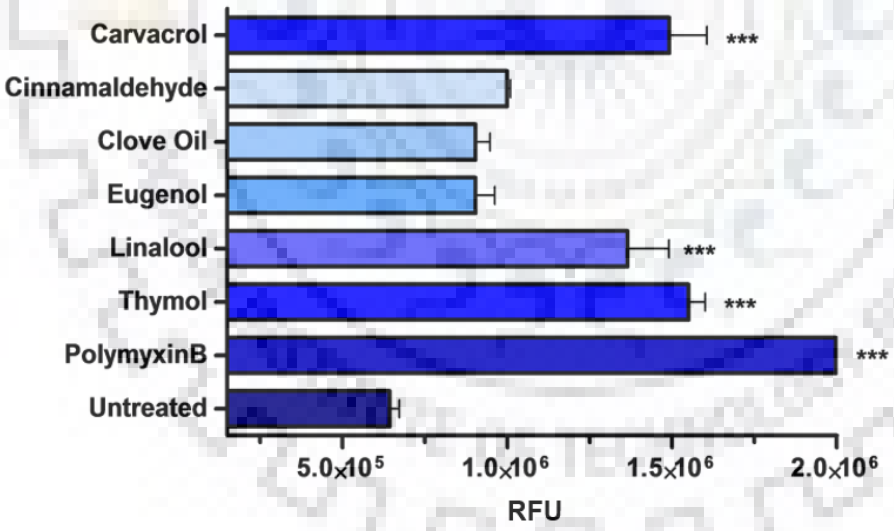

Figure 7.11: Outer Membrane permeability assay for GRAS status small molecules using fluorescent probe N-phenyl-1-napthylamine (NPN). Log phase *A. baumannii* AYE cells were resuspended in 5mM HEPES buffer to an OD_{600} of 0.3.and incubated with 0.5X MIC of small molecules for 30 minutes. NPN (10 µM) was later added and fluorescence was measured at an excitation and emission of 350 and 420 nm respectively. Polymyxin B was used as a positive control for the assay. P values were determined by one-way ANOVA followed by Tukey's multiple comparison test (*, P<0.05; **, P<0.01; ***, P<0.0001). Each value represents the mean of three values and error bars indicate standard error. RFU: Relative Fluorescence Units.

7.2.11 Thymol, carvacrol and eugenol cause inner membrane permeability in *A. baumannii*

Fluorescent probe Sytox Orange which is a DNA binding dye was used for the inner membrane permeability assay. Exponential phase cells of *A. baumannii* AYE at an OD_{600} of 0.6 were washed and resuspended in IX PBS and further diluted to an OD_{600} of 0.3. The cells were incubated with Sytox Orange (1 µM) with constant stirring to let the dye stabilize. Cells were then exposed to sub-inhibitory concentration of compounds and fluorescence was measured after 30 minutes at excitation and emission of 488 and 570 nm respectively using a plate reader. From the inner membrane permeability, it was observed that the compounds eugenol, thymol and carvacrol displayed the maximum potential to permeabilise the *A. baumannii* inner membrane (Fig. 7.12).

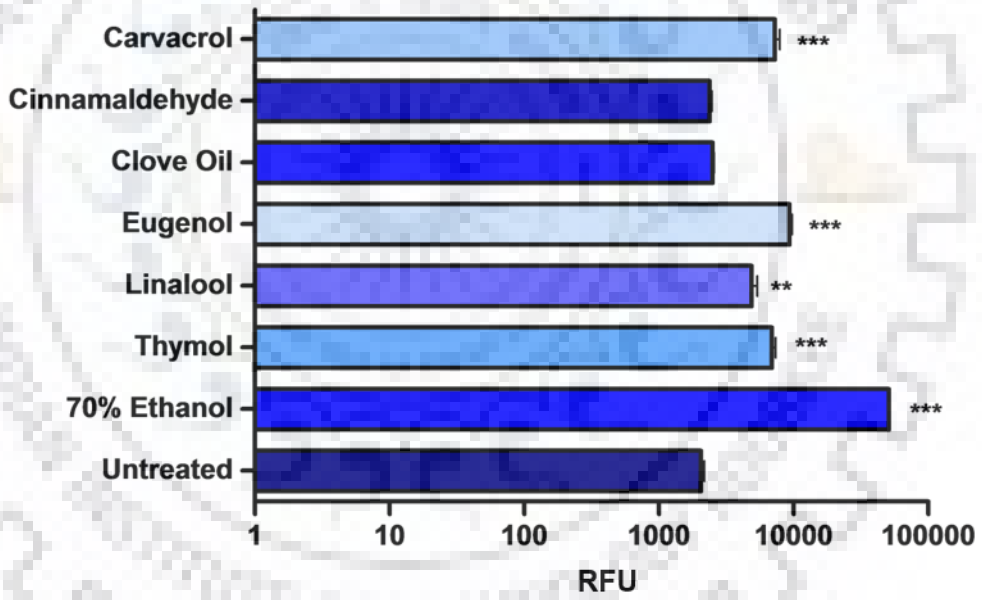

Figure 7.12: Inner Membrane permeability assay for GRAS status small molecules using fluorescent probe Sytox Orange. Log phase *A. baumannii* AYE cells were resuspended in 5 mM HEPES buffer to an OD_{600} of 0.3 and incubated with 0.5X MIC of small molecules for 30 minutes Sytox Orange (1 µM) was later added and fluorescence was measured at an excitation and emission of 488 and 570 nm respectively. 70% ethanol was used as a positive control for the assay. P values were determined by one-way ANOVA followed by Tukey's multiple comparison test (*, P<0.05; **, P<0.01; ***, P<0.0001). Each value represents the mean of three values and error bars indicate standard error. RFU: Relative Fluorescence Units.

7.2.12 Thymol, carvacrol and linalool cause increased production of reactive oxygen species (ROS) in *A. baumannii*

Bacterial cells produce reactive oxygen species (ROS) namely superoxide and hydrogen peroxide, in response to various stresses and as a metabolic by-product [323]. Since ROS can cause severe cellular damage, bacterial cells display an oxidative stress response, through the increased production of anti-oxidant enzymes, thus restoring the damage suffered. Active suppression of oxidative stress and decreased production of ROS is a known mechanism for antibiotic tolerance in bacteria [324]. Hence, screening for small molecules that can stimulate ROS production can be an effective strategy to target bacterial persisters[304]. Dichloro-dihydro-fluorescein diacetate (DCFH-DA), a non- fluorescent membrane permeable dye was used to evaluate the potential of small molecules for enhanced ROS production. DCFH-DA is broken down into Dichloro-dihydro-fluorescein (DCFH) by enzymes in the cytoplasm. In the presence of ROS, DCFH is further converted into a fluorescent product DCF that can be detected at an excitation and emission of 485 nm and 528 nm respectively.

For the assay, exponential phase cells of *A. baumannii* AYE (OD_{600} = 0.6) were washed and resuspended in IX PBS and further diluted to OD_{600} of 0.3. The cells were then incubated with DCFH-DA (10µM) for 30 minutes with constant stirring to let the dye stabilize. Cells were further washed with 1X PBS and exposed to sub-inhibitory concentration of compounds. After 30 minutes of incubation, fluorescence was measured at excitation and emission wavelengths of 485 and 528 nm respectively using a plate reader. The ROS production assay revealed that linalool, thymol and carvacrol exhibited the maximum ability to inhibit *A. baumannii* via ROS production (Fig. 7.13).

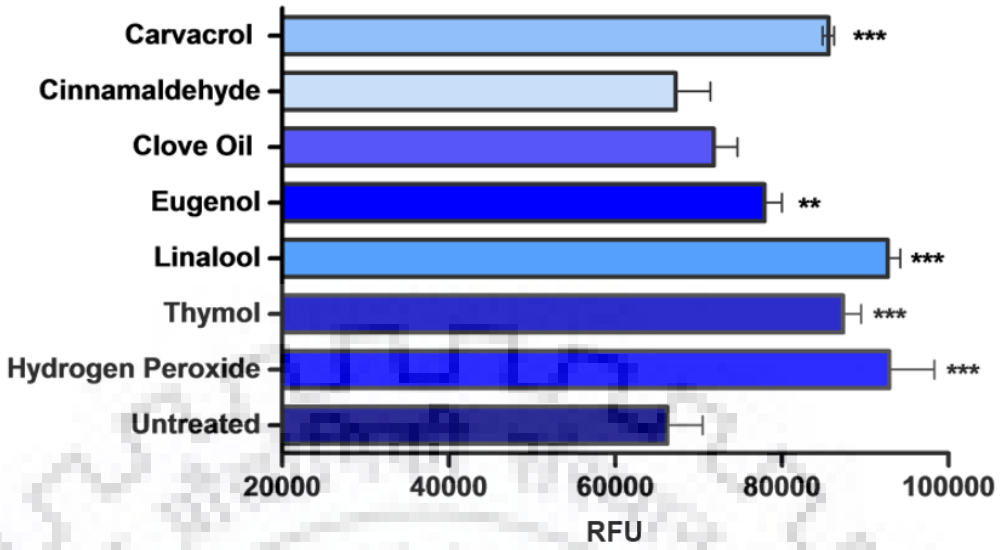

Figure 7.13: Reactive Oxygen Species (ROS) generation assay for GRAS status small molecules using fluorescent probe DCFH-DA. Log phase *A. baumannii* AYE cells were resuspended in 1X PBS buffer to an OD_{600} of 0.3 and incubated with 0.5X MIC of small molecules for 30 minutes. DCFH-DA (10µM) was later added and fluorescence was measured at an excitation and emission of 485 and 528 nm respectively. Hydrogen Peroxide was used as a positive control for the assay. P values were determined by one-way ANOVA followed by Tukey's multiple comparison test (*, P<0.05; **, P<0.01; ***, P<0.0001). Each value represents the mean of three values and error bars indicate standard error. RFU: Relative Fluorescence Units.

7.2.13 Thymol exhibits excellent ability to inhibit efflux in *A. baumannii*

More recently, active efflux mechanisms have been established to contribute significantly to antibiotic tolerance in bacteria. Therefore, administration of efflux inhibitors in combination with antibiotics is an important strategy that can target the persister phenotype. Hence, I further screened the aforementioned small molecules for their potential to inhibit the efflux of ethidium bromide (EtBr), which is a broad substrate inhibitor for most efflux pumps in Gram negative bacteria. Log phase *A. baumannii* AYE cells grown till OD_{600} of 0.5 were resuspended in 1X PBS and incubated with 10µg/mL of EtBr at 37^0C for 15 minutes. This was followed by exposing them to sub-inhibitory concentration of compounds. EtBr fluorescence at excitation and emission wavelengths of 530 nm and 600 nm respectively after 10 minutes was plotted**.** The EtBr efflux assay revealed thymol to be the most potent efflux pump inhibitor against *A. baumannii*, followed by eugenol, clove oil, linalool and carvacrol (Fig. 7.14). These observations were found to be similar to a recent study which reported the eugenol and cinnamaldehyde mediated sensitization.

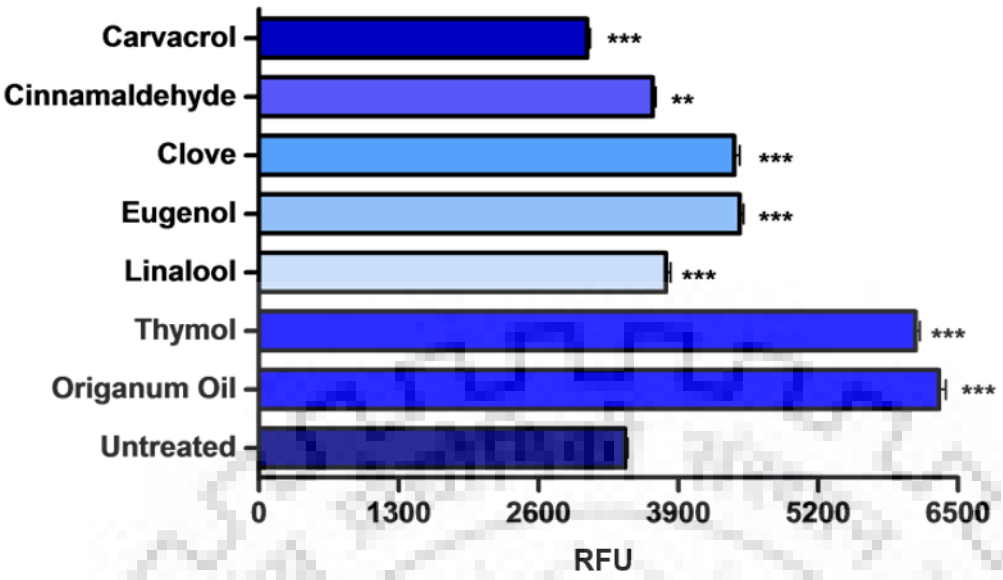

Figure 7.14: Efflux Inhibition assay for GRAS status small molecules using Ethidium Bromide (EtBr) as a substrate. *A. baumannii* AYE cells grown till an OD_{600} of 0.5 were resuspended in 1X PBS and incubated with 10µg/mL of EtBr at 37^0C for 15 minutes followed by exposure to compounds at sub-inhibitory concentration. The EtBr fluorescence observed after 10 minutes of incubation was plotted. P values were determined by one-way ANOVA and Tukey's multiple comparison test (*, P<0.05; **, P<0.01; ***, P<0.0001). Each value represents the mean of three values and error bars indicate standard error. RFU: Relative Fluorescence Units.

of *A. baumannii* to beta-lactam antibiotics by efflux inhibition [325]. Since, *carvacrol* and *thymol* represent the *two* main active components of oregano oil, it was included as a test compound and was observed to display excellent efflux inhibitory activity [326].

The results obtained from the four assays described above were further compiled in the form of heat map (Fig. 7.15). Out of the six GRAS status small molecules, Thymol was observed to outcompete others in all the four assays followed by Eugenol. As per the results obtained from the mechanistic screen, Thymol, carvacrol and eugenol were predicted to possess potential anti-persister activity and were further taken up for validation in *A. baumannii* AYE persister killing assay. It was interesting to note that since thymol and carvacrol have close structural similarity, they performed similarly in most of the assays studied except for inhibition of efflux.

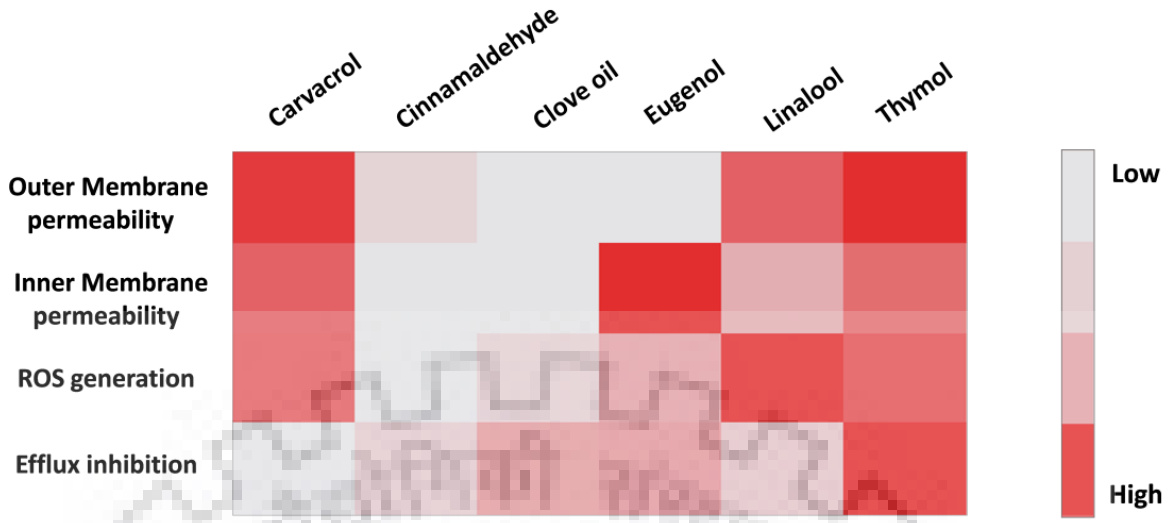

Figure 7.15: Heat map summarising the results of the mechanistic based screening of GRAS status small molecules against *A. baumannii* AYE. Thymol was chosen as the lead molecule closely followed by carvacrol and eugenol which were further taken up for validation by persister killing assays.

7.2.14 Thymol exhibits excellent inhibitory activity against meropenem persisters of *A. baumannii* in planktonic phase

Killing assays against planktonic phase *A. baumannii* persisters induced with high concentrations of a clinically important carbapenem antibiotic, meropenem were carried out to validate the anti-persister potential of the compounds screened. *A. baumannii* persisters obtained upon exposure to meropenem (at 100X MIC) were washed and resuspended in 1X PBS followed by incubation with lead compounds, thymol, eugenol and carvacrol for 12 h, both in the absence and presence of meropenem (100X MIC) in order to maintain their persistence. At the end of the incubation, the number of viable bacteria that survived the treatment were evaluated by determining the Colony Forming Units/mL in comparison to untreated control. As shown in Fig. 7.16, treatment of isolated persisters with meropenem alone (at 100X MIC) exhibited high bacterial counts, thus indicating effective persister isolation. As predicted from the results of mechanistic screen, thymol alone was observed to display complete eradication of meropenem induced *A. baumannii* persisters at 1X MIC (Fig. 7.16 A). Interestingly, in combination with meropenem, thymol caused complete eradication of persister populations at 0.5X of its MIC.

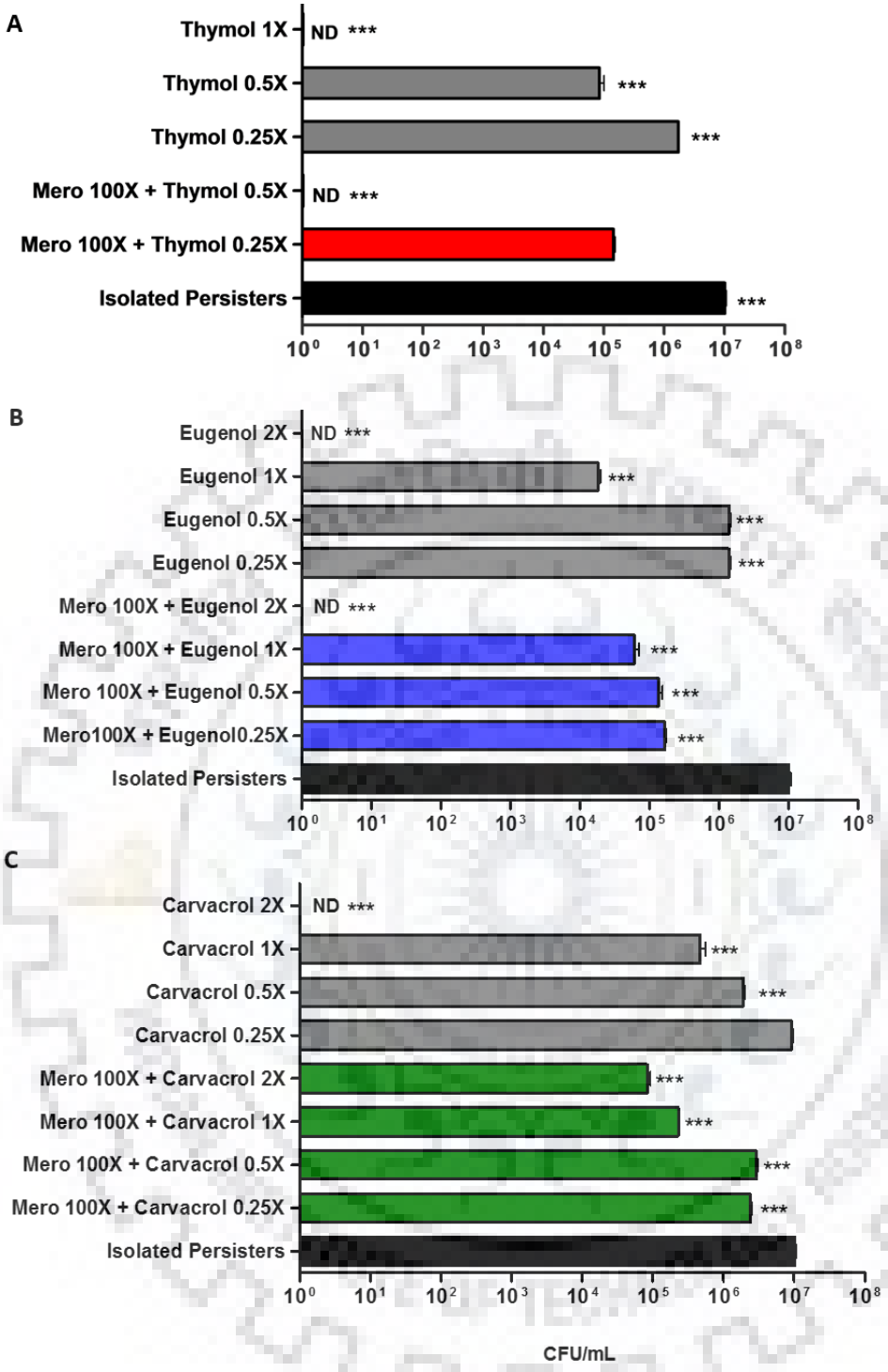

Figure 7.16: Anti-persister activity of (A) Thymol, (B) Eugenol and (C) Carvacrol against meropenem induced persisters in planktonic phase. Stationary phase cells of *A. baumannii* AYE (12 h old) were treated with meropenem (100X MIC) for 12 h followed by treatment with the GRAS status compounds at 0.25X, 0.5X, 1X and 2X MIC with and without meropenem After 12 h of incubation, the cells were plated to ennumerate the number of viable colonies. Each value represents the mean of three values and error bars indicate standard error. P values were determined by one-way ANOVA followed by Tukey's multiple comparison test (*, P<0.05; **, P<0.01; ***, P<0.0001).

Eugenol and carvacrol, on the other hand, exhibited significant ability to kill meropenem induced persisters albeit at higher concentrations than that of thymol (Fig. 7.16 B and C). Eugenol and carvacrol also displayed eradication of the persister fractions at 2X of their MIC. These results showed that all the three compounds namely thymol, eugenol and carvacrol displayed remarkable capability to kill the persister cells, both in the absence and presence of meropenem ($p < 0.0001$). The extent of killing by the small molecules was however observed to be variable and concentration dependent.

7.2.15 Thymol exhibits excellent inhibitory activity against meropenem persisters of *A. baumannii* under biofilm conditions

Recent studies have revealed that bacterial biofilms possess 100–1,000 fold more persister populations than planktonic cultures [109]. Hence, I further proceeded to evaluate the inhibitory activity of thymol, eugenol and carvacrol against the biofilm associated persisters of *A. baumannii*. 48 h old *A. baumannii* AYE biofilms were grown in 96-well microtitre plates and exposed to high concentration of meropenem alone (100X MIC), GRAS status small molecules (at 0.25X MIC, 0.5X MIC, 1X MIC and 2X MIC) or a combination of both antibiotic and small molecule. After 12 h of respective treatments, biofilm associated cells were dislodged using a bath sonicator and plated to ennumerate the number of viable colonies. It was observed that thymol showed the best inhibitory activity against the biofilm induced persisters as it completely eradicated all bacteria, at concentration corresponding to 1X of its MIC (Fig. 7.17A). However, thymol was able to cause complete elimination in biofilms at 0.5X MIC when administered in combination with meropenem, thus establishing that combination of meropenem and thymol always outcompeted the monotherapy, both in case of planktonic phase persisters and biofilm associated persisters. Eugenol on the other hand displayed eradication of persister cells in biofilms at higher concentrations corresponding to 2X of its MIC and at 1X MIC in combination with meropenem (Fig. 7.17 B). Carvacrol on the other hand showed complete eradication of the biofilm persisters at 1X MIC, both in combination as well as monotherapy (Fig. 7.17 C).

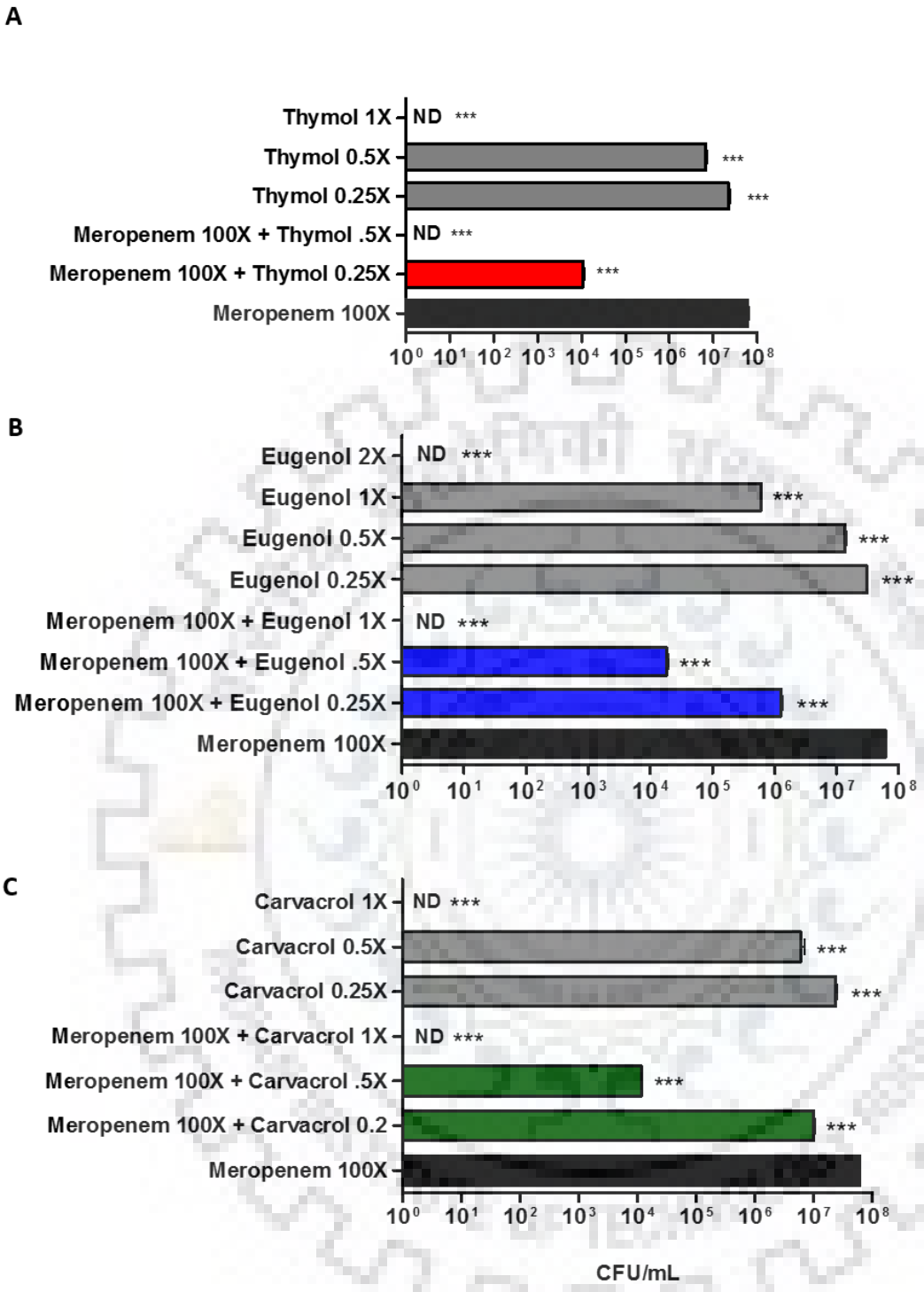

Figure 7.17: Anti-persister activity of (A) Thymol, (B) Eugenol and (C) Carvacrol against biofilm associated persister cells. 48 h old *A. baumannii* AYE biofilms were treated with meropenem alone (at 100X MIC), GRAS status small molecules (at 0.25X MIC, 0.5X MIC, IX MIC and 2X MIC) or a combination of both. After 12 h of incubation, biofilm associated cells were dislodged and plated to ennumerate the number of viable colonies. Each value represents the mean of three values and error bars indicate standard error. P values were determined by one-way ANOVA followed by Tukey's multiple comparison test (*, P<0.05; **, P<0.01; ***, P<0.0001).

7.2.16 Combination of meropenem and thymol does not show synergy in the checkerboard assay

On the basis of the above observations, where the combination of meropenem and thymol displayed a better inhibitory potential against *A. baumannii* AYE planktonic and biofilm persisters, in comparison to thymol alone; I was encouraged to see if the combination would also show a favourable synergistic interaction in the checkerboard assay. Interstingly, the meropenem and thymol combination did not exhibit synergism and the interaction between the two was observed to be additive in nature (FICI $\geq$ 0.5). This observation indicated that thymol exhibited a synergistic killing ability with meropenem against persister cells probably because it specifically targeted the mechanisms responsible for antibiotic induced persistence. Due to the absence of these targets in the normal growing populations, no synergistic interaction was observed in the checkerboard assay.

7.2.17 Thymol can inhibit stationary phase cells of *A. baumannii* AYE

It has been reported that the number of persisters in a growing population varies depending on the growth phase, with the highest persister frequency found at stationary phase [327]. Persisters have been shown to appear in the population by the mid-exponential phase and reach to a maximum of approximately 1% during stationary phase [328]. Previous experiments showed that thymol can efficiently inhibit meropenem induced persister cells. In order to examine the bactericidal potential of thymol on stationary-phase persisters of *A. baumannii*, cells were treated either with 100X MIC of meropenem or thymol alone (at 0.25X MIC to 0.5X MIC). Exposure of *A. baumannii* cells to 100X MIC of meropenem caused a decrease in the number of surviving cells and allowed the persister fractions to survive. Treatment of the stationary-phase persisters with 1X or 2X MIC of thymol alone significantly decreased the number of surviving cells compared to that of the untreated control ($p < 0.0001$) (Fig. 7.18A). Hence, the results obtained clearly showed that thymol exhibits extreme capability of killing both antibiotic induced persisters and stationary phase persisters of *A. baumannii*. The killing potential of thymol against stationary phase *A. baumannii* cells was also confirmed by microscopic studies. Scanning electron microscopy of stationary phase *A. baumannii* cells treated with thymol (at 2X MIC) displayed complete eradication of persisters and the presence of cell debris (Fig. 7.18B).

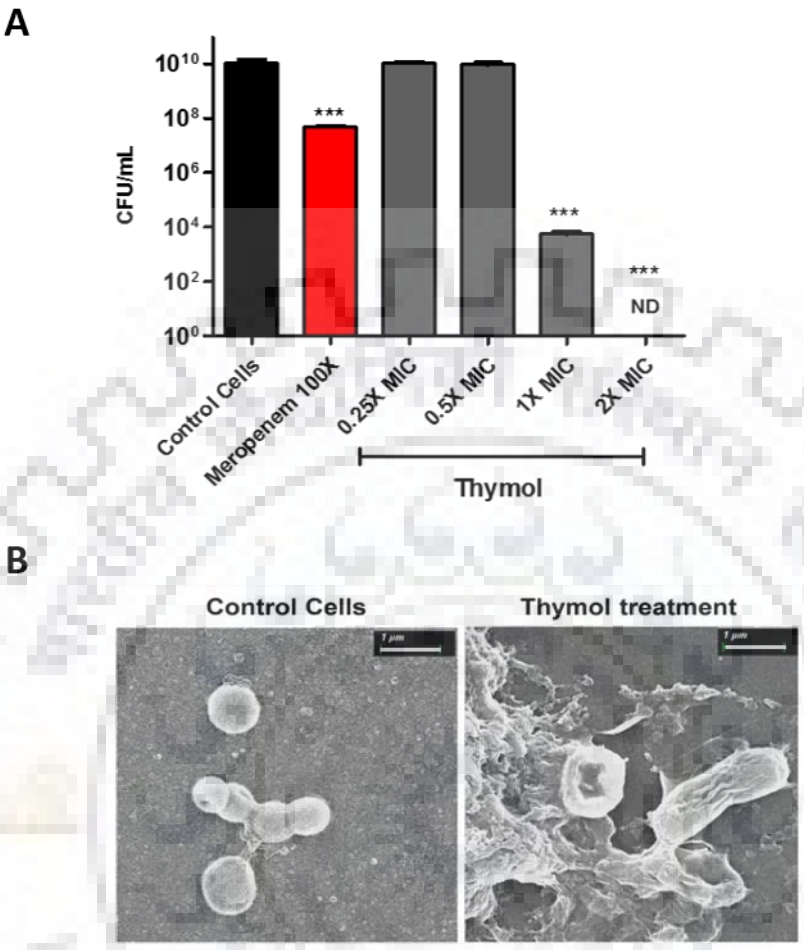

Figure 7.18: Activity of thymol against stationary phase cells of *A. baumannii*. (A) Stationary phase culture of *A. baumannii* AYE Cells were treated with 0.25X, 0.5X, 1X, 2X MIC of Thymol and 100X MIC of meropenem for 12 h. The number of viable bacterial counts were enumerated and plotted in terms of CFU/mL. (B) SEM micrographs show complete lysis of thymol treated (at 2X MIC) *A. baumannii* cells. Scale bar is 1 µm.

Fluorescence microscopy studies using the combination of dyes FM 4-64FX and Sytox green for the assessment of viability of thymol treated populations were performed. Fluorescence live-dead staining of thymol treated *A. baumannii* cells revealed complete killing of the bacterial population at 2X MIC, while partial killing was observed at 1X MIC (Fig. 7.19). These observations were found to be well in accordance with the results obtained from the CFU plating studies for assessing viability counts (Fig. 7.18A).

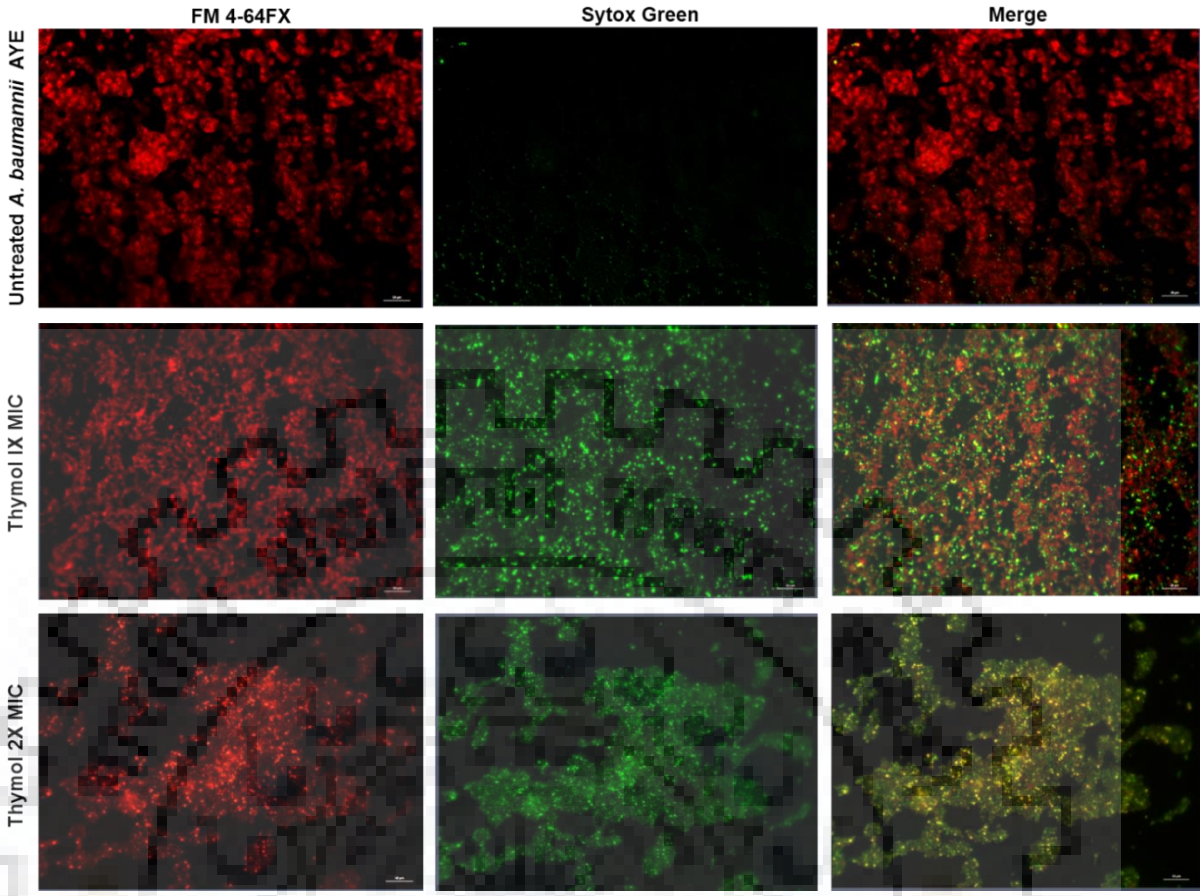

Figure 7.19: Fluorescence microscopy to assess the viability of stationary phase cells of *A. baumannii* in the presence of thymol. Stationary phase culture of *A. baumannii* AYE cells were treated with 1X and 2X MIC of Thymol for 1 h. Viability was assessed using combination of dyes FM 4-64FX and Sytox green. Scale bar represents 10 µm.

7.2.18 Thymol exhibits anti-persister activity irrespective of the time of addition to *A. baumannii* persisters

I further investigated whether thymol needs to be administered simultaneously with meropenem or could be administered at a later time point. Hence, a time kill kinetics assay was performed where thymol was added at different time points (t = 0h, 3h and 6h) during meropenem treatment (at 100X MIC) of *A. baumannii* AYE stationary phase cells. Complete eradication of *A. baumannii* cells was achieved within 1 h after the addition of thymol, irrespective of the time of its addition. These results indicate that thymol displays excellent ability to kill persister cells within a short span and could be administered during treatment at any time (Fig. 7.20)

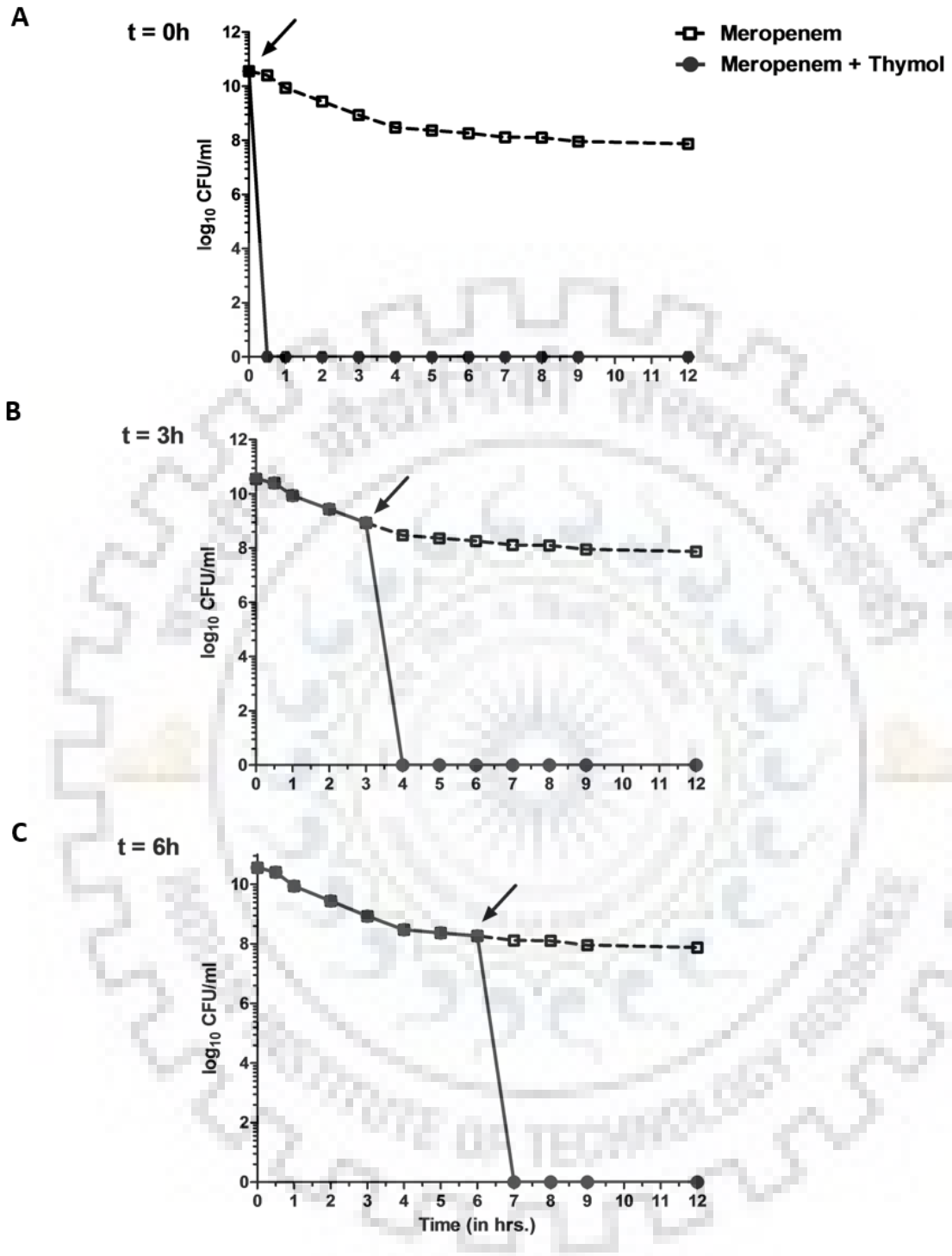

Figure 7.20: Kinetics of killing of *A. baumannii* in the presence of meropenem, upon addition of thymol at different time intervals. Stationary phase cells of *A. baumannii* AYE were treated with meropenem (100X MIC) or combination of meropenem and 1X MIC of thymol. Thymol was added to the cultures at different time points t = 0 h, 3 h and 6 h as indicated by the arrows. The number of viable cells was determined at regular intervals in terms of CFU/ml. Each value represents the mean of three values and error bars indicate standard error.

7.2.19 Anti-persister activity of thymol is antibiotic independent

In addition to meropenem, other antibiotics used to treat *A. baumannii* infections in the clinic include rifampicin, tigecycline and polymyxin B. I further sought to assess if the anti-persister activity displayed by thymol was dependent on the nature of the antibiotics used to induce persisters. Persisters of the three clinically relevant antibiotics were induced and isolated by exposing 12 h old cultures of *A. baumannii* AYE to 50X MIC of Rifampicin (MIC: 8 µg/mL), 100X MIC of Tigecycline (MIC: 0.25 µg/mL) and 10X MIC Polymyxin B (MIC: 0.5 µg/mL). Exposure to all the three antibiotics showed the isolation of large persister fractions, thus emphasising the need to tackle the problem of persistence in the clinic (Fig. 7.21).

Further to assess the inhibitory potential of thymol, persisters were treated with varying concentrations of thymol both with and without combination of antibiotics. As shown in Fig. 7.21, complete eradication of rifampicin and tigecycline induced *A. baumannii* persisters with thymol was observed at 0.25X MIC and 0.5X MIC in combination with antibiotics respectively ($p < 0.0001$). On the other hand, polymyxin B induced persisters displayed complete eradication by thymol at 1X MIC in combination with antibiotic ($p < 0.0001$). Treatment with thymol alone also displayed complete eradication although at a higher concentration i.e. at 1X MIC, in all three cases ($p < 0.0001$). These results clearly show that thymol can be combined with different classes of antibiotics and thus possesses an antibiotic independent anti- persister activity.

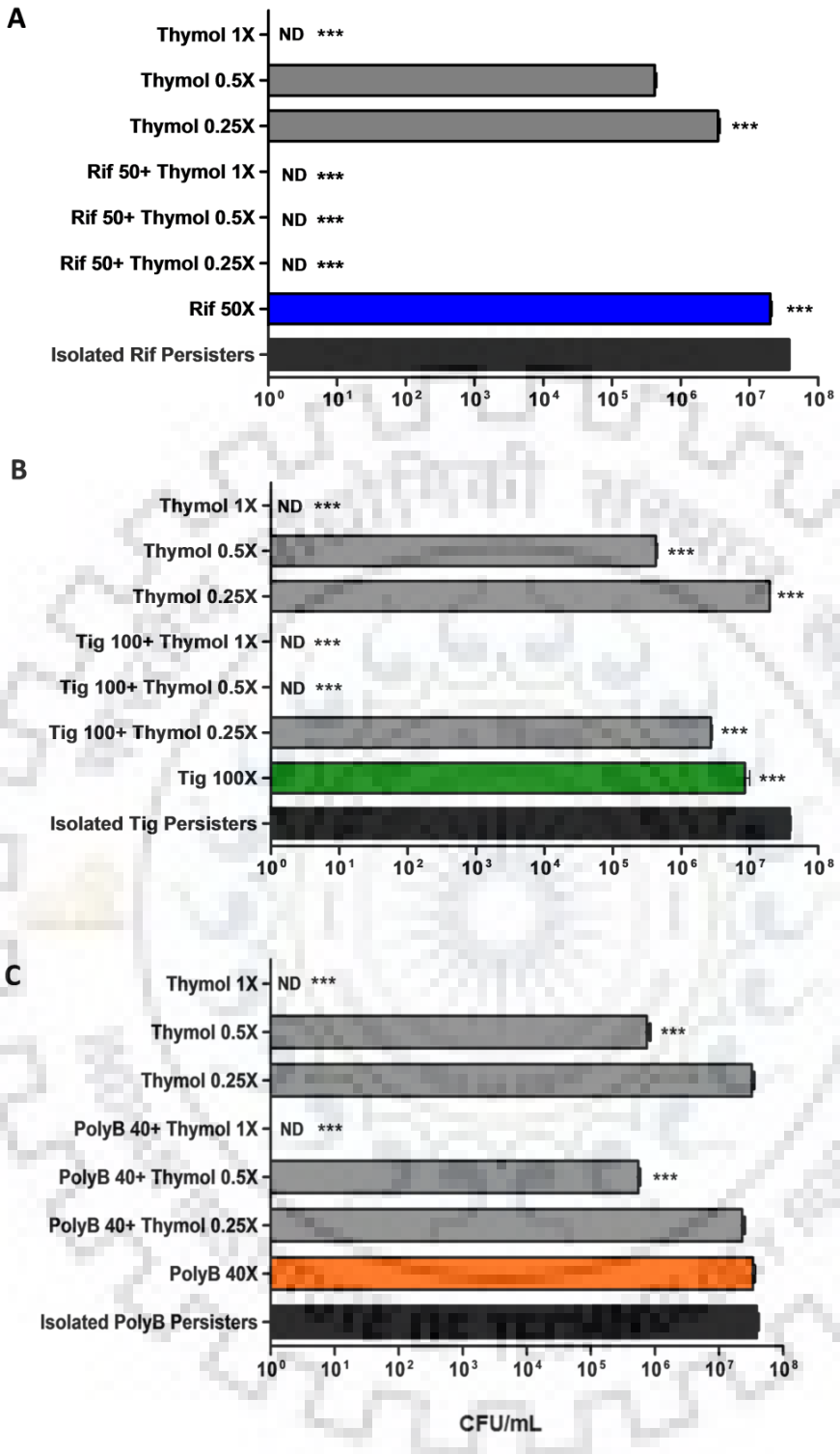

Figure 7.21: Anti-persister activity of Thymol against (A) Rifampicin (B) Tigecycline (C) Polymyxin B induced persister cells at varying concentrations of MIC. Stationary phase cells of *A. baumannii* AYE were exposed to Rifampicin, Tigecycline and Polymyxin B for 12 h followed by treatment with thymol at 0.25X, 0.5X and 1X MIC in the absence and presence of respective antibiotics at indicated concentrations. After 12 h of incubation, the cells were plated to ennumerate the number of viable colonies. P values were determined by one-way ANOVA followed by Tukey's multiple comparison test (*, P<0.05; **, P<0.01; ***, P<0.0001).

7.2.20 Thymol inhibits efflux in meropenem induced *A. baumannii* persisters

As shown previously, meropenem induced persisters of *A. baumannii* were observed to exhibit enhanced antibiotic efflux in order to survive exposure to otherwise lethal doses. In the ethidium bromide (EtBr) efflux assay of the mechanistic screen, thymol displayed excellent potential to inhibit EtBr efflux. Hence, in order to study the mechanism of persister killing by thymol, I performed the ethidium bromide efflux assay in isolated meropenem persisters. Meropenem induced *A. baumannii* persisters were isolated and incubated with 10 µg/ml of EtBr and washed with 1XPBS. The EtBr loaded cells were then added to 96-well plates containing 0.25X, 0.5X and 1X MIC of thymol. Relative increase in EtBr fluorescence upon addition of thymol with respect to no thymol control was calculated and plotted. As shown in Fig. 7.22, thymol cause a dose dependent increase in EtBr fluorescence in *A. baumannii* persisters thus indicating inhibition of efflux. This observation was further confirmed by incubating meropenem persisters with BOCILLIN FL in the presence and absence of thymol at sub inhibitory concentration. Thymol was observed to cause increased accumulation of BOCILLIN FL in the *A. baumannii* persisters in contrast to untreated persister cells (Fig. 7.23).

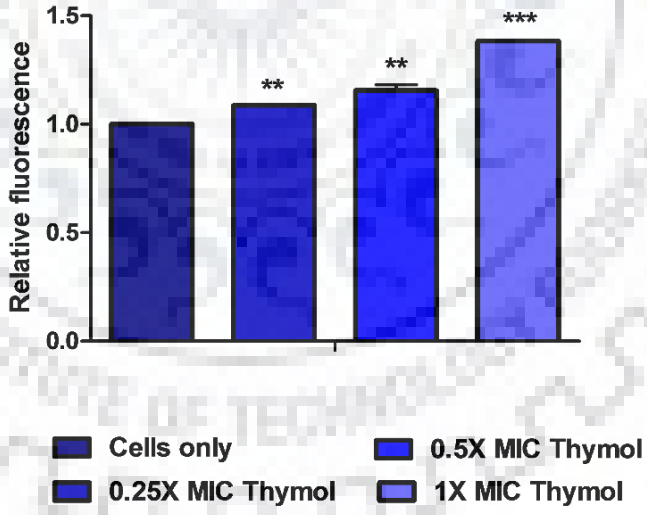

Figure 7.22: Ethidium Bromide efflux assay to study the efflux pump inhibitory activity of thymol against meropenem induced *A. baumannii* AYE persisters. Isolated persisters were incubated with 10µg/mL of EtBr at 37^0C for 15 minutes followed exposure to varying concentration of thymol. Relative increase in EtBr fluorescence upon thymol addition w.r.t. no thymol control was calculated and plotted. Each value represents the mean of three values and error bars indicate standard error.P values were determined by one-way ANOVA followed by Tukey's multiple comparison test (*, P<0.05; **, P<0.01; ***, P<0.0001).

7.2.21 Thymol causes membrane depolarization in meropenem induced *A. baumannii* persisters

As discussed previously, bacterial persisters exhibit a state of dormancy characterized by reduced cellular metabolism and low proton motive force [321]. Compounds that can modulate the PMF of dormant persister cells can act as attractive leads for anti-persister drug discovery. Moreover, since persisters are known to exhibit enhanced efflux activity and most efflux pumps are PMF driven, compounds that dissipate membrane potential can be useful in adjunct therapies with antibiotics[14]. Hence, I used the fluorescent dye $DiBAC_4(3)$ to evaluate the effect of thymol on the persister membrane potential. *A. baumannii* AYE persisters showed a significant increase in $DiBAC_4(3)$ fluorescence (P value <0.001) and thus increased membrane depolarization in response to increasing concentrations of thymol (Fig. 7.24). The ability of thymol to affect the membrane potential of *A. baumannii* persisters could also be held responsible for its impressive efflux inhibitory activity as observed previously.

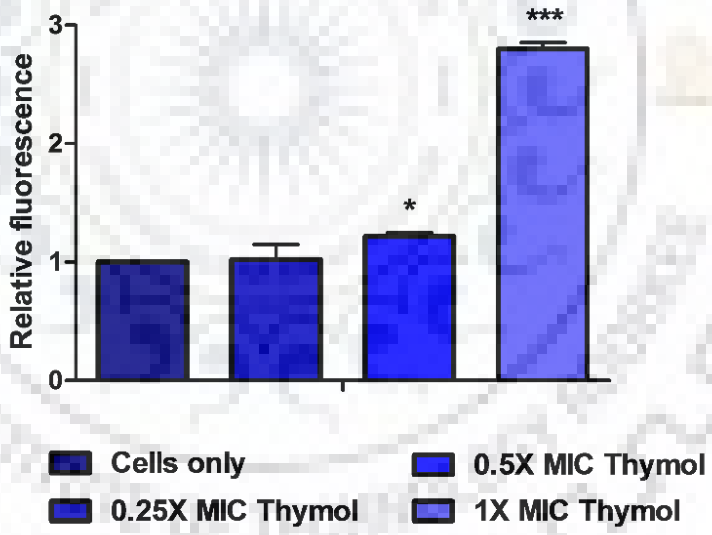

Figure 7.24: Effect of thymol on membrane potential of meropenem persisters of *A. baumannii* AYE. Cells incubated with 10 µM $DiBAC_4(3)$ for 30 minutes at 37°C were exposed to varying concentration of thymol. Fluorescence was recorded in at excitation-emission of 490/516 nm and relative increase in fluorescence w.r.t. untreated control cells was calculated. Each value represents the mean of three values and error bars indicate standard error. P values were determined by one-way ANOVA followed by Tukey's multiple comparison test (*, P<0.05; **, P<0.01; ***, P<0.0001).

7.2.22 Thymol inhibits the respiratory activity of meropenem induced *A. baumannii* persisters

As shown previously, the meropenem induced cultures of *A. baumannii* comprised of both persister and VBNC populations. The induction of VBNC state in bacterial pathogen poses a serious health threat and discovery of novel strategies that can induce their resuscitation or inhibit them is of utmost importance [107]. Hence, I further sought to assess if thymol could exhibit inhibitory potential against all of the viable cells i.e. both persisters and VBNCs, present in the meropenem treated *A. baumannii* cultures by the use of XTT assay and live-dead staining. Interestingly and encouragingly, thymol showed a significant inhibition in metabolic activity of the meropenem induced *A. baumannii* cells at 1X MIC (Fig. 7.25). The above observation was further validated by performing fluorescence based live dead staining assay. As shown in Fig. 7.26, thymol showed extreme potential to inhibit all the bacterial cells in the meropenem induced persister fractions of *A. baumannii.* Few cells in the meropenem persister fractions were observed to stain green indicating compromised membranes. These represented the susceptible bacterial cells that could not survive exposure to high concentrations of meropenem and remained in the isolated persister fractions after the washing steps.

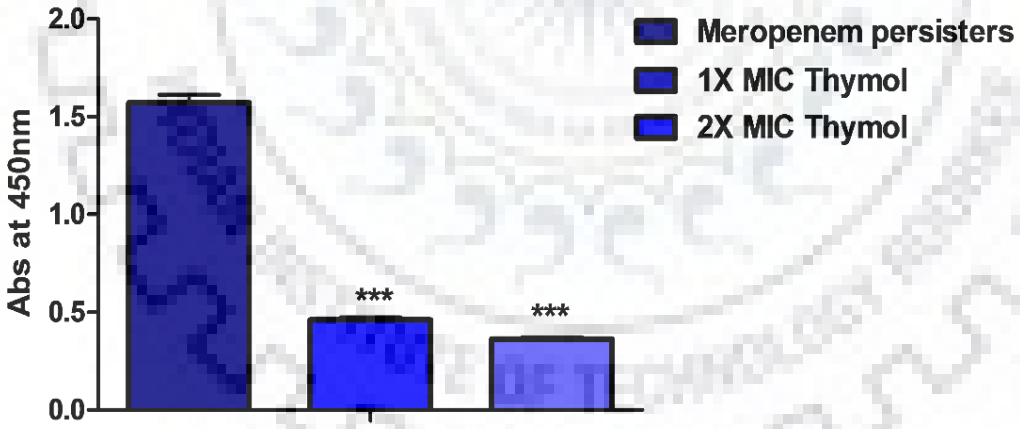

Figure 7.25: Effect of thymol on the metabolic activity of meropenem induced *A. baumannii* AYE persisters at 1X and 2X MIC. XTT (0.5 mg/ml) in combination with menadione (50 µM) was added to isolated persisters in 1X PBS and incubated for 2 h. Absorbance was read at 450 nm to assess the reduction of XTT dye. Each value represents the mean of three values and error bars indicate standard error.P values were determined by one-way ANOVA followed by Tukey's multiple comparison test (*, P<0.05; **, P<0.01; ***, P<0.0001).

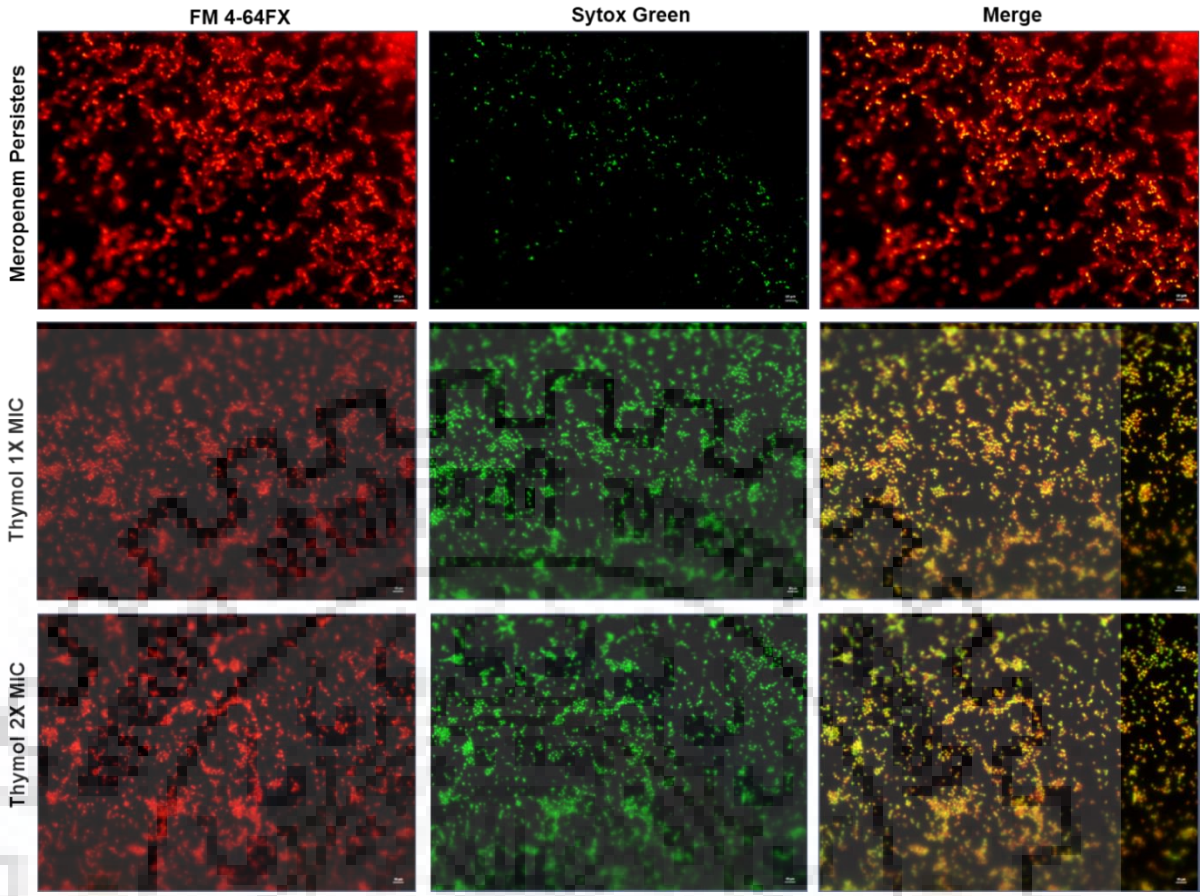

Figure 7.26: Fluorescence microscopy to determine the effect of thymol on the viability of meropenem induced persisters of *A. baumannii*. Meropenem exposed *A. baumannii* AYE cells (at 100X MIC) were treated with 1X and 2X MIC of Thymol for 1 h. Viability was assessed using combination of dyes FM 4-64FX and Sytox green. Scale bar represents 10 µm.

The effect of thymol treatment on the metabolic activity of *A. baumannii* cells in the stationary phase was also evaluated by the XTT assay. Thymol was observed to cause a significant inhibition in the metabolic activity of stationary phase cells of *A. baumannii* AYE (Fig. 7.27). Since the PMF in bacterial cells is generated by the electron transport chain (ETC), compounds that collapse the PMF can impair electron transport across the respiratory chain, also interfering with the ATP homeostasis. Hence, the ability of thymol to inhibit the respiratory activity of *A. baumannii* persisters could be attributed to its potential to dissipate the PMF, as shown previously (Fig. 7.24).

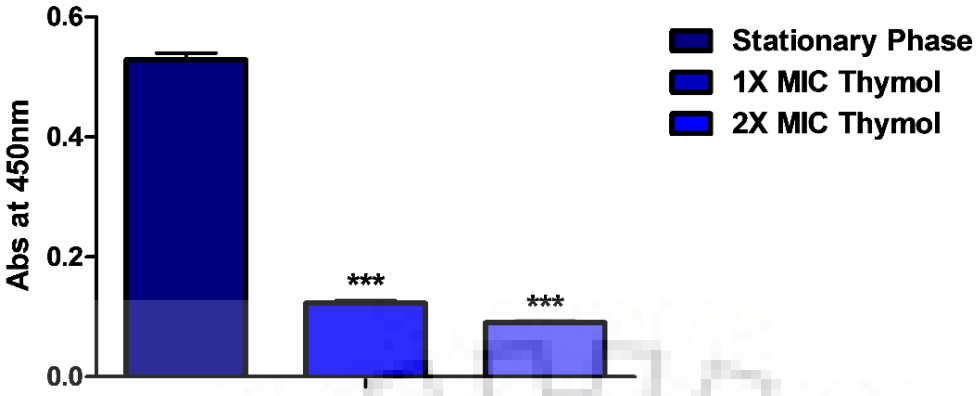

Figure 7.27: Effect of thymol on the metabolic activity of stationary phase cells of *A. baumannii* AYE at 1X and 2X MIC. XTT (0.5 mg/ml) in combination with menadione (50 µM) was added to cells in 1X PBS and incubated for 2 h. Absorbance was read at 450 nm to assess the reduction of XTT dye. Each value represents the mean of three values and error bars indicate standard error. P values were determined by one-way ANOVA followed by Tukey's multiple comparison test (*, P<0.05; **, P<0.01; ***, P<0.0001).

7.2.23 Thymol exhibits no propensity for resistance generation against *A. baumannii*

I further explored the ability of thymol to cause the emergence of resistance in *A. baumannii* AYE using the large inoculum approach to assess the frequency of resistance (FOR). 10^{10} CFU/mL of *A. baumannii* cells were exposed to thymol at 1X and 2X MIC. Rifampicin (2X MIC) was used a control for the assay. Thymol displayed no propensity towards resistance development since no colonies were obtained even after 72 h of exposure to thymol at high concentration (Table 7.2). Rifampicin, on the other hand exhibited FOR of the order 10^{-3} after 72 h of exposure in *A. baumannii* AYE. This implies that Thymol is refractory to resistance development against *A. baumannii* and holds great potential to be used as an adjuvant in clinic.

Table 7.2: Frequency of resistance generation against thymol in *A. baumannii* AYE

Frequency of Resistance (FOR)		
Thymol (1X MIC)	**Thymol (2X MIC)**	**Rifampicin (2X MIC)**
$<<< 10^{-10}$	$<<<10^{-10}$	1.2×10^{-3}

7.2.24 Activity of thymol against clinical isolates of *A. baumannii*.

The findings obtained so far were further validated by evaluating the activity of thymol against a panel of multi-drug resistant clinical isolates of *A. baumannii*. Stationary phase cultures of the clinical strains of *A. baumannii* were treated with meropenem (100-200 ug/ml) for 12 h and the fraction of surviving persisters were isolated. All the clinical strains were observed to display a high frequency of persister formation in the presence of meropenem. The persister fractions were further isolated by washing with 1X PBS and treated with 0.5X and 1X MIC of thymol for 12 h. Thymol caused a significant decrease in the persister populations of all the MDR *A. baumannii* isolates also leading to complete eradication in some strains ($p < 0.0001$) (Fig. 7.28). These observations highlight the potential of thymol to be used as an anti-persister compound in the clinics.

Table 7.3: MIC of meropenem, tigecycline, polymyxin B and rifampicin against clinical isolates of *A. baumannii.*

	Minimum Inhibitory Concentration (µg/mL)			
Strain no.	**Meropenem**	**Tigecycline**	**Polymyxin B**	**Rifampicin**
RPTC 8	4	0.25	0.5	0.5
RPTC 27	4	0.5	0.5	32
RPT U59	16	0.5	0.25	64
RPTC 10	16	0.5	0.5	0.25
RPTC 11	2	0.06	0.25	0.25
RPTC 22	4	0.25	0.25	0.25
RPTU 61	16	0.25	0.25	0.125

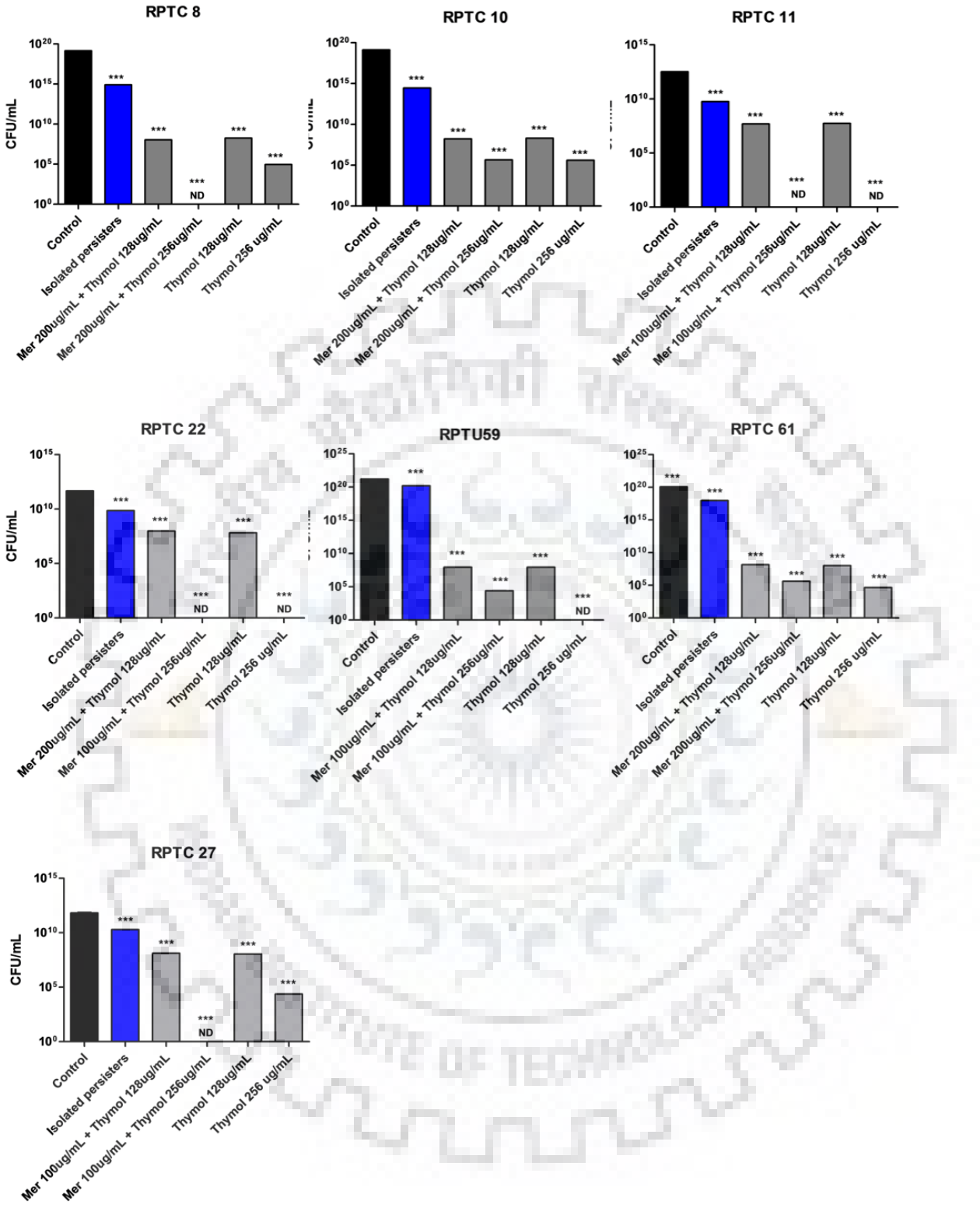

Figure 7.28: Anti-persister activity of Thymol against clinical isolates. Stationary phase cells of *A. baumannii* AYE were treated with Rifampicin, Tigecycline and Polymyxin B for 12 h followed by treatment with thymol at at indicated concentrations in the absence and presence of respective antibiotics. After 12 h of incubation, the cells were plated to ennumerate the number of viable colonies. P values were determined by one-way ANOVA followed by Tukey's multiple comparison test (*, P<0.05; **, P<0.01; ***, P<0.0001).

7.2.25 Thymol exhibits anti-persister activity against two other ESKAPE pathogens: *Klebsiella pneumoniae* and *Pseudomonas aeruginosa*

As thymol exhibited an excellent inhibitory potential against the nosocomial pathogen, *Acinetobacter baumannii*, I further sought to examine its activity against other serious ESKAPE pathogens, namely *Klebsiella pneumoniae*, *Pseudomonas aeruginosa* and *Staphylococcus aureus.*

Klebsiella pneumoniae is a Gram-negative opportunistic pathogen responsible for causing a wide range of infections such as urinary tract infections, pneumonia, and surgical wound infections [329]. Antibiotic treatment failure of *K. pneumoniae* infections has been attributed to the presence of both resistant and tolerant strains in the clinical settings [324]. Carbapenem antibiotics are frequently used to treat *K. pneumoniae* infections either as a monotherapy or in combination with other antibiotics [330]. Hence, I isolated meropenem induced persisters of *K. pneumoniae* ATCC 700698 at 100X MIC (MIC: 0.03 µg/mL) and treated them with increasing concentrations of thymol. As shown in Fig. 7.29, thymol completely eradicated all *K. pneumoniae* persisters at concentration as low as 0.25X of its MIC (i.e. at 0.5 mg/mL) ($p<0.0001$).

P. aeruginosa is another major ESKAPE pathogen known to cause chronic airway infections in patients with cystic fibrosis. Survival of *P. aeruginosa* in lungs is supported by small fractions of antibiotic tolerant subpopulations which are responsible for infection relapse. Carbapenems antibiotics such as imipenem and meropenem are frequently used for the treatment of *P. aeruginosa* infections[331]. Stationary phase cells of *P. aeruginosa* MTCC 2453 were exposed to 100X MIC of meropenem (MIC: 0.25 µg /mL) for 12 h and high fractions of persister cells were obtained. Complete eradication of the isolated persisters upon treatment with the potential anti-persister compound, thymol was observed at 0.25X MIC (i.e. 2 mg/mL) (Fig. 7.29).

S. aureus is a Gram positive ESKAPE pathogen responsible for causing endocarditis, osteomyelitis and several chronic infections that are complicated by frequent relapses through the formation of persister bacterial cells against conventional antibiotics. Vancomycin is a glycopeptide antibiotic which is a gold standard for treatment of severe Methicillin Resistant *Staphylococcus aureus* infections[332]. However, the emergence of Vancomycin tolerant strains in the clinic present a major challenge for effective antibiotic treatment. Vancomycin tolerant cells of *S. aureus* ATCC 29213 were isolated by exposing stationary phase bacteria to

50 µg/mL of vancomycin (MIC: 0.5 µg/mL). Isolated persisters were treated with IX MIC of thymol (MIC: 128 µg/mL) and the number of surviving bacteria were enumerated (Fig. 7.29). Thymol however did not display inhibitory potential against the vancomycin induced *S. aureus* persisters and thus its activity was observed to be more specific to the Gram negative pathogens.

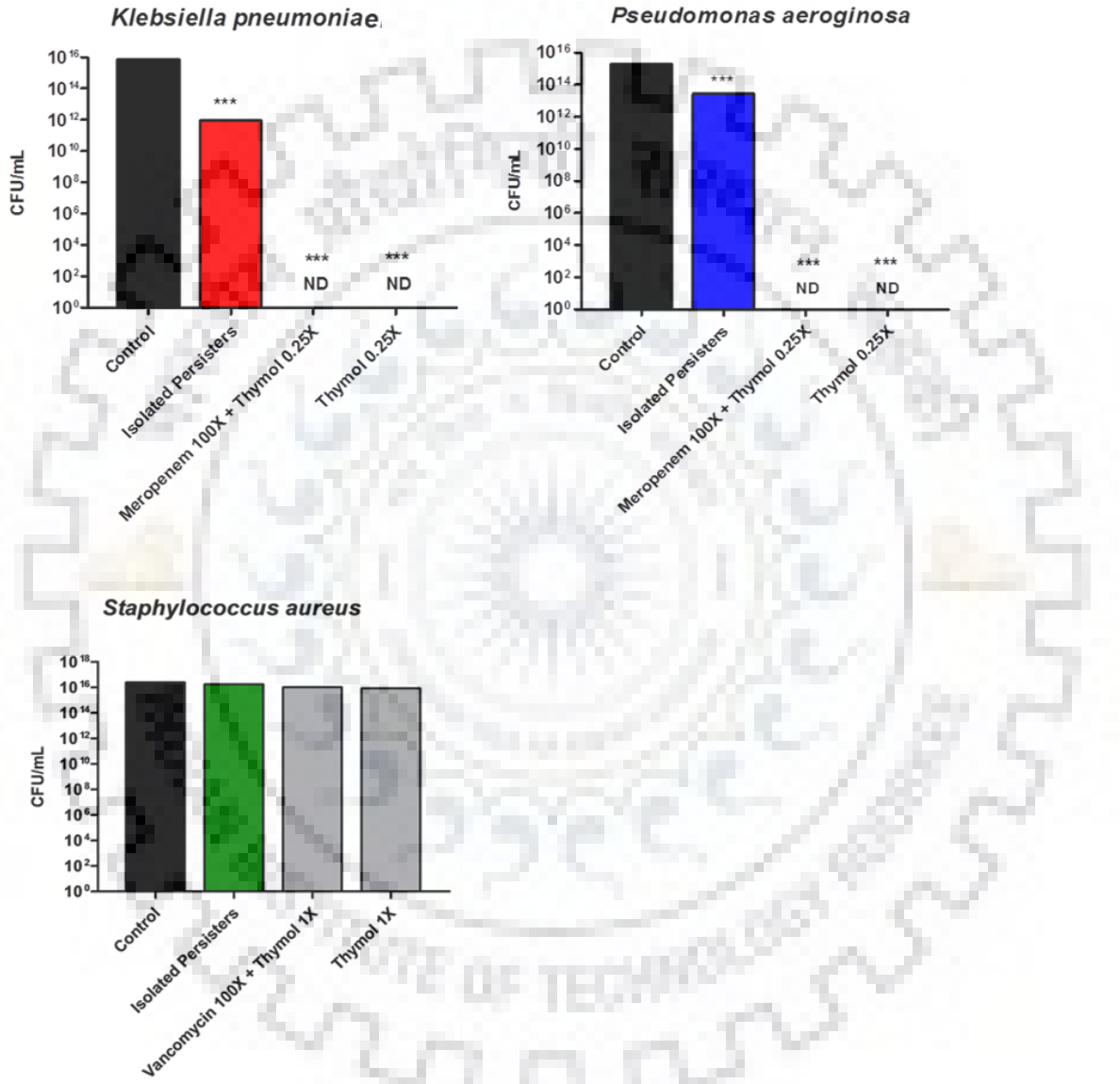

Figure 7.29: Anti-persister activity of Thymol against ESKAPE pathogens (A) *Klebsiella pneumoniae* ATCC 700698 (B) *Pseudomonas aeruginosa* MTCC 2453 (C) *Staphylococcus aureus* ATCC 29213. Stationary phase cells were treated with meropenem at 100X MIC for 12 h. Antibiotic induced persisters were treated with indicated concentrations of thymol, in the absence and presence of respective antibiotics. After 12 h of incubation, number of viable colonies were enumerated by plating. P values were determined by one-way ANOVA followed by Tukey's multiple comparison test (*, P<0.05; **, P<0.01; ***, P<0.0001).

7.3 Discussion

Besides the rapidly increasing problem of multidrug resistance, treatment of infections caused by ESKAPE pathogens is compromised by the ability of these organisms to form biofilms and comprise of antibiotic-tolerant persister populations [109]. Persister cells are able to withstand antibiotic treatment, thereby contributing to the recalcitrant nature of chronic infections and increasing the chances of resistance development [313].

In this study, the characteristics and mechanisms of persistence in the ESKAPE pathogen, *A. baumannii* were determined in response to the last resort antibiotic, meropenem. In response to antibiotic stress, *A. baumannii* persisters were observed to modulate their proton motive force and upregulate efflux mechanisms. Membrane depolarization and efflux mechanisms for antibiotic tolerance have been implicated in *E. coli*, *P. aeruginosa* and *Mycobacterium species*. To our knowledge, this is the first study that highlights the role of similar mechanisms for persistence in *A. baumannii*.

This study further identified the anti-persister activity of thymol, a plant-derived antimicrobial that can be used as monotherapy or in combination with antibiotics against bacterial infections. Thymol (2-isopropyl-5-methylphenol) is a monoterpene phenol isolated from plants belonging to the Lamiaceae family or can also be chemically synthesized [333]. The use of Thymol as a flavouring agent and food preservatives is long known such that it has been bestowed the GRAS (generally recognized as safe) status by the Food and Drug Administration (FDA), agency of the United States Department of Health and Human Services (Thymol: 21CFR172.515) [334]. Thymol has been known to possess antibacterial activity against both Gram negative and Gram positive pathogens such as *Escherichia coli*, *Salmonella typhimurium*, *E. coli* O157:H7, *Proteus mirabilis*, *Staphylococcus aureus* and *Listeria innocua* etc. [335]. Only few studies so far have reported the antibacterial activity of thymol or its derivatives against *A. baumannii* [336],[337]. However, none of the studies evaluated the inhibitory potential of thymol against *A. baumannii* persisters.

In my study, Thymol was observed to inhibit and eradicate all the “viable” cells in the antibiotic exposed populations, irrespective of their culturability. Thymol retained its activity against both non-dividing and dividing or both culturable and non-culturable

populations of *A. baumannii* by causing membrane permeability, dissipating their membrane potential and inhibiting the efflux machinery as well as respiratory activity. It was intriguing to observe that although carvacrol is an isomer of thymol, but its anti-persister activity wasn't observed to be at par with thymol. This could be again attributed to the superior efflux inhibitory activity of thymol than carvacrol, as evident from the EtBr efflux assay. Thymol was observed to have a rapid killing potential and a broad spectrum activity inhibiting three notorious Gram negative ESKAPE pathogens. Moreover, it did not exhibit the generation of resistant mutants in *A. baumannii* AYE upon prolonged exposure

Thymol is an attractive compound having its use as a food additive in the food industry and a potential bioactive compound in the pharmaceutical industry. In support of its GRAS status, recent reports have have displayed no associated toxicity in rat models, with LD50 as high as ~4000mg/kg, when administered orally [335]. The possibility of combining thymol with mechanistically different classes of antibiotics and its broad spectrum anti-persister activity, indicates thymol to have immense potential to act either alone or serve as an adjunct molecule in combination therapies against mixed bacterial infections This study encourages further research into it and the development of novel antibacterial strategies in the fight against chronic infections.

7.4 Experimental procedures

7.4.1 Bacterial strains and reagents

The strains used for the study were *Acinetobacter baumannii* AYE, *Klebsiella pneumoniae* ATCC 700698, *Pseudomonas aeruginosa* MTCC 2453 and *Staphylococcus aureus* ATCC 29213. The growth medium used was either Luria Bertani (LB) broth or LB agar. Antibiotics used in this study were procured from Sigma-Aldrich Corporation and Tokyo Chemicals Industries Limited (TCI) and were stored at conditions recommended by the seller brand. The stock solutions were prepared in water or DMSO as prescribed. Fluorescent dyes Dichloro-dihydro-fluorescein diacetate (DCFH-DA), $DiBAC_4(3)$, FM4-46FX , SYTOX green and SYTOX orange were procured from Thermofisher Scientific. BOCILLIN^{TM} FL Penicillin (BOCILLIN) was also purchased from Thermofisher Scientific. The *A. baumannii* clinical isolates used in the study were procured from AIIMS, Bhopal and Government Medical College and Hospital, Chandigarh, India.

7.4.2 Determination of Minimum Inhibitory Concentration (MIC) of antibiotics and GRAS compounds

The MIC is defined as the lowest concentration of antibiotic that completely inhibited the growth of the organism as detected with the naked eye. Serial twofold dilutions of each drug in 96 well plate was prepared according to the recommendations of CLSI immediately prior to testing. The overnight grown cultures of the required strains were sub-cultured in sterile culture tubes and were incubated at 37°C and 200 rpm, till the OD of 0.5 at 600 nm was obtained. Cultures were subsequently diluted 1000 times to achieve inoculum of 5×10^5 CFU/ml and were added to the 96 well plates containing the serially diluted antibiotics. The absorbance of the plates was recorded on a plate reader (SpectraMax M2e) at 600 nm after 12 h of incubation.

7.4.3 Inner Membrane Permeability Assay

The membrane permeability assay was determined with the fluorescent dye Sytox Orange nucleic acid stain (Thermofisher), which fluoresces upon binding to DNA. *A. baumannii* AYE cells were grown overnight in 5 ml of Luria Bertani media. The cells were then diluted 1:100 in fresh media and allowed to grow until the OD_{600} reached 0.4-0.5. Cells were then washed thrice with 1X PBS buffer and resuspended in 1X PBS to an optical density taken at 600 nm of 0.3. Sytox Orange was added to the cells at concentration of 1 µM and were incubated with constant stirring, to let the dye stabilize. Compounds (at 0.25X MIC) were then added to the

96-well opaque half area plates and fluorescence was measured at the excitation and emission wavelengths of 488 and 570 nm respectively using a plate reader (SpectraMax M2e).

7.4.4 Outer Membrane Permeability Assay

N-phenyl-1-napthylamine (NPN) dye was used to assess the outer membrane permeability in the presence of compounds. NPN binds to the outer leaflet of the cell membrane and fluoresces when in the hydrophobic environment. Overnight grown cultures of *A. baumannii* AYE were sub-cultured in fresh medium and incubated at 37°C and 200 rpm, till an OD_{600} of 0.4 was reached. These cells were then washed and resuspended in 5mM HEPES buffer to an OD_{600} of 0.3. and incubated with 0.25X MIC of the compounds for 30 minutes. To the Corning half area black plate, NPN dye was added (at 10 µM) to treated cells and fluorescence was immediately measured at an excitation/emission wavelengths of 350/420 nm respectively using a plate reader (SpectraMax M2e). Relative Fluorescence Units (RFU) were calculated by dividing the fluorescence values obtained by the absorbance at 600 nm.

7.4.5 Reactive Oxygen Species (ROS) Production Assay

Dichloro-dihydro-fluorescein diacetate (DCFH-DA) was used for the ROS detection assay. The overnight grown cultures of *A. baumannii* AYE were sub-cultured and incubated at 37°C and 180 rpm, till an OD_{600} of 0.4 was reached. These cells were then washed and resuspended in 1X PBS to an OD_{600} of 0.3 and then incubated with Dichloro-dihydro-fluorescein diacetate (DCFH-DA) at 10µM for 30 minutes at 37ºC following which they were added to the compounds (at 0.5X MIC) in the Corning half area black plate and a kinetic fluorescence spectrum was run at excitation wavelength of 485 nm and emission wavelength of 528 nm for 2 h with readings taken every 5 minutes using a plate reader (SpectraMax M2e). The values obtained at the end of 2 h were plotted for comparison.

7.4.6 Ethidium Bromide Efflux Assay

Ethidium Bromide acts as a general substrate for efflux pump and hence can be used to measure the cell's efflux activity. If a molecule acts as an efflux pump inhibitor it would show relatively higher fluorescence as compared to those which don't. The overnight grown cultures of the required strains were sub-cultured in sterile culture tubes and were incubated at 37°C and 200 rpm, till an OD_{600} of 0.4 was reached. These cells were then washed and resuspended in PBS to an OD_{600} of 0.3 and 10 µg/mL of Ethidium Bromide was added and incubated at 37ºC

for 20 minutes. The compounds were added with treated cells to the Corning half area black plate at sub-inhibitory concentrations (at 0.25X MIC) and their fluorescence was measured at excitation wavelength 480 nm and an emission wavelength of 610 nm using a plate reader (SpectraMax M2e). The fluorescence values obtained at the end of 2 h were plotted for comparison.

7.4.7 Determination of the levels of persistence in *A. baumannii* against meropenem and other clinically relevant antibiotics

A single colony of *A. baumannii* from a freshly streaked plate was inoculated in LB medium for 12 h at 37°C and 180 rpm. The cells were 100 times diluted into fresh media and further grown for 12 h under similar conditions. The antibiotics meropenem, tigecycline (at 100X MIC), rifampicin (at 50 X MIC) and polymyxin B (40X MIC) were added to the culture and incubated at 37°C under shaking conditions. The number of surviving persister fractions upon meropenem treatment were enumerated at regular intervals by the drop plate method. In case of tigecycline, rifampicin and polymyxin B, the number of surviving persister fractions were determined after 12 h of antibiotic exposure.

7.4.8 Determination of the levels of meropenem persistence in *A. baumannii* under biofilm conditions

A. baumannii cells were grown overnight in LB medium and were 100 fold diluted into fresh media until they reached OD_{600} of 0.4. Cells were added to 96-well plates and biofilms were allowed to form for 48 h at 37°C under static conditions. Planktonic cells were washed thrice with PBS and 100X MIC of meropenem in LB medium was added to the plates for 12 h. Biofilm were washed and disrupted by sonication using a bath sonicator (at 50 KHz for 10 minutes at room temperature). The number of biofilm associated *A. baumannii* cells that survived meropenem exposure was determined in comparison to untreated control.

7.4.9 Tolerance of meropenem induced *A. baumannii* persisters to other clinically relevant antibiotics

Meropenem induced persisters were isolated by the following protocol. A single colony of *A. baumannii* from a freshly streaked plate was inoculated in LB medium for 12 h at 37°C and 200 rpm. The cells were 100 times diluted into fresh media and further grown for 12 h at similar conditions. 100X MIC of meropenem was added to them and incubated further at 37°C

under shaking conditions for 12 h. The isolated persisters were washed thrice and resuspended in PBS preventing their reversion back to the normal population. To assess if meropenem induced persisters could tolerate bactericidal concentrations of other clinically relevant antibiotics, survival of *A. baumannii* cells upon exposure to high concentrations of tigecycline (50X MIC), rifampicin (50X MIC) and polymyxin B (40X MIC) was observed. The numbers of surviving persisters were enumerated after 12 h of antibiotic exposure.

7.4.10 Treatment of antibiotic induced persisters with screened natural products

Antibiotic induced persisters were isolated by the following protocol. A single colony of *A. baumannii* was inoculated in LB medium for 12 h at 37°C and 200 rpm. The cells were further 100 times diluted into fresh media and grown for 12 h at similar conditions. 100X MIC of meropenem, tigecycline; 50X MIC rifampicin and 40X MIC of polymyxin B were added to individual tubes and incubated under shaking conditions for 12 h. The isolated persisters were washed thrice and resuspended in PBS followed by treatment with 0.25X, 0.5X, 1X MIC and 2X MIC of individual natural compounds for 12 h. The numbers of surviving persisters after natural compound treatment were enumerated.

7.4.11 Fluorescence Microscopy to assess changes in cellular morphology

Fluorescence microscopy was used to evaluate the morphological changes in *A. baumannii* AYE cells after treatment with 100X MIC of meropenem. *A. baumannii* AYE persister cells were made as per the method described above and was compared with that of the control cells. Agarose pads were made using 1 % agarose. 1 µg/ml of FM 4-64FX (N-(3-Triethylammoniumpropyl)-4-(6-(4-(Diethylamino)-Phenyl)-Hexatrienyl)-Pyridinium Dibromide), a membrane staining dye was added to the control as well as persister cells and incubated for 15 minutes at room temperature. 10 µL of cells was added to the agar pad and it was covered with a cover slip and observed under AXIO A1 ZEISS fluorescence microscope.

7.4.12 Scanning Electron Microscopy to assess changes in cellular morphology

SEM was performed to evaluate the morphological changes in stationary phase *A. baumannii* AYE cells after treatment with thymol. For SEM sample preparation, *A. baumannii* AYE was exposed to thymol (1X and 2X MIC) for 12 h. Treated cells were washed thrice with 1X PBS and centrifuged at 8000 g for 4 min and fixed overnight at 4 °C with 2.5% glutaraldehyde. Fixed cells were further dehydrated with an ethanol gradient (20%, 40%, 60%, 80%, 90%, and

100%). The samples were then coated with a layer of gold and visualized under SEM. Detailed protocol has been mentioned in the experimental procedures section of chapter 4.

7.4.13 Checkerboard assay for determination of interaction between meropenem and thymol

Drug combination interactions are assessed using fractional inhibitory index (FIC) values. The ΣFICs were calculated as follows: FICI = FIC A + FIC B, where FIC A is the MIC of drug A in the combination/MIC of drug A alone, and FIC B is the MIC of drug B in the combination/MIC of drug B alone. The combination is considered synergistic when the FICI is ≤0.5, indifferent/additive when the FICI is >0.5 to <2, and antagonistic when the FICI is ≥2. A total of 100 µl of LB broth was distributed into each well of the microdilution plates. Meropenem was serially two-fold diluted along the ordinate, while thymol was diluted along the abscissa. 100 µL of *A. baumannii* AYE cells (5×10^5 CFU/ml) in LB medium were added to the 96-well microtiter well plates and incubated at 37°C for 16 h.

7.4.14 Killing assays to assess anti-persister potential of GRAS compounds against *A. baumannii* AYE

In order to assess the anti-persister potential of test compounds against *A. baumannii* AYE in planktonic phase, stationary phase cells or meropenem induced persisters were incubated with varying concentration of test compounds (0.25X, 0.5X, 1X and 2X MIC) with or without the presence of meropenem (at 100X MIC). The number of viable bacteria were enumerated after 12 h of incubation. For killing assays under biofilm conditions, 48 h old *A. baumannii* AYE biofilms were treated with meropenem alone (at 100X MIC), GRAS compounds (at 0.25X MIC, 0.5X MIC, IX MIC and 2X MIC) or a combination of both. After 12 h of incubation, biofilm associated cells were dislodged and plated to enumerate the number of viable colonies. To study the kinetics of killing of *A. baumannii* in the presence of meropenem, upon addition of thymol at different time intervals the following protocol was followed. Stationary phase cells of *A. baumannii* AYE were treated with meropenem (100X MIC) or combination of meropenem and 1X MIC of thymol. Thymol was added to the cultures at different time points t = 0 h, 3 h and 6 h. The number of viable cells was determined at regular intervals in terms of CFU/mL. In order to study the Anti-persister activity of Thymol in *A. baumannii* AYE persisters of Rifampicin, Tigecycline and Polymyxin B the following procedure was followed. Stationary phase cells of *A. baumannii* AYE were exposed to

Rifampicin (50X MIC), Tigecycline (100X MIC) and Polymyxin B (40X MIC) for 12 h to induce persister formation. Isolated persisters were then treated with thymol at 0.25X, 0.5X and 1X MIC in the absence and presence of respective antibiotics at respective concentrations. After 12 h of incubation, the cells were plated to enumerate the number of viable colonies.

7.4.15 Fluorescence microscopy studies to assess the accumulation of BOCILLIN^{TM} FL Penicillin

Isolated meropenem induced *A. baumannii* AYE persisters in IX PBS were incubated with BOCILLIN^{TM} FL Penicillin (10 µg/ml) for 30 minutes in the presence of meropenem (15 µg/ml) to maintain persistence. Cells were then washed with IX PBS, deposited on 1% agarose pads and visualised under a Zeiss Axioscope A1 fluorescence microscope equipped with an AxioCam MRC digital camera using EC Plan-Neofluar 100X objective. Stationary phase cultures of *A. baumannii* AYE were similarly washed and resuspended in 1X PBS and incubated with BOCILLIN for microscopy studies.

7.4.16 Membrane depolarization assay

A. baumannii AYE cells in the log Phase (OD_{600} = 0.5), stationary phase (12 h old) and meropenem induced persisters fractions were washed thrice with IX PBS and resuspended in the same buffer. The cells were then incubated with 10 µM $DiBAC_4(3)$ for 30 minutes and washed with 1X PBS. Fluorescence was recorded at excitation-emission wavelength of 490/516 nm in 96-well Corning half area opaque plates. Relative fluorescence unit (RFU) was calculated by dividing the fluorescence values with absorbance at 600 nm.

7.4.17 Assay for respiratory activity Tetrazolium salt (XTT) reduction assay

Meropenem induced *A. baumannii* AYE persisters, log phase and stationary phase cells of *A. baumannii* AYE were washed thrice with 1X PBS and resuspended in the same buffer. The CFU/mL of log phase and stationary phase cells were normalized in comparison to the CFU/mL of isolated meropenem persisters. XTT {2,3-bis(2-methoxy-4-nitro-5-sulfophenyl)-5-[(phenylamino)carbonyl]-2*H*-tetrazolium hydroxide} (XTT) dye (0.5 mg/ml) in combination with menadione (50 µM) was added to the cells resuspended in 1X PBS and incubated for 2 h. Absorbance was read at 450 nm to assess the reduction of XTT dye and the formation of soluble formazan.

7.4.18 Live-Dead staining to assess cell viability

Thymol treated A. baumannii AYE at 1x and 2X MIC were harvested and stained with membrane dye FM™ 4-64FX (1 μg/mL) and nucleoid stain Sytox green (1 μM) at room temperature for 15 minutes. A small volume (5μl) of cells was deposited on agarose pad and sealed with a clean coverslip. The cells were then observed under a Zeiss Axioscope A1 fluorescence microscope equipped with an AxioCam MRC digital camera using EC Plan-Neofluar 100X objective to assess viability.

7.4.19 Frequency of resistance (FOR) of thymol against *A. baumannii* AYE

A log phase culture of *A. baumannii* AYE (OD_{600} = 0.5) was centrifuged at 7000 rpm for 4 minutes and resuspended in fresh LB medium at $1/10^{th}$ the original volume in order to obtain ~ 10^{10} CFU/ml of cells as the starting inoculum. The cells were also serially diluted and plated to confirm the initial CFU count. The cell suspension was then divided into 1 mL fractions and exposed to thymol at 1X and 2X MIC for 72 h at 37°C under shaking condition. Rifampicin at 2X MIC served as the positive control for the assay. At the end of 72 h, the treated and untreated cells were serially diluted and plated. Frequency of Resistance was calculated by dividing the number of colony forming units obtained on the drug treated cultures by the number of bacteria in the untreated populations.

8 Conclusions and Future perspectives

The results of the work carried out in this thesis led to some important conclusions and opened up new avenues for more research and experimentation in the area of antibacterial drug discovery.

8.1 IITR06144 is a novel broad spectrum antibacterial displaying most features of a "theoretically ideal" antibiotic.

To address the need for compounds that can penetrate the complex envelope architecture of Gram negative bacteria, a small molecule screening of 11,000 compounds was previously performed in the lab against *E. coli.* This led to the identification of 30 antibacterial hits, out of which 4 molecules with significant antibacterial activity were observed to contain the nitrofuran nucleus. Nitrofuran compounds are prodrug antibacterials which undergo biological reduction within the host to yield active intermediates that can act on multiple cellular targets [303]. With the increasing prevalence of chronic infections and lack of novel antibiotic scaffolds, screening and identification of prodrug antibacterials is increasingly being sought [44]. Owing to their broad spectrum activity, multi-targeting nature, non-toxicity and ability to inhibit both growing and dormant persister cells, prodrugs have been considered as "theoretically ideal" antibiotics [303].

IITR06144 was observed to be structurally related to nitrofurantoin, an old prodrug antibiotic which has recently undergone revival as a frontline agent against uncomplicated Urinary Tract Infections (UTIs) [233]. However, rampant empiric use and increased over the counter (OTC) sales has led to increased percentage of nitrofurantoin resistance [338]. Moreover, nitrofurantoin failed to inhibit persistent uropathogenic *E. coli* (UPEC) infections and has been associated with frequent cases of infection relapse [207].

In comparison to nitrofurantoin, IITR06144 showed a broad spectrum activity and a superior killing ability against *E. coli* cells. IITR06144 eradicated UPEC associated biofilms and displayed a remarkable anti-persister activity along with the lack of spontaneous resistance development. IITR06144 displayed a longer PAE and a lack of cross resistance or antagonism

to clinically relevant antibiotics. IITR06144 possessed a large therapeutic index with no associated toxicity and exhibited *in vivo* efficacy in mice model. Thus, IITR06144 was observed to out-compete the existing nitrofuran antibiotics in most of the aspects studied. Moreover, IITR06144 retained its potency against nitrofurantoin resistant bacteria isolated from the clinics thereby demonstrating its potential to bypass the canonical mechanisms of nitrofurantoin resistance. Considering its superior *in vitro* and *in vivo* properties, further studies to determine the feasibility of IITR06144 as a therapeutic agent need to be undertaken in future. These could include studies to assess the *in vivo* pharmacokinetic parameters of IITR06144 followed by efficacy studies in different *in vivo* mice infection models such as urinary tract infection, wound infection, or topical infection. Since IITR06144 also exhibited excellent activity against anaerobic bacteria (*Clostridium difficile* in particular) *in vivo* studies in mice models of *Clostridium difficile* associated diarrohea (CDAD) infection could also be carried out. Furthermore, Structure Activity Relationship (SAR) studies can also be performed to optimize and enhance its *in vivo* antibacterial potential.

8.2 The combination of IITR06144 and vancomycin can inhibit Methicillin resistant *Staphylococcus aureus* (MRSA) isolates that are hVISA or VISA.

Vancomycin has been considered the "gold standard" antibiotic for the treatment of MRSA infections. However, excessive vancomycin use has led to the emergence of clinical MRSA isolates with reduced vancomycin susceptibility, such as heterogeneous vancomycin-intermediate *S. aureus* (hVISA) and vancomycin-intermediate *S. aureus* (VISA) [276]. Difficulties associated with clinical detection along with the presence of limited treatment options against hVISA/VISA infections has further complicated the problem. Therefore, combination therapy can provide a potential treatment option to tackle the threat posed by hVISA/VISA isolates. The synergistic effect of antibacterial small molecule IITR06144 with vancomycin was evaluated against MRSA strains which displayed varying levels of susceptibility to vancomycin.

Time kill kinetics studies demonstrated their superiority over the classical chequerboard method to identify probable synergistic interactions and IITR06144 exhibited synergistic interaction with vancomycin in more than 50% of the isolates studied. IITR06144-vancomycin combination was observed to be bactericidal and demonstrated favourable *in vitro* pharmacodynamics properties. IITR06144 belongs to the nitrofuran class of antibiotics which

are commonly prescribed for the treatment of uncomplicated Urinary tract infections. This is the first report which studies the combinatorial effect of a nitrofuran antibacterial with vancomycin against *Staphylococcus aureus*. The synergistic combination of IITR06144 and vancomycin reported here need to be validated further using larger no. of clinical isolates, both of VISA and hVISA. Moreover since, IITR06144 was observed to possess anti-persister activity against *E. coli* (Section 4.3.9), future studies to assess the activity of IITR06144 against *S. aureus* persisters can be carried out, and more so in combination with antibiotics frequently administered in clinics against *S. aureus* infections. These could be followed by studies evaluating the *in vivo* efficacy of the combination in mice models of *S. aureus* infections. However, the pharmacokinetic parameters of both vancomycin and IITR06144 are diverse and do not overlap, which could affect their *in vivo* efficacy [339]. Therefore, *in vivo* combination studies could be carried out against topical infection mice models, in order to overcome the pharmacokinetic barrier and evaluate its efficacy against persistent bacterial populations associated with wound/skin infections.

8.3 IITR07865 is a novel antibacterial small molecule representing a new class of cell wall inhibitors.

Chemical-chemical profiling is an unconventional approach that is used to link compound interactions with their mode of action [31]. Herein, this strategy was exploited to study the interaction profiles of 12 novel antibacterials with a panel of 14 known bioactives against *E. coli* MC1061. One of these small molecules, IITR07865 targeted the bacterial cell wall synthesis and cell membrane, which are considered to be attractive targets for antibacterial drug discovery. IITR07865 inhibited the growth of several Gram negative and Gram positive bacteria, displayed favourable pharmacodynamic properties and interacted synergistically with meropenem in time-kill kinetic studies. However, the Minimum Inhibitory Concentration of IITR07685 was high against most pathogens (MIC in the range 32-128 µg/ml) and Structure Activity Relationship (SAR) studies would be needed in future to improve its antibacterial potential. Interestingly, IITR07865 also displayed excellent anti-persister activity against *E. coli* and this property could further be explored against a broader panel of pathogenic strains in combination with clinically relevant antibiotics, more importantly carbapenems.

This study also discovered a few other molecules that act on the bacterial cells by enhancing membrane permeability and causing membrane depolarization. The compounds IITR00205,

IITR06033 and IITR07806 were found to be potential dissipaters of electric potential (ΔΨ) of the bacterial membrane, while the molecules IITR07347 and IITR08276 acted by affecting the transmembrane proton gradient (ΔpH). Previous studies have reported the strategic use of combinations of modulators of ΔΨ and ΔpH against the Gram positive pathogen, *S. aureus* [14]. Hence, the PMF modulators discovered in this study could also be further screened for their synergistic activity against antibiotic resistant and tolerant pathogens. The small molecules which dissipated the bacterial membrane potential could be also evaluated for their efflux inhibitory activity in combination with antibiotics against multidrug resistant bacteria.

8.4 Meropenem tolerant *A. baumannii* persisters exhibit active efflux mechanisms and the plant derived natural product, thymol possess excellent anti-persister activity against *A. baumannii* persisters.

Persister cells are known to be the major culprits for the recalcitrant nature of chronic infections and present a serious threat to clinical therapy [313]. *A. baumannii* is a notorious Gram negative ESKAPE pathogen which evade antibiotic action due to the occurrence of persister populations within biofilms or host environment. This study made an attempt to characterise the mechanisms of persistence in *A. baumannii* in response to the last resort antibiotic, meropenem. Meropenem induced *A. baumannii* persisters were observed to exhibit a multi-drug tolerance phenotype, depolarized membrane and upregulated efflux mechanisms. So far, this is the first study to characterise the mechanisms which confer the persistent phenotype to *A. baumannii.* Future studies could be aimed at further delineating the complex mechanisms of *A. baumannii* persiter formation by performing transcriptome analysis or the use of deletion mutants of the Toxin/Antitoxin genes, global regulators or ppGpp *etc.* This could facilitate the design and development of efficient strategies to eradicate them.

This study further identified the anti-persister activity of thymol, a plant-derived antimicrobial that could be used as monotherapy or in combination with antibiotics against *A. baumannii* infections. The GRAS (generally recognized as safe) status compound, Thymol was observed to inhibit both non-dividing and dividing as well as both culturable and non-culturable populations of *A. baumannii*. It was observed to act by increasing membrane permeability, dissipating the membrane potential and inhibiting the efflux machinery as well as respiratory activity in *A. baumannii* persisters. Nonetheless, it displayed no potential for resistance

generation, antibiotic independent activity and inhibitory potential against persister populations of *P. aeruginosa* and *K. pneumoniae.*

This indicates thymol to have an immense potential to act either alone or as an adjunct in combination therapies against mixed bacterial infections. The anti-persister activity of thymol could further be evaluated in appropriate chronic *in vivo* infection models such as mice, *C. elegans* or Zebrafish. Structure activity Relationship (SAR) studies can be also carried out followed by the synthesis of thymol derivatives with improved antibacterial activity.

Moreover, this study devised a mechanism based screen to identify potent anti-persister compounds based on their ability to target the bacterial membrane, cause increased ROS production and inhibit multidrug efflux pumps. This strategy could be further utilized to screen FDA approved libraries or other available resources in order to identify novel anti-persister compounds or aid the repurposing of already approved drugs.

9 Appendices

Appendix 9.1 Strains used in the study.

Lab stock	Strain/Relevant genotype	Source/Reference
RPT 67	*E. coli* ATCC 25922	Lab collection
RPT 2	*E. coli* BL21 DE3	Lab collection
RPT 71	*A. baumannii* ATCC 17978	ATCC, USA
RPT 73	*Acinetobacter baumannii* AYE	ATCC, USA
RPT 80	*Shigella flexneri* ATCC 9199	ATCC, USA
RPT 78	*Burkholderia cepacia* ATCC 25416	ATCC, USA
RPT 81	*Salmonella choleraesuis* ATCC 10708	ATCC, USA
NKN 5	*Salmonella enterica* Serotype Typhimurium	Lab collection
RPT 69	*Vibrio fluvialis* (BD-146)	Lab collection
RPT 68	*Vibrio fluvialis* (L-15318)	Lab collection
RPT 76	*Staphylococcus aureus* ATCC 29213	ATCC, USA
NKN 4	*Bacillus cereus* ATCC 11778	ATCC, USA
NKN 8	*Listeria monocytogenes*	Lab collection
NKN 24	*Enterococcus faecium* FH99	Lab collection
RPT 45	*Mycobacterium smegmatis*	Lab collection
RPT 313	*Mycobacterium tuberculosis* H37Ra	IMTECH, Chandigarh, India

RPT 314	*Mycobacterium bovis* BCG	IMTECH, Chandigarh, India
RPT 315	*E. coli* BW 25113	Lab collection
RPT 44	*Bacillus subtilis*	Lab collection
NKN 7	*Cronobacter sakazakii*	Lab collection
RPT 58	*Pseudomonas aeruginosa* MTCC *2453*	MTCC, India
JW0835	*E. coli* Δ*nfsA* F-, Δ(araD-araB)567, ΔlacZ4787(::rrnB-3), λ-, ΔnfsA752::kan, rph-1, Δ(rhaD-rhaB)568, hsdR514	Keio collection [1]
JW4019	*E. coli* Δ*uvrA* F-,Δ(araD-araB)567, ΔlacZ4787(::rrnB-3), λ-, rph-1, Δ(rhaD-rhaB)568, ΔuvrA753::kan, hsdR514	Keio collection [1]
JW2669	*E. coli* Δ*recA* F-, Δ(araD-araB)567, ΔlacZ4787(::rrnB-3), λ-, ΔrecA774::kan, rph-1, Δ(rhaD-rhaB)568, hsdR514	Keio collection [1]
JW3677	*E. coli* Δ*recF* F-, Δ(araD-araB)567, ΔlacZ4787(::rrnB-3), λ-, rph-1, ΔrecF735::kan, Δ(rhaD-rhaB)568, hsdR514	Keio collection [1]
JW3610	*E. coli* Δ*mutM* F-, Δ(araD-araB)567, ΔlacZ4787(::rrnB-3), λ-, ΔmutM744::kan, rph-1, Δ(rhaD-rhaB)568, hsdR514	Keio collection [1]
JW2703	*E. coli* Δ*mutS* F-, Δ(araD-araB)567, ΔlacZ4787(::rrnB-3), λ-, ΔmutS738::kan, rph-1, Δ(rhaD-rhaB)568, hsdR514	Keio collection [1]

JW1625	*E. coli* Δ*nth* F-, Δ(araD-araB)567, ΔlacZ4787(::rrnB-3), λ-, Δnth-782::kan, rph-1, Δ(rhaD-rhaB)568, hsdR514	Keio collection [1]
JW0704	*E. coli* Δ*nei* F-, Δ(araD-araB)567, ΔlacZ4787(::rrnB-3), Δnei-764::kan, λ-, rph-1, Δ(rhaD-rhaB)568, hsdR514	Keio collection [1]
RPT 308	*E. coli* MTCC 729	MTCC, India
RPT 309	*E. coli* MTCC 4296	MTCC, India
RPTC 1-25	*A. baumannii* clinical isolates	Dr. Varsha Gupta, GMCH, Chandigarh, India
RPT U6 RPT U7 RPT U10 RPT U11 RPT U14 RPT U16	*S. aureus* clinical isolates	Lab collection
RPT U20 RPT U23 RPT U26 RPT U44	*K. pneumoniae* clinical isolates	Lab collection
RPT U45 RPT U46 RPT U50 RPT U53 RPT U54	*E. coli* clinical isolates	Lab collection
NKN 51	*Lactobacillus fermentum*	Lab collection
NKN 52	*Lactobacillus brevis*	Lab collection

NKN 54	*Lactobacillus plantarum*	Lab collection
NKN 57	*Lactobacillus gasseri*	Lab collection
NKN 63	*Lactobacillus cassei*	Lab collection
NKN 189	*Lactobacillus rhamnosus*	Lab collection
NKN 188	*Streptococcus thermophiles* NCDC 74	Lab collection
NKN 190	*Leuconostoc mesenteroides* NCDC 29	Lab collection
Strain collection at AIIMS, New Delhi	*Clostridium difficile* ATCC 9689	Dr. Rama Chaudhry, AIIMS, New Delhi
Strain collection at AIIMS, New Delhi	*Clostridium perfringens* ATCC 3629	Dr. Rama Chaudhry, AIIMS, New Delhi
Strain collection at AIIMS, New Delhi	*Clostridium tetani*	Dr. Rama Chaudhry, AIIMS, New Delhi
Strain collection at AIIMS, New Delhi	*Bacteroides fragilis*	Dr. Rama Chaudhry, AIIMS, New Delhi
RPT U2	*Proteus mirabilis* clinical isolate	Lab collection

Appendix 9.2: Plasmids used in the study.

Plasmids	Origin	Resistance marker	Source or Reference
pET28a FtsZ	f1; pBR322	Kanamycin	Lab collection
pHN678	P15A ori	Chloramphenicol	Dr. Liam Good, UK [253]
pHN678 *ftsZ*	P15A ori	Chloramphenicol	Lab collection
pHN678 *murA*	P15A ori	Chloramphenicol	Lab collection
pNYL GFP	ColE1	Kanamycin	Lab collection [340]

Bibliography

1. Davies J, Davies D. Origins and evolution of antibiotic resistance. Microbiology and Molecular Biology Reviews *74*, 417–433. 2010.

2. CDC, "Antibiotic resistance threats in the United States, 2013," *Current*, p. 114, 2013.

3. "Who Publishes List of Bacteria for Which New Antibiotics Are Urgently Needed," *Saudi Med. J.*, vol. 38, no. 4, p. 444—445, 2017.

4. Boucher, H.W., Talbot, G.H., Bradley, J.S., Edwards, J.E., Gilbert, D., Rice, L.B., Scheld, M., Spellberg, B., and Bartlett, J. "Bad Bugs, No Drugs: No ESKAPE! An Update from the Infectious Diseases Society of America," *Clin. Infect. Dis.*, vol. 48, no. 1, pp. 1–12, 2009.

5. WHO, *Guidelines for the prevention and control of carbapenem-resistant* Enterobacteriaceae, *Acinetobacter baumannii and Pseudomonas aeruginosa in health care facilities*. 2017.

6. J. M. A. Blair, M. A. Webber, A. J. Baylay, D. O. Ogbolu, and L. J. V Piddock, "Molecular mechanisms of antibiotic resistance," *Nature Reviews Microbiology*, vol. 13, no. 1. pp. 42–51, 2015.

7. C. T. Kåhrström, "Entering a post-antibiotic era?," *Nat. Rev. Microbiol.*, vol. 11, no. 3, pp. 146–146, Mar. 2013.

8. Boucher, H.W., Talbot, G.H., Benjamin, D.K., Bradley, J., Guidos, R.J., Jones, R.N., Murray, B.E., Bonomo, R.A., and Gilbert, D. "10 x '20 Progress--Development of New Drugs Active Against Gram-Negative Bacilli: An Update From the Infectious Diseases Society of America," *Clin. Infect. Dis.*, vol. 56, no. 12, pp. 1685–1694, Jun. 2013.

9. Pathania, R., Zlitni, S., Barker, C., Das, R., Gerritsma, D.A., Lebert, J., Awuah, E., Melacini, G., Capretta, F.A., and Brown, E.D. "Chemical genomics in *Escherichia coli* identifies an inhibitor of bacterial lipoprotein targeting," *Nat. Chem. Biol.*, vol. 5, no. 11, pp. 849–856, Nov. 2009.

10. Ling ,L., Schneider, T., Peoples, A., Spoering, A., Engels, I., Conlon, B., Mueller, A., Schäberle,T., Hughes, D., Epstein, S., Jones, M., Lazarides, L., Steadman, V., Cohen,

D., Felix, C., Fetterman, K., Millett, W., Nitti, A., Zullo, A., Chen, C., Lewis, K. "A new antibiotic kills pathogens without detectable resistance," *Nature*, vol. 517, no. 7535, pp. 455–459, Jan. 2015.

11. Smith, P.A., Koehler, M.F.T., Girgis, H.S., Yan, D., Chen, Y., Chen, Y., Crawford, J.J., Durk, M.R., Higuchi, R.I., Kang, J., Murray, J., Paraselli, P., Park, S., Phung, W., Quinn, J., Roberts, T., Rougé, L., Schwarz, J., Skippington, E., Wai, J., Xu, M., Yu, Z., Zhang, H., Tan, M., Heise, C. "Optimized arylomycins are a new class of Gram-negative antibiotics," *Nature*, vol. 561, no. 7722, pp. 189–194, Sep. 2018.

12. R. J. Worthington and C. Melander, "Combination approaches to combat multidrug-resistant bacteria," *Trends Biotechnol.*, vol. 31, no. 3, pp. 177–184, Mar. 2013.

13. G. Cottarel and J. Wierzbowski, "Combination drugs, an emerging option for antibacterial therapy," Trends Biotechnol., vol. 25, no. 12, pp. 547–55, Dec. 2007.

14. M. A. Farha, C. P. Verschoor, D. Bowdish, and E. D. Brown, "Collapsing the Proton Motive Force to Identify Synergistic Combinations against *Staphylococcus aureus*," *Chem. Biol.*, vol. 20, no. 9, pp. 1168–1178, Sep. 2013.

15. D. R. Spring, "Chemical genetics to chemical genomics: small molecules offer big insights," *Chem. Soc. Rev.*, vol. 34, no. 6, p. 472, 2005.

16. M. Schenone, V. Dančík, B. K. Wagner, and P. A. Clemons, "Target identification and mechanism of action in chemical biology and drug discovery," *Nat. Chem. Biol.*, vol. 9, no. 4, pp. 232–240, Apr. 2013.

17. W. Zheng, N. Thorne, and J. C. McKew, "Phenotypic screens as a renewed approach for drug discovery," *Drug Discov. Today*, vol. 18, no. 21–22, pp. 1067–1073, Nov. 2013.

18. M. Schirle and J. L. Jenkins, "Identifying compound efficacy targets in phenotypic drug discovery," Drug Discov. Today, vol. 21, no. 1, pp. 82–89, 2016.

19. M. A. Farha and E. D. Brown, "Strategies for target identification of antimicrobial natural products," Nat. Prod. Rep., vol. 33, no. 5, pp. 668–80, 2016.

20. W. Zheng, G. Li, and X. Li, "Affinity purification in target identification: the specificity challenge," *Arch. Pharm. Res.*, vol. 38, no. 9, pp. 1661–1685, Sep. 2015.

21. Ong, S.-E., Schenone, M., Margolin, A.A., Li, X., Do, K., Doud, M.K., Mani, D.R., Kuai, L., Wang, X., Wood, J.L., Tolliday, N., Koehler, A., Marcaurelle, L., Golub, T., Gould, R., Schreiber, S., Carr, S. "Identifying the proteins to which small-molecule probes and drugs bind in cells," *Proc. Natl. Acad. Sci.*, vol. 106, no. 12, pp. 4617–4622, Mar. 2009.

22. X. Li, M. Zolli-Juran, J. D. Cechetto, D. M. Daigle, G. D. Wright, and E. D. Brown, "Multicopy suppressors for novel antibacterial compounds reveal targets and drug efflux susceptibility," *Chem. Biol.*, vol. 11, no. 10, pp. 1423–30, Oct. 2004.

23. C. A. Barker, M. A. Farha, and E. D. Brown, "Chemical genomic approaches to study model microbes," *Chem. Biol.*, vol. 17, no. 6, pp. 624–632, Jun. 2010.

24. Wang, J., Soisson, S.M., Young, K., Shoop, W., Kodali, S., Galgoci, A., Painter, R., Parthasarathy, G., Tang, Y.S., Cummings, R., Ha, S., Dorso, K., Motyl, M., Jayasuriya, H., Ondeyka, J., Herath, K., Zhang, C., Hernandez, L., Allocco, J., Basilio, Á., Tormo, J., Genilloud, O., Vicente, F., Pelaez, F., Colwell, L., Lee, S., Michael, B., Felcetto, T., Gill, C., Silver, L., Hermes, J., Bartizal, K., Barrett, J., Schmatz, D., Becker, J., Cully, D., Singh, S. "Platensimycin is a selective FabF inhibitor with potent antibiotic properties," *Nature*, vol. 441, no. 7091, pp. 358–361, May 2006.

25. Telenti, A., Imboden, P., Marchesi, F., Matter, L., Schopfer, K., Bodmer, T., Lowrie, D., Colston, M.J., and Cole, S. "Detection of rifampicin-resistance mutations in *Mycobacterium tuberculosis*," *Lancet*, vol. 341, no. 8846, pp. 647–651, Mar. 1993.

26. M. Fujimoto-Nakamura, H. Ito, Y. Oyamada, T. Nishino, and J. -i. Yamagishi, "Accumulation of Mutations in both gyrB and parE Genes Is Associated with High-Level Resistance to Novobiocin in *Staphylococcus aureus*," *Antimicrob. Agents Chemother.*, vol. 49, no. 9, pp. 3810–3815, Sep. 2005.

27. A.Cotsonas King and L. Wu, "Macromolecular synthesis and membrane perturbation assays for mechanisms of action studies of antimicrobial agents," Curr. Protoc. Pharmacol., vol. Chapter 13, p. Unit 13A.7, Dec. 2009.

28. P. Nonejuie, M. Burkart, K. Pogliano, and J. Pogliano, "Bacterial cytological profiling rapidly identifies the cellular pathways targeted by antibacterial molecules," *Proc. Natl. Acad. Sci. U. S. A.*, vol. 110, no. 40, pp. 16169–74, Oct. 2013.

29. A. J. O'Neill and I. Chopra, "Preclinical evaluation of novel antibacterial agents by microbiological and molecular techniques," *Expert Opin. Investig. Drugs*, vol. 13, no. 8, pp. 1045–1063, Aug. 2004.

30. S. French, M. J. Ellis, B. E. Coutts, and E. D. Brown, "Chemical genomics reveals mechanistic hypotheses for uncharacterized bioactive molecules in bacteria," *Curr. Opin. Microbiol.*, vol. 39, pp. 42–47, Oct. 2017.

31. M. A. Farha and E. D. Brown, "Chemical probes of *Escherichia coli* uncovered through chemical-chemical interaction profiling with compounds of known biological activity," *Chem. Biol.*, vol. 17, no. 8, pp. 852–862, Aug. 2010.

32. Wang, Y., Worrall, L.J., Oldfield, E., Brown, E.D., Conrady, D.G., Myers, C.L., Czarny, T.L., Strynadka, N.C.J., French, S., and Farha, M.A. "Antagonism screen for inhibitors of bacterial cell wall biogenesis uncovers an inhibitor of undecaprenyl diphosphate synthase," *Proc. Natl. Acad. Sci.*, vol. 112, no. 35, pp. 11048–11053, Sep. 2015.

33. E. M. Windels, J. E. Michiels, M. Fauvart, T. Wenseleers, B. Van den Bergh, and J. Michiels, "Bacterial persistence promotes the evolution of antibiotic resistance by increasing survival and mutation rates," *ISME J.*, vol. 13, no. 5, pp. 1239–1251, May 2019.

34. N. Dhar and J. D. McKinney, "Microbial phenotypic heterogeneity and antibiotic tolerance," *Curr. Opin. Microbiol.*, vol. 10, no. 1, pp. 30–8, Feb. 2007.

35. S. A. Waksman, "What Is an Antibiotic or an Antibiotic Substance?," *Mycologia*, vol. 39, no. 5, p. 565, Sep. 1947.

36. K. Williams, "The introduction of 'chemotherapy' using arsphenamine – the first magic bullet," *J. R. Soc. Med.*, vol. 102, no. 8, pp. 343–348, Aug. 2009.

37. L. Ludovici and A. Fleming, "Fleming: discoverer of penicillin," 1955.

38. S. Tan and Y. Tatsumura, "Alexander Fleming (1881–1955): Discoverer of penicillin," *Singapore Med. J.*, vol. 56, no. 07, pp. 366–367, Jul. 2015.

39. H. B. Woodruff, “Selman A. Waksman, Winner of the 1952 Nobel prize for physiology or medicine,” *Appl. Environ. Microbiol.*, vol. 80, no. 1, pp. 2–8, Jan. 2014.

40. R. Gaynes, “The discovery of penicillin—new insights after more than 75 years of clinical use,” *Emerg. Infect. Dis.*, vol. 23, no. 5, pp. 849–853, May 2017.

41. R. C. Moellering, “MRSA: the first half century,” *J. Antimicrob. Chemother.*, vol. 67, no. 1, pp. 4–11, Jan. 2012.

42. C. L. Ventola, “[Review] The antibiotic resistance crisis: part 1: causes and threats,” *Pharm. Ther.*, 2015.

43. L. L. Silver, “Challenges of antibacterial discovery,” *Clin. Microbiol. Rev.*, vol. 24, no. 1, pp. 71–109, Jan. 2011.

44. K. Lewis, “Platforms for antibiotic discovery,” *Nat. Rev. Drug Discov.*, vol. 12, no. 5, pp. 371–387, 2013.

45. WHO, “WHO | Global action plan on AMR,” *WHO*. 2016.

46. J. O’ Neil, “Review on antibiotic resisitance. Antimicrobial Resistance : Tackling a crisis for the health and wealth of nations,” *Heal. Wealth Nations*, no. December, 2014.

47. World Health Organization, *Prioritization of pathogens to guide discovery, research and development of new antibiotics for drug resistant bacterial infections, including tuberculosis*. 2017.

48. G. D. Wright, “Something old, something new: revisiting natural products in antibiotic drug discovery,” *Can. J. Microbiol.*, vol. 60, no. 3, pp. 147–154, Mar. 2014.

49. B. Mott *et al.*, “A report from A Scientific Roadmap for Antibiotic Discovery,” 2016.

50. D. J. Payne, M. N. Gwynn, D. J. Holmes, and D. L. Pompliano, “Drugs for bad bugs: confronting the challenges of antibacterial discovery,” *Nat. Rev. Drug Discov.*, vol. 6, no. 1, pp. 29–40, Jan. 2007.

51. K. Poole, “Outer membranes and efflux: the path to multidrug resistance in Gram-negative bacteria.,” *Curr. Pharm. Biotechnol.*, vol. 3, no. 2, pp. 77–98, Jun. 2002.

52. S. Dzidic, J. Suskovic, and K. Blazenka, "Antibiotic Resistance Mechanisms in Bacteria : Biochemical and Genetic Aspects," *Food Technol. Biotechnol.*, vol. 46, no. 1, pp. 11–21, 2008.

53. J. M. Munita and C. A. Arias, "Mechanisms of antibiotic resistance mechanisms of antibiotic resistance," *Am. Soc. Microbiol. Press*, 2016.

54. K. Bush, G. A. Jacoby, and A. A. Medeiros, "A functional classification scheme for beta-lactamases and its correlation with molecular structure," *Antimicrob. Agents Chemother.*, vol. 39, no. 6, pp. 1211–33, Jun. 1995.

55. K. Poole, "Resistance to beta-lactam antibiotics," *Cell. Mol. Life Sci.*, vol. 61, no. 17, pp. 2200–23, Sep. 2004.

56. L. P. Kotra and S. Mobashery, "Mechanistic and clinical aspects of beta-lactam antibiotics and beta-lactamases," *Arch. Immunol. Ther. Exp. (Warsz).*, vol. 47, no. 4, pp. 211–6, 1999.

57. R. Bonnet, "Growing group of extended-spectrum beta-lactamases: the CTX-M enzymes," *Antimicrob. Agents Chemother.*, vol. 48, no. 1, pp. 1–14, Jan. 2004.

58. Nakamura, A., Nakazawa, K., Miyakozawa, I., Mizukoshi, S., Tsurubuchi, K., Nakagawa, M., O'Hara, K., and Sawai, T. "Macrolide esterase-producing *Escherichia coli* clinically isolated in Japan," *J. Antibiot. (Tokyo).*, vol. 53, no. 5, pp. 516–524, 2000.

59. Y.-H. Kim, C.-J. Cha, and C. E. Cerniglia, "Purification and characterization of an erythromycin esterase from an erythromycin-resistant *Pseudomonas* sp.," *FEMS Microbiol. Lett.*, vol. 210, no. 2, pp. 239–244, May 2002.

60. K. L. Fillgrove, S. Pakhomova, M. E. Newcomer, and R. N. Armstrong, "Mechanistic diversity of Fosfomycin resistance in pathogenic microorganisms," *J. Am. Chem. Soc.*, vol. 125, no. 51, pp. 15730–15731, Dec. 2003.

61. M. W. Vetting, S. Magnet, E. Nieves, S. L. Roderick, and J. S. Blanchard, "A bacterial acetyltransferase capable of regioselective N-Acetylation of antibiotics and histones," *Chem. Biol.*, vol. 11, no. 4, pp. 565–573, Apr. 2004.

62. S. Schwarz, C. Kehrenberg, B. Doublet, and A. Cloeckaert, “Molecular basis of bacterial resistance to chloramphenicol and florfenicol,” *FEMS Microbiol. Rev.*, vol. 28, no. 5, pp. 519–42, Nov. 2004.

63. A. Nakamura, I. Miyakozawa, K. Nakazawa, K. O-Hara, and T. Sawai, “Detection and characterization of a macrolide 2’-phosphotransferase from a *Pseudomonas aeruginosa* clinical isolate,” *Antimicrob. Agents Chemother.*, vol. 44, no. 11, pp. 3241–2, Nov. 2000.

64. J. Allignet and N. el Solh, “Diversity among the gram-positive acetyltransferases inactivating streptogramin A and structurally related compounds and characterization of a new staphylococcal determinant, vatB,” *Antimicrob. Agents Chemother.*, vol. 39, no. 9, pp. 2027–2036, Sep. 1995.

65. K. Yazawa, Y. Mikami, A. Maeda, N. Morisaki, and S. Iwasaki, “Phosphorylative inactivation of rifampicin by *Nocardia otitidiscaviarum*,” *J. Antimicrob. Chemother.*, vol. 33, no. 6, pp. 1127–35, Jun. 1994.

66. M. Matsuoka and T. Sasaki, “Inactivation of macrolides by producers and pathogens.,” *Curr. Drug Targets. Infect. Disord.*, vol. 4, no. 3, pp. 217–40, Sep. 2004.

67. K. Nagai, T. A. Davies, M. R. Jacobs, and P. C. Appelbaum, “Effects of amino acid alterations in penicillin-binding proteins (PBPs) 1a, 2b, and 2x on PBP affinities of penicillin, ampicillin, amoxicillin, cefditoren, cefuroxime, cefprozil, and cefaclor in 18 clinical isolates of penicillin-susceptible, -intermediate, and -resistant *pneumococci*,” *Antimicrob. Agents Chemother.*, vol. 46, no. 5, pp. 1273–80, May 2002.

68. K. Kosowska, M. R. Jacobs, S. Bajaksouzian, L. Koeth, and P. C. Appelbaum, “Alterations of penicillin-binding proteins 1A, 2X, and 2B in *Streptococcus pneumoniae* isolates for which amoxicillin MICs are higher than penicillin MICs,” *Antimicrob. Agents Chemother.*, vol. 48, no. 10, pp. 4020–4022, Oct. 2004.

69. C. G. Dowson, T. J. Coffey, and B. G. Spratt, “Origin and molecular epidemiology of penicillin-binding-protein-mediated resistance to beta-lactam antibiotics,” *Trends Microbiol.*, vol. 2, no. 10, pp. 361–6, Oct. 1994.

70. B. Weisblum, “Erythromycin resistance by ribosome modification,” *Antimicrob. Agents Chemother.*, vol. 39, no. 3, pp. 577–85, Mar. 1995.

71. A. Canu, B. Malbruny, M. Coquemont, T. A. Davies, P. C. Appelbaum, and R. Leclercq, "Diversity of ribosomal mutations conferring resistance to macrolides, clindamycin, streptogramin, and telithromycin in *Streptococcus pneumoniae*," *Antimicrob. Agents Chemother.*, vol. 46, no. 1, pp. 125–131, Jan. 2002.

72. N. Zelinskaya, M. A. Witek, and G. L. Conn, "The pathogen-derived aminoglycoside resistance 16S rRNA methyltransferase NpmA possesses dual m 1 A1408/m 1 G1408 specificity," *Antimicrob. Agents Chemother.*, vol. 59, no. 12, pp. 7862–7865, Dec. 2015.

73. G. Wang and D. E. Taylor, "Site-specific mutations in the 23S rRNA gene of *Helicobacter pylori* confer two types of resistance to macrolide-lincosamide-streptogramin B antibiotics," *Antimicrob. Agents Chemother.*, vol. 42, no. 8, pp. 1952–8, Aug. 1998.

74. Suzuki, Y., Katsukawa, C., Tamaru, A., Abe, C., Makino, M., Mizuguchi, Y., & Taniguchi, H. "Detection of kanamycin-resistant *Mycobacterium tuberculosis* by identifying mutations in the 16S rRNA gene," *J. Clin. Microbiol.*, vol. 36, no. 5, pp. 1220–1225, 1998.

75. A. B. Khodursky, E. L. Zechiedrich, and N. R. Cozzarelli, "Topoisomerase IV is a target of quinolones in *Escherichia coli*," *Proc. Natl. Acad. Sci.*, vol. 92, no. 25, pp. 11801–11805, Dec. 1995.

76. D. Ince, X. Zhang, L. C. Silver, and D. C. Hooper, "Dual targeting of DNA gyrase and topoisomerase IV: target interactions of garenoxacin (BMS-284756, T-3811ME), a new desfluoroquinolone," *Antimicrob. Agents Chemother.*, vol. 46, no. 11, pp. 3370–80, Nov. 2002.

77. L. J. V Piddock, "Multidrug-resistance efflux pumps ? not just for resistance," *Nat. Rev. Microbiol.*, vol. 4, no. 8, pp. 629–636, Aug. 2006.

78. H. Okusu, D. Ma, and H. Nikaido, "AcrAB efflux pump plays a major role in the antibiotic resistance phenotype of *Escherichia coli* multiple-antibiotic-resistance (Mar) mutants," *J. Bacteriol.*, vol. 178, no. 1, pp. 306–8, Jan. 1996.

79. M. J. Fath and R. Kolter, "ABC transporters: bacterial exporter.," *Microbiol. Rev.*, vol. 57, no. 4, pp. 995–1017, Dec. 1993.

80. K. Poole, “Efflux-mediated antimicrobial resistance,” *J. Antimicrob. Chemother.*, vol. 56, no. 1, pp. 20–51, Jul. 2005.

81. Du, D., Wang, Z., James, N.R., Voss, J.E., Klimont, E., Ohene-Agyei, T., Venter, H., Chiu, W., and Luisi, B.F. “Structure of the AcrAB-TolC multidrug efflux pump,” *Nature*, vol. 509, no. 7501, pp. 512–515, 2014.

82. L. J. V. Piddock, “Clinically relevant chromosomally encoded multidrug resistance efflux Pumps in Bacteria,” *Clin. Microbiol. Rev.*, vol. 19, no. 2, pp. 382–402, Apr. 2006.

83. H. Nikaido, “Molecular basis of bacterial outer membrane poermeability revisited,” *Microbiol. Mol. Biol. Rev.*, vol. 67, no. 4, pp. 593–656, Dec. 2003.

84. S. P. Denyer and J.-Y. Maillard, “Cellular impermeability and uptake of biocides and antibiotics in Gram-negative bacteria,” *J. Appl. Microbiol.*, vol. 92 Suppl, pp. 35S-45S, 2002.

85. S. Gayet, R. Chollet, G. Molle, J. M. Pagès, and J. Chevalier, “Modification of outer membrane protein profile and evidence suggesting an active drug pump in *Enterobacter aerogenes* clinical strains,” *Antimicrob. Agents Chemother.*, vol. 47, no. 5, pp. 1555–1559, May 2003.

86. R. E. W. Hancock and F. S. L. Brinkman, “Function of *Pseudomonas* porins in uptake and efflux,” *Annu. Rev. Microbiol.*, vol. 56, pp. 17–38, 2002.

87. Dé, E., Baslé, A., Jaquinod, M., Saint, N., Malléa, M., Molle, G., and Pagès, J.M. “A new mechanism of antibiotic resistance in Enterobacteriaceae induced by a structural modification of the major porin,” *Mol. Microbiol.*, vol. 41, no. 1, pp. 189–198, Dec. 2001.

88. D. López, H. Vlamakis, and R. Kolter, “Biofilms,” *Cold Spring Harb. Perspect. Biol.*, vol. 2, no. 7, p. a000398, Jul. 2010.

89. P. Gupta, S. Sarkar, B. Das, S. Bhattacharjee, and P. Tribedi, “Biofilm, pathogenesis and prevention—a journey to break the wall: a review,” *Arch. Microbiol.*, vol. 198, no. 1, pp. 1–15, Jan. 2016.

90. N. Høiby, T. Bjarnsholt, M. Givskov, S. Molin, and O. Ciofu, “Antibiotic resistance of bacterial biofilms,” *Int. J. Antimicrob. Agents*, vol. 35, no. 4, pp. 322–332, Apr. 2010.

91. Montanaro, L., Poggi, A., Visai, L., Ravaioli, S., Campoccia, D., Speziale, P., and Arciola, C.R. “Extracellular DNA in biofilms,” *International Journal of Artificial Organs*. 2011.

92. M. E. Davey and G. A. O’toole, “Microbial biofilms: from ecology to molecular genetics.,” *Microbiol. Mol. Biol. Rev.*, vol. 64, no. 4, pp. 847–67, Dec. 2000.

93. T. R. Garrett, M. Bhakoo, and Z. Zhang, “Bacterial adhesion and biofilms on surfaces,” *Prog. Nat. Sci.*, vol. 18, no. 9, pp. 1049–1056, Sep. 2008.

94. H.-C. Flemming and J. Wingender, “The biofilm matrix,” *Nat. Rev. Microbiol.*, vol. 8, no. 9, pp. 623–633, Sep. 2010.

95. M. Kostakioti, M. Hadjifrangiskou, and S. J. Hultgren, “Bacterial biofilms: development, dispersal, and therapeutic strategies in the dawn of the Postantibiotic Era,” *Cold Spring Harb. Perspect. Med.*, vol. 3, no. 4, pp. a010306–a010306, Apr. 2013.

96. B. L. Bassler, “Small talk: cell-to-cell communication in bacteria,” *Cell*, vol. 109, no. 4, pp. 421–424, May 2002.

97. S. Daddi Oubekka, R. Briandet, M.-P. Fontaine-Aupart, and K. Steenkeste, “Correlative time-resolved fluorescence microscopy to assess antibiotic diffusion-reaction in biofilms,” *Antimicrob. Agents Chemother.*, vol. 56, no. 6, pp. 3349–58, Jun. 2012.

98. B. Giwercman, E. T. Jensen, N. Høiby, A. Kharazmi, and J. W. Costerton, “Induction of beta-lactamase production in *Pseudomonas aeruginosa* biofilm.,” *Antimicrob. Agents Chemother.*, vol. 35, no. 5, pp. 1008–10, May 1991.

99. W. Khan, S. P. Bernier, S. L. Kuchma, J. H. Hammond, F. Hasan, and G. A. O’Toole, “Aminoglycoside resistance of Pseudomonas aeruginosa biofilms modulated by extracellular polysaccharide,” *Int. Microbiol.*, vol. 13, no. 4, pp. 207–12, Dec. 2010.

100. C. W. Hall and T.-F. Mah, “Molecular mechanisms of biofilm-based antibiotic resistance and tolerance in pathogenic bacteria,” *FEMS Microbiol. Rev.*, vol. 41, no. 3, pp. 276–301, May 2017.

101. T.-F. Mah, “Biofilm-specific antibiotic resistance,” *Future Microbiol.*, vol. 7, no. 9, pp. 1061–1072, Sep. 2012.

102. R. T. Merod and S. Wuertz, “Extracellular polymeric substance architecture influences natural genetic transformation of *Acinetobacter baylyi* in biofilms,” *Appl. Environ. Microbiol.*, vol. 80, no. 24, pp. 7752–7, Dec. 2014.

103. S. Borgeaud, L. C. Metzger, T. Scrignari, and M. Blokesch, “The type VI secretion system of Vibrio cholerae fosters horizontal gene transfer,” *Science (80-.).*, vol. 347, no. 6217, pp. 63–67, Jan. 2015.

104. M. R. Brown, D. G. Allison, and P. Gilbert, “Resistance of bacterial biofilms to antibiotics: a growth-rate related effect?,” *J. Antimicrob. Chemother.*, vol. 22, no. 6, pp. 777–80, Dec. 1988.

105. Amato, S.M., Fazen, C.H., Henry, T.C., Mok, W.W.K., Orman, M.A., Sandvik, E.L., Volzing, K.G., and Brynildsen, M.P. “The role of metabolism in bacterial persistence,” *Front. Microbiol.*, vol. 5, no. MAR, 2014.

106. M. Monzón, C. Oteiza, J. Leiva, M. Lamata, and B. Amorena, “Biofilm testing of *Staphylococcus epidermidis* clinical isolates: low performance of vancomycin in relation to other antibiotics.,” *Diagn. Microbiol. Infect. Dis.*, vol. 44, no. 4, pp. 319–24, Dec. 2002.

107. L. Li, N. Mendis, H. Trigui, J. D. Oliver, and S. P. Faucher, “The importance of the viable but non-culturable state in human bacterial pathogens,” *Front. Microbiol.*, vol. 5, p. 258, Jun. 2014.

108. T. Ramamurthy, A. Ghosh, G. P. Pazhani, and S. Shinoda, “Current perspectives on Viable but Non-Culturable (VBNC) pathogenic bacteria.,” *Front. public Heal.*, vol. 2, p. 103, 2014.

109. B. P. Conlon, S. E. Rowe, and K. Lewis, “Persister cells in biofilm associated infections,” *Advances in experimental medicine and biology*, vol. 831, 2015, pp. 1–9.

110. M. Ayrapetyan, T. C. Williams, and J. D. Oliver, “Bridging the gap between viable but non-culturable and antibiotic persistent bacteria,” *Trends Microbiol.*, vol. 23, no. 1, pp. 7–13, Jan. 2015.

111. S. Helaine and E. Kugelberg, “Bacterial persisters: formation, eradication, and experimental systems,” *Trends Microbiol.*, vol. 22, no. 7, pp. 417–424, Jul. 2014.

112. I. Keren, S. Minami, E. Rubin, and K. Lewis, “Characterization and transcriptome analysis of *Mycobacterium tuberculosis* persisters.,” *MBio*, vol. 2, no. 3, pp. e00100-11, Jul. 2011.

113. K. Lewis, “Persister cells and the riddle of biofilm survival.,” *Biochemistry. (Mosc).*, vol. 70, no. 2, pp. 267–74, Feb. 2005.

114. K. Lewis, “Multidrug tolerance of biofilms and persister cells.,” *Curr. Top. Microbiol. Immunol.*, vol. 322, pp. 107–31, 2008.

115. S. Singh, S. K. Singh, I. Chowdhury, and R. Singh, “Understanding the mechanism of bacterial biofilms resistance to antimicrobial agents.,” *Open Microbiol. J.*, vol. 11, pp. 53–62, 2017.

116. S. J. Pamp, M. Gjermansen, H. K. Johansen, and T. Tolker-Nielsen, “Tolerance to the antimicrobial peptide colistin in *Pseudomonas aeruginosa* biofilms is linked to metabolically active cells, and depends on the pmr and mexAB-oprM genes,” *Mol. Microbiol.*, vol. 68, no. 1, pp. 223–240, Apr. 2008.

117. S. J. Pamp, M. Gjermansen, H. K. Johansen, and T. Tolker-Nielsen, “Tolerance to the antimicrobial peptide colistin in *Pseudomonas aeruginosa* biofilms is linked to metabolically active cells, and depends on the pmr and mexAB-oprM genes,” *Mol. Microbiol.*, vol. 68, no. 1, pp. 223–240, Apr. 2008.

118. A. Sharma, R. Sharma, T. Bhattacharyya, T. Bhando, and R. Pathania, “Fosfomycin resistance in *Acinetobacter baumannii* is mediated by efflux through a major facilitator superfamily (MFS) transporter—AbaF,” *J. Antimicrob. Chemother.*, vol. 72, no. 1, pp. 68–74, Jan. 2017.

119. P. Fernandes, B. S. Ferreira, and J. M. S. Cabral, “Solvent tolerance in bacteria: role of efflux pumps and cross-resistance with antibiotics.,” *Int. J. Antimicrob. Agents*, vol. 22, no. 3, pp. 211–6, Sep. 2003.

120. Wakimoto, N., Nishi, J., Sheikh, J., Nataro, J.P., Sarantuya, J., Iwashita, M., Manago, K., Tokuda, K., Yoshinaga, M., and Kawano, Y. “Quantitative biofilm assay using a

microtiter plate to screen for enteroaggregative *Escherichia Coli*," *Am. J. Trop. Med. Hyg.*, vol. 71, no. 5, pp. 687–690, 2004

121. K. Matsumura, S. Furukawa, H. Ogihara, and Y. Morinaga, "Roles of multidrug efflux pumps on the biofilm formation of *Escherichia coli* K-12.," *Biocontrol Sci.*, vol. 16, no. 2, pp. 69–72, Jun. 2011.

122. J. Bigger, "Treatment of Staphylococcal infections wih penicillin by intermittent sterszation," *Lancet*, vol. 244, no. 6320, pp. 497–500, Oct. 1944.

123. M. Fauvart, V. N. De Groote, and J. Michiels, "Role of persister cells in chronic infections: clinical relevance and perspectives on anti-persister therapies," *J. Med. Microbiol.*, vol. 60, no. 6, pp. 699–709, Jun. 2011.

124. H. Honda and D. K. Warren, "Central nervous system Infections: meningitis and brain abscess," *Infect. Dis. Clin. North Am.*, vol. 23, no. 3, pp. 609–623, Sep. 2009.

125. K. Lewis, "Persister cells.," *Annu. Rev. Microbiol.*, vol. 64, pp. 357–72, 2010.

126. M. A. Kohanski, D. J. Dwyer, and J. J. Collins, "How antibiotics kill bacteria: from targets to networks.," *Nat. Rev. Microbiol.*, vol. 8, no. 6, pp. 423–35, Jun. 2010.

127. Pu, Y., Zhao, Z., Li, Y., Zou, J., Ma, Q., Zhao, Y., Ke, Y., Zhu, Y., Chen, H., Baker, M.A.B., Ge, H., Sun, Y., Xie, X., Bai, F. "Enhanced efflux activity facilitates drug tolerance in dormant bacterial cells," *Mol. Cell*, vol. 62, no. 2, pp. 284–294, Apr. 2016.

128. Wexselblatt, E., Oppenheimer-Shaanan, Y., Kaspy, I., London, N., Schueler-Furman, O., Yavin, E., Glaser, G., Katzhendler, J., and Ben-Yehuda, S. "Relacin, a novel antibacterial agent targeting the stringent response," *PLoS Pathog.*, vol. 8, no. 9, p. e1002925, Sep. 2012.

129. T. L. Renbarger, J. M. Baker, and W. M. Sattley, "Slow and steady wins the race: an examination of bacterial persistence.," *AIMS Microbiol.*, vol. 3, no. 2, pp. 171–185, 2017.

130. G. Schreiber, E. Z. Ron, and G. Glaser, "ppGpp-mediated regulation of DNA replication and cell division in *Escherichia coli*," *Curr. Microbiol.*, vol. 30, no. 1, pp. 27–32, Jan. 1995.

131. D. Wilmaerts, E. M. Windels, N. Verstraeten, and J. Michiels, “General mechanisms leading to persister formation and awakening,” *Trends Genet.*, vol. 35, no. 6, pp. 401–411, Jun. 2019.

132. R. Page and W. Peti, “Toxin-antitoxin systems in bacterial growth arrest and persistence,” *Nat. Chem. Biol.*, vol. 12, no. 4, pp. 208–214, Apr. 2016.

133. D., W., M., B., L., D., W., K., J.T., M., J., H., P., D., G., M., and N., V. “The persistence-inducing toxin HokB forms dynamic pores that cause ATP leakage,” *MBio*, vol. 9, no. 4, Aug. 2018.

134. P. A. Gurnev, R. Ortenberg, T. Dörr, K. Lewis, and S. M. Bezrukov, “Persister-promoting bacterial toxin TisB produces anion-selective pores in planar lipid bilayers,” *FEBS Lett.*, vol. 586, no. 16, pp. 2529–2534, Jul. 2012.

135. T. Dörr, M. Vulić, and K. Lewis, “Ciprofloxacin causes persister formation by inducing the TisB toxin in *Escherichia coli*,” *PLoS Biol.*, vol. 8, no. 2, p. e1000317, Feb. 2010.

136. K. Pedersen, A. V. Zavialov, M. Y. Pavlov, J. Elf, K. Gerdes, and M. Ehrenberg, “The bacterial toxin RelE displays codon-specific cleavage of mRNAs in the Ribosomal A site,” *Cell*, vol. 112, no. 1, pp. 131–140, Jan. 2003.

137. M. A. Griffin, J. H. Davis, and S. A. Strobel, “Bacterial toxin RelE: a highly efficient ribonuclease with exquisite substrate specificity using atypical catalytic residues,” *Biochemistry*, vol. 52, no. 48, pp. 8633–8642, Dec. 2013.

138. S. K. Christensen and K. Gerdes, “RelE toxins from bacteria and archaea cleave mRNAs on translating ribosomes, which are rescued by tmRNA,” *Mol. Microbiol.*, vol. 48, no. 5, pp. 1389–1400, May 2003.

139. Prysak, M. H., Mozdzierz, C. J., Cook, A. M., Zhu, L., Zhang, Y., Inouye, M., & Woychik, N. A. “Bacterial toxin YafQ is an endoribonuclease that associates with the ribosome and blocks translation elongation through sequence-specific and frame-dependent mRNA cleavage,” *Mol. Microbiol.*, vol. 71, no. 5, pp. 1071–1087, 2009.

140. Y. Zhang, J. Zhang, K. P. Hoeflich, M. Ikura, G. Qing, and M. Inouye, “MazF cleaves cellular mRNAs specifically at ACA to block protein synthesis in *Escherichia coli*,” *Mol. Cell*, vol. 12, no. 4, pp. 913–923, 2003.

141. Y. Yamaguchi, J. H. Park, and M. Inouye, “MqsR, a crucial regulator for quorum sensing and biofilm formation, is a GCU-specific mRNA interferase in Escherichia coli,” *J. Biol. Chem.*, vol. 284, no. 42, pp. 28746–28753, 2009.

142. J. P. Norton and M. A. Mulvey, “Toxin-Antitoxin systems are important for niche-specific colonization and stress resistance of uropathogenic *Escherichia coli*,” *PLoS Pathog.*, vol. 8, no. 10, 2012.

143. I. Kaspy, E. Rotem, N. Weiss, I. Ronin, N. Q. Balaban, and G. Glaser, “HipA-mediated antibiotic persistence via phosphorylation of the glutamyl-tRNA-synthetase,” *Nat. Commun.*, vol. 4, no. 1, p. 3001, Dec. 2013.

144. E. Germain, D. Castro-Roa, N. Zenkin, and K. Gerdes, “Molecular mechanism of bacterial persistence by HipA,” *Mol. Cell*, vol. 52, no. 2, pp. 248–254, Oct. 2013.

145. Z. Baharoglu and D. Mazel, “SOS, the formidable strategy of bacteria against aggressions,” *FEMS Microbiol. Rev.*, vol. 38, no. 6, pp. 1126–45, Nov. 2014.

146. Goneau LW, Yeoh NS, MacDonald KW, Cadieux PA, Burton JP, Razvi H, Reid G. “Selective target inactivation rather than global metabolic dormancy causes antibiotic tolerance in uropathogens,” *Antimicrob. Agents Chemother.*, vol. 58, no. 4, pp. 2089–2097, Apr. 2014.

147. Bernier, S.P., Lebeaux, D., DeFrancesco, A.S., Valomon, A., Soubigou, G., Coppée, J.Y., Ghigo, J.M., and Beloin, C. “Starvation, together with the SOS response, mediates high biofilm-specific tolerance to the fluoroquinolone ofloxacin,” *PLoS Genet.*, vol. 9, no. 1, p. e1003144, Jan. 2013.

148. Wu N, He L, Cui P, Wang W, Yuan Y, Liu S, Xu T, Zhang S, Wu J, Zhang W, Zhang Y. “Ranking of persister genes in the same *Escherichia coli* genetic background demonstrates varying importance of individual persister genes in tolerance to different antibiotics,” *Front. Microbiol.*, vol. 6, no. SEP, Sep. 2015.

149. K. G. Völzing and M. P. Brynildsen, “Stationary-phase persisters to ofloxacin sustain DNA damage and require repair systems only during recovery,” *MBio*, vol. 6, no. 5, pp. e00731-15, Sep. 2015.

150. Ejim L, Farha MA, Falconer SB, Wildenhain J, Coombes BK, Tyers M, Brown ED, Wright GD. "Combinations of antibiotics and nonantibiotic drugs enhance antimicrobial efficacy," *Nature chemical biology*, vol. 7, no. 6, pp. 348–50, 2011.

151. P. A. Masters, T. A. O'Bryan, J. Zurlo, D. Q. Miller, and N. Joshi, "Trimethoprim-sulfamethoxazole revisited," *Arch. Intern. Med.*, vol. 163, no. 4, pp. 402–10, Feb. 2003.

152. R. J. Worthington and C. Melander, "Overcoming resistance to β-Lactam antibiotics," *The Journal of Organic Chemistry*, vol. 78, no. 9, pp. 4207–4213, Mar. 2013.

153. L. Kalan and G. D. Wright, "Antibiotic adjuvants: multicomponent anti-infective strategies," *Expert reviews in molecular medicine*, vol. 13, p. e5, 2011.

154. AD Pagliotto, KR Caleffi-Ferracioli, MA Lopes, VP Baldin, CQ Leite, FR Pavan, RB Scodro, VL Siqueira, RF Cardoso, "Anti-Mycobacterium tuberculosis activity of antituberculosis drugs and amoxicillin/clavulanate combination," *Journal of microbiology, immunology, and infection* vol. 49, no. 6, pp. 980–983, 2016.

155. T. G. Winstanley and J. G. Hastings, "Penicillin-aminoglycoside synergy and post-antibiotic effect for enterococci.," *J. Antimicrob. Chemother.*, vol. 23, no. 2, pp. 189–99, Feb. 1989.

156. A. Leigh, "Augmentin (amoxycillin and clavulanic acid) in the treatment of urinary tract infections," *Scott. Med. J.*, vol. 27 Spec No., pp. S28-34, 1982.

157. T T. Kish, "New antibiotics in development target highly resistant Gram-negative organisms," *P & T : a peer-reviewed journal for formulary management*, vol. 43, no. 2, pp. 116–120, 2018.

158. King AM, Reid-Yu SA, Wang W, King DT, De Pascale G, Strynadka NC, Walsh TR, Coombes BK, Wright GD., "Aspergillomarasmine A overcomes metallo-β-lactamase antibiotic resistance," *Nature*, vol. 510, no. 7506, pp. 503–6, 2014.

159. A. M. Kalle and A. Rizvi, "Inhibition of bacterial multidrug resistance by celecoxib, a cyclooxygenase-2 inhibitor," *Antimicrob. Agents Chemother.*, vol. 55, no. 1, pp. 439–442, Jan. 2011.

160. T. Bhattacharyya, A. Sharma, J. Akhter, and R. Pathania, “The small molecule IITR08027 restores the antibacterial activity of fluoroquinolones against multidrug-resistant *Acinetobacter baumannii* by efflux inhibition,” *Int. J. Antimicrob. Agents*, vol. 50, no. 2, pp. 219–226, 2017.

161. Corbett D, Wise A, Langley T, Skinner K, Trimby E, Birchall S, Dorali A, Sandiford S, Williams J, Warn P, Vaara M, Lister T. “Potentiation of antibiotic activity by a novel cationic peptide: Potency and spectrum of activity of SPR741,” *Antimicrob. Agents Chemother.*, e00200-17.vol. 61, no. 8, Aug. 2017.

162. Lenhard, Bulman, Tsuji, and Kaye, “Shifting Gears: The Future of polymyxin antibiotics,” *Antibiotics*, vol. 8, no. 2, p. 42, Apr. 2019.

163. C. T. O’Loughlin, L. C. Miller, A. Siryaporn, K. Drescher, M. F. Semmelhack, and B. L. Bassler, “A quorum-sensing inhibitor blocks *Pseudomonas aeruginosa* virulence and biofilm formation,” *Proc. Natl. Acad. Sci.*, vol. 110, no. 44, pp. 17981–17986, Oct. 2013.

164. J. Y. Chow, Y. Yang, S. B. Tay, K. L. Chua, and W. S. Yew, “Disruption of biofilm formation by the human pathogen *Acinetobacter baumannii* using engineered quorum-quenching lactonases,” *Antimicrob. Agents Chemother.*, vol. 58, no. 3, pp. 1802–1805, Mar. 2014.

165. J. J. Martinez-Irujo, M. L. Villahermosa, E. Alberdi, and E. Santiago, “A checkerboard method to evaluate interactions between drugs.,” *Biochem. Pharmacol.*, vol. 51, no. 5, pp. 635–44, Mar. 1996.

166. M. M. Sopirala *et al.*, “Synergy Testing by Etest, microdilution checkerboard and time-kill methods for Pan-Drug-Resistant *Acinetobacter baumannii*,” *Antimicrob. Agents Chemother.*, vol. 54, no. 11, pp. 4678–4683, 2010.

167. Saginur R, Stdenis M, Ferris W, Aaron SD, Chan F, Lee C, Ramotar K “Multiple combination bactericidal testing of staphylococcal biofilms from implant-associated infections,” *Antimicrob. Agents Chemother.*, vol. 50, no. 1, pp. 55–61, Jan. 2006.

168. H. Saini, S. Chhibber, and K. Harjai, “Azithromycin and ciprofloxacin: a possible synergistic combination against *Pseudomonas aeruginosa* biofilm-associated urinary tract infections.,” *Int. J. Antimicrob. Agents*, vol. 45, no. 4, pp. 359–67, Apr. 2015.

169. O. Ciofu, E. Rojo-Molinero, M. D. Macià, and A. Oliver, "Antibiotic treatment of biofilm infections," *APMIS*, vol. 125, no. 4, pp. 304–319, Apr. 2017.

170. K. A. Hammer, C. F. Carson, and T. V. Riley, "Antimicrobial activity of essential oils and other plant extracts," *J. Appl. Microbiol.*, vol. 86, no. 6, pp. 985–990, Jun. 1999.

171. F. Nazzaro, F. Fratianni, L. De Martino, R. Coppola, and V. De Feo, "Effect of essential oils on pathogenic bacteria.," *Pharmaceuticals (Basel).*, vol. 6, no. 12, pp. 1451–74, Nov. 2013.

172. Nostro, A., Roccaro, A.S., Bisignano, G., Marino, A., Cannatelli, M.A., Pizzimenti, F.C., Cioni, P.L., Procopio, F., and Blanco, A.R. "Effects of oregano, carvacrol and thymol on *Staphylococcus aureus* and *Staphylococcus epidermidis* biofilms," *J. Med. Microbiol.*, vol. 56, no. 4, pp. 519–523, Apr. 2007.

173. F. L. Coelho and M. O. Pereira, "Exploring new treatment strategies for *Pseudomonas aeruginosa* biofilm infections based on plant essential oils," *Formatex*, pp. 83–89, 2013.

174. I. C. S. Cirino, S. M. P. Menezes-Silva, H. T. D. Silva, E. L. de Souza, and J. P. Siqueira-Júnior, "The essential oil from *Origanum vulgare* L. and its individual constituents carvacrol and thymol enhance the effect of tetracycline against *Staphylococcus aureus*," *Chemotherapy*, vol. 60, no. 5–6, pp. 290–3, 2014.

175. Martinez-Gutierrez, F., Boegli, L., Agostinho, A., Sánchez, E.M., Bach, H., Ruiz, F., and James, G. "Anti-biofilm activity of silver nanoparticles against different microorganisms," *Biofouling*, vol. 29, no. 6, pp. 651–660, Jul. 2013.

176. J.-H. Lee, Y.-G. Kim, M. H. Cho, and J. Lee, "ZnO nanoparticles inhibit *Pseudomonas aeruginosa* biofilm formation and virulence factor production," *Microbiol. Res.*, vol. 169, no. 12, pp. 888–896, Dec. 2014.

177. Lambadi, P.R., Sharma, T.K., Kumar, P., Vasnani, P., Thalluri, S.M., Bisht, N., Pathania, R., and Navani, N.K. "Facile biofunctionalization of silver nanoparticles for enhanced antibacterial properties, endotoxin removal, and biofilm control," *Int. J. Nanomedicine*, 10, pp.2155–2171.Mar. 2015.

178. S. Uroz, Y. Dessaux, and P. Oger, "Quorum sensing and quorum quenching: The yin and yang of bacterial communication," *ChemBioChem*, vol. 10, no. 2, pp. 205–216, Jan. 2009.

179. Paczkowski JE, Mukherjee S, McCready AR, Cong JP, Aquino CJ, Kim H, Henke BR, Smith CD, Bassler BL "Flavonoids suppress *Pseudomonas aeruginosa* virulence through allosteric inhibition of quorum-sensing receptors.," *J. Biol. Chem.*, vol. 292, no. 10, pp. 4064–4076, Mar. 2017.

180. T. Chen, F. Li, and B.-S. Chen, "Cross-talks of sensory transcription networks in response to various environmental stresses.," *Interdiscip. Sci.*, vol. 1, no. 1, pp. 46–54, Mar. 2009.

181. M. Korem, Y. Gov, M. D. Kiran, and N. Balaban, "Transcriptional profiling of target of RNAIII-activating protein, a master regulator of staphylococcal virulence.," *Infect. Immun.*, vol. 73, no. 10, pp. 6220–8, Oct. 2005.

182. Pompilio, A., Scocchi, M., Pomponio, S., Guida, F., Di Primio, A., Fiscarelli, E., Gennaro, R., and Di Bonaventura, G. "Antibacterial and anti-biofilm effects of cathelicidin peptides against pathogens isolated from cystic fibrosis patients," *Peptides*, vol. 32, no. 9, pp. 1807–1814, Sep. 2011.

183. S. Dosler and E. Mataraci, "In vitro pharmacokinetics of antimicrobial cationic peptides alone and in combination with antibiotics against methicillin resistant *Staphylococcus aureus* biofilms," *Peptides*, vol. 49, pp. 53–58, Nov. 2013.

184. T. K. Lu and J. J. Collins, "Dispersing biofilms with engineered enzymatic bacteriophage," *Proc. Natl. Acad. Sci.*, vol. 104, no. 27, pp. 11197–11202, Jul. 2007.

185. D. Pires, L. Melo, D. Vilas Boas, S. Sillankorva, and J. Azeredo, "Phage therapy as an alternative or complementary strategy to prevent and control biofilm-related infections," *Curr. Opin. Microbiol.*, vol. 39, pp. 48–56, Oct. 2017.

186. H. Koo, R. N. Allan, R. P. Howlin, P. Stoodley, and L. Hall-Stoodley, "Targeting microbial biofilms: current and prospective therapeutic strategies," *Nat. Rev. Microbiol.*, vol. 15, no. 12, pp. 740–755, Sep. 2017.

187. V. Singh, N. Verma, B. Banerjee, K. Vibha, S. Haque, and C. K. M. Tripathi, "Enzymatic degradation of bacterial biofilms using *Aspergillus clavatus* MTCC 1323," *Microbiology*, vol. 84, no. 1, pp. 59–64, Jan. 2015.

188. [1] E. A. Izano, H. Wang, C. Ragunath, N. Ramasubbu, and J. B. Kaplan, "Detachment and killing of *Aggregatibacter actinomycetemcomitans* biofilms by dispersin B and SDS," *J. Dent. Res.*, vol. 86, no. 7, pp. 618–622, Jul. 2007.

189. B. J. Kalpana, S. Aarthy, and S. K. Pandian, "Antibiofilm activity of α-Amylase from *Bacillus subtilis* S8-18 against biofilm forming human bacterial pathogens," *Appl. Biochem. Biotechnol.*, vol. 167, no. 6, pp. 1778–1794, Jul. 2012.

190. Spaulding CN, Klein RD, Ruer S, Kau AL, Schreiber HL, Cusumano ZT, Dodson KW, Pinkner JS, Fremont DH, Janetka JW, Remaut H, Gordon JI, Hultgren SJ. "Selective depletion of uropathogenic *E. coli* from the gut by a FimH antagonist," *Nature*, vol. 546, no. 7659, p. 528, Jun. 2017.

191. Cusumano, C.K., Pinkner, J.S., Han, Z., Greene, S.E., Ford, B.A., Crowley, J.R., Henderson, J.P., Janetka, J.W., and Hultgren, S.J. "Treatment and prevention of urinary tract infection with orally active FimH inhibitors," *Sci. Transl. Med.*, vol. 3, no. 109, pp. 109ra115-109ra115, Nov. 2011.

192. Cegelski L, Pinkner JS, Hammer ND, Cusumano CK, Hung CS, Chorell E, Aberg V, Walker JN, Seed PC, Almqvist F, Chapman MR, Hultgren SJ "Small-molecule inhibitors target *Escherichia coli* amyloid biogenesis and biofilm formation.," *Nat. Chem. Biol.*, vol. 5, no. 12, pp. 913–9, Dec. 2009.

193. Liebens V, Defraine V, Knapen W, Swings T, Beullens S, Corbau R, Marchand A, Chaltin P, Fauvart M, Michiels J. "Identification of 1-((2,4-Dichlorophenethyl)Amino)-3-Phenoxypropan-2-ol, a novel antibacterial compound active against persisters of *Pseudomonas aeruginosa*," *Antimicrob. Agents Chemother.*, vol. 61, no. 9, 2017.

194. Defraine V, Verstraete L, Van Bambeke F, Anantharajah A, Townsend EM, Ramage G, Corbau R, Marchand A, Chaltin P, Fauvart M, Michiels J "Antibacterial activity of 1-[(2,4-Dichlorophenethyl)amino]-3-Phenoxypropan-2-ol against antibiotic-resistant strains of diverse bacterial pathogens, biofilms and in pre-clinical infection models.," *Front. Microbiol.*, vol. 8, p. 2585, 2017.

195. J. Feng, S. Zhang, W. Shi, N. Zubcevik, J. Miklossy, and Y. Zhang, "Selective essential oils from spice or culinary herbs have high activity against stationary phase and biofilm *Borrelia burgdorferi*," *Front. Med.*, vol. 4, p. 169, 2017.

196. Defraine V, Schuermans J, Grymonprez B, Govers SK, Aertsen A, Fauvart M, Michiels J, Lavigne R, Briers Y "Efficacy of artilysin art-175 against resistant and persistent *Acinetobacter baumannii*," *Antimicrob. Agents Chemother.*, vol. 60, no. 6, pp. 3480–3488, Jun. 2016.

197. Briers Y, Walmagh M, Grymonprez B, Biebl M, Pirnay JP, Defraine V, Michiels J, Cenens W, Aertsen A, Miller S, Lavigne R. "Art-175 is a highly efficient antibacterial against multidrug-resistant strains and persisters of *Pseudomonas aeruginosa," Antimicrob. Agents Chemother.*, vol. 58, no. 7, pp. 3774–84, Jul. 2014.

198. Kim JS, Heo P, Yang TJ, Lee KS, Cho DH, Kim BT, Suh JH, Lim HJ, Shin D, Kim SK, Kweon DH. "Selective killing of bacterial persisters by a single chemical compound without affecting normal antibiotic-sensitive cells," *Antimicrob. Agents Chemother.*, vol. 55, no. 11, pp. 5380–5383, Nov. 2011.

199. C. N. H. Marques, A. Morozov, P. Planzos, and H. M. Zelaya, "The fatty acid signaling molecule cis-2-decenoic acid increases metabolic activity and reverts persister cells to an antimicrobial-susceptible state," *Appl. Environ. Microbiol.*, vol. 80, no. 22, pp. 6976–6991, 2014.

200. David Lebeaux, Ashwini Chauhan, Sylvie Létoffé, Frédéric Fischer, Hilde de Reuse, Christophe Beloin, Jean-Marc Ghigo, "pH-mediated potentiation of aminoglycosides kills bacterial persisters and eradicates in vivo biofilms," *J. Infect. Dis.*, vol. 210, no. 9, pp. 1357–1366, Nov. 2014.

201. Duan, X., Huang, X., Wang, X., Yan, S., Guo, S., Abdalla, A.E., Huang, C., and Xie, J. "L-Serine potentiates fluoroquinolone activity against *Escherichia coli* by enhancing endogenous reactive oxygen species production," *J. Antimicrob. Chemother.*, vol. 71, no. 8, pp. 2192–2199, Aug. 2016.

202. Y. Shan, D. Lazinski, S. Rowe, A. Camilli, and K. Lewis, "Genetic basis of persister tolerance to aminoglycosides in *Escherichia coli*," *MBio*, vol. 6, no. 2, Apr. 2015.

203. N. Barraud, A. Buson, W. Jarolimek, and S. A. Rice, "Mannitol enhances antibiotic sensitivity of persister bacteria in *Pseudomonas aeruginosa* biofilms," *PLoS One*, vol. 8, no. 12, p. e84220, Dec. 2013.

204. J. RubenMorones-Ramirez, J. A. Winkler, C. S. Spina, and J. J. Collins, “Silver enhances antibiotic activity against gram-negative bacteria,” *Sci. Transl. Med.*, vol. 5, no. 190, 2013.

205. Adams KN, Takaki K, Connolly LE, Wiedenhoft H, Winglee K, Humbert O, Edelstein PH, Cosma CL, Ramakrishnan L. “Drug tolerance in replicating mycobacteria mediated by a macrophage-induced efflux mechanism.,” *Cell*, vol. 145, no. 1, pp. 39–53, Apr. 2011.

206. J. Feng, P. G. Auwaerter, and Y. Zhang, “Drug combinations against *Borrelia burgdorferi* persisters *In Vitro*: eradication achieved by using daptomycin, cefoperazone and doxycycline,” *PLoS One*, vol. 10, no. 3, p. e0117207, Mar. 2015.

207. Cui P, Niu H, Shi W, Zhang S, Zhang H, Margolick J, Zhang W, Zhang Y. “Disruption of membrane by colistin kills uropathogenic *Escherichia coli* persisters and enhances killing of other antibiotics.,” *Antimicrob. Agents Chemother.*, vol. 60, no. 11, pp. 6867–6871, Nov. 2016.

208. E. S. Chung and K. S. Ko, “Eradication of persister cells of *Acinetobacter baumannii* through combination of colistin and amikacin antibiotics,” *J. Antimicrob. Chemother.*, vol. 74, no. 5, pp. 1277–1283, 2019.

209. Starkey M, Lepine F, Maura D, Bandyopadhaya A, Lesic B, He J, Kitao T, Righi V, Milot S, Tzika A, Rahme L. “Identification of anti-virulence compounds that disrupt quorum-sensing regulated acute and persistent pathogenicity,” *PLoS Pathog.*, vol. 10, no. 8, p. e1004321, Aug. 2014.

210. Allegretta G, Maurer CK, Eberhard J, Maura D, Hartmann RW, Rahme L, Empting M. “In-depth profiling of MvfR-regulated small molecules in *Pseudomonas aeruginosa* after Quorum Sensing inhibitor treatment,” *Front. Microbiol.*, vol. 8, May 2017.

211. Dahl JU, Gray MJ, Bazopoulou D, Beaufay F, Lempart J, Koenigsknecht MJ, Wang Y, Baker JR, Hasler WL, Young VB, Sun D, Jakob U. “The anti-inflammatory drug mesalamine targets bacterial polyphosphate accumulation,” *Nat. Microbiol.*, vol. 2, no. 4, p. 16267, Apr. 2017.

212. E. D. Brown and G. D. Wright, “Antibacterial drug discovery in the resistance era.,” *Nature*, vol. 529, no. 7586, pp. 336–43, Jan. 2016.

213. R. Tommasi, D. G. Brown, G. K. Walkup, J. I. Manchester, and A. A. Miller, "ESKAPEing the labyrinth of antibacterial discovery.," *Nat. Rev. Drug Discov.*, vol. 14, no. 8, pp. 529–42, 2015.

214. M. A. Farha and E. D. Brown, "Unconventional screening approaches for antibiotic discovery.," *Ann. N. Y. Acad. Sci.*, vol. 1354, pp. 54–66, Sep. 2015.

215. D. Schnappinger, "Genetic approaches to facilitate antibacterial drug development," *Cold Spring Harb. Perspect. Med.*, vol. 5, no. 7, p. a021139, Jul. 2015.

216. J. M. Stokes, J. H. Davis, C. S. Mangat, J. R. Williamson, and E. D. Brown, "Discovery of a small molecule that inhibits bacterial ribosome biogenesis.," *Elife*, vol. 3, p. e03574, Sep. 2014.

217. P. L. Taylor, L. Rossi, G. De Pascale, and G. D. Wright, "A forward chemical screen identifies antibiotic adjuvants in *Escherichia coli*," *ACS Chem. Biol.*, vol. 7, no. 9, pp. 1547–1555, 2012.

218. R. Guimerà and M. Sales-Pardo, "A network inference method for large-scale unsupervised identification of novel drug-drug interactions," *PLoS Comput. Biol.*, vol. 9, no. 12, 2013.

219. Hartkoorn RC, Sala C, Neres J, Pojer F, Magnet S, Mukherjee R, Uplekar S, Boy-Röttger S, Altmann KH, Cole ST. "Towards a new tuberculosis drug: Pyridomycin - nature's isoniazid," *EMBO Mol. Med.*, vol. 4, no. 10, pp. 1032–1042, Oct. 2012.

220. Lomenick B, Hao R, Jonai N, Chin RM, Aghajan M, Warburton S, Wang J, Wu RP, Gomez F, Loo JA, Wohlschlegel JA, Vondriska TM, Pelletier J, Herschman HR, Clardy J, Clarke CF, Huang J. "Target identification using drug affinity responsive target stability (DARTS)," *Proc. Natl. Acad. Sci.*, vol. 106, no. 51, pp. 21984–21989, Dec. 2009.

221. P. Canepari, M. Boaretti, M. Del Mar Lleo, and G. Satta, "Lipoteichoic acid as a new target for activity of antibiotics: Mode of action of daptomycin (LY146032)," *Antimicrob. Agents Chemother.*, vol. 34, no. 6, pp. 1220–1226, Jun. 1990.

222. Thangamani S, Mohammad H, Abushahba MF, Sobreira TJ, Hedrick VE, Paul LN, Seleem MN. "Antibacterial activity and mechanism of action of auranofin against multi-drug resistant bacterial pathogens," *Sci. Rep.*, vol. 6, no. 1, p. 22571, Mar. 2016.

223. Htut Htut Htoo, Lauren Brumage, Vorrapon Chaikeeratisak, Hannah Tsunemoto, Joseph Sugie, Chanwit Tribuddharat, Joe Pogliano, Poochit Nonejuie "Bacterial cytological profiling as a tool to study mechanisms of action of antibiotics that are active against *Acinetobacter baumannii*," *Antimicrob. Agents Chemother.*, vol. 63, no. 4, Feb. 2019.

224. A. C. Palmer and R. Kishony, "Opposing effects of target overexpression reveal drug mechanisms," *Nat. Commun.*, vol. 5, no. 1, p. 4296, Sep. 2014.

225. Baba T, Ara T, Hasegawa M, Takai Y, Okumura Y, Baba M, Datsenko KA, Tomita M, Wanner BL, Mori H. "Construction of *Escherichia coli* K-12 in-frame, single-gene knockout mutants: the Keio collection," *Mol. Syst. Biol.*, vol. 2, p. 2006.0008, Feb. 2006.

226. S. D. Patil, R. Sharma, S. Srivastava, N. K. Navani, and R. Pathania, "Downregulation of *yidC* in *Escherichia coli* by antisense RNA expression results in sensitization to antibacterial essential oils eugenol and carvacrol.," *PLoS One*, vol. 8, no. 3, p. e57370, 2013.

227. T. Elad, H. Bin Seo, S. Belkin, and M. B. Gu, "High-throughput prescreening of pharmaceuticals using a genome-wide bacterial bioreporter array," *Biosens. Bioelectron.*, vol. 68, pp. 699–704, Jun. 2015.

228. Pasquina L, Santa Maria JP Jr, McKay Wood B, Moussa SH, Matano LM, Santiago M, Martin SE, Lee W, Meredith TC, Walker S. "A synthetic lethal approach for compound and target identification in *Staphylococcus aureus*," *Nat. Chem. Biol.*, vol. 12, no. 1, pp. 40–45, Jan. 2016.

229. Gupta, V.K., Gaur, R., Sharma, A., Akther, J., Saini, M., Bhakuni, R.S., and Pathania, R. "A novel bi-functional chalcone inhibits multi-drug resistant *Staphylococcus aureus* and potentiates the activity of fluoroquinolones," *Bioorg. Chem.*, vol. 83, pp. 214–225, Mar. 2019.

230. J.-H. Zhang, T. D. Y. Chung, and K. R. Oldenburg, "A simple statistical parameter for use in evaluation and validation of high throughput screening assays," *J. Biomol. Screen.*, vol. 4, no. 2, pp. 67–73, 1999.

231. M. R. Ghadir, A. Shafaghi, A. Iranikhah, A. Pakdin, F. Joukar, and F. Mansour-

Ghanaei, “Furazolidone, amoxicillin and omeprazole with or without bismuth for eradication of *Helicobacter pylori* in peptic ulcer disease,” *Turkish J. Gastroenterol. Off. J. Turkish Soc. Gastroenterol.*, vol. 22, no. 1, pp. 1–5, 2011.

232. K. Gupta *et al.*, “International clinical practice guidelines for the treatment of acute uncomplicated cystitis and pyelonephritis in women: A 2010 update by the Infectious Diseases Society of America and the European Society for Microbiology and Infectious Diseases,” *Clin. Infect. Dis.*, vol. 52, no. 5, pp. e103–e120, Mar. 2011.

233. Theuretzbacher, U., Van Bambeke, F.V., Cantón, R., Giske, C.G., Mouton, J.W., Nation, R.L., Paul, M., Turnidge, J.D., and Kahlmeter, G. “Reviving old antibiotics,” *J. Antimicrob. Chemother.*, vol. 70, no. 8, pp. 2177–2181, 2015.

234. S. C. Valentine, D. Contreras, S. Tan, L. J. Real, S. Chu, and H. H. Xu, “Phenotypic and molecular characterization of *Acinetobacter baumannii* clinical isolates from nosocomial outbreaks in Los Angeles county, California,” *J. Clin. Microbiol.*, vol. 46, no. 8, pp. 2499–2507, 2008.

235. Khalil IA, Troeger C, Blacker BF, Rao PC, Brown A, Atherly DE, Brewer TG, Engmann CM, Houpt ER, Kang G, Kotloff KL, Levine MM, Luby SP, MacLennan CA, Pan WK, Pavlinac PB, Platts-Mills JA, Qadri F, Riddle MS, Ryan ET, Shoultz DA, Steele AD, Walson JL, Sanders JW, Mokdad AH, Murray CJL, Hay SI, Reiner RC Jr “Morbidity and mortality due to shigella and enterotoxigenic *Escherichia coli* diarrhoea: the Global Burden of Disease Study 1990–2016,” *Lancet Infect. Dis.*, vol. 18, no. 11, pp. 1229–1240, Nov. 2018.

236. I. Brook, H. M. Wexler, and E. J. C. Goldstein, “Antianaerobic antimicrobials: spectrum and susceptibility testing,” *Clin. Microbiol. Rev.*, vol. 26, no. 3, pp. 526–546, Jul. 2013.

237. Matthew A. Wikler, *Development of in vitro susceptibility testing criteria and quality control parameters*, 5th ed. 2018.

238. F. M. MacKenzie and I. M. Gould, “The post-antibiotic effect,” *J. Antimicrob. Chemother.*, vol. 32, no. 4, pp. 519–537, 1993.

239. D. Lebeaux, J.-M. Ghigo, and C. Beloin, “Biofilm-related infections: bridging the gap between clinical management and fundamental aspects of recalcitrance toward antibiotics.,” *Microbiol. Mol. Biol. Rev.*, vol. 78, no. 3, pp. 510–43, Sep. 2014.

240. C. T. M. Mascio, J. D. Alder, and J. A. Silverman, “Bactericidal action of daptomycin against stationary-phase and nondividing *Staphylococcus aureus* cells,” *Antimicrob. Agents Chemother.*, vol. 51, no. 12, pp. 4255–4260, 2007.

241. E. E. Obaseiki-Ebor, “Enhanced *Escherichia coli* susceptibility to nitrofurantoin by EDTA and multiple aminoglycoside antibiotics resistance mutation,” *Chemotherapy*, vol. 30, no. 2, pp. 88–91, 1984.

242. P. Yeh, A. I. Tschumi, and R. Kishony, “Functional classification of drugs by properties of their pairwise interactions,” *Nat. Genet.*, vol. 38, no. 4, pp. 489–494, Apr. 2006.

243. Sisson G, Goodwin A, Raudonikiene A, Hughes NJ, Mukhopadhyay AK, Berg DE, Hoffman PS “Enzymes associated with reductive activation and action of nitazoxanide, nitrofurans, and metronidazole in *Helicobacter pylori*,” *Antimicrob. Agents Chemother.*, vol. 46, no. 7, pp. 2116–23, Jul. 2002.

244. Whiteway J, Koziarz P, Veall J, Sandhu N, Kumar P, Hoecher B, Lambert IB. “Oxygen-insensitive nitroreductases: Analysis of the roles of nfsA and nfsB in development of resistance to 5-Nitrofuran derivatives in *Escherichia coli*,” *J. Bacteriol.*, vol. 180, no. 21, pp. 5529–5539, 1998.

245. L. Sandegren, A. Lindqvist, G. Kahlmeter, and D. I. Andersson, “Nitrofurantoin resistance mechanism and fitness cost in *Escherichia coli*,” *J. Antimicrob. Chemother.*, vol. 62, no. 3, pp. 495–503, 2008.

246. M. S. Chadfield and M. H. Hinton, “*In vitro* activity of nitrofuran derivatives on growth and morphology of *Salmonella enterica* serotype Enteritidis,” *J. Appl. Microbiol.*, vol. 96, no. 5, pp. 1002–1012, 2004.

247. K. N. Kreuzer, “DNA damage responses in prokaryotes: regulating gene expression, modulating growth patterns, and manipulating replication forks.,” *Cold Spring Harb. Perspect. Biol.*, vol. 5, no. 11, p. a012674, Nov. 2013.

248. S. T. Jenkins and P. M. Bennett, “Effect of mutations in deoxyribonucleic acid repair pathways on the sensitivity of *Escherichia coli* K-12 strains to nitrofurantoin,” *J. Bacteriol.*, vol. 125, no. 3, pp. 1214–1216, 1976.

249. K. R. Ona, C. T. Courcelle, and J. Courcelle, “Nucleotide excision repair Is a predominant mechanism for processing nitrofurazone-induced DNA damage in *Escherichia coli*,” *J. Bacteriol.*, vol. 191, no. 15, pp. 4959–4965, 2009.

250. H. Strahl and L. W. Hamoen, “Membrane potential is important for bacterial cell division,” *Proc. Natl. Acad. Sci.*, vol. 107, no. 27, pp. 12281–12286, Jul. 2010.

251. J. Cambridge, A. Blinkova, D. Magnan, D. Bates, and J. R. Walker, “A replication-inhibited unsegregated nucleoid at mid-cell blocks Z-ring formation and cell division independently of SOS and the SlmA nucleoid occlusion protein in *Escherichia coli,” J. Bacteriol.*, vol. 196, no. 1, pp. 36–49, 2014.

252. C. Ortiz, P. Natale, L. Cueto, and M. Vicente, “The keepers of the ring: regulators of FtsZ assembly,” *FEMS Microbiol. Rev.*, vol. 40, no. 1, pp. 57–67, 2016.

253. J. M. Boberek, J. Stach, and L. Good, “Genetic evidence for inhibition of bacterial division protein FtsZ by Berberine,” *PLoS One*, vol. 5, no. 10, p. e13745, 2010.

254. F. M. Kahan, J. S. Kahan, P. J. Cassidy, and H. Kropp, “The mechanism of action of fosfomycin (phosphonomycin),” *Ann. N. Y. Acad. Sci.*, vol. 235, no. 1, pp. 364–386, 1974.

255. Dwyer DJ, Belenky PA, Yang JH, MacDonald IC, Martell JD, Takahashi N, Chan CT, Lobritz MA, Braff D, Schwarz EG, Ye JD, Pati M, Vercruysse M, Ralifo PS, Allison KR, Khalil AS, Ting AY, Walker GC, Collins JJ .“Antibiotics induce redox-related physiological alterations as part of their lethality,” *Proc. Natl. Acad. Sci. U. S. A.*, vol. 111, no. 20, pp. E2100-2109, 2014.

256. Miyamoto Y, Kalisiak J, Korthals K, Lauwaet T, Cheung DY, Lozano R, Cobo ER, Upcroft P, Upcroft JA, Berg DE, Gillin FD, Fokin VV, Sharpless KB, Eckmann L. “Expanded therapeutic potential in activity space of next-generation 5-nitroimidazole antimicrobials with broad structural diversity,” *Proc. Natl. Acad. Sci.*, vol. 110, no. 43, pp. 17564–17569, Oct. 2013.

257. L. E. Fleck, E. J. North, R. E. Lee, L. R. Mulcahy, G. Casadei, and K. Lewis, "A screen for and validation of prodrug antimicrobials," *Antimicrob. Agents Chemother.*, vol. 58, no. 3, pp. 1410–1419, 2014.

258. Stover CK, Warrener P, VanDevanter DR, Sherman DR, Arain TM, Langhorne MH, Anderson SW, Towell JA, Yuan Y, McMurray DN, Kreiswirth BN, Barry CE, Baker WR. "A small-molecule nitroimidazopyran drug candidate for the treatment of tuberculosis," *Nature*, vol. 405, no. 6789, pp. 962–966, Jun. 2000.

259. RP Tangallapally , R Yendapally, RE Lee, K Hevener K, VC Jones , AJ Lenaerts MR McNeil , Y Wang ,S Franzblau S, RE Lee RE. "Synthesis and evaluation of nitrofuranylamides as novel antituberculosis agents," *Journal of Medicinal Chemistry*, vol. 47, no. 21, pp. 5276–5283, Oct. 2004

260. A. Huttner, E. M. Verhaegh, S. Harbarth, A. E. Muller, U. Theuretzbacher, and J. W. Mouton, "Nitrofurantoin revisited: a systematic review and meta-analysis of controlled trials," *J. Antimicrob. Chemother.*, vol. 70, no. 9, pp. 2456–2464, Sep. 2015.

261. C. Lu and D. R. McCalla, "Action of some nitrofuran derivatives on glucose metabolism, ATP levels, and macromolecule synthesis in *Escherichia coli*," *Can. J. Microbiol.*, vol. 24, no. 6, pp. 650–657, 1978.

262. "M11-A6-Methods for Antimicrobial Susceptibility Testing of Anaerobic Bacteria; Approved Standard—Sixth Edition," p. 60.

263. G. A. Pankuch, M. R. Jacobs, and P. C. Appelbaum, "Postantibiotic effects of gatifloxacin against Gram-positive and -negative organisms," *Antimicrob. Agents Chemother.*, vol. 43, no. 10, pp. 2574–2575, 1999.

264. Charrier C, Salisbury AM, Savage VJ, Duffy T, Moyo E, Chaffer-Malam N, Ooi N, Newman R, Cheung J, Metzger R, McGarry D, Pichowicz M, Sigerson R, Cooper IR, Nelson G, Butler HS, Craighead M, Ratcliffe AJ, Best SA, Stokes NR. "Novel bacterial topoisomerase inhibitors with potent broad-spectrum activity against drug-resistant bacteria," *Antimicrob. Agents Chemother.*, vol. 61, no. 5, pp. e02100-16, 2017.

265. N. Asthana, S. P. Yadav, and J. K. Ghosh, "Dissection of antibacterial and toxic activity of melittin: a leucine zipper motif plays a crucial role in determining its hemolytic

activity but not antibacterial activity.," *J. Biol. Chem.*, vol. 279, no. 53, pp. 55042–50, Dec. 2004.

266. Otta DA, de Araújo FF, de Rezende VB, Souza-Fagundes EM, Elói-Santos SM, Costa-Silva MF, Santos RA, Costa HA, Siqueira-Neto JL, Martins-Filho OA, Teixeira-Carvalho A. "Identification ofaAnti-*Trypanosoma* cruzi lead compounds with putative immunomodulatory activity," *Antimicrobial agents and chemotherapy*, vol. 62, no. 4, pp. e01834-17, 2018.

267. A. Böyum, "Isolation of mononuclear cells and granulocytes from human blood. Isolation of monuclear cells by one centrifugation, and of granulocytes by combining centrifugation and sedimentation at 1 g.," *Scand. J. Clin. Lab. Invest. Suppl.*, vol. 97, pp. 77–89, 1968.

268. C. Ghosh, P. Sarkar, S. Samaddar, D. S. S. M. Uppu, and J. Haldar, "L-Lysine based lipidated biphenyls as agents with anti-biofilm and anti-inflammatory properties that also inhibit intracellular bacteria," *Chem. Commun.*, vol. 53, no. 60, pp. 8427–8430, 2017.

269. J. Hong, J. Hu, and F. Ke, "Experimental induction of bacterial resistance to the antimicrobial peptide Tachyplesin I and investigation of the resistance mechanisms.," *Antimicrob. Agents Chemother.*, vol. 60, no. 10, pp. 6067–75, 2016.

270. F. Rohwer and F. Azam, "Detection of DNA damage in prokaryotes by Terminal Deoxyribonucleotide Transferase-Mediated dUTP Nick End Labeling," *Appl. Environ. Microbiol.*, vol. 66, no. 3, pp. 1001–1006, 2000.

271. P. A. Levin, "6 Light microscopy techniques for bacterial cell biology," in *Methods in Microbiology*, vol. 31, Academic Press, pp. 115–132. 2002

272. N. Nakashima, T. Tamura, and L. Good, "Paired termini stabilize antisense RNAs and enhance conditional gene silencing in *Escherichia coli*," *Nucleic Acids Res.*, vol. 34, no. 20, p. e138, 2006.

273. D. Hwang and Y.-H. Lim, "Resveratrol antibacterial activity against *Escherichia coli* is mediated by Z-ring formation inhibition via suppression of FtsZ expression," *Sci. Rep.*, vol. 5, no. 1, p. 10029, Sep. 2015.

274. S. C. Valentine, D. Contreras, S. Tan, L. J. Real, S. Chu, and H. H. Xu, "Phenotypic and molecular Characterization of *Acinetobacter baumannii* Clinical Isolates from Nosocomial Outbreaks in Los Angeles County, California," *J. Clin. Microbiol.*, vol. 46, no. 8, pp. 2499–2507, Aug. 2008.

275. Matthew A. Wikler, *M23Ed5 | In Vitro Susceptibility Testing Criteria & QC*, 5th ed. 2018.

276. P. C. Appelbaum, "The emergence of vancomycin-intermediate and vancomycin-resistant *Staphylococcus aureus*," *Clinical Microbiology and Infection*, vol. 12, pp. 16–23, 2006.

277. R. Khatib, K. Riederer, M. Sharma, S. Shemes, S. P. Iyer, and S. Szpunar, "Screening for intermediately Vancomycin-Susceptible and Vancomycin-Heteroresistant *Staphylococcus aureus* by Use of Vancomycin-Supplemented Brain Heart Infusion Agar Biplates: Defining Growth Interpretation Criteria Based on Gold Standard Confirmation," *Journal of Clinical Microbiology*, vol. 53, no. 11, pp. 3543–3546, Aug. 2015.

278. F. M. MacKenzie and I. M. Gould, "The post-antibiotic effect," *J. Antimicrob. Chemother.*, vol. 32, no. 4, pp. 519–537, Oct. 1993.

279. A. S. Bayer and J. O. Morrison, "Disparity between timed-kill and checkerboard methods for determination of in vitro bactericidal interactions of vancomycin plus rifampin versus methicillin-susceptible and -resistant Staphylococcus aureus.," *Antimicrobial Agents and Chemotherapy*, vol. 26, no. 2, pp. 220–223, 1984.

280. Y. Hu and A. R. M. Coates, "Enhancement by novel anti-methicillin-resistant *Staphylococcus aureus* compound HT61 of the activity of neomycin, gentamicin, mupirocin and chlorhexidine: *in vitro* and *in vivo* studies.," *J. Antimicrob. Chemother.*, vol. 68, no. 2, pp. 374–84, Feb. 2013.

281. M. Arditi and R. Yogev, "*In vitro* interaction between rifampin and clindamycin against pathogenic coagulase-negative *staphylococci*," *Antimicrob. Agents Chemother.*, vol. 33, no. 2, pp. 245–7, Feb. 1989.

282. L. Alou, F. Cafini, D. Sevillano, I. Unzueta, and J. Prieto, "*In vitro* activity of mupirocin and amoxicillin-clavulanate alone and in combination against *staphylococci*

including those resistant to methicillin," *International Journal of Antimicrobial Agents*, vol. 23, no. 5, pp. 513–516, May 2004.

283. Jamal, M., Ahmad, W., Andleeb, S., Jalil, F., Imran, M., Nawaz, M.A., Hussain, T., Ali, M., Rafiq, M., and Kamil, M.A. "Bacterial biofilm and associated infections," *J. Chinese Med. Assoc.*, vol. 81, no. 1, pp. 7–11, Jan. 2018.

284. S. Ward, Y. Argon, and G. A. Nelson, "Sperm Morphogenesis in wild-type and fertilization-defective mutants of *Caenorhabditis elegans," J. Cell Biol.*, vol. 91, pp. 26–44, 1981.

285. D. Uccelletti, E. Zanni, L. Marcellini, C. Palleschi, D. Barra, and M. L. Mangoni, "Anti-*Pseudomonas* activity of frog skin antimicrobial peptides in a *Caenorhabditis elegans* infection model: a plausible mode of action *in vitro* and *in vivo*," *Antimicrobial Agents and Chemotherapy*, vol. 54, no. 9, pp. 3853–3860, Jul. 2010.

286. S. Brenner, "The genetics of *Caenorhabditis elegans*," *Genetics*, vol. 77, no. 1, pp. 71–94, 1974.

287. K. Ooi, T.-Y. Lim, S.-H. Lee, and S. Nathan, "*Burkholderia pseudomallei* kills *Caenorhabditis elegans* through virulence mechanisms distinct from intestinal lumen colonization.," *Virulence*, vol. 3, no. 6, pp. 485–96, Oct. 2012.

288. M. J. Casadaban and S. N. Cohen, "Analysis of gene control signals by DNA fusion and cloning in *Escherichia coli*.," *J. Mol. Biol.*, vol. 138, no. 2, pp. 179–207, Apr. 1980.

289. P. Gilbert and A. J. McBain, "Potential impact of increased use of biocides in consumer products on prevalence of antibiotic resistance.," *Clin. Microbiol. Rev.*, vol. 16, no. 2, pp. 189–208, Apr. 2003.

290. S. Zlitni, J. E. Blanchard, and E. D. Brown, "High-throughput screening of model bacteria.," *Methods Mol. Biol.*, vol. 486, pp. 13–27, 2009.

291. V. Dartois *et al.*, "Systemic antibacterial activity of novel synthetic cyclic peptides," *Antimicrob. Agents Chemother.*, vol. 49, no. 8, pp. 3302–3310, 2005.

292. R. Daugelavicius, E. Bakiene, and D. H. Bamford, "Stages of polymyxin B interaction with the *Escherichia coli* cell envelope," *Antimicrobial agents and chemotherapy*, vol. 44, no. 11, pp. 2969–78, 2000.

293. T. P. T. Cushnie, N. H. O'Driscoll, and A. J. Lamb, "Morphological and ultrastructural changes in bacterial cells as an indicator of antibacterial mechanism of action.," *Cell. Mol. Life Sci.*, vol. 73, no. 23, pp. 4471–4492, 2016.

294. X.-Z. Li and H. Nikaido, "Efflux-mediated drug resistance in bacteria.," *Drugs*, vol. 64,

no. 2, pp. 159–204, 2004.

295. B. G. Spratt, “Distinct penicillin binding proteins involved in the division, elongation, and shape of Escherichia coli K12.,” *Proceedings of the National Academy of Sciences*, vol. 72, no. 8, pp. 2999–3003, Aug. 1975.
296. T. Den Blaauwen, M. E. G. Aarsman, N. O. E. Vischer, and N. Nanninga, “Penicillin-binding protein PBP2 of *Escherichia coli* localizes preferentially in the lateral wall and at mid-cell in comparison with the old cell pole.,” *Mol. Microbiol.*, vol. 47, no. 2, pp. 539–47, Jan. 2003.
297. N. A. Curtis, D. Orr, G. W. Ross, and M. G. Boulton, “Affinities of penicillins and cephalosporins for the penicillin-binding proteins of *Escherichia coli* K-12 and their antibacterial activity.,” *Antimicrob. Agents Chemother.*, vol. 16, no. 5, pp. 533–9, Nov. 1979.
298. T. A. Davies, W. Shang, K. Bush, and R. K. Flamm, “Affinity of doripenem and comparators to penicillin-binding proteins in *Escherichia coli* and *Pseudomonas aeruginosa*,” *Antimicrobial Agents and Chemotherapy*, vol. 52, no. 4, pp. 1510–1512, Feb. 2008.
299. E. Lacasse, E. Brouillette, A. Larose, T. R. Parr, A. Rubio, and F. Malouin, “*In vitro* activity of Tebipenem (SPR859) against penicillin-binding proteins of Gram-negative and Gram-positive bacteria.,” *Antimicrob. Agents Chemother.*, vol. 63, no. 4, Apr. 2019.
300. G. Zhao, T. I. Meier, S. D. Kahl, K. R. Gee, and L. C. Blaszczak, “BOCILLIN FL, a sensitive and commercially available reagent for detection of penicillin-binding proteins.,” *Antimicrob. Agents Chemother.*, vol. 43, no. 5, pp. 1124–8, May 1999.
301. P. C. Maloney, E. R. Kashket, and T. H. Wilson, “A Proton motive force drives ATP synthesis in bacteria,” *Proceedings of the National Academy of Sciences*, vol. 71, no. 10, pp. 3896–3900, Oct. 1974.
302. C. L. Andersen, I. B. Holland, and A. Jacq, “Verapamil, a Ca2+ channel inhibitor acts as a local anesthetic and induces the sigma E dependent extra-cytoplasmic stress response in *E. coli*.,” *Biochim. Biophys. Acta*, vol. 1758, no. 10, pp. 1587–95, Oct. 2006.
303. L. E. Fleck, E. J. North, R. E. Lee, L. R. Mulcahy, G. Casadei, and K. Lewis, “A screen for and validation of prodrug antimicrobials,” *Antimicrob. Agents Chemother.*, vol. 58, no. 3, pp. 1410–1419, Mar. 2014.
304. V. Defraine, M. Fauvart, and J. Michiels, “Fighting bacterial persistence: current and emerging anti-persister strategies and therapeutics.,” *Drug Resist. Updat.*, vol. 38, pp.

12–26, 2018.

305. J. B. Fitzgerald, B. Schoeberl, U. B. Nielsen, and P. K. Sorger, “Systems biology and combination therapy in the quest for clinical efficacy.,” *Nat. Chem. Biol.*, vol. 2, no. 9, pp. 458–66, Sep. 2006.
306. A. Y. Peleg, H. Seifert, and D. L. Paterson, “*Acinetobacter baumannii*: emergence of a successful pathogen,” *Clinical Microbiology Reviews*, vol. 21, no. 3, pp. 538–582, Jul. 2008.
307. V. C. Barth, B. Á. Rodrigues, G. D. Bonatto, S. W. Gallo, V. E. Pagnussatti, C. A. S. Ferreira, and S. D. D. Oliveira, “Heterogeneous persister cells formation in *Acinetobacter baumannii*,” *PLoS ONE*, vol. 8, no. 12, 2013.
308. B. K. Donamore, S. W. Gallo, P. M. Abreu Ferreira, C. A. Sanchez Ferreira, and S. D. de Oliveira, “Levels of persisters influenced by aeration in *Acinetobacter calcoaceticus-baumannii*.,” *Future Microbiol.*, vol. 13, pp. 209–219, 2018.
309. A. Michalopoulos and M. E. Falagas, “Treatment of *Acinetobacter* infections.,” *Expert Opin. Pharmacother.*, vol. 11, no. 5, pp. 779–88, Apr. 2010.
310. R. A. Fisher, B. Gollan, and S. Helaine, “Persistent bacterial infections and persister cells,” *Nat. Rev. Microbiol.*, vol. 15, no. 8, pp. 453–464, May 2017.
311. J. G. Hurdle, A. J. O’Neill, I. Chopra, and R. E. Lee, “Targeting bacterial membrane function: an underexploited mechanism for treating persistent infections,” *Nature Reviews Microbiology*, vol. 9, no. 1, pp. 62–75, Dec. 2010.
312. S. S. Grant, B. B. Kaufmann, N. S. Chand, N. Haseley, and D. T. Hung, “Eradication of bacterial persisters with antibiotic-generated hydroxyl radicals,” *Proceedings of the National Academy of Sciences*, vol. 109, no. 30, pp. 12147–12152, Jul. 2012.
313. I. Keren, N. Kaldalu, A. Spoering, Y. Wang, and K. Lewis, “Persister cells and tolerance to antimicrobials.,” *FEMS Microbiol. Lett.*, vol. 230, no. 1, pp. 13–8, Jan. 2004.
314. Etthel M. Windels, Zacchari Ben Meriem, Taiyeb Zahir, Kevin J. Verstrepen, PascalHersen, Bram Van den Bergh, Jan Michiels., “Isolation of persisters enabled by ß-lactam-induced filamentation reveals their single-cell awakening characteristics,” bioRxiv, https://doi.org/10.1101/600700, 2019.
315. N. Hofsteenge, E. van Nimwegen, and O. K. Silander, “Quantitative analysis of persister fractions suggests different mechanisms of formation among environmental isolates of *E. coli*,” *BMC Microbiology*, vol. 13, no. 1, p. 25, 2013.
316. M. Bernabeu-Wittel, A. García-Curiel, C. Pichardo, M. E. Pachón-Ibáñez, M. E.

Jiménez-Mejías, and J. Pachón, “Morphological changes induced by imipenem and meropenem at sub-inhibitory concentrations in *Acinetobacter baumannii*.,” *Clin. Microbiol. Infect.*, vol. 10, no. 10, pp. 931–4, Oct. 2004.

317. W. F. Penwell *et al.*, “Molecular mechanisms of sulbactam antibacterial activity and resistance determinants in *Acinetobacter baumannii.,” Antimicrob. Agents Chemother.*, vol. 59, no. 3, pp. 1680–9, Mar. 2015.
318. R. L. Soon, R. L. Nation, P. G. Hartley, I. Larson, and J. Li, “Atomic force microscopy investigation of the morphology and topography of colistin-heteroresistant *Acinetobacter baumannii* strains as a function of growth phase and in response to colistin treatment.,” *Antimicrob. Agents Chemother.*, vol. 53, no. 12, pp. 4979–86, Dec. 2009.
319. N. Verstraeten *et al.*, “Obg and membrane depolarization are part of a microbial bet-hedging strategy that leads to antibiotic tolerance.,” *Mol. Cell*, vol. 59, no. 1, pp. 9–21, Jul. 2015.
320. C. T. Bot and C. Prodan, “Quantifying the membrane potential during *E. coli* growth stages.,” *Biophys. Chem.*, vol. 146, no. 2–3, pp. 133–7, Feb. 2010.
321. T. K. Wood, S. J. Knabel, and B. W. Kwan, “Bacterial persister cell formation and dormancy.,” *Appl. Environ. Microbiol.*, vol. 79, no. 23, pp. 7116–21, Dec. 2013.
322. S. L. McKay and D. A. Portnoy, “Ribosome hibernation facilitates tolerance of stationary-phase bacteria to aminoglycosides,” *Antimicrobial Agents and Chemotherapy*, vol. 59, no. 11, pp. 6992–6999, Aug. 2015.
323. X. Zhao and K. Drlica, “Reactive oxygen species and the bacterial response to lethal stress,” *Current Opinion in Microbiology*, vol. 21, pp. 1–6, Oct. 2014.
324. R. Trastoy., “Mechanisms of bacterial tolerance and persistence in the gastrointestinal and respiratory environments,” *Clinical Microbiology Reviews*, vol. 31, no. 4, Aug. 2018.
325. D. P. Karumathil, M. S. Nair, J. Gaffney, A. Kollanoor-Johny, and K. Venkitanarayanan, “Trans-cinnamaldehyde and eugenol increase *Acinetobacter baumannii* sensitivity to beta-lactam antibiotics,” *Frontiers in Microbiology*, vol. 9, 2018.
326. N. Leyva-López, E. P. Gutiérrez-Grijalva, G. Vazquez-Olivo, and J. B. Heredia, Essential oils of Oregano: biological activity beyond their antimicrobial properties,” *Molecules*, vol. 22, no. 6, p. 989, Jun. 2017.
327. P. Patra and S. Klumpp, “Population dynamics of bacterial persistence,” *PLoS ONE*,

vol. 8, no. 5, p. e62814, May 2013.

328. K. Lewis, “Persister cells, dormancy and infectious disease.,” *Nat. Rev. Microbiol.*, vol. 5, no. 1, pp. 48–56, Jan. 2007.
329. M. K. Paczosa and J. Mecsas, *“Klebsiella pneumoniae*: Going on the Offense with a Strong Defense,” *Microbiology and molecular biology reviews : MMBR*, vol. 80, no. 3, pp. 629–61, 2016.
330. E. B. Hirsch and V. H. Tam, “Detection and treatment options for *Klebsiella pneumoniae* carbapenemases (KPCs): an emerging cause of multidrug-resistant infection.,” *J. Antimicrob. Chemother.*, vol. 65, no. 6, pp. 1119–25, Jun. 2010.
331. A. A. El Solh and A. Alhajhusain, “Update on the treatment of *Pseudomonas aeruginosa* pneumonia,” *Journal of Antimicrobial Chemotherapy*, vol. 64, no. 2, pp. 229–238, Jun. 2009.
332. A. Srinivasan, J. D. Dick, and T. M. Perl, “Vancomycin resistance in *Staphylococci*,” *Clinical Microbiology Reviews*, vol. 15, no. 3, pp. 430–438, Jul. 2002.
333. A. Marchese *et al.*, “Antibacterial and antifungal activities of thymol: A brief review of the literature.,” *Food Chem.*, vol. 210, pp. 402–14, Nov. 2016.
334. “CFR - Code of Federal Regulations Title 21.”
335. F. C. Fachini-Queiroz *et al.*, “Effects of thymol and carvacrol, constituents of *Thymus vulgaris* L. essential oil, on the inflammatory response,” *Evidence-Based Complementary and Alternative Medicine*, vol. 2012, pp. 1–10, 2012.
336. M. Zengin *et al.*, “Novel thymol bearing oxypropanolamine derivatives as potent some metabolic enzyme inhibitors - Their antidiabetic, anticholinergic and antibacterial potentials.,” *Bioorg. Chem.*, vol. 81, pp. 119–126, 2018.
337. P. Raei *et al.*, “Thymol and carvacrol strongly inhibit biofilm formation and growth of carbapenemase-producing Gram negative bacilli.,” *Cell. Mol. Biol. (Noisy-le-grand).*, vol. 63, no. 5, pp. 108–112, May 2017.
338. B. A. Cunha, P. E. Schoch, and J. R. Hage, “Nitrofurantoin: preferred empiric therapy for community-acquired lower urinary tract infections.,” *Mayo Clin. Proc.*, vol. 86, no. 12, pp. 1243–4; author reply 1244, Dec. 2011.
339. R. G. Finch, *Antibiotic and chemotherapy : anti-infective agents and their use in therapy.*
340. S. K. Srivastava, V. R. Iyer, T. Ghosh, P. R. Lambadi, R. Pathania, and N. K. Navani, “Isolation of a non-genomic origin fluoroquinolone responsive regulatory element using a combinatorial bioengineering approach,” *Nucleic Acids Res.*, vol. 44, no. 5, pp. 2451–

2461, 2016.

341. J. Vervoort, B. B. Xavier, A. Stewardson, S. Coenen, M. Godycki-Cwirko, N. Adriaenssens, A. Kowalczyk, C. Lammens, S. Harbarth, H. Goossens, S. M. Kumar., "An *in vitro* deletion in *ribE* encoding Lumazine Synthase contributes to nitrofurantoin resistance in *Escherichia coli*," *Antimicrobial Agents and Chemotherapy*, vol. 58, no. 12, pp. 7225–7233, Sep. 2014.

Publications

Publications/Patents out of this thesis work

Publications:

Bhando T., Bhattacharya T., Gaurav A., Akhter J., Saini M., Gupta V. K., Srivastava S., Sen H., Navani N. K., Gupta V., Biswas D., Chaudhary R., Pathania R. Antibacterial properties and *in vivo* efficacy of a novel nitrofuran, IITR06144 against multidrug resistant pathogens. (Accepted in Journal of Antimicrobial Chemotherapy, September 2019).

Bhando T., Casius A., Pathania R. Mechanism based screen identifies an FDA-approved compound with Anti-persister activity against *Acinetobacter baumannii*. (Manuscript under preparation).

Bhando T., M. Safuwan, Gupta R., Pathania R. Chemical-Chemical Interaction Profiling uncovers a novel small molecule exhibiting *in vitro* synergy with cell wall targeting antibiotics. (Manuscript under preparation).

Bhando T., Sen H., Saini M., Pathania R. Synergistic interaction of IITR06144 and Vancomycin against heterogenous vancomycin intermediate *Staphylococcus aureus* (hVISA) and VISA. (Manuscript under preparation)

Patents:

Pathania R., **Bhando T**., Casius A. Methods and compositions for identification of novel anti-persister activity of GRAS compounds (Provisional patent application No. 201911023795).

Pathania R., **Bhando T**., Saini M., Novel combinations of furan derivatives with glycopeptide antibiotics for the treatment of bacterial infections. (Provisional patent application filed)

Pathania R., **Bhando T**. Use of novel biguanide derivatives and combinations thereof with antibiotics against persistent bacterial infections. (Provisional patent application filed).

Book Chapter:

Bhando T., Dubey V., Pathania R., Biofilms in antimicrobial activity and drug resistance, Bacterial Adaptation to Co-resistance, Springer Nature. (Accepted, July 2019).

Other Publications/Patent

Publications:

Singh S.*, **Bhando T.***, Dikshit K.L. Fibrin targeted plasminogen activation by plasminogen activator from *Streptococcus dysgalactiae*. Protein Science. 2014 June 23;(6):714-722; *Equal contribution.

Singh S., Rathore Y. S., **Bhando T.**, Ashish, Dikshit K.L. Bilobed shape of PadA reveals the connectivity from single to multi-domain bacterial plasminogen activators. International journal of biological macromolecules 2015 Apr; 78:370-378.

Sharma A., Sharma R., Bhattacharya T., **Bhando T.**, Pathania R. Fosfomycin resistance in *Acinetobacter baumannii* is mediated by efflux through a major facilitator superfamily (MFS) transporter—AbaF. Journal of Antimicrobial Chemotherapy. 2016 Sep; 20:72(1):68-74.

Bhatia A., Singh NK, **Bhando T.**, Pathania R., Kazmi AA. "Effect of intermittent aeration on microbial diversity in an intermittently aerated IFAS reactor treating municipal waste water: A field study. Journal of Environ Science and Health A Toxicology Hazard Subst Environ Eng. 2017 Apr; 52(5):440-448.

Sharma A., Dubey V., Sharma R., Devnath K., Gupta V., Akhter J., **Bhando T.**, Verma A., Ambatipudi K. S., Pathania R. The unusual glycine rich C-terminus of the *Acinetobacter baumannii* RNA chaperone Hfq plays an important role in bacterial physiology. Journal of Biological Chemistry. 2018 Aug; 293(35):13377-88.

Bhando T.*, Singh S.*, Hade M.D., Dikshit K.L. A novel staphylokinase derivative having VEK-30 peptide with improved fibrinolytic properties. (Under review in Applied Microbiology and Biotechnology) *Equal contribution.

Patent:

Singh, S., **Bhando T.,** Dikshit K.L. Construction and purification of novel staphylokinase derivatives having enhanced plasminogen activation and clot dissolution ability. (US Patent Application No. 0070NF2013N: dated 28-03-2013).

Conferences/Poster Presentations

Bhando T., Pathania R. A novel small RNA AbSR28 mediates resistance to osmotic stress in *A. baumannii* ATCC 17978. International Conference on NextGen Genomics, Biology, Bioinformatics and Technologies (NGBT), Jaipur, India. 30th Sept-2nd October, 2018.
(Best Poster Award)

Bhando T., Bhattacharya T., Gaurav A., Akhter J., Saini M., Gupta V. K., Pathania R. A novel nitrofuran small molecule - IITR06144 inhibits multidrug resistant Gram negative pathogens**.** 1st National Biomedical Research Competition held at AIIMS, Rishikesh, India. 15th Oct, 2018.
(Certificate of Appreciation)

Bhando T., Bhattacharya T., Gaurav A., Akhter J., Saini M., Gupta V. K., Pathania R. Small molecule screening identifies a novel antibacterial with broad spectrum activity against multidrug resistant pathogens. International Symposium on Antimcrobial Resistance - One health Perspective, IIT Roorkee, India. 5th-8th March, 2019.
(Best Poster Award)

M. Safuwan, **Bhando T.,** Gupta R., Pathania R. Chemical-Chemical Interaction Profiling uncovers a novel small molecule exhibiting *in vitro* synergy with cell wall targeting antibiotics. International Symposium on Antimcrobial Resistance - One health Perspective, IIT Roorkee, India. 5th-8th March, 2019.
(Best Poster Award)

Casius A., **Bhando T.,** Pathania R. Mechanism based screen identifies a GRAS status small molecule with Anti-persister activity against *Acinetobacter baumannii*. International Symposium on Antimcrobial Resistance - One health Perspective, IIT Roorkee, India. 5th-8th March, 2019.